

Analysis of Laminated Anisotropic Plates and Shells Via a Modified Complementary Energy Principle Approach

Martin Claude Domfang
Marquette University

Recommended Citation

Domfang, Martin Claude, "Analysis of Laminated Anisotropic Plates and Shells Via a Modified Complementary Energy Principle Approach" (2013). *Dissertations (2009 -)*. 253.
https://epublications.marquette.edu/dissertations_mu/253

ANALYSIS OF LAMINATED ANISOTROPIC PLATES AND SHELLS VIA A
MODIFIED COMPLEMENTARY ENERGY PRINCIPLE APPROACH

by

Martin Claude Domfang, S.J., M.S.

A Dissertation submitted to the Faculty of the Graduate School,
Marquette University,
in Partial Fulfillment of the Requirements for
the Degree of Doctor of Philosophy

Milwaukee, Wisconsin

May 2013

ABSTRACT
ANALYSIS OF LAMINATED ANISOTROPIC PLATES AND SHELLS VIA A
MODIFIED COMPLEMENTARY ENERGY PRINCIPLE APPROACH

Martin Claude Domfang, S.J., M.S.

Marquette University, 2013

The present work is concerned with the finite element structural analysis of laminated anisotropic plates and shells. New elements based on a modified complementary energy principle are proposed to improve the analysis of such composite structures. Third order deformation plate and shell models incorporating a convergence parameter are developed to govern the general displacement field.

An eight-node isoparametric quadrilateral element with two independent cross-sectional rotations and three normal displacements is utilized to describe the displacement field. The present modified complementary energy formulation incorporates a number of in-plane strain functions of various orders. The corresponding in-plane stresses for each lamina are derived from the constitutive relations. The transverse stresses are then computed from the application of equilibrium equations. The element comprises an arbitrary number of lamina rigidly bonded together.

The analysis technique employed, although using a higher order formulation, does not increase the number of variables associated with each lamina. Moreover, the use of a convergence parameter permits one to achieve excellent results for very thin as well as thick composite plates and shells. The static bending analysis of several example problems for various geometries, transverse loads and material properties is analyzed via a code written in MATLAB. The results are compared with those from technical theories, other finite element models and three-dimensional elasticity solutions available in the literature. It is demonstrated that marked improvements in the results for stress and displacement can be achieved by the use of the new modified complementary energy elements incorporating a convergence parameter.

ACKNOWLEDGEMENTS

Martin Claude Domfang, S.J., M.S.

I am grateful to my family, especially my sister Suzanne Youveup and my nephew and nieces, for their unfailing love and continuous support, and to my Jesuits companions, in particular those of the Wisconsin Province, for their friendship in the Lord, and their spiritual and financial support.

I would like to express my deepest gratitude to Professor G. E. Otto Widera. You have been more than an academic advisor; you are a mentor for me. You boosted my energy and eagerness to pursue excellence in a field with a little background (finite element analysis) and another with no background whatsoever (composite materials). Thank you for your guidance and inspiration during the course of the research leading to this dissertation.

My thanks go to Dr. Hyunjae Park for his assistance and advice. Your remarks and suggestions were invaluable.

I am grateful to Dr. Kyuil Kim, Dr Raymond Fournelle, and Dr. Baolin Wan for also being members of my dissertation committee and to the professors and staff (especially Annette Wolak) of the Department of Mechanical Engineering for their support and encouragement.

I extend my gratitude to the Chinang family, the Gesu Companions of Christian Life Community, the Cercle des Amis du Cameroon and the member of “Marie Reine du Monde” community of St Camillus Parish in Silver Spring (MD). Their prayers and genuine love made the tension between priesthood and study bearable and enjoyable.

TABLE OF CONTENTS

ACKNOWLEDGEMENTS	i
LIST OF FIGURES.....	vii
LIST OF TABLES	xii
CHAPTER 1 INTRODUCTION	1
1.1. Introduction to Laminated Composite Materials	1
1.2. Statement of the Problem	2
1.3. Review of Relevant Literature.....	5
1.3.1 Composite Laminated Plates.....	5
<i>a) Exact Elasticity Solutions</i>	<i>5</i>
<i>b) Analytical Approaches.....</i>	<i>6</i>
<i>c) Finite Element Methods.....</i>	<i>7</i>
1.3.2 Laminated Composite Cylindrical Shells.....	9
<i>a) Elasticity Theory and Analytical Methods.....</i>	<i>9</i>
<i>b) Finite Element Analysis of Laminated Composite Cylindrical Shells</i>	<i>11</i>
1.3.3 Failure Criteria in Composite Material Structures	12
1.4. Objective and Scope of Present Study	14
CHAPTER 2 REVIEW OF COMPOSITE LAMINATED PLATE AND SHELL THEORIES	16
2.1. Anisotropic Linear Elasticity Theory	16
2.1.1 Kinematics or Strain-Displacements Relations.	16
2.1.2 Kinetics or Equilibrium Equations.....	18
2.1.3 Constitutive Equations.....	20
2.1.4 Mechanics of Orthotropic Lamina.....	21
<i>a) Constitutive Equations in Material and Global Coordinates</i>	<i>21</i>

<i>b) Displacement Continuity and Traction Free Conditions</i>	24
2.2 Technical Theories – Analytical Approach	25
2.2.1 Classical Plate and Shell Theories	25
<i>a) Plate and Shell Theory Assumptions</i>	25
<i>b) Equilibrium Equations</i>	28
<i>b) Constitutive Equations</i>	29
<i>c) Solution Methods</i>	31
2.2.2 Classical Lamination Plate and Shell Theories.....	31
<i>a) Displacement and Strain Fields</i>	31
<i>b) State of Stress</i>	32
<i>c) Governing Equations</i>	33
<i>e) Analytical Solution</i>	36
<i>d) Tractions Continuity or Interface Boundary Conditions</i>	36
2.2.3 First Order Deformation Theory	37
<i>a) Displacement and Strain Fields</i>	37
<i>b) Governing Equations</i>	40
<i>c) Analytical Solutions</i>	43
2.2.3 Higher Order Deformation Theories (HSDT)	45
<i>a) Displacement Assumptions</i>	45
<i>b) Governing Equations - Constitutive Equations</i>	47
<i>c) Analytical Solutions</i>	48
2.3 Technical Theories – Finite Element Approach (Via Variational Principle)	48
2.3.1 Principal of Minimum Potential Energy	48
2.3.2 Principle of Minimum Complementary Energy	50
2.3.3 Mixed Formulation	51

CHAPTER 3 STRAIN-BASED MODIFIED COMPLEMENTARY ENERGY PRINCIPLE	54
3.1 General Element Formulation	54
3.2 Definition of the Functional for a Multilayered Plate or Shell Element.	56
3.3 Proposed Element Formulation.....	60
3.3.1 Strain Functions Choices.....	60
3.3.2 First Order Element Formulation.....	62
3.3.3 Third Order Strain Element.....	64
CHAPTER 4 Finite Element Formulation (Analysis and Implementation)	73
4.1 Plate Element Formulation	73
4.1.1 Geometry	73
4.1.2 Displacement Field.....	76
4.1.3 Kinematics.....	76
4.1.4 Stress Interpolation.....	79
4.1.5 Interlaminar Boundary Conditions	81
4.1.6 Development of Stiffness Matrix.....	87
4.1.7 Stress Calculation.....	89
4.2 Shell Element Formulation.....	89
4.2.1 Geometry Definition and Description of the Element.....	90
4.2.2 Displacement Field.....	92
4.2.3 Kinematics.....	94
4.2.4 Strain Transformation	98
4.2.5 Constitutive Equations.....	100
4.2.6 Stress Interpolation.....	101
4.2.7 Development of Stiffness Matrix.....	109

4.3 Numerical Implementation (Development of FE code)	113
4.3.1 Flowchart	113
4.3.2 Matlab Code Input.....	117
CHAPTER 5 SAMPLE ANALYSES AND VERIFICATION	118
5.1 Displacement Examples	120
5.1.1 Deflection of an Isotropic Square Plate.....	121
<i>a) Boundary Conditions 1: Simply Supported Edges</i>	121
<i>b) Boundary Conditions 2: Clamped Edges</i>	125
5.1.2 Displacements of Two-Layered Angle-Ply Composite Square Plate.....	128
5.1.3 Deflection of a Three-Layered Semi-Infinite Strip	132
5.1.4 Deflection of an Anti-Symmetric Cross-Ply Square Plate with Various Edge Boundary Conditions.....	144
5.1.5 Barrel Vault Under Gravity Load	162
5.1.6 Pinched Cylinder Analysis	164
5.1.7 Maximum Transverse Deflections of a Two-Layered Cross-Ply Laminated Cylindrical Shell Roof of Various Thickness.....	166
5.2 Stress Examples	171
5.2.1 Bending Stresses of a Simply Supported Isotropic Square Plate	171
5.2.2 Stress Analysis of a Three-Layered Semi-Infinite Strip.....	173
5.2.3 Stress Analysis of an Anti-Symmetric Cross-Ply Square Plate with Various Edge Boundaries Conditions.....	177
5.2.4 Stress Analysis of a Two-Layered Cross-Ply Laminated Cylindrical Shell Roof of Various Thicknesses	194
Chapter 6 Summary – Conclusion and Future Work	202
6.1 Summary and Conclusion	202

6.2 Suggestion for Future Work	206
REFERENCES	207
APPENDIX A	219
APPENDIX B	226

LIST OF FIGURES

Figure 1. 1: Illustration of the two levels of characterizing composite laminated structures	2
Figure 1. 2: Interconnection between the knowledge needed to analyze a laminated composite structure.	4
Figure 2. 1: Deformed body under external forces.	17
Figure 2. 2: 3-D state of stress acting on an infinitesimal parallelepiped element.	19
Figure 2. 3: Illustration of material and global coordinate systems.....	22
Figure 2. 4: Transverse displacement based on <i>Kirchhoff hypothesis</i>	27
Figure 2. 5: Force and moment resultants acting on an element plate or shell.....	29
Figure 2. 6. Equivalent single layer laminated composite structure	32
Figure 2. 7: Interlayer traction continuity conditions	37
Figure 2. 8: Illustration of the first order shear deformation theory. a) Undeformed geometry, b) Deformed geometry.....	38
Figure 3. 1: Prescribed traction and boundary equilibrium on an element boundary.....	55
Figure 3. 2: Multilayer element numbering.	57
Figure 3. 3: Pascal triangle.....	61
Figure 4. 1: Multi-layer geometry and nodal degree of freedom for plate element.....	74
Figure 4. 2: Node numbering of quadratic element.	75
Figure 4. 3: Multi-layer composite shell element	91
Figure 4. 4: Unit vectors at node i	91
Figure 4. 5: Nodal displacements.....	94
Figure 5. 1: Geometry and axes orientation for a plate.....	121
Figure 5.2: Convergence rate of the center deflection for a thin isotropic simply supported plate ($S=0.01$).	124
Figure 5.3: Convergence rate for a moderately thin isotropic simply supported plate ($S=0.005$).	124

Figure 5. 4: Normalized center deflection of an isotropic clamped square plate ($S=0.01$).	127
Figure 5. 5: Normalized center deflection of an isotropic clamped square plate ($S=0.005$).	127
Figure 5. 6: Boundary conditions, fiber orientation and stacking lay up of angle-ply square plate.	130
Figure 5. 7: Center deflection error of a thin ($S=0.0375$) symmetric 3-layered semi- infinite strip using Type I elements.	134
Figure 5. 8: Center deflection error of a moderately thin ($S=0.05$) symmetric 3- layered semi-infinite strip using Type I elements.	135
Figure 5. 9: Center deflection error of a moderately thick ($S=0.1$) symmetric 3- layered semi-infinite strip using Type I elements.	136
Figure 5. 10: Center deflection error of a very thick ($S=0.25$) symmetric 3-layered semi-infinite strip using Type I elements.	137
Figure 5. 11: Center deflection error of a very thin ($S=0.01$) symmetric 3-layered semi-infinite strip using Type II elements.	138
Figure 5. 12: Center deflection error of a thin ($S=0.0375$) symmetric 3-layered semi-infinite strip using Type II elements.	139
Figure 5. 13: Center deflection error of a moderately thin ($S=0.05$) symmetric 3- layered semi-infinite strip using Type II elements.	140
Figure 5. 14: Center deflection error of a moderately thick ($S=0.1$) symmetric 3- layered semi-infinite strip using Type II elements.	141
Figure 5. 15: Center deflection error of a very thick ($S=0.25$) symmetric 3-layered semi-infinite strip using Type II elements.	142
Figure 5. 16: Center deflection of antisymmetric cross-ply square plates (SS BCs) using Type I elements.	146
Figure 5. 17: Center deflection of antisymmetric cross-ply square plates (CC BCs) using Type I elements.	147
Figure 5. 18: Center deflection of antisymmetric cross-ply square plates (FF BCs) using Type I elements.	148
Figure 5. 19: Center deflection of antisymmetric cross-ply square plates (SC BCs) using Type I elements.	149

Figure 5. 20: Center deflection of antisymmetric cross-ply square plates (SS BCs) using Type I elements.	150
Figure 5. 21: Center deflection of antisymmetric cross-ply square plates (FC BCs) using Type I elements.	151
Figure 5. 22: Center deflection comparison of antisymmetric cross-ply square plates with various edge BCs.....	153
Figure 5. 23: Center deflection of antisymmetric cross-ply square plates (SS BCs) using Type II elements.....	155
Figure 5. 24: Center deflection of antisymmetric cross-ply square plates (CC BCs) using Type II elements.....	156
Figure 5. 25 : Center deflection of antisymmetric cross-ply square plates (FF BCs) using Type II elements.....	157
Figure 5. 26: Center deflection of antisymmetric cross-ply square plates (SC BCs) using Type II elements.....	158
Figure 5. 27: Center deflection of antisymmetric cross-ply square plates (FS BCs) using Type II elements.....	159
Figure 5. 28: Center deflection of antisymmetric cross-ply square plates (FC BCs) using Type II elements.....	160
Figure 5. 29: Barrel Vault geometry and meshing (Scordelis-Lo Roof problem).	163
Figure 5. 30: Pinched cylinder geometry and meshing.....	165
Figure 5. 31: Center deflection of a very thin ($S = 0.01$) cross-ply Barrel Vault using Type I element.....	168
Figure 5. 32: Center deflection of a thin ($S=0.02$) cross-ply Barrel Vault using Type I element.....	169
Figure 5. 33: Center deflection of a moderately thin ($S=0.05$) cross-ply Barrel Vault using Type I element.....	170
Figure 5.34: Maximum In-plane distribution of an isotropic square plate	172
Figure 5. 35: Normal stress evaluation of a symmetric 3-layered semi-infinite strip.....	175
Figure 5. 36: Transverse shear stress evaluation of a symmetric 3-layered semi-infinite strip.....	176
Figure 5. 37: Axial stress ($S1$) of antisymmetric cross-ply square plates (FF BCs) using Type I elements.	179

Figure 5. 38: Axial stress (S1) of antisymmetric cross-ply square plates (CC BCs) using Type I elements.	180
Figure 5. 39: Axial stress (S1) of antisymmetric cross-ply square plates (SS BCs) using Type I elements.	181
Figure 5. 40: Axial stress (S2) of antisymmetric cross-ply square plates (FF BCs) using Type I elements.	182
Figure 5. 41: Axial stress (S2) of antisymmetric cross-ply square plates (CC BCs) using Type I elements.	183
Figure 5. 42: Axial stress (S2) of antisymmetric cross-ply square plates (SS BCs) using Type I elements.	184
Figure 5. 43: Transverse shear stress (S4) of antisymmetric cross-ply square plates (FF BCs) using Type I elements.	185
Figure 5. 44: Transverse shear stress (S4) of antisymmetric cross-ply square plates (CC BCs) using Type I elements.	186
Figure 5. 45: Transverse shear stress (S4) of antisymmetric cross-ply square plates (SS BCs) using Type I elements.	187
Figure 5. 46: Axial stress (S1) of antisymmetric cross-ply square plates (SS BCs) using Type II and bests of Type I elements.	188
Figure 5. 47: Axial stress (S1) of antisymmetric cross-ply square plates (CC BCs) using Type II and bests of Type I elements.	189
Figure 5. 48: Axial stress (S1) of antisymmetric cross-ply square plates (FF BCs) using Type II and bests of Type I elements.	190
Figure 5. 49: Transverse shear stress (S4) of antisymmetric cross-ply square plates (SS BCs) using Type II and bests of Type I elements.	191
Figure 5. 50: Transverse shear stress (S4) of antisymmetric cross-ply square plates (CC BCs) using Type II and bests of Type I elements.	192
Figure 5. 51: Transverse shear stress (S4) of antisymmetric cross-ply square plates (FF) (BCs) using Type II and bests of Type I elements.	193
Figure 5. 52: Axial stress (Sx) of thin cross-ply Barrel Vault	195
Figure 5. 53: Axial stress (Sx) of a moderately thin cross-ply Barrel Vault.	196
Figure 5. 54: Axial stress (Sx) of a moderately thick cross-ply Barrel Vault.....	197
Figure 5. 55: Axial stress (Sy) of a thin cross-ply Barrel Vault	198

Figure 5. 56: Axial stress (S_y) of a moderately thin cross-ply Barrel Vault	199
Figure 5. 57: Axial stress (S_y) of a moderately thick cross-ply Barrel Vault.....	200

LIST OF TABLES

Table 5.1: Third order elements used to analyze different case problems.....	119
Table 5.2: Normalized center deflection of an isotropic simply supported square plate.....	123
Table 5. 3: Normalized center deflection of an isotropic clamped square plate.....	126
Table 5. 4: Displacement of a simply supported two layer anti-symmetric square composite plate with fiber orientation $\theta=\pm 35^\circ$	131
Table 5. 5: Displacement of a simply supported two layer anti-symmetric square composite plate with fiber orientation $\theta=\pm 45^\circ$	131
Table 5. 6: Center deflection error of a very thick ($S=0.25$) symmetric 3-layered semi-infinite strip using Type II elements.	143
Table 5. 7: Nomenclature for the boundary condition.....	144
Table 5. 8: Nondimensional center deflection of antisymmetric cross-ply square plates with Various Edge BCs – Comparison with other results.	152
Table 5.9: Center deflection of the free edge of a Barrel Vault and comparison with other results.....	163
Table 5.10: Center deflection of a pinched cylinder and comparison with other results.....	165

CHAPTER 1

INTRODUCTION

The present dissertation deals with the structural analysis of laminated anisotropic plates and shells via the use of the finite element method. New elements based on the use of a modified complementary energy principle are proposed to improve the analysis of such composite structures. Third order plate and shell models incorporating a convergence parameter are obtained to govern the general stress and displacement fields.

1.1. Introduction to Laminated Composite Materials

Laminated composite materials can be defined as “combinations of material elements which differ in composition or form on a macroscopic level with respect to each other. The individual fibrous constituent elements can be man-made, are generally insoluble, retain their identities within the composite, and may be continuous or discontinuous” [1]. The fibers are the main load-carrying members, while the matrix material bonds them together. It is established that fiber materials are stronger and stiffer than their bulk-form counterpart, whereas matrix components retain their usual bulk-form properties. The fiber materials are usually made of common metals like aluminum, copper, iron, nickel, steel, and titanium or materials like glass, boron and graphite. Matrix materials are generally epoxy or resin. A full understanding of the behavior of fiber and matrix properties at the microscopic level requires the use of the field of material science. The present study is entirely devoted to a macroscopic level study as illustrated in Figure 1.1.

Laminated composite materials are often made by stacking many thin layers, each generally called a lamina. A lamina is a macro unit of material whose properties are

determined through an appropriate experimental test. A desired strength and stiffness for a particular structural application such as bars, beams, plates and shells is obtained by stacking many lamina together resulting in a laminate construction. Each lamina may have a different thickness, elastic properties or fiber orientation.

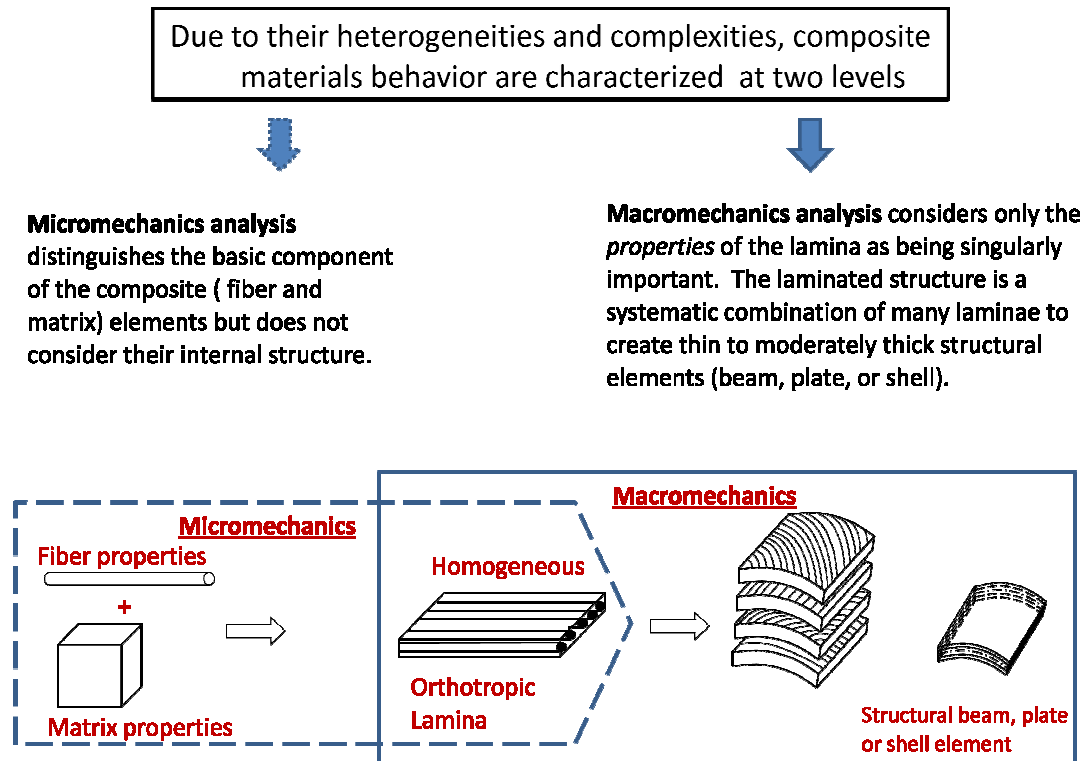


Figure 1. 1: Illustration of the two levels of characterizing composite laminated structures

1.2. Statement of the Problem

Multilayer composite materials continue to be widely used in the form of plate and shell-type structures for various industries such as pressure vessels and piping, transportation, construction, aerospace, nuclear and fossil power, chemical and petro-chemical. In structures such as fuel tanks, oxidizer tanks, motor cases, etc., composite materials are replacing the traditional metallic alloys. Their high strength, high stiffness,

light weight and high corrosion resistance give them an advantage over the traditional isotropic materials. Moreover, they offer to the designer a great deal of freedom in tailoring mechanical properties that suit the loading conditions and the geometric and environmental restrictions. Examples are helically wound cylinders which are common structures used in the pressure vessel and piping industry. Since many of these vessels work at high pressure, their safe design is of utmost importance. The regulatory authorities require designers to prove that the primary structure will sustain all the different failures modes that can cause extensive property damage, personal injury, environmental pollution, and even loss of life.

Usually, as illustrated in Figure 1.2, there are five methods available for the analysis of laminated composite plates and shells: namely, various structural lamination plate and shell theories, the numerical method of finite element analysis, failure theories to predict modes of failure and determine failure loads, and the experimental method. Although the latter is very important for establishing an assortment of data for acceptable analytical and numerical results comparison, and for proof testing, it is often materials and apparatus sensitive as well as being costly. Therefore, a variety of analytical methods that can provide consistently accurate results have been developed.

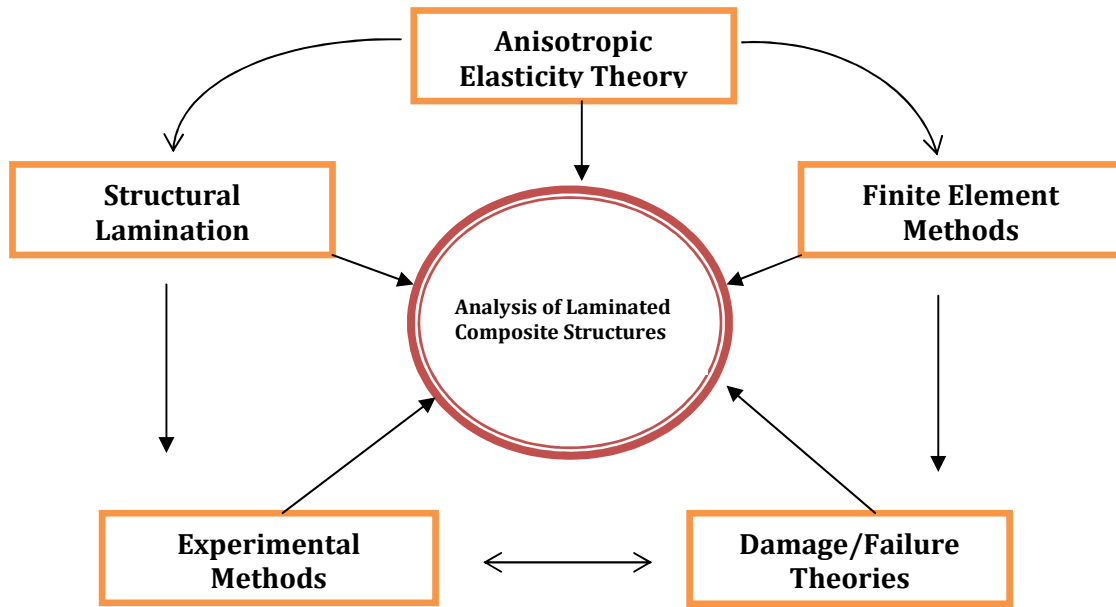


Figure 1. 2: Interconnection between the knowledge needed to analyze a laminated composite structure.

Many previous studies have been carried out on the stress and displacement analysis of composite plates and shells. These, however, yielded unsatisfactory results as far as the stress state (especially the transverse stresses) and failure predictions were concerned. This is mainly due to how the transverse shear deformation (TSD) was incorporated in the analysis. An important distinction between a composite structure and its isotropic counterpart is that transverse shear deformation plays a significant role in the structural behavior of the composite plate or shell. For isotropic thin plates and shells, the effect of TSD can often be neglected. However, it cannot be ignored for laminated composite structures, even for very thin ones. Also, the difference in material properties and geometry of each layer causes many coupling effects such as extension-bending, twisting-extension and twisting-bending, which complicate the analysis. That explains why there are many sophisticated approaches for analyzing composites plates and shells.

In this dissertation a finite element formulation based on a modified complementary energy principle is developed. One of the unique contributions of this study is the use of higher order strain functions in the variational principle to accomplish the finite element implementation. Examined also is whether the present formulation developed for laminated plates can also be applied to curved shell structures.

1.3. Review of Relevant Literature

1.3.1 Composite Laminated Plates

a) Exact Elasticity Solutions

The first publication on anisotropic plates may be attributed to Kaczkowski [2], followed by that of Ambartsumyan [3]. The latter published a book, “Theory of Anisotropic Plates”, which included an analysis of the transverse shear effect. The early papers on exact elasticity solutions for laminated composites structures are often credited to Pagano [4-6]. His first paper, published in 1969, provided exact elasticity solutions for semi-infinite cross-ply laminated strips. The next year, he studied the exact solution of rectangular bi-directional composite layered plates, and found out that the curvature of the transverse shear stresses at any point is discontinuous in its first derivative at the inter-layer boundary. He also demonstrated that the same curvature is a function of the thickness coordinate. Many other researchers such as Srinivas et al. [7-10], Jones [11], Lee [12,13], Whitney [14], Pagano and Hatfield [15], Noor [16], and Fan and Ye [17] have made a significant contribution in solving composite laminated plates by using the theory of elasticity. Recent studies include Kant et al. [18, 19], who proposed an elasticity solution for a cross-ply composite and sandwich laminate, and Teo and Liew [20] who

studied the three-dimensional elasticity behavior of some orthotropic structures. The paper by Civalek and Baltacioglu [21], investigated a three-dimensional elasticity solution for rectangular composite plates. The approach is based on the discrete singular convolution method. Their results show good agreement with the ones obtained by Srinivas, Kant and Teo. However, the smallest number of elements they used to obtain a 1% error is 343 ($7 \times 7 \times 7$). Also, the method appears to be a finite element type of approximation since they used meshed elements. Other 3-D elasticity studies can be found in [22-23].

b) Analytical Approaches

Very often, in-plane laminated composite structures are used in applications that entail both membrane and bending strengths. Many of these composite laminates can be studied by the use of plate theories. The textbook of Reddy [24] provides many details about the different theories that can be used to analyze laminated composite plates.

The common mode of failure of composite laminates are matrix or fiber cracking and delamination which are essentially three dimensional in nature, due primarily to transverse stresses. While classical plate lamination theory (CLT) is commonly used for simple analysis, it cannot handle the problem of shear deformation. Many alternate theories have therefore been proposed, such as the first order shear deformation theory (FSDT). Two other theories, namely the higher order shear deformation theory (HSDT) and the layerwise theories are also in use mostly to overcome the problem of the assumption of linear shear strain variation posed by the FSDT [25]. More details on this will be given in the next chapter. Considerable attention has been given to CLT (see Wang et al. [26] and [27-30]) which is derived from Kirchhoff plate theory as an

extension of Euler- Lagrange beam theory. The FSDT has also been extensively studied [31-34]. Some of the FSDT theories require shear correction factors [35-37] which are difficult to determine for any given laminated composite plate application. According to Reddy [2004], “the shear correction factor depends not only on the lamination and geometric parameters, but also on the loading and boundary conditions.” Higher-order plate theories (HSDT) used higher order polynomials in the expansion of the displacement components through the thickness of the laminate [38-41]. These higher order formulations introduce additional unknowns that are often difficult to interpret in physical terms. Complete derivations of the governing equations of the theories and some of their solutions are presented in the next Chapter.

c) Finite Element Methods

Solutions by use of analytical methods are available only for problems with simplified geometries, loads, boundary conditions and material orientation. Therefore, numerical methods like finite element analysis are practical substitute formulations to treat the more complicated problems. Considerable literature has been devoted to the finite element analysis of laminated composite plates [42-60]. However, their formulations differ widely from one another. Zhang and Yang [61] provide an extensive review on recent developments in this area. Finite element analysis methods are usually formulated using one of the three variational principles: namely, the minimum potential energy principle, the minimum complementary energy principle, and the modified complementary energy principle or mixed and hybrid formulations (see, for example, [62-64]). More details on each principle will be provided in Chapter 2.

The assumed displacement method based on the Minimum Potential Energy Principle has been the most studied of the variational principles and is the easiest to develop. There exists a vast amount of literature for this method (see, for example, [65]). As for the hybrid formulation that is the concern of the present study, there have also been a number of authors who have contributed to its development. Pian [66] pioneered the studies of the hybrid stress finite element theories. They are derived from the modified complementary energy statement, in which the requirements of inter-element traction compatibility and boundary traction compatibility are relaxed via the use of the Lagrange multiplier method. Pian [67-70] has continued to lead the research in the field of hybrid-stress finite element methods. It is worth mentioning that, in 1995, Pian [71] wrote an article in which he describes how hybrid and mixed finite element methods have evolved and how different versions of the variational functional have been utilized for the construction of more robust finite elements, especially for composite materials analysis. Mau et al. [72] used the hybrid stress method to formulate quadrilateral elements for the analysis of thick laminated plates. They used five nodal degrees of freedom, namely three displacements and two cross-sectional rotations for each individual layer. Their results for thick plates were good; however, the computational time was high. Spilker [73] also used the modified complementary finite element formulation to analyze composite laminates. He focused on the through-the-thickness distributions for both the stress and displacement components. His investigation was restricted to the cylindrical bending of cross-ply laminates. A comparison between his results and the elasticity solutions exhibited a good agreement. Since then, Spilker [74-76] has used the hybrid stress formulation to successfully develop additional elements. The majority of these elements

were implemented with an eight-node isoparametric formulation based on the plate bending elements developed by Spilker and Munir [77].

1.3.2 Laminated Composite Cylindrical Shells

a) Elasticity Theory and Analytical Methods

There is a vast amount of literature on the theoretical and numerical analysis of composite shells. Here, the focus is on laminated composite cylindrical shells. The first research on anisotropic cylindrical shells was reported in 1924 by Shtayerman [78]. Since then, considerable progress has been made in the analysis of such laminated shells. Most of the early publications were limited to predicting general response characteristics (vibrations frequencies, buckling loads, average through-the-thickness displacements and rotations) and employed the assumptions of classical thin shell theory. An adequate theory for this purpose is the Classical Lamination Theory [79, 80]. The roots of CLT for plates and shells can be found in the first works of Lekhnitskii [81-83]. However, the variation of material properties through the thickness direction associated with a laminated structure makes the Kirchhoff-Love hypotheses inappropriate for the study of moderately thin to thick walled composite structures.

The increased use of composites materials in such high-tech industries as aircraft and petro-chemical has enhanced the interest in a more accurate prediction of the detailed response characteristics during the design and analysis of laminated anisotropic cylindrical shells, especially when employed as pressure vessels. It is commonly admitted that when the diameter ratio (outside to inside) is larger than 1.1 the vessel should no longer be considered thin-walled [84]. Therefore, a design method based on three-dimensional stress-strain analysis is quite appropriate. Many authors [85-90][8-13] have

included the analysis of laminated cylindrical vessels in their investigation, but only a few have carried out a 3-D analysis.

Full-scale 3-D analyses of cylindrical laminated shells were developed starting in the 1980s [91-92]. The problem statement was uniquely formulated in terms of the equations of elasticity of a laminated anisotropic body (therefore this did not require any specifications, especially on the symmetry of the laminate). The research then shifted from developing analytical plate and shell theories to developing approximate numerical 3-D solutions for them [93,94]. In the second edition of his famous book, *Theory of Elasticity of an Anisotropic Body*, Lekhnitskii [82] studied the particular case of plane strain cylindrical structures. Roy and Tsai [92] extended the work of Lekhnitskii and proposed a simple and efficient design method for thick composite cylinders. Their analysis, based on cylinders in the state of generalized plane strain, can be used for both pipes and pressure vessels and was proven to be accurate and efficient [18]. Parnas and Katirci [95] studied the design of such pressure vessels under various loading conditions based on a linear elasticity solution of the thick-walled multi-layered filament-wound cylindrical shell.

The method of asymptotic expansion [96-98] can also be used to develop approximate shell theories to any order for anisotropic laminated media. Chung et al. [99] accomplished this via the method of asymptotic integration of the three-dimensional elasticity equations, while Logan et al. [100, 101] used this method in conjunction with Reissner's variational principle to derive these equations for composite cylindrical shells. Widera et al. [102] showed, for the problem of a layered tube under in plane loadings, that the asymptotic expansion approach, when compared with the elasticity solution,

results in approximate shell theories which converge uniformly for all thickness to radius ratios less than one.

b) Finite Element Analysis of Laminated Composite Cylindrical Shells

The finite element analysis of composite shell structures is still a great challenge for the research community. Numerous numerical approaches have been developed and Yang et al. provide an extensive review of them [103]. The most popular because of its simplicity and efficiency, and the one which is adopted in this investigation, is the solid shell degenerated approach. The earliest paper is attributed to Ahmad et al. [104]. Since then, significant contributions have been provided by Ramm [105], Hallquist et al. [106], and Liu et al. [107]. The shell degenerated elements are successful with structures not exhibiting enough warping as, for example, a cylindrical shell under internal pressure or uniformly loaded folded plates. To overcome this limit, degenerated shell elements with “drilling” degrees of freedom were proposed in the literature. A displacement-type modified variational formulation was developed and numerically assessed by Hughes et al. [108]. Flat shell elements are obtained by combining a plate bending element with a membrane element. At present, there still exists a considerable interest in using flat shell elements to model curved shells [109], mainly due to the simplicity of their formulation. Some authors have combined finite element methods with theoretical and experimental analysis to determine the burst pressure of cylindrical shells. The first-ply failure in composite pressure vessels was investigated by Chang [110] by using the acoustic emission technique. He obtained close results between finite element method (FEM) and experimental results. Mirza et al. [111] investigated composite vessels under concentrated moments applied at discrete lug positions by also using the finite element method. A

more recent study of the burst failure load of composite pressure vessels was carried out by Onder et al. [112]. They came to the conclusion that a FEM analysis using ANSYS was not sufficiently accurate in predicting the failure pressure, while their analytical method gave close results when compared to the experimental result. This remark was also made by Bogdanovich and Pastore [94]. They found that interlaminar stress predictions using the 3-D FEM ANSYS code were not accurate. Even after refining the mesh in the through-the thickness direction, the in-plane stress predictions were still not sufficiently accurate at the interfaces.

1.3.3 Failure Criteria in Composite Material Structures

As mentioned earlier, failure analysis is an important part of today's requirement in analyzing composite materials. Although not covered in the dissertation, a review of the state of the art is deemed important in order to complete the discussion on the necessity of needing an effective and accurate stress analysis of cylindrical composite shells.

The increase in the usage of composite structures means that factors such as reliability and durability are becoming more and more important. Many types of failure, such as fiber rupture, interfiber matrix cracking, delamination, etc., were taken into account in the pioneering work of Timoshenko [113], Tsai [114-119], Hashin [120-122] and Puck [123]. However, it emerged from an 'experts meeting' held at St. Albans (UK) in 1991 on the subject of 'Failure of Polymeric Composites and Structures: Mechanisms and Criteria for the Prediction of Performance' [124], that there is no universal definition of what constitutes 'failure' of a composite and that there is a lack of faith in the failure criteria in current use [125]. In 1992, following on that meeting, the participants launched

an international exercise to determine the accuracy of the current theories employed for predicting failure in composite laminates. This 'Failure Olympics' named "World Wide Failure Exercise" involved recognized experts in the area of fiber composite failure theories, including leading academics and developers of software/numerical codes. A summary of the methodologies employed in each theory, a direct comparison of the predictions made for each test case, and the overall predictive capabilities of the various theories when compared with the experimental results was presented in [126] and [127]. The World-Wide Failure Exercise evaluated 19 theoretical approaches for predicting the deformation and failure response of polymer composite laminates when subjected to 14 different test cases of complex states of stress. In 2004, they provided recommendations as to how the theories can be best utilized to provide safe and economic predictions in a wide range of engineering design applications [128]. The leading five theories were explored in great detail to demonstrate their strengths and weaknesses. It was shown that there still appeared some shortfalls in the theories, especially in predicting the final strength (burst failure) of composite material pressure vessels.

Many authors have integrated the analysis of burst failure prediction into their investigation. For example, Adali et al. [129] presented a method of optimizing multi-layered composite pressure vessels using an exact elasticity solution. A three-dimensional theory for anisotropic thick composite cylinders subjected to axisymmetrical loading conditions was derived. The three-dimensional interactive Tsai-Wu failure criterion was employed to predict the maximum burst pressure. The optimization analysis of these pressure vessels shows that the stacking sequence of the layers can be employed effectively for maximizing the burst pressure. Sun et al. [130] calculated the stresses and

the burst pressure of filament wound solid-rocket motor cases. The maximum stress failure criterion and a stiffness-degradation model were introduced in the failure analysis. Bakaiyan et al. [131] analyzed multi-layered filament-wound composite pipes under combined internal pressure and thermomechanical loading with thermal variations and then integrated Tsai-Hill failure criteria into the elasticity solution.

Many studies used the plain strain elasticity solution as developed by Lekniski [82] to develop a theoretical burst pressure expression for cylinders. Others have carried out the finite element analysis of laminated composites under internal pressure by using commercial software (ANSYS) and failure criteria. Very few of these studies, however, have questioned the accuracy of the so-determined stresses applied in the failure criteria. From the WWE [128] conclusions, there is still enough investigative work needed to improve the failure analysis of laminated composite structures. It is the belief here that this improvement needs to start with a more accurate stress analysis using an appropriate computational formulation. An accurate representation of the transverse shear deformation will play a significant role in the development of structural theories for the composite plates or shells. It is expected that this effect will vary a lot depending on the type of lamina material, boundary conditions, loading and stacking sequence.

1.4. Objective and Scope of Present Study

The intent of this study is to contribute to a more accurate as well as efficient displacement and stress analysis of laminated composite plates and shells by using specially developed finite elements to adequately represent the non-homogeneous, anisotropic nature of such laminated structures. The proposed analysis technique, although using a higher order formulation, does not increase the number of variables

associated with each layer. Moreover, the inclusion of a shear convergence parameter allows one to account for the disparities of loading, boundary conditions, layer thickness and material properties. A finite element formulation based on a modified complementary energy principle is used to develop the new elements. The second objective of this dissertation is to use the developed plate elements in a shell formulation to assess the stress and displacement analysis of shell structures.

The remainder of the current study is outlined as follows:

Chapter 2 provides a review of the theoretical basis composite of laminated plate and shell theories. It includes a summary of the main governing equations applicable to theories employed in the present investigation. Assessments of these theories are also presented.

Chapter 3 presents the new displacement field formulation with the shear convergence parameter integrated into a modified complementary energy principle. A detailed procedure is given for the derivation of the stiffness matrix.

Chapter 4 contains the plate and shell finite element formulations and their implementation within a numerical code written in Matlab. A detailed flowchart is provided and the coding process using Matlab is discussed.

Chapter 5 discusses the effectiveness of the new elements by studying plates and shells problems with different geometries, boundary conditions, and loading type. The relevance of the convergence parameter is also covered.

Chapter 6 summarizes the conclusions drawn from this investigation and presents future studies in terms of a discussion of the particular case of the stress analysis of laminated cylindrical shells under internal pressure.

CHAPTER 2

REVIEW OF COMPOSITE LAMINATED PLATE AND SHELL THEORIES

The goal of this Chapter is to present some of the important aspects about the theories of laminated plates and shell that will be employed during the course of this study. The development of the governing equations of these theories references an anisotropic linear elastic body, and can be carried out by use of the following basic principles:

- (1) Kinetics or conservation of momenta.
- (2) Kinematics or strain-displacements relations.
- (3) Principle of virtual work and its variants.
- (4) Constitutive equations or the stress-strain relations.

The equations resulting from these principles are supplemented by appropriate boundary and initial conditions from the problem statement. In the present study, a time non-dependent linear elastic deformation will be considered.

2.1. Anisotropic Linear Elasticity Theory

2.1.1 Kinematics or Strain-Displacements Relations.

Consider a loaded body as shown in Figure 2.1. The body experiences relative displacements and changes in geometry. Let $\{u\}$ be the displacement vector from an initial position to an actual position after deformation, with (u, v, w) as components with reference to the Cartesian coordinate system (x, y, z) . The strain analysis aims at quantifying all possible kinds of changes in the relative positions of the part of a deformed body. The engineering components of the strains are then given by:

$$\begin{aligned}\varepsilon_x(x, y, z) &= \frac{\partial u}{\partial x} \\ \varepsilon_y(x, y, z) &= \frac{\partial v}{\partial y} \\ \varepsilon_z(x, y, z) &= \frac{\partial w}{\partial z} \\ \gamma_{xy}(x, y, z) &= \frac{\partial u}{\partial y} + \frac{\partial v}{\partial x} \\ \gamma_{yz}(x, y, z) &= \frac{\partial v}{\partial z} + \frac{\partial w}{\partial y} \\ \gamma_{xz}(x, y, z) &= \frac{\partial u}{\partial z} + \frac{\partial w}{\partial x}\end{aligned}\tag{2.1}$$

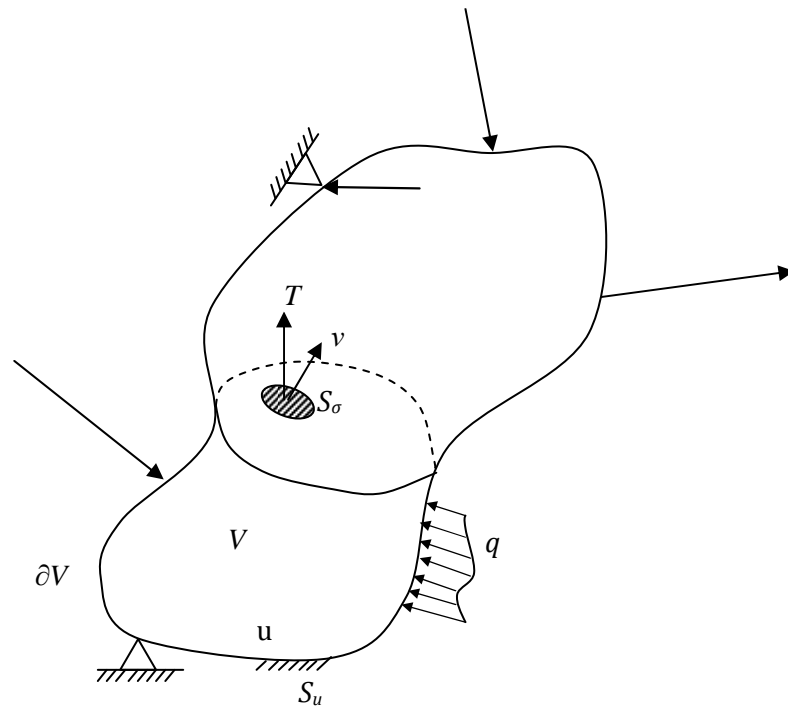


Figure 2. 1: Deformed body under external forces.

These equations define six different strain functions, three normal strains ($\varepsilon_x, \varepsilon_y, \varepsilon_z$) and three shear strains ($\gamma_{xy}, \gamma_{yz}, \gamma_{xz}$), which are expressed in terms of the three displacement vector components. It indicates that if displacement functions are specified, all six strain components will be determined thereby. Hence, the strain functions cannot be defined subjectively. However, if the strain components are specified, the following equations of compatibility are required to insure unique values of the displacement components, and thus have displacement continuity within the deformed body.

$$\begin{aligned}
 \frac{\partial^2 \varepsilon_x}{\partial y^2} + \frac{\partial^2 \varepsilon_y}{\partial x^2} &= \frac{\partial^2 \gamma_{xy}}{\partial x \partial y} \\
 \frac{\partial^2 \varepsilon_y}{\partial z^2} + \frac{\partial^2 \varepsilon_z}{\partial y^2} &= \frac{\partial^2 \gamma_{yz}}{\partial y \partial z} \\
 \frac{\partial^2 \varepsilon_z}{\partial x^2} + \frac{\partial^2 \varepsilon_x}{\partial z^2} &= \frac{\partial^2 \gamma_{xz}}{\partial x \partial z} \\
 \frac{\partial}{\partial z} \left(\frac{\partial \gamma_{yz}}{\partial x} + \frac{\partial \gamma_{xz}}{\partial y} - \frac{\partial \gamma_{xy}}{\partial z} \right) &= 2 \frac{\partial^2 \varepsilon_z}{\partial x \partial y} \\
 \frac{\partial}{\partial x} \left(\frac{\partial \gamma_{yz}}{\partial y} + \frac{\partial \gamma_{xy}}{\partial y} - \frac{\partial \gamma_{yz}}{\partial x} \right) &= 2 \frac{\partial^2 \varepsilon_x}{\partial y \partial z} \\
 \frac{\partial}{\partial y} \left(\frac{\partial \gamma_{yz}}{\partial z} + \frac{\partial \gamma_{yz}}{\partial x} - \frac{\partial \gamma_{xz}}{\partial y} \right) &= 2 \frac{\partial^2 \varepsilon_y}{\partial x \partial z}
 \end{aligned} \tag{2.2}$$

2.1.2 Kinetics or Equilibrium Equations.

Consider again the loaded body as shown in Figure 2.1. The applied loads induce internal forces in the body which can be grouped in two categories: body forces and surface forces. Figure 2.2 shows a three dimensional state of stress acting on an infinitesimal parallelepiped element of the body without body forces. The stresses acting on one face of the parallelepiped body are called traction stresses.

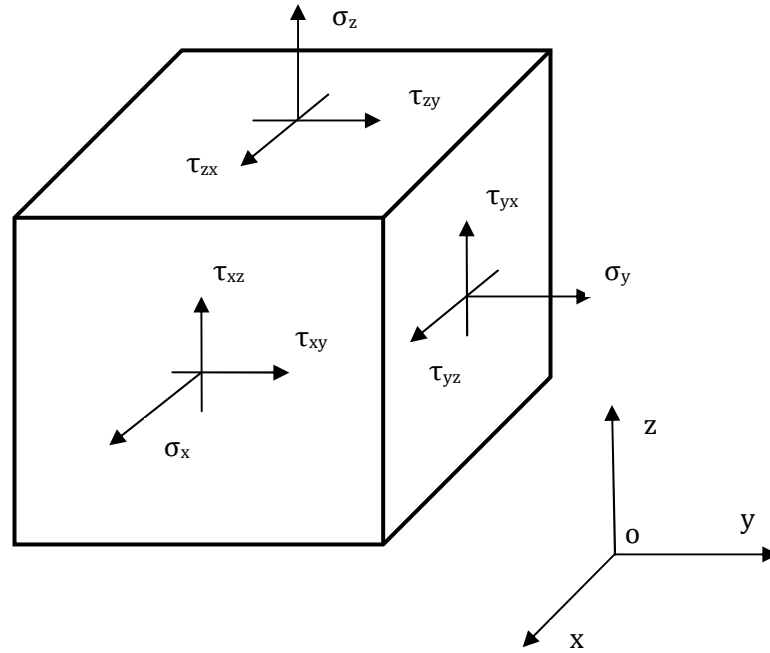


Figure 2. 2: 3-D state of stress acting on an infinitesimal parallelepiped element.

Assuming that there is an internal stress gradients throughout the body and that the stress components and their first derivatives are continuous, some differences will exist between the surface stresses (tractions) acting on the opposite sides of the parallelepiped. The equilibrium of the infinitesimal element including body forces components (F_x , F_y , F_z) can be expressed as

$$\begin{aligned}
 \frac{\partial \sigma_x}{\partial x} + \frac{\partial \tau_{xy}}{\partial y} + \frac{\partial \tau_{xz}}{\partial z} + F_x &= 0 \\
 \frac{\partial \tau_{xy}}{\partial x} + \frac{\partial \sigma_y}{\partial y} + \frac{\partial \tau_{yz}}{\partial z} + F_y &= 0 \\
 \frac{\partial \tau_{xz}}{\partial x} + \frac{\partial \tau_{yz}}{\partial y} + \frac{\partial \sigma_z}{\partial z} + F_z &= 0
 \end{aligned} \tag{2.3}$$

or using standard tensor notation,

$$\frac{\partial \sigma_{ji}}{\partial x_i} + F_i = 0 \quad (2.4)$$

where $i = 1, 2, 3$ and the summation over j is taken from 1 to 3.

2.1.3 Constitutive Equations

The relationship between the stress components and strain components depends on the material properties of the structure. In the case of a linear elastic anisotropic body, as considered in this study, the constitutive equations take the form of generalized Hooke's law and in Cartesian coordinates are expressed as:

$$\begin{aligned} \sigma_x &= C_{11} \varepsilon_x + C_{12} \varepsilon_y + C_{13} \varepsilon_z + C_{14} \gamma_{xy} + C_{15} \gamma_{yz} + C_{16} \gamma_{xz} \\ \sigma_y &= C_{21} \varepsilon_x + C_{22} \varepsilon_y + C_{23} \varepsilon_z + C_{24} \gamma_{xy} + C_{25} \gamma_{yz} + C_{26} \gamma_{xz} \\ \sigma_z &= C_{31} \varepsilon_x + C_{32} \varepsilon_y + C_{33} \varepsilon_z + C_{34} \gamma_{xy} + C_{35} \gamma_{yz} + C_{36} \gamma_{xz} \\ \tau_{xy} &= C_{41} \varepsilon_x + C_{42} \varepsilon_y + C_{43} \varepsilon_z + C_{44} \gamma_{xy} + C_{45} \gamma_{yz} + C_{46} \gamma_{xz} \\ \tau_{yz} &= C_{51} \varepsilon_x + C_{52} \varepsilon_y + C_{53} \varepsilon_z + C_{54} \gamma_{xy} + C_{55} \gamma_{yz} + C_{56} \gamma_{xz} \\ \tau_{xz} &= C_{61} \varepsilon_x + C_{62} \varepsilon_y + C_{63} \varepsilon_z + C_{64} \gamma_{xy} + C_{65} \gamma_{yz} + C_{66} \gamma_{xz} \end{aligned} \quad (2.5)$$

Note that the number of independent stiffness components C_{ij} is equal to 21 [132]. The stress-strain relations for a generally anisotropic linear elastic body can be expressed in matrix form as follows:

$$\{\sigma\} = [C] \{\varepsilon\} \quad (2.6)$$

or the strain - stress relations given by

$$\{\varepsilon\} = [S] \{\sigma\} \quad (2.7)$$

where

$$\begin{aligned}
\{\sigma\} &= \{\sigma_x, \sigma_y, \sigma_z, \tau_{xy}, \tau_{yz}, \tau_{xz}\}^T \\
\{\varepsilon\} &= \{\varepsilon_x, \varepsilon_y, \varepsilon_z, \gamma_{xy}, \gamma_{yz}, \gamma_{xz}\}^T \\
[C] &= \begin{bmatrix} C_{11} & C_{12} & C_{13} & C_{14} & C_{15} & C_{16} \\ & C_{22} & C_{23} & C_{24} & C_{25} & C_{26} \\ & & C_{33} & C_{34} & C_{35} & C_{36} \\ & & & C_{44} & C_{45} & C_{46} \\ & Sym & & & C_{55} & C_{56} \\ & & & & & C_{66} \end{bmatrix} \\
[S] &= \begin{bmatrix} S_{11} & S_{12} & S_{13} & S_{14} & S_{15} & S_{16} \\ & S_{22} & S_{23} & S_{24} & S_{25} & S_{26} \\ & & S_{33} & S_{34} & S_{35} & S_{36} \\ & & & S_{44} & S_{45} & S_{46} \\ & Sym & & & S_{55} & S_{56} \\ & & & & & S_{66} \end{bmatrix}
\end{aligned} \tag{2.8}$$

where $[C]$ and $[S]$ are the stiffness and compliance matrices, respectively.

All six stress components and six strain components have been considered with no restriction on the geometry, loading conditions or material properties. The strain-displacement relations (2.1), the equilibrium equations (2.3) and the stress-strain relations (2.6) constitute together with the prescribed boundary conditions, the conditions that must be satisfied by any anisotropic elastic body in equilibrium.

2.1.4 Mechanics of Orthotropic Lamina

a) Constitutive Equations in Material and Global Coordinates

Three important aspects are to be taken into account when modeling a laminated composite structure. First, since each lamina is considered a macroscopic homogeneous anisotropic body which possesses three planes of symmetry, the constitutive equations of

each lamina are orthotropic. Second, the constitutive equations depend on the kinematics assumptions of the theory used. Finally, material symmetry has to be added to the geometric and loading symmetry when considering the use of symmetry conditions in the analysis. For an orthotropic lamina, the stiffness matrix takes the form of

$$[C] = \begin{bmatrix} C_{11} & C_{12} & C_{13} & 0 & 0 & 0 \\ & C_{22} & C_{23} & 0 & 0 & 0 \\ & & C_{33} & 0 & 0 & 0 \\ & & & C_{44} & 0 & 0 \\ Sym & & & & C_{55} & 0 \\ & & & & & C_{66} \end{bmatrix} \quad (2.9)$$

In general, the uni-directional mechanical properties of one lamina are obtained experimentally. They are expressed in the material coordinate system (x_1, x_2, x_3) as E_i , G_{ij} , and ν_{ij} , with $i, j = 1, 2, 3$ and are, respectively, the elastic moduli, shear moduli and Poisson's ratios.

Consider that the material coordinate system is rotated about the global coordinate system (x, y, z) of an angle, α , as shown in Figure 2.3.

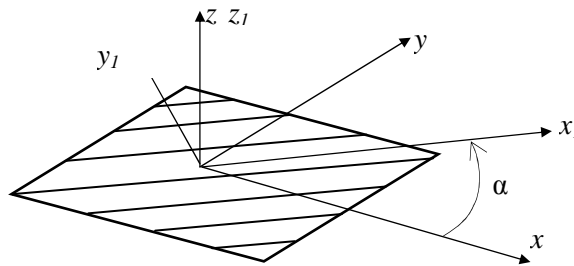


Figure 2.3: Illustration of material and global coordinate systems

Define l_i , m_i and n_i as the components of the direction cosines matrix such that

$$x_i = l_i x + m_i y + n_i z \quad (2.10)$$

with $i = 1, 2, 3$.

For orthotropic material, the compliance matrix in material coordinates system is given as

$$[S]_{mc} = \begin{bmatrix} \frac{1}{E_1} & \frac{-\nu_{21}}{E_2} & \frac{-\nu_{31}}{E_3} & 0 & 0 & 0 \\ & \frac{1}{E_2} & \frac{-\nu_{32}}{E_3} & 0 & 0 & 0 \\ & & \frac{1}{E_3} & 0 & 0 & 0 \\ & & & \frac{1}{G_{23}} & 0 & 0 \\ & \text{Sym} & & & \frac{1}{G_{13}} & 0 \\ & & & & & \frac{1}{G_{22}} \end{bmatrix} \quad (2.11)$$

while the stiffness matrix is defined by

$$[C]_{mc} = [S]_{mc}^{-1} \quad (2.12)$$

Consider the stress and strain components in material coordinates expressed as

$$\begin{aligned} \{\sigma\}_{mc} &= \{\sigma_1, \sigma_2, \sigma_3, \tau_{12}, \tau_{23}, \tau_{13}\}^T \\ \{\varepsilon\}_{mc} &= \{\varepsilon_1, \varepsilon_2, \varepsilon_3, \gamma_{12}, \gamma_{23}, \gamma_{13}\}^T \end{aligned} \quad (2.13)$$

The constitutive equation in material coordinates is then given as

$$\{\sigma\}_{mc} = [C]_{mc} \{\varepsilon\}_{mc} \quad (2.14)$$

The relationship between stress and strain components expressed in material coordinate system (Eq. (2.11)) to stress and strain components formulated in global coordinate system are stated in matrix form as [85]

$$\begin{aligned} \{\sigma\} &= [T] \{\sigma\}_{mc} \\ \{\varepsilon\} &= [T_e] \{\varepsilon\}_{mc} \end{aligned} \quad (2.15)$$

where

$$[T] = \begin{bmatrix} l_1^2 & l_2^2 & l_3^2 & 2l_1l_2 & 2l_1l_3 & 2l_2l_3 \\ m_1^2 & m_2^2 & m_3^2 & 2m_1m_2 & 2m_1m_3 & 2m_2m_3 \\ n_1^2 & n_2^2 & n_3^2 & 2n_1n_2 & 2n_1n_3 & 2n_2n_3 \\ l_1m_1 & l_2m_2 & l_3m_3 & l_1m_2 + l_2m_1 & l_1m_3 + l_3m_1 & l_2m_3 + l_3m_2 \\ l_1n_1 & l_2n_2 & l_3n_3 & l_1n_2 + l_2n_1 & l_1n_3 + l_3n_1 & l_2n_3 + l_3n_2 \\ m_1n_1 & m_2n_2 & m_3n_3 & m_1n_2 + m_2n_1 & m_1n_3 + m_3n_1 & m_2n_3 + m_3n_2 \end{bmatrix} \quad (2.16)$$

$$[T_e] = [T]^{-T}$$

Upon substituting using Eqs. (2.14) and (2.15b) in Eq. (2.6), the transformed constitutive equations are obtained as

$$\{\sigma\} = [T][C]_{mc}[T_e]^{-1}\{\varepsilon\} \quad (2.17)$$

with the stiffness matrix in global coordinates defines as

$$[C] = [T][C]_{mc}[T_e]^{-1} \quad (2.18)$$

In the three dimensional theory of a laminated composite, each layer is modeled as a 3-D body using Eqs. (2.2), (2.4) and (2.9). However, each set of governing equations is related to the lamina layer position and marked with a superscript (m). For example, the constitutive equation (2.9) becomes

$$\{\sigma\}^m = [C]^m\{\varepsilon\}^m \quad (2.19)$$

Assuming perfect bonding between layers, the interlayer boundary conditions in terms of stresses and/or displacements become important.

b) Displacement Continuity and Traction Free Conditions

The assumption of homogeneous anisotropic lamina (perfect bonded continuum) implies that a C^0 displacement continuity must be satisfied at every point within the lamina. On any free surface, there must be no stresses. For orthotropic laminated

structures loaded in bending, that means the transverse shear stresses at the top and the bottom of the surface are zero. It follows that at $z = \pm \frac{h}{2}$

$$\gamma_{yz}(x, y, z) = \frac{\partial v}{\partial z} + \frac{\partial w}{\partial y} = 0; \text{ and } \gamma_{xz}(x, y, z) = \frac{\partial u}{\partial z} + \frac{\partial w}{\partial x} = 0 \quad (2.20)$$

where h is the thickness of the structure.

The anisotropic linear elasticity theory (herein presented) is the reference theory because it has no assumptions on the geometry of deformation, and no restrictions on the type of loadings or boundary conditions. Subsequent theories are derived from this reference theory by transforming a three-dimensional formulation to a two-dimensional one.

An example of elasticity solution for orthotropic cylinder is given in Appendix A (it is a plane strain case).

2.2 Technical Theories – Analytical Approach

2.2.1 Classical Plate and Shell Theories

a) Plate and Shell Theory Assumptions

Here, a plate or a shell is an isotropic body or a homogeneous anisotropic (one lamina) elastic structure whose thickness is small compared to the span and width. It is loaded in such a way that bending deformation in addition to stretching are caused. The thickness coordinate is eliminated from the governing elasticity equations such that the 3D problem is reduced to a 2D case. The thickness thus becomes a known parameter that is provided. A plate can be considered as a particular case of shell with no initial curvatures. In many other cases, especially for FEA, a shell can often be modeled as an assembly of small plate elements.

Classical plate theory (CPT) is an extension of the Euler-Bernoulli beam theory to plates by Kirchhoff [3]. It is based on three kinematic assumptions (Figure 2.4) known as the *Kirchhoff hypothesis*. They are:

- (1) Straight lines normal to the plate mid-surface remain straight after deformation.
- (2) There is no change of elongation in the thickness direction; the thickness is inextensible.
- (3) Straight lines normal to the plate mid-surface rotate such that they remain perpendicular to the mid-surface after deformation.

The consequence of the inextensibility of the thickness is that the strain in the thickness direction is zero:

$$\varepsilon_z(x, y, z) = \frac{\partial w}{\partial z} = 0 \quad (2.21)$$

this suggests that the transverse displacement w is independent of the z -coordinate. By definition, the third hypothesis implies that there are no transverse shear strains:

$$\gamma_{yz}(x, y, z) = \frac{\partial v}{\partial z} + \frac{\partial w}{\partial y} = 0; \text{ and } \gamma_{xz}(x, y, z) = \frac{\partial u}{\partial z} + \frac{\partial w}{\partial x} = 0 \quad (2.22)$$

If the transverse shear strains are all zero, then according to Hooke's law the transverse shear stresses are also zero. This can not be because these shear stresses are needed for equilibrium. In order to accommodate this contradiction, one assumes that Hooke's law only holds for the in- plane quantities. It is also assumed that σ_z is negligible compared to σ_x and σ_y . Laminae elements parallel to the middle surface ($z = 0$) are thus assumed to be very nearly in a plane state of stress.

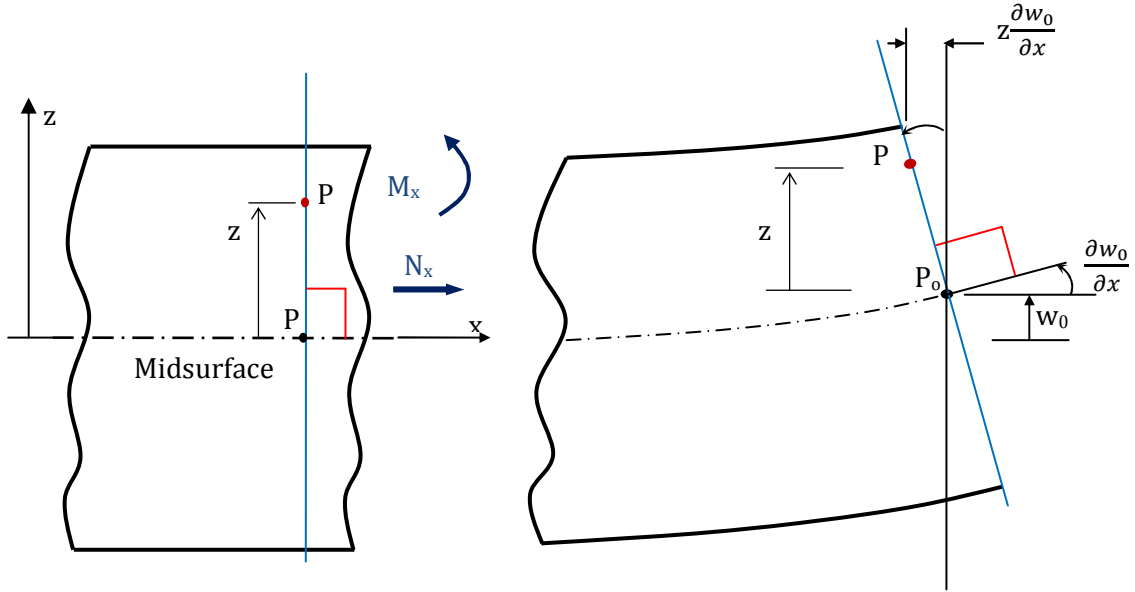


Figure 2. 4: Transverse displacement based on *Kirchhoff hypothesis*.

After integrating Eq. (2.22), Kirchhoff assumptions imply the following displacement field:

$$\begin{aligned} u(x, y, z) &= u_0(x, y) - z \frac{\partial w_0}{\partial x} \\ v(x, y, z) &= v_0(x, y) - z \frac{\partial w_0}{\partial y} \end{aligned} \quad (2.23)$$

$$w(x, y, z) = w_0(x, y)$$

where (u_0, v_0, w_0) are the displacement along the mid-surface of the plate (see Figure 2.4). Using the Eq. (2.23) in Eq. (2.2), the strain field is derived as

$$\begin{aligned} \varepsilon_x(x, y, z) &= \varepsilon_x^{(0)}(x, y) + z\varepsilon_x^{(1)}(x, y) \\ \varepsilon_y(x, y, z) &= \varepsilon_y^{(0)}(x, y) + z\varepsilon_y^{(1)}(x, y) \\ \gamma_{xy}(x, y, z) &= \gamma_{xy}^{(0)}(x, y) + z\gamma_{xy}^{(1)}(x, y) \end{aligned} \quad (2.24)$$

where

$$\begin{aligned}
\varepsilon_x^{(0)}(x, y) &= \frac{\partial u_0(x, y)}{\partial x}, & \varepsilon_x^{(1)} &= -\frac{\partial^2 w_0(x, y)}{\partial x^2} \\
\varepsilon_y^{(0)}(x, y) &= \frac{\partial v_0(x, y)}{\partial y}, & \varepsilon_y^{(1)}(x, y) &= -\frac{\partial^2 w_0(x, y)}{\partial y^2} \\
\gamma_{xy}^{(0)}(x, y) &= \frac{\partial u_0(x, y)}{\partial y} + \frac{\partial v_0(x, y)}{\partial x}, & \gamma_{xy}^{(1)}(x, y) &= -\frac{\partial^2 w_0(x, y)}{\partial x \partial y}
\end{aligned} \tag{2.25}$$

Notice that the *membrane strains* are $(\varepsilon_x^{(0)}, \varepsilon_y^{(0)}, \gamma_{xy}^{(0)})$ while the *bending strains* are given by $(\varepsilon_x^{(1)}, \varepsilon_y^{(1)}, \gamma_{xy}^{(1)})$.

b) Equilibrium Equations

When a transverse load q acts on the top surface of a plate as shown in Figure 2.5, it produces in plane stresses $\sigma_x, \sigma_y, \tau_{xy}$, and transverse stresses τ_{xz}, τ_{yz} . In classical plate theory, these stresses are replaced by their resultant forces acting at the middle surface of the plate. These are bending moments, M_x and M_y , twisting moment M_{xy} , shear force N_{xy} , transverse shear forces Q_x and Q_y and transverse normal forces N_x and N_y . These quantities are forces and moments per unit length (also called stress resultants). They are obtained by integration through the thickness and expressed as follows:

$$\begin{aligned}
N_x &= \int_{-\frac{h}{2}}^{\frac{h}{2}} \sigma_x dz, & N_y &= \int_{-\frac{h}{2}}^{\frac{h}{2}} \sigma_y dz, & N_{xy} &= \int_{-\frac{h}{2}}^{\frac{h}{2}} \sigma_{xy} dz, \\
Q_x &= \int_{-\frac{h}{2}}^{\frac{h}{2}} \tau_{xz} dz, & Q_y &= \int_{-\frac{h}{2}}^{\frac{h}{2}} \tau_{yz} dz \\
M_x &= \int_{-\frac{h}{2}}^{\frac{h}{2}} z \sigma_x dz, & M_y &= \int_{-\frac{h}{2}}^{\frac{h}{2}} z \sigma_y dz, & M_{xy} &= \int_{-\frac{h}{2}}^{\frac{h}{2}} z \sigma_{xy} dz
\end{aligned} \tag{2.26}$$

The equilibrium equations can be obtained either by considering the state of equilibrium for an infinitesimal element or by using the principle of virtual work. Details derivation can be found in many textbooks [24, 88]. The Euler-Lagrange equations of the principle of virtual displacement provide the equilibrium of an isotropic structure as

$$\begin{aligned}\frac{\partial N_x}{\partial x} + \frac{\partial N_{xy}}{\partial y} &= 0 \\ \frac{\partial N_{xy}}{\partial x} + \frac{\partial N_y}{\partial y} &= 0 \\ \frac{\partial^2 M_x}{\partial x^2} + \frac{\partial^2 M_y}{\partial y^2} + 2 \frac{\partial^2 M_{xy}}{\partial x \partial y} + q &= 0\end{aligned}\tag{2.27}$$

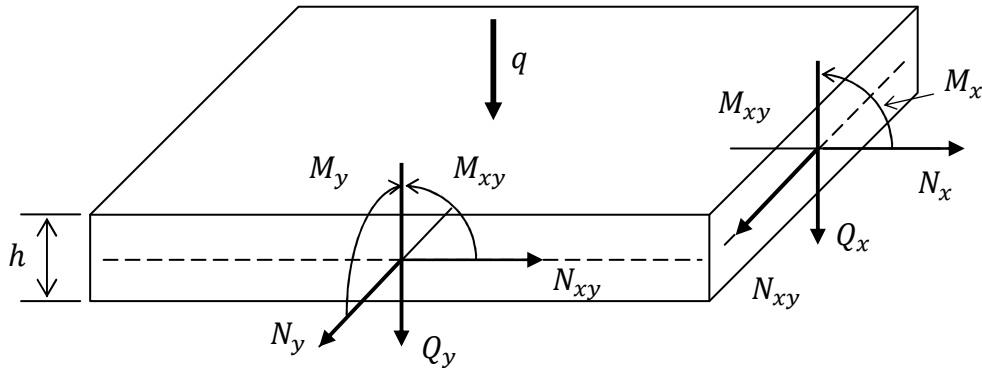


Figure 2. 5: Force and moment resultants acting on an element plate or shell.

b) Constitutive Equations

The constitutive equations for classical isotropic plate theory are the two dimensional version of the generalized constitutive equation (2.4) applied to isotropic homogeneous plates or shells in which ε_z , γ_{yz} and γ_{xz} are all zero. The constitutive equations in matrix form are given as

$$\begin{Bmatrix} \sigma_x \\ \sigma_y \\ \tau_{xy} \end{Bmatrix} = \begin{bmatrix} \frac{E}{1-\nu^2} & \frac{E\nu}{1-\nu^2} & 0 \\ \frac{E\nu}{1-\nu^2} & \frac{E}{1-\nu^2} & 0 \\ 0 & 0 & G \end{bmatrix} \begin{Bmatrix} \varepsilon_x \\ \varepsilon_y \\ \varepsilon_{xy} \end{Bmatrix} \quad (2.28)$$

where, E , G , and ν are the Young modulus, the shear modulus and Poisson ratio respectively.

Substituting the strain displacement relation (Eq. (2.23)) into Eq. (2.26c), the expressions for the bending and twisting moments in terms of displacements are given as

$$\begin{aligned} M_x &= -D \left(\frac{\partial^2 w}{\partial x^2} + \nu \frac{\partial^2 w}{\partial y^2} \right) \\ M_y &= -D \left(\nu \frac{\partial^2 w}{\partial x^2} + \frac{\partial^2 w}{\partial y^2} \right) \\ M_{xy} &= -D(1-\nu) \frac{\partial^2 w}{\partial x \partial y} \end{aligned} \quad (2.29)$$

where D is the flexural rigidity of the plate defined as

$$D = \frac{Eh^3}{12(1-\nu^2)} \quad (2.30)$$

Upon substituting Eq. (2.29) into Eq. (2.27) the governing differential equation for deflection of thin plates and shells are derived as

$$\frac{\partial^4 w}{\partial x^4} + 2 \frac{\partial^2 w}{\partial x^2 \partial y^2} + \frac{\partial^4 w}{\partial y^4} = \frac{q}{D} \quad (2.31)$$

which can be written in a concise form as

$$\nabla^2 \nabla^2 w = \frac{q}{D} \quad (2.32)$$

where

$$\nabla^2 = \frac{\partial^2}{\partial x^2} + \frac{\partial^2}{\partial y^2} \quad (2.33)$$

is the Laplace operator.

c) Solution Methods

It is often difficult to find a solution for the governing equation (2.32), except for problems having a simple geometry and loading conditions. Very often, what is called the “inverse method” is used to attempt a solution. The method consists of assuming solutions for displacements which satisfy both the governing equation and the boundary conditions. This method can provide “exact” solutions for simple problems, and one can then use these solutions as the basis for approximation methods for the analysis of more complex configurations. For example, Timoshenko and Young [107] present the solutions for a square plate with two boundary conditions, namely simply supported and clamped edges. Their solutions will be used for comparison in the course of this study.

2.2.2 Classical Lamination Plate and Shell Theories

a) Displacement and Strain Fields

The classical lamination plate theory (CLT) first developed by Reissner and Stavsky [27] is simply an extension of the classical plate theory from the previous section, but applied to a multi-layered composite plate. It differs from the elasticity laminated theory in the assumptions made about the transverse deformation. While the elasticity theory considers an independent rotation of each layer, the CLT reduces all the layers to an equivalent single layer in terms of geometry of deformation (Figure 2.6) and material properties (equivalent stiffness and compliance properties, also known as

Equivalent Single Layer (ESL) theory). The assumptions imply that the transverse strains (normal and shear) are all neglected.

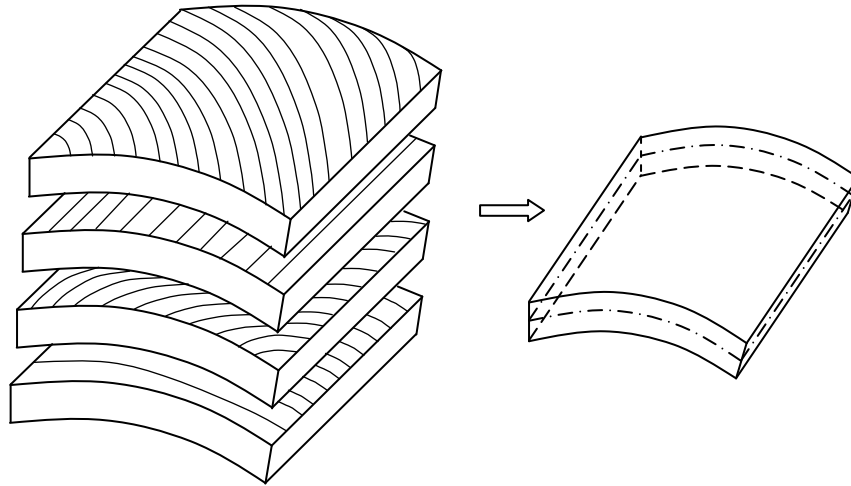


Figure 2. 6. Equivalent single layer laminated composite structure

b) State of Stress

The displacement and strain fields expression are identical to Eqs (2.23) and (2.25). However, the orthotropic properties of the laminates induce another consequence for the state of stress. The transverse shear stresses are neglected like in isotropic materials. The problem is that composite materials have a very low shear modulus ($G < E/10$), and many failures are due to transverse deformation especially for moderately thick to thick plates. The first order shear deformation theory tries to remediate this drawback.

c) *Governing Equations*

The Euler-Lagrange equations (equilibrium) are the same as Eq. (2.27).

The constitutive equations are similar to the one of CPT (equation (2.26)) with the difference that the integration is performed for each lamina, since the material properties vary through the thickness. The force and moment resultants are given as

$$\begin{aligned}
 N_x &= \sum_{m=1}^{NL} \int_{Z_m}^{Z_{m+1}} \sigma_x dz, & N_y &= \sum_{m=1}^{NL} \int_{Z_m}^{Z_{m+1}} \sigma_y dz, \\
 N_{xy} &= \sum_{m=1}^{NL} \int_{Z_m}^{Z_{m+1}} \sigma_{xy} dz, \\
 M_x &= \sum_{m=1}^{NL} \int_{Z_m}^{Z_{m+1}} z \sigma_x dz, & M_y &= \sum_{m=1}^{NL} \int_{Z_m}^{Z_{m+1}} z \sigma_y dz, \\
 M_{xy} &= \sum_{m=1}^{NL} \int_{Z_m}^{Z_{m+1}} z \sigma_{xy} dz
 \end{aligned} \tag{2.34}$$

Using the 2-D form of Eq. (2.5) and the strain expression of Eq. (2.24) in Eq. (2.34), the force and moment resultants in global coordinates and matrix form become:

$$\begin{aligned}
 \begin{Bmatrix} N_x \\ N_y \\ N_{xy} \end{Bmatrix} &= \sum_{m=1}^{NL} \int_{Z_m}^{Z_{m+1}} \begin{bmatrix} \bar{Q}_{11} & \bar{Q}_{12} & \bar{Q}_{16} \\ \bar{Q}_{21} & \bar{Q}_{22} & \bar{Q}_{26} \\ \bar{Q}_{16} & \bar{Q}_{26} & \bar{Q}_{66} \end{bmatrix}^m \begin{Bmatrix} \varepsilon_x^{(0)} + z\varepsilon_x^{(1)} \\ \varepsilon_y^{(0)} + z\varepsilon_y^{(1)} \\ \varepsilon_{xy}^{(0)} + z\varepsilon_{xy}^{(1)} \end{Bmatrix} dz \\
 \begin{Bmatrix} M_x \\ M_y \\ M_{xy} \end{Bmatrix} &= \sum_{m=1}^{NL} \int_{Z_m}^{Z_{m+1}} z \begin{bmatrix} \bar{Q}_{11} & \bar{Q}_{12} & \bar{Q}_{16} \\ \bar{Q}_{21} & \bar{Q}_{22} & \bar{Q}_{26} \\ \bar{Q}_{16} & \bar{Q}_{26} & \bar{Q}_{66} \end{bmatrix}^m \begin{Bmatrix} \varepsilon_x^{(0)} + z\varepsilon_x^{(1)} \\ \varepsilon_y^{(0)} + z\varepsilon_y^{(1)} \\ \varepsilon_{xy}^{(0)} + z\varepsilon_{xy}^{(1)} \end{Bmatrix} dz
 \end{aligned} \tag{2.35}$$

where \bar{Q}_{ij} are the lamina stiffness coefficients.

Define the extensional stiffness components as

$$A_{ij} = \int_{-\frac{h}{2}}^{\frac{h}{2}} \bar{Q}_{ij} dz = \sum_{m=1}^{NL} \int_{z_m}^{z_{m+1}} \bar{Q}_{ij} dz = \sum_{m=1}^{NL} \bar{Q}_{ij}^m (z_{m+1} - z_m) \quad (2.36)$$

the bending stiffness components

$$B_{ij} = \frac{1}{2} \sum_{m=1}^{NL} \bar{Q}_{ij}^m (z_{m+1}^2 - z_m^2) \quad (2.37)$$

and the bending-extensional coupling stiffness components as

$$D_{ij} = \frac{1}{3} \sum_{m=1}^{NL} \bar{Q}_{ij}^m (z_{m+1}^3 - z_m^3) \quad (2.38)$$

The laminate constitutive equations are then expressed as

$$\begin{Bmatrix} N_x \\ N_y \\ N_{xy} \end{Bmatrix} = \begin{bmatrix} A_{11} & A_{12} & A_{16} \\ A_{12} & A_{22} & A_{26} \\ A_{16} & A_{26} & A_{66} \end{bmatrix} \begin{Bmatrix} \varepsilon_x^{(0)} \\ \varepsilon_y^{(0)} \\ \varepsilon_{xy}^{(0)} \end{Bmatrix} + \begin{bmatrix} B_{11} & B_{12} & B_{16} \\ B_{12} & B_{22} & B_{26} \\ B_{16} & B_{26} & B_{66} \end{bmatrix} \begin{Bmatrix} \varepsilon_x^{(1)} \\ \varepsilon_y^{(1)} \\ \varepsilon_{xy}^{(1)} \end{Bmatrix} \quad (2.39)$$

$$\begin{Bmatrix} M_x \\ M_y \\ M_{xy} \end{Bmatrix} = \begin{bmatrix} B_{11} & B_{12} & B_{16} \\ B_{12} & B_{22} & B_{26} \\ B_{16} & B_{26} & B_{66} \end{bmatrix} \begin{Bmatrix} \varepsilon_x^{(0)} \\ \varepsilon_y^{(0)} \\ \varepsilon_{xy}^{(0)} \end{Bmatrix} + \begin{bmatrix} D_{11} & D_{12} & D_{16} \\ D_{12} & D_{22} & D_{26} \\ D_{16} & D_{26} & D_{66} \end{bmatrix} \begin{Bmatrix} \varepsilon_x^{(1)} \\ \varepsilon_y^{(1)} \\ \varepsilon_{xy}^{(1)} \end{Bmatrix} \quad (2.40)$$

Using a compact form notation, Eqs. (2.39) and (2.40) can be presented as

$$\begin{Bmatrix} \{N\} \\ \{M\} \end{Bmatrix} = \begin{bmatrix} [A] & [B] \\ [B] & [D] \end{bmatrix} \begin{Bmatrix} \{\varepsilon_0\} \\ \{\varepsilon_1\} \end{Bmatrix} \quad (2.41)$$

where $\{\varepsilon_0\}$ and $\{\varepsilon_1\}$ are defined in Eq. (2.25).

The governing equations are obtained in terms of displacements (u_0 , v_0 , w_0) by substituting only the in-plane components of the strain-displacement equations (2.1) into the laminate constitutive equations (2.39) and (2.40),

$$\begin{aligned}
& A_{11} \frac{\partial^2 u_0}{\partial x^2} + A_{12} \frac{\partial^2 v_0}{\partial x \partial y} + A_{16} \left(\frac{\partial^2 u_0}{\partial x \partial y} + \frac{\partial^2 v_0}{\partial x^2} \right) - B_{11} \frac{\partial^3 w_0}{\partial x^3} \\
& - B_{12} \frac{\partial^3 w_0}{\partial x \partial y^2} - 2B_{16} \frac{\partial^3 w_0}{\partial y \partial x^2} + A_{16} \frac{\partial^2 u_0}{\partial x \partial y} + A_{26} \frac{\partial^2 v_0}{\partial y^2} \\
& + A_{66} \left(\frac{\partial^2 u_0}{\partial y^2} + \frac{\partial^2 v_0}{\partial x \partial y} \right) - B_{26} \frac{\partial^3 w_0}{\partial y^3} - B_{16} \frac{\partial^3 w_0}{\partial x^2 \partial y} + 2B_{66} \frac{\partial^3 w_0}{\partial x \partial y^2} \\
& = 0
\end{aligned} \tag{2.42}$$

$$\begin{aligned}
& A_{16} \frac{\partial^2 u_0}{\partial x^2} + A_{26} \frac{\partial^2 v_0}{\partial x \partial y} + A_{66} \left(\frac{\partial^2 u_0}{\partial x \partial y} + \frac{\partial^2 v_0}{\partial x^2} \right) - B_{16} \frac{\partial^3 w_0}{\partial x^3} \\
& - B_{66} \frac{\partial^3 w_0}{\partial x \partial y^2} - 2B_{66} \frac{\partial^3 w_0}{\partial y \partial x^2} + A_{12} \frac{\partial^2 u_0}{\partial x \partial y} + A_{22} \frac{\partial^2 v_0}{\partial y^2} \\
& + A_{26} \left(\frac{\partial^2 u_0}{\partial y^2} + \frac{\partial^2 v_0}{\partial x \partial y} \right) - B_{22} \frac{\partial^3 w_0}{\partial y^3} - B_{12} \frac{\partial^3 w_0}{\partial x^2 \partial y} - 2B_{26} \frac{\partial^3 w_0}{\partial x \partial y^2} \\
& = 0
\end{aligned} \tag{2.43}$$

$$\begin{aligned}
& B_{11} \frac{\partial^3 u_0}{\partial x^3} + B_{12} \frac{\partial^3 v_0}{\partial y \partial x^2} + B_{16} \left(\frac{\partial^3 u_0}{\partial x^2 \partial y} + \frac{\partial^3 w_0}{\partial x^3} \right) - D_{11} \frac{\partial^4 w_0}{\partial x^4} - D_{12} \frac{\partial^4 w_0}{\partial x^2 \partial y^2} \\
& - 2D_{16} \frac{\partial^4 w_0}{\partial x^3 \partial y} - 2B_{16} \frac{\partial^3 u_0}{\partial x^2 \partial y} + 2B_{26} \frac{\partial^3 v_0}{\partial x \partial y^2} \\
& + 2B_{66} \left(\frac{\partial^3 v_0}{\partial y \partial x^2} + \frac{\partial^3 w_0}{\partial x \partial y^2} \right) - 2D_{16} \frac{\partial^4 w_0}{\partial x^3 \partial y} - 4D_{26} \frac{\partial^4 w_0}{\partial x \partial y^3} \\
& - 4D_{66} \frac{\partial^4 w_0}{\partial x^2 \partial y^2} + B_{12} \frac{\partial^3 u_0}{\partial x \partial y^2} + B_{22} \frac{\partial^3 v_0}{\partial y^3} + B_{26} \frac{\partial^3 v_0}{\partial y \partial x^2} \\
& + B_{26} \left(\frac{\partial^3 v_0}{\partial y^2 \partial x} + \frac{\partial^3 u_0}{\partial y^3} \right) - D_{12} \frac{\partial^4 w_0}{\partial x^2 \partial y^2} - D_{22} \frac{\partial^4 w_0}{\partial y^4}
\end{aligned} \tag{2.44}$$

e) Analytical Solution

A solution of these equations for orthotropic composite laminated structures with simply supported boundary conditions and using Navier type method can be found in [24] and is made used of in Chapter 5. The Navier method is explained in Section 2.2.3.

d) Tractions Continuity or Interface Boundary Conditions

As stated before, these governing equations are very often solved exactly through the inverse method using simple problems. However, all solutions must integrate the interface boundary conditions as a consequence of the assumption of perfect bonding between laminae. Equilibrium conditions require that the traction components must be continuous across any surface. Figure 2.7 illustrates the stress continuity on two surfaces (imaginatively separated).

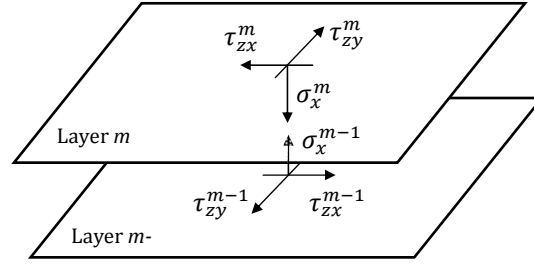


Figure 2. 7: Interlayer traction continuity conditions

In terms of equations they are expressed at the interface where $z = h_m$ as

$$\begin{aligned}\sigma_{xz}^m &= \sigma_{xz}^{m-1}, \\ \sigma_{yz}^m &= \sigma_{yz}^{m-1}, \\ \sigma_z^m &= \sigma_z^{m-1}\end{aligned}\tag{2.45}$$

These conditions will be entirely satisfied in the first and third order formulation of the present work.

2.2.3 First Order Deformation Theory

a) Displacement and Strain Fields

Reissner [133] and Mindlin [134] proposed a refined classical laminated theory which includes the effect of transverse shear deformation, known as First Order Shear Deformation Theory (FSDT). The new kinematic assumption is that the straight lines normal to the midplane remain straight but not normal after deformation (Figure 2.5). Therefore, the displacement field becomes

$$\begin{aligned}
 u(x, y, z) &= u_0(x, y) - z\psi_x(x, y) \\
 v(x, y, z) &= v_0(x, y) - z\psi_y(x, y) \\
 w(x, y, z) &= w_0(x, y)
 \end{aligned}
 \tag{2.46}$$

where $(u_0, v_0, w_0, \psi_x, \psi_y)$ are the *generalized displacements* which are to be determined. They dependent only on the in-plane coordinates (x, y) .

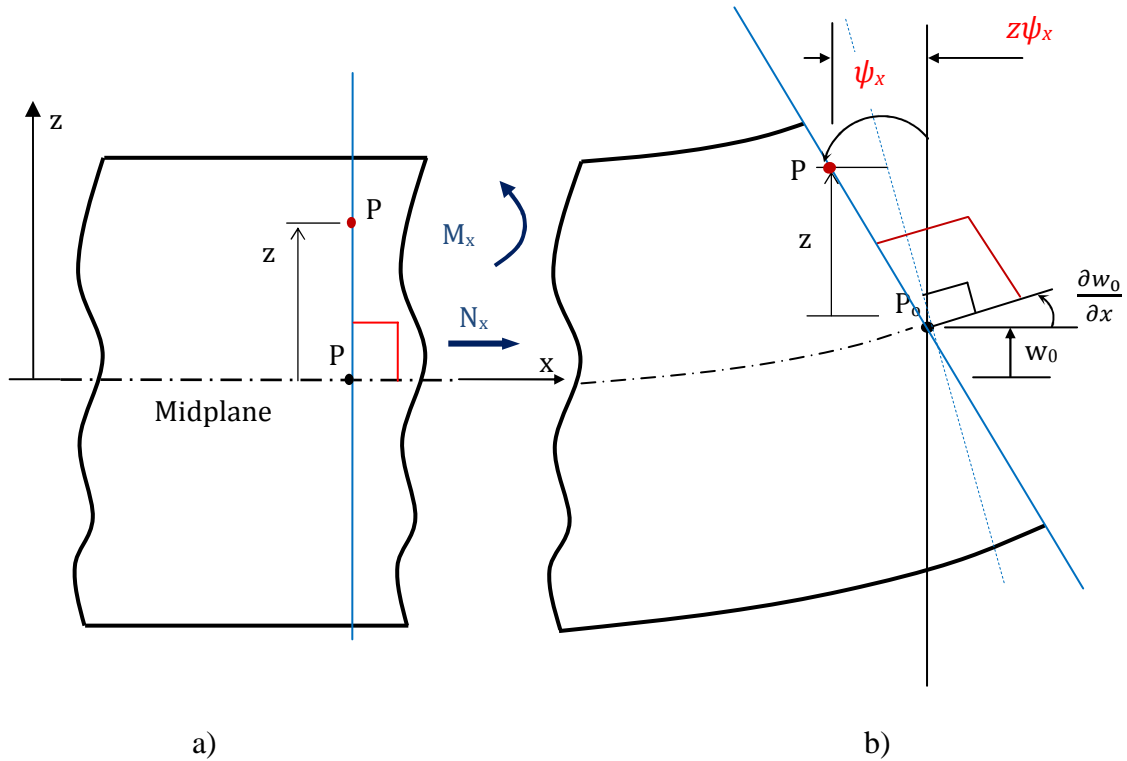


Figure 2. 8: Illustration of the first order shear deformation theory. a) Undeformed geometry, b) Deformed geometry.

The strains are obtained by substituting Eq. (2.33) into Eq. (2.2):

$$\begin{aligned}
 \varepsilon_x(x, y, z) &= \varepsilon_x^{(0)}(x, y) + z\varepsilon_x^{(1)}(x, y) \\
 \varepsilon_y(x, y, z) &= \varepsilon_y^{(0)}(x, y) + z\varepsilon_y^{(1)}(x, y) \\
 \gamma_{xy}(x, y, z) &= \gamma_{xy}^{(0)}(x, y) + z\gamma_{xy}^{(1)}(x, y)
 \end{aligned}
 \tag{2.47}$$

$$\gamma_{yz}(x, y, z) = \gamma_{yz}^{(0)}(x, y)$$

$$\gamma_{xz}(x, y, z) = \gamma_{xz}^{(0)}(x, y)$$

$$\varepsilon_z(x, y, z) = 0$$

where

$$\begin{aligned} \varepsilon_x^{(0)}(x, y) &= \frac{\partial u_0(x, y)}{\partial x}, & \varepsilon_x^{(1)} &= -\frac{\partial \psi_x(x, y)}{\partial x} \\ \varepsilon_y^{(0)}(x, y) &= \frac{\partial v_0(x, y)}{\partial y}, & \varepsilon_y^{(1)}(x, y) &= -\frac{\partial \psi_y(x, y)}{\partial y} \\ \gamma_{xy}^{(0)}(x, y) &= \frac{\partial u_0(x, y)}{\partial y} + \frac{\partial v_0(x, y)}{\partial x}, & \gamma_{xy}^{(1)}(x, y) &= \frac{\partial \psi_x(x, y)}{\partial y} + \frac{\partial \psi_y(x, y)}{\partial x} \\ \gamma_{yz}^{(0)}(x, y) &= \frac{\partial w_0(x, y)}{\partial y} + \psi_y(x, y) \\ \gamma_{xz}^{(0)}(x, y) &= \frac{\partial w_0(x, y)}{\partial x} + \psi_x(x, y) \end{aligned} \quad (2.48)$$

It can be noticed that the transverse shear strains (γ_{yz}, γ_{xz}) are constant through the laminate thickness. So will also be the transverse shear stresses. However, it is established from the elementary theory of homogeneous beams that the transverse shear stress has a quadratic variation in the thickness direction. For laminated composite plates and shells, the transverse shear stresses should have at least a quadratic variation. To remedy this, a shear correction factor is used in computing the transverse force resultants. It is obtained by equating the strain energy due to the FSDT transverse shear stresses to the strain energy due to the true transverse stresses predicted by the three-dimensional elasticity theory. Modified complementary energy formulations, in general, do not require the use of such a correction factor.

Many of the FSDT theories are successful in predicting the transverse deflections, natural frequencies and buckling loads (see Yang et al. [135]), but they do not adequately predict the interlaminar stresses. Therefore, higher order theories which account for the variation in the transverse shear deformation are necessary.

b) Governing Equations

The process of deriving the governing equations for the first order shear deformation theory is very similar to the one developed in the previous Sections for CPT and CLT. The Euler-Lagrange equations (equilibrium) are similar Eq. (2.27) but augmented by the transverse force resultants Q_x and Q_y defined as

$$Q_x = C_f \int_{-\frac{h}{2}}^{\frac{h}{2}} \sigma_{xz} dz, \quad Q_y = C_f \int_{-\frac{h}{2}}^{\frac{h}{2}} \sigma_{yz} dz \quad (2.49)$$

where C_f is the shear correction factor.

The final expression of the Euler-Lagrange equations are given as

$$\begin{aligned} \frac{\partial N_x}{\partial x} + \frac{\partial N_{xy}}{\partial y} &= 0 \\ \frac{\partial N_{xy}}{\partial x} + \frac{\partial N_y}{\partial y} &= 0 \\ \frac{\partial Q_x}{\partial x} + \frac{\partial Q_y}{\partial y} &= -q \\ \frac{\partial M_x}{\partial x} + \frac{\partial M_{xy}}{\partial y} &= Q_x \\ \frac{\partial M_{xy}}{\partial x} + \frac{\partial M_y}{\partial y} &= Q_y \end{aligned} \quad (2.50)$$

The transverse forces are also added to the CLT constitutive equations so that the constitutive equations for FSDT are

$$\begin{Bmatrix} N_x \\ N_y \\ N_{xy} \end{Bmatrix} = \begin{bmatrix} A_{11} & A_{12} & A_{16} \\ A_{12} & A_{22} & A_{26} \\ A_{16} & A_{26} & A_{66} \end{bmatrix} \begin{Bmatrix} \varepsilon_x^{(0)} \\ \varepsilon_y^{(0)} \\ \varepsilon_{xy}^{(0)} \end{Bmatrix} + \begin{bmatrix} B_{11} & B_{12} & B_{16} \\ B_{12} & B_{22} & B_{26} \\ B_{16} & B_{26} & B_{66} \end{bmatrix} \begin{Bmatrix} \varepsilon_x^{(1)} \\ \varepsilon_y^{(1)} \\ \varepsilon_{xy}^{(1)} \end{Bmatrix} \quad (2.51)$$

$$\begin{Bmatrix} M_x \\ M_y \\ M_{xy} \end{Bmatrix} = \begin{bmatrix} B_{11} & B_{12} & B_{16} \\ B_{12} & B_{22} & B_{26} \\ B_{16} & B_{26} & B_{66} \end{bmatrix} \begin{Bmatrix} \varepsilon_x^{(0)} \\ \varepsilon_y^{(0)} \\ \varepsilon_{xy}^{(0)} \end{Bmatrix} + \begin{bmatrix} D_{11} & D_{12} & D_{16} \\ D_{12} & D_{22} & D_{26} \\ D_{16} & D_{26} & D_{66} \end{bmatrix} \begin{Bmatrix} \varepsilon_x^{(1)} \\ \varepsilon_y^{(1)} \\ \varepsilon_{xy}^{(1)} \end{Bmatrix} \quad (2.52)$$

augmented with

$$\begin{Bmatrix} Q_x \\ Q_y \end{Bmatrix} = \begin{bmatrix} A_{44} & A_{45} \\ A_{45} & A_{55} \end{bmatrix} \begin{Bmatrix} \gamma_{xz}^{(0)} \\ \gamma_{yz}^{(0)} \end{Bmatrix} \quad (2.53)$$

The equilibrium equations (2.50) in terms of generalized displacements (u_0 , v_0 , w_0 , ψ_x , ψ_y) are obtained by substituting the strain-displacement relations, Eq. (2.47), into Eq. (2.52). The final expressions are given as

$$\begin{aligned} & A_{11} \frac{\partial^2 u_0}{\partial x^2} + A_{12} \frac{\partial^2 v_0}{\partial x \partial y} + A_{16} \left(\frac{\partial^2 u_0}{\partial x \partial y} + \frac{\partial^2 v_0}{\partial x^2} \right) + B_{11} \frac{\partial^2 \psi_x}{\partial x^2} \\ & + B_{12} \frac{\partial^2 \psi_y}{\partial x \partial y} + 2B_{16} \left(\frac{\partial^2 \psi_x}{\partial x \partial y} + \frac{\partial^2 \psi_y}{\partial x^2} \right) + A_{16} \frac{\partial^2 u_0}{\partial x \partial y} + A_{26} \frac{\partial^2 v_0}{\partial y^2} \\ & + A_{66} \left(\frac{\partial^2 u_0}{\partial y^2} + \frac{\partial^2 v_0}{\partial x \partial y} \right) + B_{26} \frac{\partial^2 \psi_y}{\partial x \partial y} + B_{66} \left(\frac{\partial^2 \psi_y}{\partial x \partial y} + \frac{\partial^2 \psi_x}{\partial y^2} \right) = 0 \end{aligned} \quad (2.54)$$

$$\begin{aligned}
& A_{16} \frac{\partial^2 u_0}{\partial x^2} + A_{26} \frac{\partial^2 v_0}{\partial x \partial y} + A_{66} \left(\frac{\partial^2 u_0}{\partial x \partial y} + \frac{\partial^2 v_0}{\partial x^2} \right) + B_{16} \frac{\partial^2 \psi_x}{\partial x^2} \\
& + B_{26} \frac{\partial^2 \psi_y}{\partial x \partial y} + B_{66} \left(\frac{\partial^2 \psi_x}{\partial x \partial y} + \frac{\partial^2 \psi_y}{\partial x^2} \right) + A_{12} \frac{\partial^2 u_0}{\partial x \partial y} + A_{22} \frac{\partial^2 v_0}{\partial y^2} \\
& + A_{26} \left(\frac{\partial^2 u_0}{\partial y^2} + \frac{\partial^2 v_0}{\partial x \partial y} \right) \\
& + B_{12} \frac{\partial^2 \psi_x}{\partial x \partial y} + B_{22} \frac{\partial^2 \psi_x}{\partial y^2} + B_{26} \left(\frac{\partial^2 \psi_y}{\partial x \partial y} + \frac{\partial^2 \psi_x}{\partial y^2} \right) = 0
\end{aligned} \tag{2.55}$$

$$\begin{aligned}
& C_f A_{55} \left(\frac{\partial^2 w_0}{\partial x^2} + \frac{\partial \psi_x}{\partial x} \right) + C_f A_{55} \left(\frac{\partial^2 w_0}{\partial x \partial y} + \frac{\partial \psi_y}{\partial x} \right) + C_f A_{45} \left(\frac{\partial^2 w_0}{\partial x \partial y} + \frac{\partial \psi_x}{\partial y} \right) \\
& + C_f A_{44} \left(\frac{\partial^2 w_0}{\partial y^2} + \frac{\partial \psi_y}{\partial y} \right) = 0
\end{aligned} \tag{2.56}$$

$$\begin{aligned}
& B_{11} \frac{\partial^2 u_0}{\partial x^2} + B_{12} \frac{\partial^2 v_0}{\partial y \partial x} + B_{16} \frac{\partial^2 u_0}{\partial x \partial y} + D_{11} \frac{\partial^2 \psi_x}{\partial x^2} + D_{12} \frac{\partial^2 \psi_y}{\partial x \partial y} \\
& + D_{16} \left(\frac{\partial^2 \psi_x}{\partial x \partial y} + \frac{\partial^2 \psi_y}{\partial x^2} \right) + B_{16} \frac{\partial^2 u_0}{\partial x \partial y} + B_{26} \frac{\partial^2 u_0}{\partial y^2} \\
& + B_{66} \left(\frac{\partial^2 v_0}{\partial y \partial x} + \frac{\partial^2 u_0}{\partial y^2} \right) + D_{16} \frac{\partial^2 \psi_x}{\partial x \partial y} + D_{26} \frac{\partial^2 \psi_y}{\partial y^2} \\
& + D_{66} \left(\frac{\partial^2 \psi_y}{\partial x \partial y} + \frac{\partial^2 \psi_x}{\partial y^2} \right) - C_f A_{55} \left(\frac{\partial w_0}{\partial x} + \psi_x \right) \\
& - C_f A_{45} \left(\frac{\partial w_0}{\partial y} + \psi_y \right) = 0
\end{aligned} \tag{2.57}$$

$$\begin{aligned}
& B_{16} \frac{\partial^2 u_0}{\partial x^2} + B_{26} \frac{\partial^2 v_0}{\partial y \partial x} + B_{66} \frac{\partial^2 u_0}{\partial x \partial y} + D_{16} \frac{\partial^2 \psi_x}{\partial x^2} + D_{26} \frac{\partial^2 \psi_y}{\partial x \partial y} \\
& + D_{66} \left(\frac{\partial^2 \psi_x}{\partial x \partial y} + \frac{\partial^2 \psi_y}{\partial x^2} \right) + B_{12} \frac{\partial^2 u_0}{\partial x \partial y} + B_{22} \frac{\partial^2 u_0}{\partial y^2} \\
& + B_{26} \left(\frac{\partial^2 v_0}{\partial y \partial x} + \frac{\partial^2 u_0}{\partial y^2} \right) + D_{12} \frac{\partial^2 \psi_x}{\partial x \partial y} + D_{22} \frac{\partial^2 \psi_y}{\partial y^2} \\
& + D_{26} \left(\frac{\partial^2 \psi_y}{\partial x \partial y} + \frac{\partial^2 \psi_x}{\partial y^2} \right) - C_f A_{45} \left(\frac{\partial w_0}{\partial x} + \psi_x \right) \\
& - C_f A_{44} \left(\frac{\partial w_0}{\partial y} + \psi_y \right) = 0
\end{aligned} \tag{2.58}$$

Once the displacements are found, the stresses and strains can be computed through the strain-displacement relations and the constitutive equations.

c) Analytical Solutions

An exact solution for linear partial differential equations (2.53)-(2.58) is cumbersome. For some particular geometry, boundary and loading conditions, analytical solutions are developed, such as Navier or Levy type solutions for a simply supported rectangular plate loaded in bending only. If the plate is considered as specially orthotropic, the bending-stretching terms B_{ij} and the bending-twisting terms (D_{16}, D_{26}) are all neglected. Therefore, the governing equations (2.44) become

$$D_{11} \frac{\partial^4 w_0}{\partial x^4} + 2(D_{12} + 2D_{66}) \frac{\partial^4 w_0}{\partial x^2 \partial y^2} + D_{22} \frac{\partial^4 w_0}{\partial y^4} = -q \tag{2.59}$$

A Navier solution for the above equation is considered when the four edges of the plate are simply supported while a Levy type solution is developed when two opposite edges are simply supported and the two others are a combination of free, simple support or fixed boundary conditions (Figure 2.5). The Navier technique consist of finding a solution function which satisfies the boundary conditions such as a double trigonometric series in terms of unknown parameters in the form

$$w_0(x, y) = \sum_{k=1}^{\infty} \sum_{l=1}^{\infty} W_{kl} \sin\left(\frac{k\pi x}{a}\right) \sin\left(\frac{l\pi y}{b}\right) \quad (2.60)$$

where W_{kl} are coefficients to be determined.

The load is also expanded in double trigonometric series function as

$$q(x, y) = \sum_{k=1}^{\infty} \sum_{l=1}^{\infty} Q_{kl} \sin\left(\frac{k\pi x}{a}\right) \sin\left(\frac{l\pi y}{b}\right) \quad (2.61)$$

Substituting Eqs (2.60) and (2.61) into Eq. (2.59) yields

$$\sum_{k=1}^{\infty} \sum_{l=1}^{\infty} \{-W_{kl}[D_{11}d^4 + 2(D_{12} + 2D_{66})d^2f^2 + D_{22}f^4] + Q_{kl}\} \sin dx \sin fy = 0 \quad (2.62)$$

where $d=k\pi x/a$, and $f=l\pi y/a$. Solving for W_{kl} for any x and y, the solution is then given as

$$w_0(x, y) = \sum_{k=1}^{\infty} \sum_{l=1}^{\infty} \frac{Q_{kl}}{R_m} \sin\left(\frac{k\pi x}{a}\right) \sin\left(\frac{l\pi y}{b}\right) \quad (2.63)$$

where

$$R_m = \frac{b^2 \pi^4}{a^2 b^4} \left[D_{11} \frac{b^2}{a^2} k^4 + 2(D_{12} + 2D_{66})k^2 l^2 + D_{22} l^4 \right] \quad (2.64)$$

This example is also used for comparison later on.

2.2.3 Higher Order Deformation Theories (HSDT)

a) Displacement Assumptions

Higher order theories refer to the order of the displacement expression in terms of the z-coordinate. HSDT can represent the kinematics better than the CLT and FSDT.

They do not require shear correction factors and they yield more accurate interlaminar stress distributions [24]. In order to avoid using shear correction factors, the displacement field can be expanded up to any desired order. However, due to algebraic complexity and computational time involved in HSDT, theories higher than third order have not been attempted.

A very limited number of second order-theories has been proposed, the most important being

- (i) Essenburg [136], who proposed a theory based on the following displacement fields:

$$\begin{aligned} u &= u_0 + z\psi_x \\ v &= v_0 + z\psi_y \end{aligned} \quad (2.65)$$

$$w = w_0 + z\psi_z + z^2\varphi_z$$

- (ii) Whitney and Sun [137],

$$\begin{aligned} u &= u_0 + z\psi_x + z^2\varphi_x \\ v &= v_0 + z\psi_y + z^2\varphi_y \end{aligned} \quad (2.66)$$

$$w = w_0 + z\psi_z$$

(iii) and Nelson and Lorch [138]

$$\begin{aligned} u &= u_0 + z\psi_x + z^2\varphi_x \\ v &= v_0 + z\psi_y + z^2\varphi_y \\ w &= w_0 + z\psi_z + z^2\varphi_z \end{aligned} \quad (2.67)$$

where ψ_z , and φ_y are dependent on the midplane coordinates.

Since the present study deals with a Third Order Shear Deformation Theory (TSDT), a brief account of earlier significant TSDTs will be provided in the following.

The earliest TSDT is attributed to Reissner [139]. He used a displacement field in the form of

$$\begin{aligned} u &= z\psi_x + z^3\vartheta_x \\ v &= z\psi_y + z^3\vartheta_y \\ w &= w_0 + z^2\varphi_z \end{aligned} \quad (2.68)$$

The midsurface deformation is neglected. Reissner demonstrated that this theory, applied to the bending of a plate with a circular hole, gives very accurate results when compared with the elasticity solution.

Reissner's theory was extended by Lo et al. [140,141] to include the effects of the midsurface and out-of-plane deformations. The formulation is based on

$$\begin{aligned} u &= u_0 + z\psi_x + z^2\varphi_x + z^3\vartheta_x \\ v &= v_0 + z\psi_y + z^2\varphi_y + z^3\vartheta_y \\ w &= w_0 + z\psi_z + z^2\varphi_z \end{aligned} \quad (2.69)$$

They investigated a simply supported thick isotropic and laminated plate subjected to cylindrical bending. The governing equations were obtained from the principle of minimum potential energy.

Later on, a new class of third order shear deformation theories began to flourish in the literature [40, 41, 142-144] with the displacement field very similar to that given by Eq. (2. 21). The main difference is that the effect of normal strain is neglected by assuming a constant transverse displacement w_0 through the thickness direction. The advantage of this new formalations is that by satisfying the condition of zero transverse shear stresses on the top and bottom surfaces of the plate or shell, the number of dependent unknowns can be successfully reduced to the same number as for the FSDT, without using any shear correction factors. The displacements are given in the following form

$$\begin{aligned} u &= u_0 + z \left[\psi_x - \frac{4}{3} \left(\frac{z}{h} \right)^2 \left(\psi_x + \frac{\partial w}{\partial x} \right) \right] \\ v &= v_0 + z \left[\psi_y - \frac{4}{3} \left(\frac{z}{h} \right)^2 \left(\psi_y + \frac{\partial w}{\partial y} \right) \right] \\ w &= w_0 \end{aligned} \tag{2.70}$$

where h is the thickness of the laminate.

b) Governing Equations - Constitutive Equations

Many authors derived the governing equations in terms of displacements. The procedure is similar to the one developed in the previous Section. Also, there are many different types of displacement fields. Reddy [41] proposed an analytical solution for his TSDT based on Eq. (2.22). However, he used the variational principle of virtual displacements to develop the governing equations. Analytical solutions are limited to

simple cases. For complex problems, the FEM is needed to provide excellent approximate numerical solutions.

c) Analytical Solutions

A TSDT solution of an anti-symmetric cross-ply laminated composite plate, with simply supported boundary conditions, was obtained by Reddy [24] using a Navier solution technique as presented in the previous section. Reddy's solution will be made use of in Chapter 5.

2.3 Technical Theories – Finite Element Approach (Via Variational Principle)

The objective of this section is to give a brief overview of the finite element formulation of the FSDT and HSDT of laminated composite plate and shell structures. These theories can be classified into displacement formulation, mixed formulation and hybrid stress or strain models.

2.3.1 Principal of Minimum Potential Energy.

The principle of minimum potential energy is a displacement based method. It is also a particular case of the Principle of Virtual Displacement applied to linear elastic bodies, since they exhibit an elastic potential energy. There is a significant volume of writings related to the use of this variational method to elasticity problems. Pryor and Barker [42] developed a displacement finite element based on the FSDT to analyze thick laminated composite plates. They used a rectangular four-node element with seven degrees of freedom per node. The transverse stresses in each lamina are derived by integrating the local differential equilibrium equation, Eq. (2.4). With a restriction on the loading condition (applied load should not caused severe warping of the cross section),

their transverse stresses were in good agreement with those of the elasticity solutions. Panda and Natarajan [145] improved the results of Pryor and Barker by using an eight-node quadrilateral plate element with only five degrees of freedom. However, when thickness to length ration is larger than 0.1 (moderately thick), the accuracy of the results is diminished. Pandya and Kant [146] also used the principle of minimum potential energy to investigate a TSDT plate element. They used a nine-node Lagrange isoparametric plate bending element with six degree of freedom per node (two transverse rotations, one transverse displacement, and three unknown displacement terms). The formulation and example analysis were limited only to symmetrical laminates. Their results were in good agreement with those of the exact elasticity solution.

Details of the derivation of the formulation of the Principle of Minimum Potential Energy can be found in recent textbooks written by Wunderlich and Pilkey [147], and by Cook [148]. Here, we present only a summary of the procedure, since it is part of the modified complementary energy principle (MCEP) formulation. To formulate this principle, let's consider again the loaded body of Figure 2.1., in which some of the portion of the body surface, ∂V , has prescribed displacements \bar{u} – denoted by S_u – while the other portion, S_σ , is where the tractions \bar{T} are prescribed. Here, ν is the direction cosine of the normal to the boundary. The strain energy is expressed in terms of strain vector $\{\varepsilon\}$. The principal of minimum potential energy can then be stated [149] in the form of minimizing the following potential energy functional:

$$\Pi_p(u) = \int_V \frac{1}{2} \{\varepsilon\}^T [C] \{\varepsilon\} dV - \int_{S_\sigma} \{\bar{T}\}^T \{u\} dS = Min. \quad (2.71)$$

where $[C]$ is the elastic stiffness matrix, $\{\varepsilon\}$ is the strain vector, and $\{u\}$, the boundary displacement.

In the assumed displacement approach, the displacements are the only field variables, and must be continuous within the domain. Therefore, the stresses, which are very important for moderately thick to thick laminated composite plates and shells, are not directly determined. Afshari demonstrated in his dissertation [150] that the assumed displacement method was not accurate for composite thin plates.

2.3.2 Principle of Minimum Complementary Energy

The principle of minimum complementary energy is the “dual” form of the principle of minimum potential energy in which the strains are expressed in terms of stresses and the equilibrium conditions for the stresses and the prescribed tractions along the element boundary are satisfied. The only field variable are the stresses and the complementary energy principle can be stated as [68]

$$\Pi_c(\sigma) = \int_V \frac{1}{2} \{\sigma\}^T [S] \{\sigma\} dV - \int_{S_u} \{T\}^T \{\bar{u}\} dS = Min. \quad (2.72)$$

Here, S_u refers to portion of the boundary ∂V over which the surface displacement $\{\bar{u}\}$ are prescribed (Figure 2.1).

The assembly of these functions for stresses $\{\sigma\}$ may be taken as admissible functions for this functional if they satisfy the following requirements; i) they are continuous, single-valued and satisfy equilibrium equation within the body, and ii) they satisfy the equilibrium conditions on the boundaries. There are very few accounts of the finite element analysis of laminated composite plates and shells using the principle of

minimum complementary energy. The reason is that they are less accurate compared to those from the original mixed-formulation by the Hellinger-Reissner principle [71].

2.3.3 Mixed Formulation

The expression *mixed* methods is applied to the finite element formulations in which the resulting matrix equations consist of more than one set of field variables. They are also called modified variational principles, and are obtained by including the constraint conditions in the functional through the application of the Lagrange multiplier method [151]. For instance, by using the stresses as Lagrange multipliers to relax the constraining strain-displacement relation ($\{\varepsilon\} = [B]\{u\}$), Washizu [151] obtained a three-field variational principle as

$$\begin{aligned} \Pi_{KW}(\varepsilon, \sigma, u) = & \int_V \left[\frac{1}{2} \{\varepsilon\}^T [C] \{\varepsilon\} - \{\sigma\}^T (\{\varepsilon\} - [B]\{u\}) \right] dV - \int_{S_\sigma} \{\bar{T}\}^T \{u\} dS \\ & - \int_{S_u} \{\bar{T}\}^T (\{u\} - \{\bar{u}\}) dS = \text{Stationary} \end{aligned} \quad (2.73)$$

where S_σ is the portion over which the surface tractions are prescribed.

By using the constitutive relations to replace the strain expressions in Eq. (2.32), the two-field original Hellinger-Reissner principle is derived as

$$\begin{aligned} \Pi_{HR}(\sigma, u) = & \int_V \left[-\frac{1}{2} \{\sigma\}^T [S] \{\sigma\} - \{\sigma\}^T ([B]\{u\}) \right] dV - \int_{S_\sigma} \{\bar{T}\}^T \{u\} dS \\ & - \int_{S_u} \{\bar{T}\}^T (\{u\} - \{\bar{u}\}) dS = \text{Stationary} \end{aligned} \quad (2.74)$$

The entire domain is discretized into finite elements which are summed up to obtain the variational principles. There are many papers on mixed formulations and Felippa [152] gives a very good review of their further development as well as applications.

For laminated composites, of all these variational principles, the conventional assumed displacement model is still by far the simplest scheme if an appropriate interpolation function can be constructed that will satisfy the inter-laminar compatibility conditions. These conditions can be easily satisfied for problems such as plane elasticity, axisymmetric solids, and three-dimensional solids for which the continuity of the normal derivatives along the inter-element boundaries is not required.

However, when conditions of transverse displacement and independent cross-sectional rotation are imposed, the assumed displacement method (and assumed force method) exhibits some shortcomings. Since each method is a unique field variable principle (either displacement or stress) the variables must satisfy either the compatibility or the equilibrium equations. The assumed displacement method, most of the time, leads to unnecessary stiffness (locking). To overcome this shortcoming, the mixed and hybrid formulation are used, since they allow for independent fields within an element and for a boundary element (e.g., equilibrium within the element and displacement continuity along the boundaries [153]). K. J. William demonstrated that hybrid and mixed formulation methods perform better than the assumed displacement method [154].

In the case of thick composite plates and shells, the determination of transverse stresses is necessary in order to perform an adequate failure analysis of these laminated structures. The assumed displacement method does not predict these stresses accurately

[155]. On the other hand, a hybrid method, based on the Modified Complementary Energy Principle, is capable of predicting these stresses by satisfying equilibrium and the inter-laminar transverse stress continuity conditions. The assumed stress model first developed by Pian [66, 67] and Spilker [74-77] has been shown to perform well where transverse stresses are to be determined. The next Chapter will present a strain-based hybrid type method which will have the advantage of predicting both stresses and displacements accurately.

CHAPTER 3

STRAIN-BASED MODIFIED COMPLEMENTARY ENERGY PRINCIPLE

There are different types of modified complementary energy principles. This Chapter focused on a higher order strain-based formulation. Compared to other formulations, it does not use displacement functions of a third order (Section 2.3.3) but rather uses a third order strain formulation (which is new) to formulate a solution for the analysis of composite laminates by use of finite element methods. The first section will present the general concept of how the complementary energy principle is modified through the Lagrange multiplier method to obtain a so called modified complementary energy principle. The second section will describe the process of obtaining the stiffness matrix and the last section will present what is original in the proposed formulation.

3.1 General Element Formulation

In order to weigh the equilibrium and compatibility conditions more equally, Reissner [27, 96, and 97] formulated an alternative principle in which both the stresses and strains are the admitted variables. The modified complementary energy principle is derived from Reissner's principle and is obtained by extending the complementary energy with the addition of the global (integral) form of the static boundary conditions:

- i) along an element boundary S (Figure 3.1a), where the boundary tractions are prescribed,

$$T - \bar{T} = 0 \quad (3.1)$$

- ii) along the inter-element boundary S_{ab} (Figure 3.1b) between two elements a and b ,

$$T^a - T^b = 0 \quad (3.2)$$

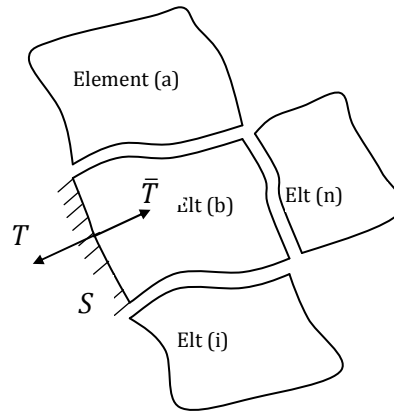


Figure 3.1a. Prescribed traction on an element boundary S

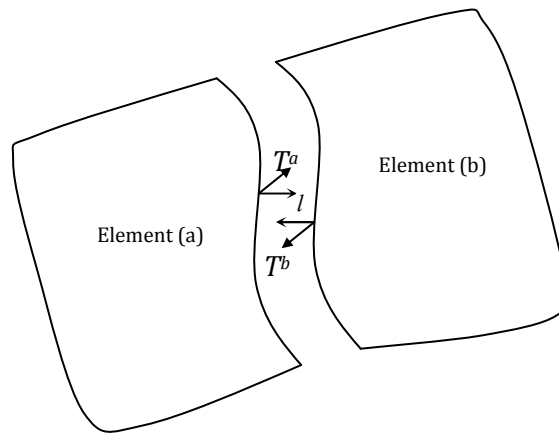


Figure 3.1b. Two continuous elements with boundary equilibrium

Figure 3. 1: Prescribed traction and boundary equilibrium on an element boundary

With the aid of the boundary displacements, $\{u\}$, as Lagrange multipliers defined on S_{ab} , the principle can be expressed as

$$\prod_{mc} = \prod_c - \sum G_{ab} \quad (3.3)$$

where

$$G_{ab} = \iint_{S_{ab}} \{u\}^T (\{T\}^a + \{T\}^b) dS \quad (3.4)$$

Thus, the requirement i) above is relaxed in the variational equation and the functions for stresses in each element may be selected independently without concern for inter-element stress continuity requirements.

For the whole body, the modified complementary function may be rewritten as

[74]

$$\prod_{mc} = \sum_n \left(\int_{V_n} \frac{1}{2} \{\sigma\}^T [S] \{\sigma\} dV - \int_{\partial V_n} \{T\}^T \{u\} dS + \int_{S_{\sigma n}} \{\bar{T}\}^T \{u\} dS \right) \quad (3.5)$$

where $[S]$ is the compliance matrix, $\{\sigma\}$ is the stress matrix, $\{u\}$ is the boundary displacement; ∂V_n is the n th element boundary which includes the inter-element boundary, S_{ab} ; S_{un} , the portion over which the surface displacement are prescribed, and $S_{\sigma n}$, the portion over which the surface tractions are prescribed. As noted earlier, the component of the element boundary traction $\{T\}$ is related to the stress components by

$$\{T\} = \{l\}^T \{\sigma\} \quad (3.6)$$

In Eq. (3,5), the independent quantities subjected to variations are $\{\sigma\}$ and $\{u\}$. It is thus seen that the present functional has the stresses within the elements and the displacements along the element boundaries as the field variables.

3.2 Definition of the Functional for a Multilayered Plate or Shell Element.

The multilayered plate or shell is assumed to lie in the (x, y) plane within the local coordinate system. The laminate reference surface ($z = 0$) is located arbitrarily at the geometric mid-surface. The laminate consists of N perfectly bounded layers numbered bottom to top, with $z = h_1, h_2, \dots, h_m, \dots, h_{N+1}$ (see Figure 3.2).

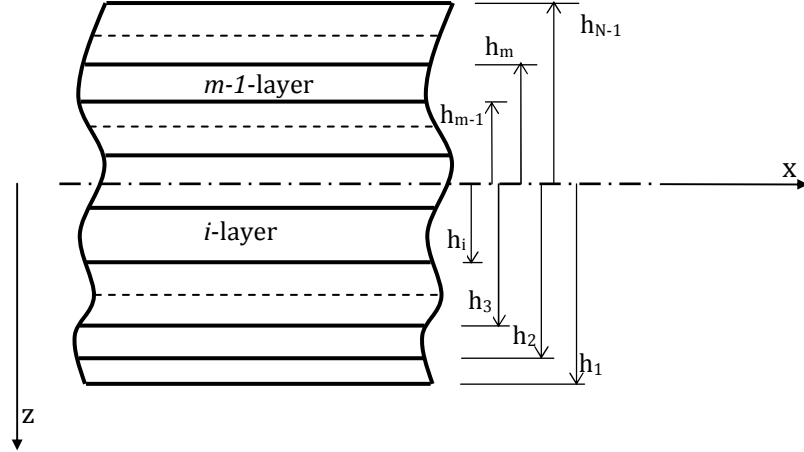


Figure 3. 2: Multilayer element numbering.

Assuming that the plate or the shell element is approximated by a sum of small elements in local coordinate, the modified complementary principle for a multilayer composite structure is given by Pian [66] as:

$$\begin{aligned} \Pi_{mc} = \sum_n \sum_i \left(\int_{V_{ni}} \frac{1}{2} \{\sigma\}^{iT} [S]^i \{\sigma\}^i dV - \int_{V_{ni}} \{\sigma\}^{iT} \{\epsilon\}^i dV \right. \\ \left. + \int_{S_{\sigma n}} \{\bar{T}\}^T \{u\} dS \right) = \text{stationary} \end{aligned} \quad (3.7)$$

where $\{\epsilon\}$ are the components of the strain as computed from the displacements via the strain displacement relations (note that in a hybrid-stress model, strains are computed from the stresses through the constitutive equations). The superscript n and i refer to the n -th element and i -th layer, respectively.

For the application of Π_{mc} to laminated composites structures incorporating independent cross-sectional rotations, the stresses within the layer i are assumed in terms of finite number of stress parameters $\{\beta\}^i$ in the form

$$\{\sigma\}^i = [P]_i \{\beta\}^i \quad (3.8)$$

where $[P]_i$ is a function of the coordinates whose form is such that the homogeneous equilibrium equations, the equilibrium conditions of the tractions in the interlayer surface and the traction-free conditions on the cylindrical surface are satisfied. The $\{\beta\}^i$ are parameters that are yet to be determined.

To avoid calculating the β 's for each layer, adequate strain functions can be chosen (see Afshari [72]) instead of stress functions as required for the complementary energy method. The type of strain functions chosen defines the type of element, meaning first order or higher order displacement field. One of the contributions of this dissertation is the choice of appropriate strain functions. That will be discussed in the next Section.

The in-plane strain vector $\{\epsilon\}_{in}$ for the whole laminate can be expressed as

$$\{\epsilon\}_{in} = [P]_{in} \{\beta\} \quad (3.9)$$

The in-plane stress – strain relation is given by

$$\{\sigma\}_{in}^i = [C]^i \{\epsilon\}_{in} \quad (3.10)$$

Substituting Eq. (3.9) into Eq. (3.10), the in-plane stresses can be expressed as:

$$\{\sigma\}_{in}^i = [C]^i [P]_{in} \{\beta\} \quad (3.11)$$

Then, one substitutes the in-plane stresses into the equilibrium equations (2.4) to determine the other stress components. All the stress components can be related to the strain parameters by

$$\{\sigma\}^i = [P]^i \{\beta\} \quad (3.12)$$

The boundary displacements, $\{u\}$, can be expressed in terms of generalized nodal displacement parameters, $\{q\}$, by

$$\{\epsilon\} = [B]\{u\} = [B]\{q\} \quad (3.13)$$

Substituting Eqs. (3.9), (3.12), and (3.13) into the functional expression Π_{mc} , Eq. (3.7), one obtains

$$\begin{aligned} \Pi_{mc} = \sum_n \sum_i & \left(\int_{V_n} \frac{1}{2} \{\beta\}^T \{P\}^{iT} [S]^i [P]^i \{\beta\} dV - \int_{V_n} \{\beta\}^T [P]^{iT} [B] \{q\} dV \right. \\ & \left. + \int_{S_n} \{Q\}^T \{q\} dS \right) \end{aligned} \quad (3.14)$$

Defining the element $[H]$ and $[G]$ matrices as

$$[H] = \begin{bmatrix} [H]^1 & & & \\ & [H]^2 & & \\ & & \ddots & \\ (diag) & & & [H]^k \end{bmatrix} \quad \text{with} \quad [H]^i = \int_{V_n} [P]^{iT} [S]^i [P]^i dV, \quad (3.15)$$

$$[G] = \begin{Bmatrix} G^1 \\ G^2 \\ \vdots \\ G^k \end{Bmatrix} \quad \text{with} \quad [G]^i = \int_{V_n} [P]^{iT} [B] dV \quad (3.16)$$

$$\{Q\}^T = \int_{S_n} \{\bar{T}\}^T dS \quad (3.17)$$

with $i = 1, 2, \dots, k$, where k is the total layer number of the element; $\{Q\}$ is the prescribed generalized nodal force; β and q are the strain parameters and nodal displacements respectively for the element,

$$\{\beta\}^T = \{\beta^1, \beta^2, \dots, \beta^k\}^T \quad \{q\}^T = \{q^1, q^2, \dots, q^k\}^T$$

and substituting Eq. (3.15) through (3.17) into Eq. (3.14), the modified complementary energy becomes

$$\Pi_{mc} = \sum_n \left\{ \frac{1}{2} \{\beta\}^T [H] \{\beta\} - \{\beta\}^T [G] \{q\} + \{q\}^T \{Q\} \right\} \quad (3.18)$$

The stationary value of the energy expression is obtained by taking the partial derivative of Equation (3.18) with respect to β and setting it equal to zero (i.e; $\partial \Pi_{mc} / \partial \beta = 0$). This yields a relation between $\{q\}$ and $\{\beta\}$ as

$$\{\beta\} = [H]^{-1}[G]\{q\} \quad (3.19)$$

Upon substituting Eq. (3.19) into Eq. (3.18), the energy expression in terms of the nodal displacement parameters becomes

$$\Pi_{mc} = \sum_n \left\{ -\frac{1}{2} \{q\}^T [G]^T [H]^{-1} [G] \{q\} + \{q\}^T \{Q\} \right\} \quad (3.20)$$

From the stationary condition of Π_{mc} , the element matrix is obtained:

$$[K]\{q\} = \{Q\} \quad (3.21)$$

where

$$[K] = [G]^T [H]^{-1} [G]. \quad (3.22)$$

This formulation is independent of the coordinate system, the element type and the displacement field formulation.

3.3 Proposed Element Formulation

3.3.1 Strain Functions Choices

Two categories of element are proposed. Both are based on assumed in-plane strain functions and on the modified complementary energy principle method adopted herein.

An eight-node isoparametric “serendipity” element is used because of its practicability in overcoming the shear locking effect that was observed with the four node quadrilateral element [6]. The assumed in-plane displacement functions used to obtain the

3.3.2 First Order Element Formulation

This formulation is based on in-plane strain functions as follows

$$\begin{aligned}
 \epsilon_x(x, y, z) &= \epsilon_{x0}(x, y) + z\epsilon_{x1}(x, y) \\
 \epsilon_y(x, y, z) &= \epsilon_{y0}(x, y) + z\epsilon_{y1}(x, y) \\
 \epsilon_{xy}(x, y, z) &= \epsilon_{xy0}(x, y) + z\epsilon_{xy1}(x, y)
 \end{aligned} \tag{3.23}$$

where ϵ_{x0} , ϵ_{x1} , ϵ_{y0} , ϵ_{y1} , ϵ_{xy0} and ϵ_{xy1} are functions to be determined. Note that the notation is changed from that previously employed in order to conform to the strain-based modified complementary energy formulation.

The number of strain parameters and the type of displacement assumptions used will be the main characteristic of the element nomenclature. A sample nomenclature is FELM36 or TELM54 to designate a first order element with 36 betas or a third order element with 54 betas, respectively. When two elements have the same number of strain parameters with different strain functions, the number 2 will be added at the end of the second element. There are only two of these cases, namely TELM422 and TELM482. As an example, the in-plane strain field for FELM36 is given by

$$\begin{aligned}
 \epsilon_x &= \beta_1 + \beta_4x + \beta_7y + \beta_{10}xy + \beta_{13}x^2 + \beta_{16}y^2 + \beta_{19}x^3 + \beta_{22}y^3 \\
 &\quad + z(\beta_{25} + \beta_{28}x + \beta_{31}y + \beta_{34}xy) \\
 \epsilon_y &= \beta_2 + \beta_5x + \beta_8y + \beta_{11}xy + \beta_{14}x^2 + \beta_{17}y^2 + \beta_{19}x^3 + \beta_{23}y^3 \\
 &\quad + z(\beta_{26} + \beta_{29}x + \beta_{32}y + \beta_{35}xy) \\
 \epsilon_{xy} &= \beta_3 + \beta_6x + \beta_9y + \beta_{12}xy + \beta_{15}x^2 + \beta_{18}y^2 + \beta_{21}x^3 + \beta_{24}y^3 \\
 &\quad + z(\beta_{27} + \beta_{30}x + \beta_{33}y + \beta_{36}xy)
 \end{aligned} \tag{3.24}$$

or in matrix notation,

$$\begin{aligned}
\epsilon_x &= \{\beta_{x0}\}^T \{\psi_0\} + z\{\beta_{x1}\}^T \{\psi_1\} \\
\epsilon_y &= \{\beta_{y0}\}^T \{\psi_0\} + z\{\beta_{y1}\}^T \{\psi_1\} \\
\epsilon_{xy} &= \{\beta_{xy0}\}^T \{\psi_0\} + z\{\beta_{xy1}\}^T \{\psi_1\}
\end{aligned} \tag{3.25}$$

where

$$\begin{aligned}
\{\beta_{x0}\}^T &= \{\beta_1, \beta_4, \beta_7, \beta_{10}, \beta_{13}, \beta_{16}, \beta_{19}, \beta_{22}\}; & \{\beta_{x1}\}^T &= \{\beta_{25}, \beta_{28}, \beta_{30}, \beta_{34}\} \\
\{\beta_{y0}\}^T &= \{\beta_2, \beta_5, \beta_8, \beta_{11}, \beta_{14}, \beta_{17}, \beta_{20}, \beta_{23}\}; & \{\beta_{y1}\}^T &= \{\beta_{26}, \beta_{29}, \beta_{32}, \beta_{35}\} \\
\{\beta_{xy0}\}^T &= \{\beta_3, \beta_6, \beta_9, \beta_{12}, \beta_{15}, \beta_{18}, \beta_{21}, \beta_{24}\}; & \{\beta_{xy1}\}^T & \\
& & &= \{\beta_{27}, \beta_{30}, \beta_{33}, \beta_{36}\}
\end{aligned} \tag{3.26}$$

and

$$\begin{aligned}
\{\psi_0\} &= \{1, x, y, xy, x^2, y^2, x^3, y^3\} \\
\{\psi_1\} &= \{1, x, y, xy\}
\end{aligned}$$

The expressions of the basis functions $\{\psi_0\}$ and $\{\psi_1\}$ are chosen to be the same for ϵ_x , ϵ_y and ϵ_{xy} , for two reasons. First, to have the same order for the matrix of strain functions, avoiding therefore the matrix mismatching error during the numerical implementation using Matlab. Secondly, having identical basis functions assumes an initial balance of in-plane behavior where all the parameters have equal weight. For instance, if the basis function for ϵ_x has more x variables than the one of ϵ_y , then the formulation would suggest a particular influence of the x components on the behavior of the plate. In what follows, the strain functions will be identified only by the form of the basis functions $\{\psi_0\}$ and $\{\psi_1\}$.

There are two FSDT elements investigated in this study; the above mentioned FELM36 which uses two incomplete quadratic and cubic in-plane strain functions and FELM48 for which the first component of the strain function is

$$\begin{aligned} \epsilon_x = & \{\beta_{x0}\}^T \{1, x, y, xy, x^2, y^2, x^2y, xy^2, x^3, y^3\} \\ & + z\{\beta_{x1}\}^T \{1, x, y, xy, x^2, y^2\} \end{aligned} \quad (3.27)$$

It is seen that FELM48 is characterized by one complete quadratic and one complete cubic in-plane strain function.

3.3.3 Third Order Strain Element

Similar to the notation type Eq. (3.25), the proposed third order strain element has the strain field expressed as follow:

$$\begin{aligned} \epsilon_x = & \{\beta_{x0}\}^T \{\psi_0\} + z\{\beta_{x1}\}^T \{\psi_1\} + (\alpha z)^3 \{\beta_{x2}\}^T \{\psi_2\} \\ \epsilon_y = & \{\beta_{y0}\}^T \{\psi_0\} + z\{\beta_{y1}\}^T \{\psi_1\} + (\alpha z)^3 \{\beta_{y2}\}^T \{\psi_2\} \\ \epsilon_{xy} = & \{\beta_{xy0}\}^T \{\psi_0\} + z\{\beta_{xy1}\}^T \{\psi_1\} + (\alpha z)^3 \{\beta_{xy2}\}^T \{\psi_2\} \end{aligned} \quad (3.28)$$

where ψ_0 , ψ_1 , and ψ_2 are functions which depend only on in-plane coordinates x and y .

The convergence parameter, α , is incorporated the z -cube terms for comparison purposes with the linear ones. As stated before, there is no special physical meaning to the z -cube term, besides the fact that it permits the strain function to be non-linear, allowing for a non-linear variation of the transverse stresses. The z^2 terms have not been incorporated to meet the requirement of free transverse shear stresses at the top and bottom surface of a plate or shell loaded in bending, as stated in Section 2.1.4 (Eq. (2.20)). The proposed expressions are more general in form and by using a convergence parameter, α , one will have more flexible elements which can account for special type of boundary conditions and the structural geometry of laminated composites. The proposed formulation is based

on strain functions. It is necessary and important that the choice of the strain functions be such that they are consistent with the displacement expressions. This is especially true for the strain based modified complementary energy principle where one can develop two independent strain fields. The first is the in-plane strain field used to define the constitutive equation within the formulation (Eq. (3.12)). The second is the strain field involved in the boundary displacements (Eq. (3.13)). In what follows, a detailed analysis of the relationship between strain and displacement assumptions in the proposed formulation is presented.

From the third order strain field above (Eq. (3.28)), the general form of the in-plane displacement field can be derived as

$$\begin{aligned} u &= u_0 + z\varphi_{x1} + (\alpha z)^3\varphi_{x2} \\ v &= v_0 + z\varphi_{y1} + (\alpha z)^3\varphi_{y2} \end{aligned} \quad (3.29)$$

This expression assumes traction free conditions on the top and bottom surface. For the sake of coherence and compatibility in formulation, the relationship between strain and displacement functions is now discussed. The traction free conditions, Eq. (2.20), suggests that

$$\text{at } z = \pm \frac{h}{2}: \quad \frac{\partial v}{\partial z} = -\frac{\partial w}{\partial y}; \quad \text{and} \quad \frac{\partial u}{\partial z} = -\frac{\partial w}{\partial x} \quad (3.30)$$

Substituting the expression of u and v from Eq. (3.29) into Eq. (3.30), one obtains

$$\frac{\partial w}{\partial y} = -(\varphi_{y1} + 3(\alpha z)^2\varphi_{y2}); \quad \text{and} \quad \frac{\partial w}{\partial x} = -(\varphi_{x1} + 3(\alpha z)^2\varphi_{x2}) \quad (3.31)$$

At $z = \pm \frac{h}{2}$, these become

$$\varphi_{x2} = -\frac{4}{3\alpha^2 h^2} \left(\varphi_{x1} + \frac{\partial w}{\partial x} \right); \quad \text{and} \quad \varphi_{y2} = -\frac{4}{3\alpha^2 h^2} \left(\varphi_{y1} + \frac{\partial w}{\partial y} \right) \quad (3.32)$$

The in-plane strain displacement relations are given as

$$\epsilon_x = \frac{\partial u}{\partial x}; \quad \epsilon_y = \frac{\partial v}{\partial y} \quad \text{and} \quad \epsilon_{xy} = \frac{\partial u}{\partial y} + \frac{\partial v}{\partial x} \quad (3.33)$$

Upon substituting the expressions of u and v from Eq. (3.29) into Eq. (3.33), one obtains

$$\begin{aligned} \epsilon_x &= u_{0,x} + z\varphi_{x1,x} + (\alpha z)^3 \varphi_{x2,x} \\ \epsilon_y &= v_{0,y} + z\varphi_{y1,y} + (\alpha z)^3 \varphi_{y2,y} \end{aligned} \quad (3.34)$$

$$\epsilon_{xy} = (u_{0,y} + v_{0,x}) + z\varphi_{x1,y} + z\varphi_{y1,x} + (\alpha z)^3 \varphi_{x2,y} + (\alpha z)^3 \varphi_{y2,x}$$

Differentiating the expression of φ_{x2} and φ_{y2} from Eq. (3.32) and substituting them into

Eq. (3.34), the strain components are expressed as

$$\begin{aligned} \epsilon_x &= u_{0,x} + z\varphi_{x1,x} - \alpha z^3 \frac{4}{3h^2} \left(\varphi_{x1,x} + \frac{\partial^2 w}{\partial x^2} \right) \\ \epsilon_y &= v_{0,y} + z\varphi_{y1,y} - \alpha z^3 \frac{4}{3h^2} \left(\varphi_{y1,x} + \frac{\partial^2 w}{\partial y^2} \right) \\ \epsilon_{xy} &= (u_{0,y} + v_{0,x}) + z(\varphi_{x1,y} + \varphi_{y1,x}) \\ &\quad - \alpha z^3 \frac{4}{3h^2} \left((\varphi_{x1,y} + \varphi_{y1,x}) + 2 \frac{\partial^2 w}{\partial x \partial y} \right) \end{aligned} \quad (3.35)$$

By comparing Eqs (3.28) and (3.35) one may formally identify the expression of the proposed strain functions with the compatible assumed strain fields, such that

$$\begin{aligned} \epsilon_x &= \{\psi_{x0}\} + z\{\psi_{x1}\} + (\alpha z)^3 \{\psi_{x2}\} \\ \epsilon_y &= \{\psi_{y0}\} + z\{\psi_{y1}\} + (\alpha z)^3 \{\psi_{y2}\} \\ \epsilon_{xy} &= \{\psi_{xy0}\} + z\{\psi_{xy1}\} + (\alpha z)^3 \{\psi_{xy2}\} \end{aligned} \quad (3.36)$$

where

$$\begin{aligned} \{\psi_{x0}\} &= \{\beta_{x0}\}^T \{\psi_0\} = u_{0,x} \\ \{\psi_{x1}\} &= \{\beta_{x1}\}^T \{\psi_1\} = \varphi_{x1,x} \end{aligned} \quad (3.37)$$

$$\begin{aligned}\{\psi_{x2}\} &= \{\beta_{x2}\}^T \{\psi_2\} = -\frac{4}{3\alpha^3 h^2} \left(\varphi_{x1,x} + \frac{\partial^2 w}{\partial x^2} \right) \\ \{\psi_{y0}\} &= \{\beta_{y0}\}^T \{\psi_0\} = v_{0,y} \\ \{\psi_{y1}\} &= \{\beta_{y1}\}^T \{\psi_1\} = \varphi_{y1,y}\end{aligned}\tag{3.38}$$

$$\begin{aligned}\{\psi_{y2}\} &= \{\beta_{y2}\}^T \{\psi_2\} = -\frac{4}{3\alpha^3 h^2} \left(\varphi_{y1,x} + \frac{\partial^2 w}{\partial y^2} \right) \\ \{\psi_{xy0}\} &= \{\beta_{xy0}\}^T \{\psi_0\} = (u_{0,y} + v_{0,x}) \\ \{\psi_{xy1}\} &= \{\beta_{xy1}\}^T \{\psi_1\} = (\varphi_{x1,y} + \varphi_{y1,x})\end{aligned}\tag{3.39}$$

$$\{\psi_{xy2}\} = \{\beta_{xy2}\}^T \{\psi_2\} = -\frac{4}{3\alpha^3 h^2} \left((\varphi_{x1,y} + \varphi_{y1,x}) + 2 \frac{\partial^2 w}{\partial x \partial y} \right)$$

The choice of basis functions $\{\psi_0\}$, $\{\psi_1\}$, and $\{\psi_2\}$ will define the strain-based elements. There is no particular condition imposed on w beside the fact that it depends only on the in-plane coordinates x and y , and must be at least C^1 continuous in order to allow warping behavior (due to x and y components in w expression). Thus, w should be at least a bi-quadratic function of x and y . In classical plate theory, the expressions $(\partial^2 w / \partial x^2)$ and $(\partial^2 w / \partial y^2)$ are the curvatures about x and y axis, respectively. They are expected to influence the behavior of the structure and will also be selected freely. All the basis in-plane strain functions are linearly independent, but are related to the in-plane displacement functions used in the isoparametric approximation of the shape functions. Since isoparametric formulation is used, the basis shape functions and displacement basis functions must be identical. The in-plane displacement functions used to derived the shape functions of an eight-node isoparametric *serendipity* element are given by [148]

$$u = a_1 + a_2 x + a_3 y + a_4 xy + a_5 x^2 + a_6 y^2 + a_7 x^2 y + a_8 xy^2\tag{3.40}$$

$$v = a_9 + a_{10}x + a_{11}y + a_{12}xy + a_{13}x^2 + a_{14}y^2 + a_{15}x^2y + a_{16}xy^2$$

The in-plane strain functions, which are the first derivative of displacements do not have to be of the same form, but must be compatible with the isoparametric formulation. However, one must expect that strain functions that are not close to a bi-quadratic form may yield inaccurate result. This is one of the reasons why bi-linear strain functions used for the first and third order formulations do not work. Therefore, the in-plane basis strain function, $\{\psi_0\}$, will be chosen with a slight variation of the bi-quadratic functions. The basis function $\{\psi_1\}$ is associated with the independent linear transverse rotations $(\partial w/\partial x)$, and $(\partial w/\partial y)$, which are defined as unknown degrees of freedom (DOF) θ_x , and θ_y , respectively. Therefore, they will be selected freely. The most important aspect of the formulation is involved with the choice of the basis function $\{\psi_2\}$. The strain functions can be considered as independent functions which are associated with new nodal degrees of freedom (the three higher order rotations), therefore increasing the total number of DOF to eight for a single node, and as well as increasing the number of strain parameters. The advantage is that the tractions free boundary conditions will be *a priori* satisfied. Another formulation method would be to consider $\{\psi_2\}$ as a simple contribution to the general transverse behavior of the structure without association to any degree of freedom. The advantages are keeping the original number of DOF and independently choosing the basis function. However, one still has a larger number of strain parameters when compared to the first order formulation. This case was the first one investigated with several elements and will be discussed further later. Since basis functions $\{\psi_1\}$ and $\{\psi_2\}$ are chosen freely, another possibility is to choose them to be identical. Note that the strain functions $\{\psi_{x1}\}$ and $\{\psi_{x2}\}$ associated to the basis

functions are still linearly independent, but are non-linearly dependent in a αz -cube terms, which is consistent with the third order strain-based formulation adopted in this study. The advantage is that the number of strain parameters is reduced considerably, while saving computing time. This option was also investigated by selecting basis functions as variations of the eight-node serendipity shape functions.

Twenty one elements are investigated in the following: thirteen of which have complete independence between basis functions $\{\psi_1\}$ and $\{\psi_2\}$, and eight for which the basis functions are non-linearly z -cube dependent and which are consistent with the traction free boundary conditions. For the elements associated with the independent basis function, the letter “I” will be added at the end of the nomenclature. For instance, TELM66I represents a third order strain based element with 66 strain parameters associated with independent first and third order basis functions. A listing of the strain functions is as follows:

1 - TELM422I

$$\varepsilon_x = [1, x, y, xy, x^2, y^2] \beta_a^T + z[1, x, y, xy] \beta_b^T + (\alpha z)^3 [1, x, y, xy] \beta_c^T$$

2 - TELM45I

$$\varepsilon_x = [1, x, y, xy, x^2, y^2, x^2y, xy^2] \beta_a^T + z[1, x, y, xy] \beta_b^T + (\alpha z)^3 [1, x, y] \beta_c^T$$

3 - TELM51I

$$\varepsilon_x = [1, x, y, xy, x^2, y^2, x^2y, xy^2] \beta_a^T + z[1, x, y, xy, x^2, y^2] \beta_b^T + (\alpha z)^3 [1, x, y] \beta_c^T$$

4 - TELM54I

$$\varepsilon_x = [1, x, y, xy, x^2, y^2, x^2y, xy^2] \beta_a^T + z[1, x, y, xy, x^2, y^2] \beta_b^T + (\alpha z)^3 [1, x, y, xy] \beta_c^T$$

5 - TELM542I

$$\begin{aligned}\varepsilon_x &= [1, x, y, xy, x^2, y^2, x^2y, xy^2, x^3, y^3]\beta_a^T + z[1, x, y, xy]\beta_b^T \\ &\quad + (\alpha z)^3[1, x, y, xy]\beta_c^T\end{aligned}$$

6 - TELM57I

$$\begin{aligned}\varepsilon_x &= [1, x, y, xy, x^2, y^2, x^2y, xy^2, x^3, y^3]\beta_a^T + z[1, x, y, xy, x^2, y^2]\beta_b^T \\ &\quad + (\alpha z)^3[1, x, y]\beta_c^T\end{aligned}$$

7 - TELM60I

$$\begin{aligned}\varepsilon_x &= [1, x, y, xy, x^2, y^2, x^2y, xy^2]\beta_a^T + z[1, x, y, xy, x^2, y^2]\beta_b^T \\ &\quad + (\alpha z)^3[1, x, y, xy, x^2, y^2]\beta_c^T\end{aligned}$$

8 - TELM602I

$$\begin{aligned}\varepsilon_x &= [1, x, y, xy, x^2, y^2, x^2y, xy^2, x^3, y^3]\beta_a^T + z[1, x, y, xy, x^2, y^2]\beta_b^T \\ &\quad + (\alpha z)^3[1, x, y, xy]\beta_c^T\end{aligned}$$

9 - TELM66I

$$\begin{aligned}\varepsilon_x &= [1, x, y, xy, x^2, y^2, x^2y, xy^2, x^3, y^3]\beta_a^T + z[1, x, y, xy, x^2, y^2]\beta_b^T \\ &\quad + (\alpha z)^3[1, x, y, xy, x^2, y^2]\beta_c^T\end{aligned}$$

10 - TELM72I

$$\begin{aligned}\varepsilon_x &= [1, x, y, xy, x^2, y^2, x^2y, xy^2]\beta_a^T + z[1, x, y, xy, x^2, y^2, x^2y, xy^2]\beta_b^T \\ &\quad + (\alpha z)^3[1, x, y, xy, x^2, y^2, x^2y, xy^2]\beta_c^T\end{aligned}$$

11 - TELM78I

$$\begin{aligned}\varepsilon_x &= [1, x, y, xy, x^2, y^2, x^2y, xy^2, x^3, y^3]\beta_a^T + z[1, x, y, xy, x^2, y^2, x^2y, xy^2]\beta_b^T \\ &\quad + (\alpha z)^3[1, x, y, xy, x^2, y^2, x^2y, xy^2]\beta_c^T\end{aligned}$$

12 - TELM84I

$$\begin{aligned}\varepsilon_x &= [1, x, y, xy, x^2, y^2, x^2y, xy^2, x^3, y^3]\beta_a^T \\ &\quad + z[1, x, y, xy, x^2, y^2, x^2y, xy^2, x^3, y^3]\beta_b^T \\ &\quad + (\alpha z)^3[1, x, y, xy, x^2, y^2, x^2y, xy^2]\beta_c^T\end{aligned}$$

13 - TELM90I

$$\begin{aligned}\varepsilon_x &= [1, x, y, xy, x^2, y^2, x^2y, xy^2, x^3, y^3]\beta_a^T + z[1, x, y, xy, x^2, y^2, x^2y, xy^2, x^3, y^3]\beta_b^T \\ &\quad + (\alpha z)^3[1, x, y, xy, x^2, y^2, x^2y, xy^2, x^3, y^3]\beta_c^T\end{aligned}$$

14 - TELM30

$$\varepsilon_x = [1, x, y, xy, x^2, y^2]\beta_a^T + [z+(\alpha z)^3][\{1, x, y, xy\}]\beta_b^T$$

15 - TELM36

$$\varepsilon_x = [1, x, y, xy, x^2, y^2, x^2y, xy^2]\beta_a^T + [z+(\alpha z)^3][\{1, x, y, xy\}]\beta_b^T$$

16 - TELM42

$$\varepsilon_x = [1, x, y, xy, x^2, y^2, x^2y, xy^2, x^3, y^3]\beta_a^T + [z+(\alpha z)^3][1, x, y, xy]\beta_b^T$$

17 - TELM422

$$\varepsilon_x = [1, x, y, xy, x^2, y^2, x^2y, xy^2]\beta_a^T + [z+(\alpha z)^3][1, x, y, xy, x^2, y^2]\beta_b^T$$

18 - TELM54

$$\varepsilon_x = [1, x, y, xy, x^2, y^2, x^2y, xy^2, x^3, y^3]\beta_a^T + [z+(\alpha z)^3][1, x, y, xy, x^2, y^2]\beta_b^T$$

19 - TELM482

$$\begin{aligned}\varepsilon_x &= [1, x, y, xy, x^2, y^2, x^2y, xy^2]\beta_a^T \\ &\quad + [z+(\alpha z)^3][1, x, y, xy, x^2, y^2, x^2y, xy^2]\beta_b^T\end{aligned}$$

20 - TELM54

$$\begin{aligned}\varepsilon_x &= [1, x, y, xy, x^2, y^2, x^2y, xy^2, x^3, y^3]\beta_a^T \\ &\quad + [z+(\alpha z)^3][1, x, y, xy, x^2, y^2, x^2y, xy^2]\beta_b^T\end{aligned}$$

21 - TELM60

$$\begin{aligned}\varepsilon_x = & [1, x, y, xy, x^2, y^2, x^2y, xy^2, x^3, y^3]\beta_a^T \\ & + [z+(\alpha z)^3][1, x, y, xy, x^2, y^2, x^2y, xy^2, x^3, y^3]\beta_b^T\end{aligned}$$

In this Section the main characteristics of the proposed element formulations were presented and a discussion on how they were chosen was given. More details on their incorporation in a strain-based approach of the modified complementary energy principle will be presented in the next Chapter.

CHAPTER 4

FINITE ELEMENT FORMULATION (ANALYSIS AND IMPLEMENTATION)

In this chapter, the finite element method is used as the numerical technique to implement formulations which are subsequently used to solve laminated composite plate and shell problems. The strain-based modified complementary energy principle and two different in-plane fields as presented in the previous chapter are used for both plate and shell element development. A detailed description of the plate element development is given first, followed by a brief presentation of the shell element formulation. To avoid redundancy, only the higher order strain elements will be presented, assuming that the lower ones order can be easily deduced from them. A computer program written in Matlab is used to implement all the formulations and sample problem solutions.

4.1 Plate Element Formulation

4.1.1 Geometry

The geometry characteristics of the multi-layer plate element are shown in Figure 4.1. The structure is made of several layers through the wall thickness, each of which may have a different thickness, fiber orientation and material properties. The layers are assumed to be perfectly bonded. The mid-surface of the plate is taken as the reference surface for the geometry of the element. The Cartesian coordinate system (x, y, z) is used to describe the global coordinate system and its origin is located on the middle surface.

The element consists of eight nodes: four corner nodes and four mid-side nodes. The normalized coordinates system (ξ, η, ζ) is used for the isoparametric element. All three normalized coordinates vary between -1 and 1 on the respective faces of the

element. A two-dimensional shape function, $N_i(\xi, \eta)$, lies in the x-y mid-surface of the plate element while ζ is a linear coordinate in the thickness direction.

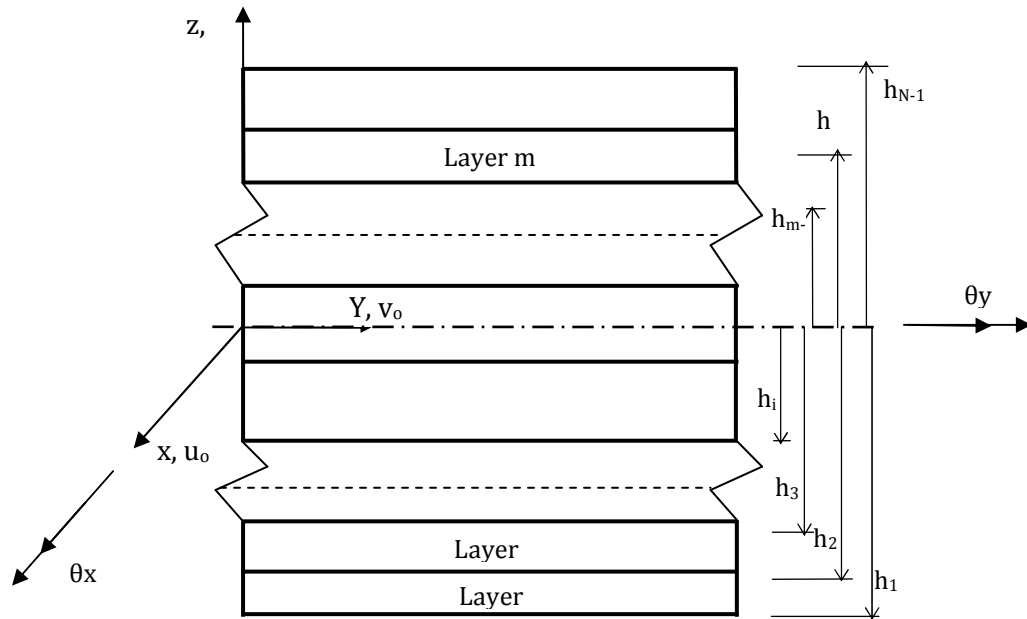


Figure 4. 1: Multi-layer geometry and nodal degree of freedom for plate element.

The position of a point with coordinates x and y is expressed in terms of the normalized coordinates by the isoparametric transformation as

$$\begin{Bmatrix} x \\ y \end{Bmatrix} = \sum_{i=1}^8 N_i(\xi, \eta) \begin{Bmatrix} x_i \\ y_i \end{Bmatrix} \quad (4.1)$$

where x_i , y_i and $N_i(\xi, \eta)$ are, respectively, the global in-plane coordinates of node i and the bi-quadratic serendipity shape function. Figure 4.2 shows the numbering pattern of a typical element. The shape functions associate to each node are given as [148]:

$$\begin{aligned}
N_1 &= 0.25(\xi - 1)(1 - \eta)(\xi + \eta + 1) \\
N_2 &= 0.5(1 - \xi^2)(1 - \eta) \\
N_3 &= 0.25(\xi + 1)(1 - \eta)(\xi - \eta - 1) \\
N_4 &= 0.5(1 - \eta^2)(1 + \xi) \\
N_5 &= 0.25(\xi + 1)(1 + \eta)(\xi + \eta - 1) \\
N_6 &= 0.5(1 - \xi^2)(1 + \eta) \\
N_7 &= 0.25(\xi - 1)(1 + \eta)(\xi - \eta + 1) \\
N_8 &= 0.5(1 - \eta^2)(1 - \xi)
\end{aligned} \tag{4.2}$$

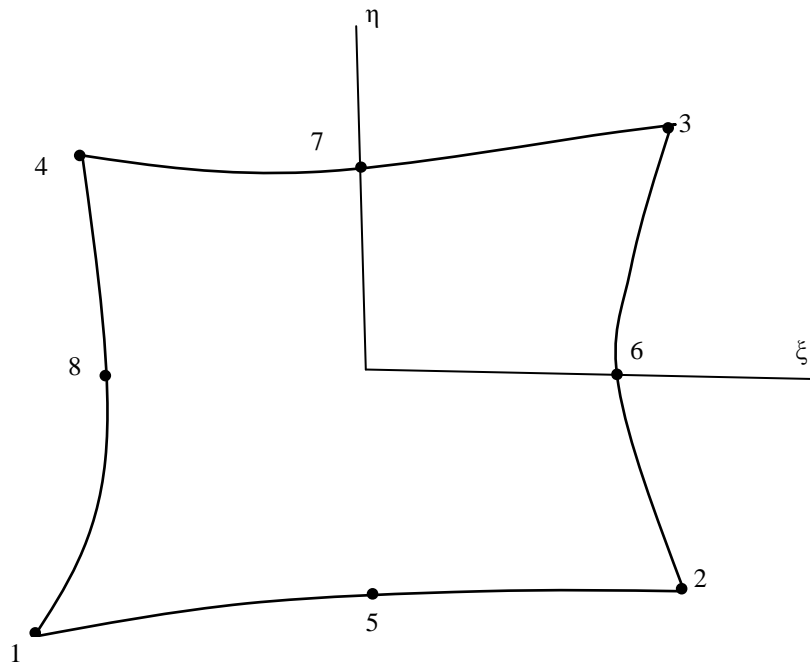


Figure 4. 2: Node numbering of quadratic element.

Since the element consist of layers, the normalized transverse coordinate for each layer is given by Spilker [73] as:

$$z = \frac{1}{2}[(h_i + h_{i+1}) + \zeta(h_{i+1} - h_i)] \quad (4.3)$$

such that ζ varies from (-1) to (+1) between the bottom and the top of layer i .

4.1.2 Displacement Field

The displacement field is derived from the type of strain field assumed in Eq. (3.28). The element displacements consist of the mid-surface nodal displacement, namely u_{oi} , v_{oi} , w_i and two small rotations θ_{xi} and θ_{yi} about x -axis and y -axis, respectively, as shown in Figure 4.1.

The nodal and element degrees of freedom may be expressed, respectively, by the vectors

$$\begin{aligned} \{q_i\} &= \{u_{oi}, v_{oi}, w_i, \theta_{xi}, \theta_{yi}\}^T \\ \{q\} &= \{q_1, q_2, \dots, q_8\}^T \end{aligned} \quad (4.4)$$

The displacement components u , v , w , of an arbitrary point in the element in Cartesian coordinates can be expressed in terms of nodal displacements as follows:

$$\begin{Bmatrix} u \\ v \\ w \end{Bmatrix} = \sum_{i=1}^8 N_i(\xi, \eta) \begin{Bmatrix} u_{oi} \\ v_{oi} \\ w_i \end{Bmatrix} + z \sum_{i=1}^8 N_i(\xi, \eta) \begin{Bmatrix} \theta_{yi} \\ \theta_{xi} \\ 0 \end{Bmatrix} + (az)^3 \sum_{i=1}^8 N_i(\xi, \eta) \begin{Bmatrix} \theta_{yi} \\ \theta_{xi} \\ 0 \end{Bmatrix} \quad (4.5)$$

Since an isoparametric formulation is employed, the N_i are the same shape functions as those used in the geometric definition (Eq. 4.2). As each node has five degrees of freedom, each element thus has forty degrees of freedom.

4.1.3 Kinematics

The kinematic equations (2.2) and the displacement fields equations (4.1) are used to obtain the matrix [B] of the strain-displacement relations. Using simplified derivative notation ($\frac{\partial u_0(x,y)}{\partial x} = u_{0,x}$), the linear kinematic relations can be written as

$$\begin{aligned}
 \epsilon_x &= u_{,x} \\
 \epsilon_y &= v_{,y} \\
 \epsilon_{xy} &= u_{,y} + v_{,x} \\
 \epsilon_{yz} &= v_{,z} + w_{,y} \\
 \epsilon_{xz} &= u_{,z} + w_{,x}
 \end{aligned} \tag{4.6}$$

In terms of the shape functions, they become

$$\begin{aligned}
 \epsilon_x &= \sum_{i=1}^8 N_{i,x} u_{oi} + z \sum_{i=1}^8 N_{i,x} \theta_{yi} + (\alpha z)^3 \sum_{i=1}^8 N_{i,x} \theta_{yi} \\
 \epsilon_y &= \sum_{i=1}^8 N_{i,y} v_{oi} + z \sum_{i=1}^8 N_{i,y} \theta_{xi} + (\alpha z)^3 \sum_{i=1}^8 N_{i,y} \theta_{xi} \\
 \epsilon_{xy} &= \sum_{i=1}^8 N_{i,y} u_{oi} + \sum_{i=1}^8 N_{i,x} v_{oi} + z \sum_{i=1}^8 N_{i,x} \theta_{xi} + (\alpha z)^3 \sum_{i=1}^8 N_{i,x} \theta_{xi} \\
 &\quad + z \sum_{i=1}^8 N_{i,y} \theta_{yi} + (\alpha z)^3 \sum_{i=1}^8 N_{i,y} \theta_{yi} \\
 \epsilon_{yz} &= \sum_{i=1}^8 N_{i,y} w_i + \sum_{i=1}^8 N_i \theta_{xi} + 3(\alpha z)^2 \sum_{i=1}^8 N_i \theta_{xi} \\
 \epsilon_{xz} &= \sum_{i=1}^8 N_{i,x} w_i + z \sum_{i=1}^8 N_i \theta_{yi} + 3(\alpha z)^2 \sum_{i=1}^8 N_i \theta_{yi}
 \end{aligned} \tag{4.7}$$

Putting equation (4.3) in a matrix form, one obtains

$$\{\epsilon\} = \sum_{i=1}^8 [B_i] \{q_i\} \quad (4.8)$$

where the strain vector and the $[B]_i$ matrix for a single node are expressed as

$$[B]_i = \begin{bmatrix} N_{i,x} & 0 & 0 & 0 & [z + (\alpha z)^3]N_{i,x} \\ 0 & N_{i,y} & 0 & [z + (\alpha z)^3]N_{i,y} & 0 \\ N_{i,y} & N_{i,x} & 0 & [z + (\alpha z)^3]N_{i,x} & [z + (\alpha z)^3]N_{i,y} \\ 0 & 0 & N_{i,y} & [1 + 3(\alpha z)^2]N_i & 0 \\ 0 & 0 & N_{i,x} & 0 & [1 + 3(\alpha z)^2]N_i \end{bmatrix} \quad (4.9)$$

$$\{\epsilon\} = \{\epsilon_x, \epsilon_y, \epsilon_z, \epsilon_{xy}, \epsilon_{yz}, \epsilon_{xz}\}^T$$

The derivatives of $N_i(\xi, \eta)$ with respect to the global coordinates x and y are not available directly. Using the chain rule of differentiation, one obtains

$$N_{i,\xi} = N_{i,x}x_{,\xi} + N_{i,y}y_{,\xi} \quad (4.10)$$

$$N_{i,\eta} = N_{i,x}x_{,\eta} + N_{i,y}y_{,\eta}$$

Equation (4.4) in a matrix form becomes

$$\begin{Bmatrix} N_{i,\xi} \\ N_{i,\eta} \end{Bmatrix} = \begin{bmatrix} x_{,\xi} & y_{,\xi} \\ x_{,\eta} & y_{,\eta} \end{bmatrix} \begin{Bmatrix} N_{i,x} \\ N_{i,y} \end{Bmatrix} = [J] \begin{Bmatrix} N_{i,x} \\ N_{i,y} \end{Bmatrix} \quad (4.11)$$

where $[J]$ is the *Jacobian Matrix*. The components of the Jacobian matrix are derived

from Eq. (4.1) as follows:

$$\begin{aligned} x_{,\xi} &= \sum_{i=1}^8 N_{i,\xi} x_i; & x_{,\eta} &= \sum_{i=1}^8 N_{i,\eta} x_i \\ y_{,\xi} &= \sum_{i=1}^8 N_{i,\xi} y_i; & y_{,\eta} &= \sum_{i=1}^8 N_{i,\eta} y_i \end{aligned} \quad (4.12)$$

Using Eq. (4.5), $N_{i,x}$, and $N_{i,y}$ are determined as

$$\begin{Bmatrix} N_{i,x} \\ N_{i,y} \end{Bmatrix} = [J]^{-1} \begin{Bmatrix} N_{i,\xi} \\ N_{i,\eta} \end{Bmatrix} \quad (4.13)$$

Therefore, all the components of the nodal $[B]_i$ are determined. The strain displacement relation for an element in matrix form can then be expressed as

$$\{\epsilon\} = [B]\{q\} \quad (4.14)$$

The $[B]$ matrix is made up of eight (5x5) blocks of the $[B]_i$.

4.1.4 Stress Interpolation

The stresses are obtained by used of the strain functions defined in the previous chapter. Here, element TELM36 is used to demonstrate the detailed procedure of obtaining the element stiffness matrix. The expression of the in-plane strain functions for TELM36 are given by

$$\begin{aligned} \epsilon_x &= \beta_1 + \beta_4 x + \beta_7 y + \beta_{10} xy + \beta_{13} x^2 + \beta_{16} y^2 + \beta_{19} x^2 y + \beta_{22} xy^2 + (z \\ &\quad + (\alpha z)^3) (\beta_{25} + \beta_{28} x + \beta_{31} y + \beta_{34} xy) \\ \epsilon_y &= \beta_2 + \beta_5 x + \beta_8 y + \beta_{11} xy + \beta_{14} x^2 + \beta_{17} y^2 + \beta_{20} x^2 y + \beta_{23} xy^2 + (z \\ &\quad + (\alpha z)^3) (\beta_{26} + \beta_{29} x + \beta_{32} y + \beta_{35} xy) \\ \epsilon_{xy} &= \beta_3 + \beta_6 x + \beta_9 y + \beta_{12} xy + \beta_{15} x^2 + \beta_{18} y^2 + \beta_{21} x^2 y + \beta_{24} xy^2 \\ &\quad + (z + (\alpha z)^3) (\beta_{27} + \beta_{30} x + \beta_{33} y + \beta_{36} xy) \end{aligned} \quad (4.15)$$

From the constitutive equations, the in-plane stresses are

$$\begin{aligned} \sigma_x^m &= c_{11}^m \epsilon_x + c_{12}^m \epsilon_y + c_{14}^m \epsilon_{xy} \\ \sigma_y^m &= c_{12}^m \epsilon_x + c_{22}^m \epsilon_y + c_{24}^m \epsilon_{xy} \\ \sigma_{xy}^m &= c_{14}^m \epsilon_x + c_{24}^m \epsilon_y + c_{44}^m \epsilon_{xy} \end{aligned} \quad (4.16)$$

Substituting Eq. (4.15) into Eq. (4.16) the expressions of in-plane stresses become as follows:

$$\begin{aligned}
\sigma_x^m = & c_{11}^m[\beta_1 + \beta_4x + \beta_7y + \beta_{10}xy + \beta_{13}x^2 + \beta_{16}y^2 + \beta_{19}x^2y + \beta_{22}xy^2 \\
& + (z + (\alpha z)^3)(\beta_{25} + \beta_{28}x + \beta_{31}y + \beta_{34}xy)] + c_{12}^m[\beta_2 \\
& + \beta_5x + \beta_8y + \beta_{11}xy + \beta_{14}x^2 + \beta_{17}y^2 + \beta_{20}x^2y \\
& + \beta_{23}xy^2 + (z + (\alpha z)^3)(\beta_{26} + \beta_{29}x + \beta_{32}y + \beta_{35}xy)] \\
& + c_{14}^m[\beta_3 + \beta_6x + \beta_9y + \beta_{12}xy + \beta_{15}x^2 + \beta_{18}y^2 + \beta_{21}x^2y \\
& + \beta_{24}xy^2 + (z + (\alpha z)^3)(\beta_{27} + \beta_{30}x + \beta_{33}y + \beta_{36}xy)]
\end{aligned} \tag{4.17}$$

$$\begin{aligned}
\sigma_y^m = & c_{12}^m[\beta_1 + \beta_4x + \beta_7y + \beta_{10}xy + \beta_{13}x^2 + \beta_{16}y^2 + \beta_{19}x^2y + \beta_{22}xy^2 \\
& + (z + (\alpha z)^3)(\beta_{25} + \beta_{28}x + \beta_{31}y + \beta_{34}xy)] + c_{22}^m[\beta_2 \\
& + \beta_5x + \beta_8y + \beta_{11}xy + \beta_{14}x^2 + \beta_{17}y^2 + \beta_{20}x^2y \\
& + \beta_{23}xy^2 + (z + (\alpha z)^3)(\beta_{26} + \beta_{29}x + \beta_{32}y + \beta_{35}xy)] \\
& + c_{24}^m[\beta_3 + \beta_6x + \beta_9y + \beta_{12}xy + \beta_{15}x^2 + \beta_{18}y^2 + \beta_{21}x^2y \\
& + \beta_{24}xy^2 + (z + (\alpha z)^3)(\beta_{27} + \beta_{30}x + \beta_{33}y + \beta_{36}xy)]
\end{aligned} \tag{4.18}$$

$$\begin{aligned}
\sigma_{xy}^m = & c_{14}^m[\beta_1 + \beta_4x + \beta_7y + \beta_{10}xy + \beta_{13}x^2 + \beta_{16}y^2 + \beta_{19}x^2y + \beta_{22}xy^2 \\
& + (z + (\alpha z)^3)(\beta_{25} + \beta_{28}x + \beta_{31}y + \beta_{34}xy)] + c_{24}^m[\beta_2 \\
& + \beta_5x + \beta_8y + \beta_{11}xy + \beta_{14}x^2 + \beta_{17}y^2 + \beta_{20}x^2y \\
& + \beta_{23}xy^2 + (z + (\alpha z)^3)(\beta_{26} + \beta_{29}x + \beta_{32}y + \beta_{35}xy)] \\
& + c_{44}^m[\beta_3 + \beta_6x + \beta_9y + \beta_{12}xy + \beta_{15}x^2 + \beta_{18}y^2 + \beta_{21}x^2y \\
& + \beta_{24}xy^2 + (z + (\alpha z)^3)(\beta_{27} + \beta_{30}x + \beta_{33}y + \beta_{36}xy)]
\end{aligned} \tag{4.19}$$

The transverse stresses are obtained from the equilibrium equations (2.4) as follows:

$$\sigma_{xz}^m = - \int (\sigma_{x,x}^m + \sigma_{xy,y}^m) dz + Cst1^m \tag{4.20}$$

$$\sigma_{yz}^m = - \int (\sigma_{xy,x}^m + \sigma_{y,y}^m) dz + Cst2^m \tag{4.21}$$

$$\sigma_z^m = - \int (\sigma_{xz,x}^m + \sigma_{yz,y}^m) dz + Cst3^m \quad (4.22)$$

where $Cst1^m$, $Cst2^m$, and $Cst3^m$ are constants of integration.

It is important to note that the integrations are performed within one layer thickness and not through the structure thickness. They express the transverse equilibrium within the element. Therefore, the transverse stresses are not the resultants as in the equivalent single layer theory. This is another advantage of the modified complementary energy principle.

4.1.5 Interlaminar Boundary Conditions

In the present study, three boundary conditions are satisfied to determine the constants of integration. They are:

- a) The transverse stresses are equal at the interface of the layers. That implies that

at $z = h_m$,

$$\begin{aligned} \sigma_{xz}^m &= \sigma_{xz}^{m-1}, \\ \sigma_{yz}^m &= \sigma_{yz}^{m-1}, \\ \sigma_z^m &= \sigma_z^{m-1} \end{aligned} \quad (4.23)$$

- b) The transverse stresses are zero on the bottom surface of the element. Thus,

at $z = h_1$

$$\begin{aligned} \sigma_{xz}^1 &= 0 \\ \sigma_{yz}^1 &= 0 \\ \sigma_z^1 &= 0 \end{aligned} \quad (4.24)$$

By satisfying the above conditions, the constants of integration are determined for each layer. Note that there are no specific restrictions on the top surface tractions (eq. (2.20)) although they are partially assumed in the strain field assumptions.

The final expression for all stresses are given as

$$\begin{aligned}
\sigma_x^m = & c_{11}^m[\beta_1 + \beta_4x + \beta_7y + \beta_{10}xy + \beta_{13}x^2 + \beta_{16}y^2 + \beta_{19}x^2y + \beta_{22}xy^2 \\
& + (z + (\alpha z)^3) (\beta_{25} + \beta_{28}x + \beta_{31}y + \beta_{34}xy)] + c_{12}^m[\beta_2 + \beta_5x \\
& + \beta_8y + \beta_{11}xy + \beta_{14}x^2 + \beta_{17}y^2 + \beta_{20}x^2y + \beta_{23}xy^2 + (z \\
& + (\alpha z)^3) (\beta_{26} + \beta_{29}x + \beta_{32}y + \beta_{35}xy)] + c_{14}^m[\beta_3 + \beta_6x \\
& + \beta_9y + \beta_{12}xy + \beta_{15}x^2 + \beta_{18}y^2 + \beta_{21}x^2y + \beta_{24}xy^2 + (z \\
& + (\alpha z)^3) (\beta_{27} + \beta_{30}x + \beta_{33}y + \beta_{36}xy)]
\end{aligned} \tag{4.25a}$$

$$\begin{aligned}
\sigma_y^m = & c_{12}^m[\beta_1 + \beta_4x + \beta_7y + \beta_{10}xy + \beta_{13}x^2 + \beta_{16}y^2 + \beta_{19}x^2y + \beta_{22}xy^2 \\
& + (z + (\alpha z)^3) (\beta_{25} + \beta_{28}x + \beta_{31}y + \beta_{34}xy)] + c_{22}^m[\beta_2 + \beta_5x \\
& + \beta_8y + \beta_{11}xy + \beta_{14}x^2 + \beta_{17}y^2 + \beta_{20}x^2y + \beta_{23}xy^2 + (z \\
& + (\alpha z)^3) (\beta_{26} + \beta_{29}x + \beta_{32}y + \beta_{35}xy)] + c_{24}^m[\beta_3 + \beta_6x \\
& + \beta_9y + \beta_{12}xy + \beta_{15}x^2 + \beta_{18}y^2 + \beta_{21}x^2y + \beta_{24}xy^2 + (z \\
& + (\alpha z)^3) (\beta_{27} + \beta_{30}x + \beta_{33}y + \beta_{36}xy)]
\end{aligned} \tag{4.25b}$$

$$\begin{aligned}
\sigma_{xy}^m = & c_{14}^m[\beta_1 + \beta_4x + \beta_7y + \beta_{10}xy + \beta_{13}x^2 + \beta_{16}y^2 + \beta_{19}x^2y + \beta_{22}xy^2 \\
& + (z + (\alpha z)^3) (\beta_{25} + \beta_{28}x + \beta_{31}y + \beta_{34}xy)] + c_{24}^m[\beta_2 + \beta_5x \\
& + \beta_8y + \beta_{11}xy + \beta_{14}x^2 + \beta_{17}y^2 + \beta_{20}x^2y + \beta_{23}xy^2 + (z \\
& + (\alpha z)^3) (\beta_{26} + \beta_{29}x + \beta_{32}y + \beta_{35}xy)] + c_{44}^m[\beta_3 + \beta_6x \\
& + \beta_9y + \beta_{12}xy + \beta_{15}x^2 + \beta_{18}y^2 + \beta_{21}x^2y + \beta_{24}xy^2 + (z \\
& + (\alpha z)^3) (\beta_{27} + \beta_{30}x + \beta_{33}y + \beta_{36}xy)]
\end{aligned} \tag{4.25c}$$

$$\begin{aligned}
\sigma_z^m = -2z & \left[\left(A_{14}^m + \left(\frac{1}{2}z + z^2 \right) C_{14}^m + SA_{14}^m + 2DF_{14}^m \right) \beta_{10} \right. \\
& + \left(A_{24}^m + \left(\frac{1}{2}z + z^2 \right) C_{24}^m + SA_{24}^m + 2DF_{24}^m \right) \beta_{11} \\
& + \left(A_{44}^m + \left(\frac{1}{2}z + z^2 \right) C_{44}^m + SA_{44}^m + 2DF_{44}^m \right) \beta_{12} \\
& + \left(A_{11}^m + \left(\frac{1}{2}z + z^2 \right) C_{11}^m + SA_{11}^m + 2DF_{11}^m \right) \beta_{13} \\
& + \left(A_{12}^m + \left(\frac{1}{2}z + z^2 \right) C_{12}^m + SA_{12}^m + 2DF_{12}^m \right) \beta_{14} \\
& + \left(A_{14}^m + \left(\frac{1}{2}z + z^2 \right) C_{14}^m + SA_{14}^m + 2DF_{14}^m \right) \beta_{15} \\
& + \left(A_{12}^m + \left(\frac{1}{2}z + z^2 \right) C_{12}^m + SA_{12}^m + 2DF_{12}^m \right) \beta_{16} \\
& + \left(A_{22}^m + \left(\frac{1}{2}z + z^2 \right) C_{22}^m + SA_{22}^m + 2DF_{22}^m \right) \beta_{17} \\
& + \left(A_{24}^m + \left(\frac{1}{2}z + z^2 \right) C_{24}^m + SA_{24}^m + 2DF_{24}^m \right) \beta_{18} \\
& + \left(DF_{14}^m + \frac{2}{3}z^2 C_{14}^m + SD_{14}^m + F_{14}^m \right) \beta_{28} \\
& + \left(DF_{24}^m + \frac{2}{3}z^2 C_{24}^m + SD_{24}^m + F_{24}^m \right) \beta_{29} \\
& + \left(DF_{44}^m + \frac{2}{3}z^2 C_{44}^m + SD_{44}^m + F_{44}^m \right) \beta_{30} \\
& + \left(DF_{11}^m + \frac{2}{3}z^2 C_{11}^m + SD_{11}^m + F_{11}^m \right) \beta_{31} \\
& + \left(DF_{12}^m + \frac{2}{3}z^2 C_{12}^m + SD_{12}^m + F_{12}^m \right) \beta_{32} \\
& + \left(DF_{14}^m + \frac{2}{3}z^2 C_{14}^m + SD_{14}^m + F_{14}^m \right) \beta_{33} \\
& + \left(DF_{12}^m + \frac{2}{3}z^2 C_{12}^m + SD_{12}^m + F_{12}^m \right) \beta_{34} \\
& + \left(DF_{22}^m + \frac{2}{3}z^2 C_{22}^m + SD_{22}^m + F_{22}^m \right) \beta_{35} \\
& \left. + \left(DF_{24}^m + \frac{2}{3}z^2 C_{24}^m + SD_{24}^m + F_{24}^m \right) \beta_{36} \right] \tag{4.25d}
\end{aligned}$$

$$\begin{aligned}
\sigma_{xz}^m = & A_{11}^m \beta_4 + A_{12}^m \beta_5 + A_{14}^m \beta_6 + A_{14}^m \beta_7 + A_{24}^m \beta_8 + A_{44}^m \beta_9 \\
& + (A_{14}^m x + A_{11}^m y) \beta_{10} + (A_{14}^m x + A_{11}^m y) \beta_{11} \\
& + (A_{44}^m x + A_{14}^m y) \beta_{12} + 2A_{11}^m x \beta_{13} + 2A_{12}^m x \beta_{15} \\
& + 2A_{14}^m y \beta_{16} + 2A_{24}^m y \beta_{17} + 2A_{44}^m y \beta_{18} + DF_{11}^m y \beta_{22} \\
& + DF_{12}^m \beta_{23} + DF_{14}^m \beta_{24} + DF_{14}^m \beta_{25} + DF_{24}^m \beta_{26} \\
& + DF_{44}^m \beta_{27} + (DF_{14}^m x + DF_{11}^m y) \beta_{28} \\
& + (DF_{24}^m x + DF_{12}^m y) \beta_{29} + (DF_{44}^m x + DF_{14}^m y) \beta_{30} \\
& + 2DF_{11}^m x \beta_{31} + 2DF_{12}^m x \beta_{32} + 2DF_{14}^m x \beta_{33} \\
& + 2DF_{14}^m y \beta_{34} + 2DF_{24}^m y \beta_{35} + 2DF_{44}^m y \beta_{36}
\end{aligned} \tag{4.25e}$$

$$\begin{aligned}
\sigma_{yz}^m = & A_{14}^m \beta_4 + A_{24}^m \beta_5 + A_{44}^m \beta_6 + A_{12}^m \beta_7 + A_{22}^m \beta_8 + A_{24}^m \beta_9 \\
& + (A_{14}^m y + A_{11}^m x) \beta_{10} + (A_{22}^m x + A_{24}^m y) \beta_{11} \\
& + (A_{24}^m x + A_{44}^m y) \beta_{12} + 2A_{14}^m x \beta_{13} + 2A_{24}^m x \beta_{15} \\
& + 2A_{12}^m y \beta_{16} + 2A_{22}^m y \beta_{17} + 2A_{24}^m y \beta_{18} + DF_{14}^m y \beta_{22} \\
& + DF_{24}^m \beta_{23} + DF_{44}^m \beta_{24} + DF_{12}^m \beta_{25} + DF_{22}^m \beta_{26} \\
& + DF_{24}^m \beta_{27} + (DF_{12}^m x + DF_{14}^m y) \beta_{28} + (DF_{22}^m x \\
& + DF_{24}^m y) \beta_{29} + (DF_{24}^m x + DF_{44}^m y) \beta_{30} + 2DF_{14}^m x \beta_{31} \\
& + 2DF_{24}^m x \beta_{32} + 2DF_{44}^m x \beta_{33} + 2DF_{12}^m y \beta_{34} \\
& + 2DF_{22}^m y \beta_{35} + 2DF_{24}^m y \beta_{36}
\end{aligned} \tag{4.25f}$$

with

$$A_{kl}^m = \sum_{i=2}^m h_i (C_{kl}^i - C_{kl}^{i-1}) - z C_{kl}^m + C_{kl}^1 h_1 \tag{4.26a}$$

$$DF_{kl}^m = \frac{1}{2} \left[\sum_{i=2}^m \alpha^2 h_i^2 (C_{kl}^i - C_{kl}^{i-1}) - (\alpha z)^2 C_{kl}^m + C_{kl}^1 h_1^2 \right] \tag{4.26b}$$

$$SA_{kl}^m = 2 \sum_{i=2}^m h_i (A_{kl}^i - A_{kl}^{i-1}) + 2A_{kl}^1 h_1 \quad (4.26c)$$

$$SF_{kl}^m = 2 \sum_{i=2}^m h_i (DF_{kl}^i - DF_{kl}^{i-1}) + 2DF_{kl}^1 h_1 \quad (4.26d)$$

$$F_{kl}^m = \sum_{i=2}^m \frac{4}{3} h_i^3 (C_{kl}^i - C_{kl}^{i-1}) + \frac{4}{3} C_{kl}^1 h_1^3; \quad (4.26e)$$

Defining

$$AF_{kl}^m = -2 * z \left(A_{kl}^m + \left(\frac{1}{2}z + z^2 \right) C_{kl}^m + SA_{kl}^m + 2 * DF_{kl}^m \right) \quad (4.26f)$$

$$FF_{kl}^m = -2 * z \left(DF_{kl}^m + \left(\frac{2}{3}z^2 \right) C_{kl}^m + SF_{kl}^m + F_{kl}^m \right) \quad (4.26g)$$

the stresses can be written in matrix form in terms of strain parameters, β 's, as follows

$$\{\sigma\}^m = [P]^m \{\beta\} \quad (4.27)$$

where

$$[P]^m = (\text{see next page}) \quad (4.28)$$

$$[P]^m = \begin{bmatrix} C_{11} & C_{12} & C_{14} & C_{11}x & C_{12}x & C_{14}x & C_{11}y & C_{12}y & C_{14}y \\ C_{12} & C_{22} & C_{24} & C_{12}x & C_{22}x & C_{24}x & C_{12}y & C_{22}y & C_{24}y \\ 0 & 0 & 0 & 0 & 0 & 0 & 0 & 0 & 0 \\ C_{14} & C_{24} & C_{44} & C_{14}x & C_{24}x & C_{44}x & C_{14}y & C_{24}y & C_{44}y \\ 0 & 0 & 0 & A_{11} & A_{12} & A_{14} & A_{14} & A_{24} & A_{44} \\ 0 & 0 & 0 & A_{14} & A_{24} & A_{44} & A_{12} & A_{22} & A_{24} \end{bmatrix}$$

$$\begin{bmatrix} C_{11}xy & C_{12}xy & C_{14}xy & C_{11}x^2 & C_{12}x^2 & C_{14}x^2 & C_{11}y^2 & C_{12}y^2 & C_{14}y^2 \\ C_{12}xy & C_{22}xy & C_{24}xy & C_{12}x^2 & C_{22}x^2 & C_{24}x^2 & C_{12}y^2 & C_{22}y^2 & C_{24}y^2 \\ AD_{14} & AD_{24} & AD_{44} & AD_{11} & AD_{12} & AD_{14} & AD_{12} & AD_{22} & AD_{24} \\ C_{14}xy & C_{24}xy & C_{44}xy & C_{14} & C_{24}x^2 & C_{44}x^2 & C_{14}y^2 & C_{24}y^2 & C_{44}y^2 \\ A_{14}x + A_{11}y & A_{24}x + A_{12}y & A_{44}x + A_{14}y & 2A_{11}x & 2A_{12}x & 2A_{14}x & 2A_{14}y & 2A_{24}y & 2A_{44}y \\ A_{12}x + A_{14}y & A_{22}x + A_{24}y & A_{24}x + A_{44}y & 2A_{14}x & 2A_{24}x & 2A_{44}x & 2A_{12}y & 2A_{22}y & 2A_{24}y \end{bmatrix}$$

$$\begin{bmatrix} C_{11}z & C_{12}z & C_{14}z & C_{11}zx & C_{12}zx & C_{14}zx & C_{11}zy & C_{12}zy & C_{14}zy \\ C_{12}z & C_{22}z & C_{24}z & C_{12}zx & C_{22}zx & C_{24}zx & C_{12}zy & C_{22}zy & C_{24}zy \\ 0 & 0 & 0 & 0 & 0 & 0 & 0 & 0 & 0 \\ C_{14}z & C_{24}z & C_{44}z & C_{14}zx & C_{24}zx & C_{44}zx & C_{14}zy & C_{24}zy & C_{44}zy \\ 0 & 0 & 0 & DF_{11} & DF_{12} & DF_{14} & DF_{14} & DF_{24} & DF_{44} \\ 0 & 0 & 0 & DF_{14} & DF_{24} & DF_{44} & DF_{12} & DF_{22} & DF_{24} \end{bmatrix}$$

$$\begin{bmatrix} C_{11}zxy & C_{12}zxy & C_{14}zxy & C_{11}zx^2 & C_{12}zx^2 & C_{14}zx^2 & C_{11}zy^2 & C_{12}zy^2 & C_{14}zy^2 \\ C_{12}zxy & C_{22}zxy & C_{24}zxy & C_{12}zx^2 & C_{22}zx^2 & C_{24}zx^2 & C_{12}zy^2 & C_{22}zy^2 & C_{24}zy^2 \\ FF_{14} & FF_{24} & FF_{44} & FF_{11} & FF_{12} & FF_{14} & FF_{12} & FF_{22} & FF_{24} \\ C_{14}zxy & C_{24}zxy & C_{44}zxy & C_{14}zx^2 & C_{24}zx^2 & C_{44}zx^2 & C_{14}zy^2 & C_{24}zy^2 & C_{44}zy^2 \\ DF_{14}x + DF_{11}y & DF_{24}x + DF_{12}y & DF_{44}x + DF_{14}y & 2DF_{11}x & 2DF_{12}x & 2DF_{14}x & 2DF_{14}y & 2DF_{24}y & 2DF_{44}y \\ DF_{12}x + DF_{14}y & DF_{22}x + DF_{24}y & DF_{24}x + DF_{44}y & 2DF_{14}x & 2DF_{24}x & 2DF_{44}x & 2DF_{12}y & 2DF_{22}y & 2DF_{24}y \end{bmatrix}^m$$

4.1.6 Development of Stiffness Matrix

After forming the $[P]^m$ and $[B]$ matrices, the following matrices are found:

$$[H]^m = \int_{V_n} [P]^{mT} [S]^m [P]^m dV \quad (4.29)$$

$$[G]^m = \int_{V_n} [P]^{mT} [B] dV$$

Since the matrices $[P]^m$ and $[B]$ are expressed in the normalized coordinates system, the element volume is rewritten using the following standard transformation formula demonstrated by Murnaghan [81]:

$$dV = |J| d\xi d\eta d\zeta \quad (4.30)$$

By substituting Eq. (4.30) into Eq. (4.29) and Eq. (4.28), the $[H]^m$ and $[G]^m$ matrices can be expressed as

$$[H]^m = \int_{-1}^{+1} \int_{-1}^{+1} \int_{-1}^{+1} P^{mT} S^{mT} P^{mi} |J| d\xi d\eta d\zeta, \quad (4.31)$$

$$[G]^m = \int_{-1}^{+1} \int_{-1}^{+1} \int_{-1}^{+1} P^{mT} B |J| d\xi d\eta d\zeta \quad (4.32)$$

These integral are carried out numerically using the Gaussian quadrature method.

However, the compliance and stress-parameter matrices change from one layer to another; and are not continuous functions of ζ . Therefore, the thickness concept is utilized by splitting the limits of integration through each layer. This is done by modifying the variable ζ to ζ_k in any m -th layer such that ζ_k varies from -1 to +1 in the layer (see Figure 4.1). The change of variable is obtained from

$$\zeta = -1 + 2 \left[\sum_{i=1}^k t_m - t_m(1 - \zeta_k) \right] / t \quad (4.33)$$

and thus

$$d\zeta = \frac{t_m}{t} d\zeta_k \quad (4.34)$$

Here, t_m is the thickness of layer m and t the element thickness.

Upon substituting of Eq. (4.29) into Eqs (4.27) and (4.28), the $[H]^m$ and $[G]^m$ matrices take the following form:

$$[H]^m = \frac{t_m}{t} \int_{-1}^{+1} \int_{-1}^{+1} \int_{-1}^{+1} P^{mT} S^{mT} P^m |J| d\xi d\eta d\zeta_k, \quad (4.35)$$

$$[G]^m = \frac{t_m}{t} \int_{-1}^{+1} \int_{-1}^{+1} \int_{-1}^{+1} P^{mT} B |J| d\xi d\eta d\zeta_k \quad (4.36)$$

Applying the Gauss quadrature formula, one obtains:

$$[H]^m = \sum_1^{NX} \sum_1^{NY} \sum_1^{NZ} P^{mT} S^{mT} P^m |J| W_x W_y W_z, \quad (4.37)$$

$$[G]^m = \sum_1^{NX} \sum_1^{NY} \sum_1^{NZ} P^{mT} B |J| W_x W_y W_z \quad (4.38)$$

Here, NX , NY , and NZ are the number of Gauss points with associated convergence parameters, W_x , W_y , and W_z , respectively. The element matrices $[H]$ and $[G]$ can then be obtained by summing the contribution of all layers:

$$[H] = \sum_{m=1}^N [H]^m \quad (4.39)$$

$$[G] = \sum_{m=1}^N [G]^m$$

where N is the total number of layers.

After computing the inverse of the H matrix, the stiffness matrix for that element is formed by using Eq (3.22),

$$[K] = [G]^T [H]^{-1} [G]. \quad (4.40)$$

4.1.7 Stress Calculation

Upon assembling the global stiffness matrix for all the elements, the stresses can be found. First, determine the generalized displacements, $\{q\}$, using Eq. (3.21) as follows:

$$\{q\} = [K]^{-1} \{Q\} \quad (4.41)$$

where $\{Q\}$ is the external load matrix. The strain parameters, $\{\beta\}$, are found using Eq.

(3.19)

$$\{\beta\} = [H]^{-1} [G] \{q\} \quad (4.42)$$

Then the stresses at each layer can be computed by

$$\{\sigma\}^m = [P]^m \{\beta\} \quad (4.43)$$

The same procedure is going to be used to formulate the shell elements proposed in this study.

4.2 Shell Element Formulation

The curved shell elements proposed here is degenerated from a 3-D solid structure. They are applied to any type of shell, not only to cylindrical shells as some of the figures may suggest.

4.2.1 Geometry Definition and Description of the Element

Similar to the plate element, the multi-layer shell element (Figure 4.3) is an eight node isoparametric element with five degree of freedom at each node. The shell element is derived from the three-dimensional solid structure in which a point can be expressed by the sum of two vectors. The first is the position vector from the origin of the Cartesian coordinate system (x, y, z) which is also used to describe the global coordinate system, to a point on the reference surface of the shell element. The mid-surface of the shell is again taken as the reference surface for the geometry of the element. The second vector is a position vector from the mid-surface to the point of consideration. The normalized curvilinear coordinates system (ξ, η, ζ) is used for the isoparametric element.

At a typical node i , Figure 4.4, a unit vector \mathbf{V}_{3i} , in the thickness direction is defined as

$$\mathbf{V}_{3i} = \begin{Bmatrix} l_{3i} \\ m_{3i} \\ n_{3i} \end{Bmatrix} \quad (4.44)$$

where l_{3i} , m_{3i} and n_{3i} are direction cosines.

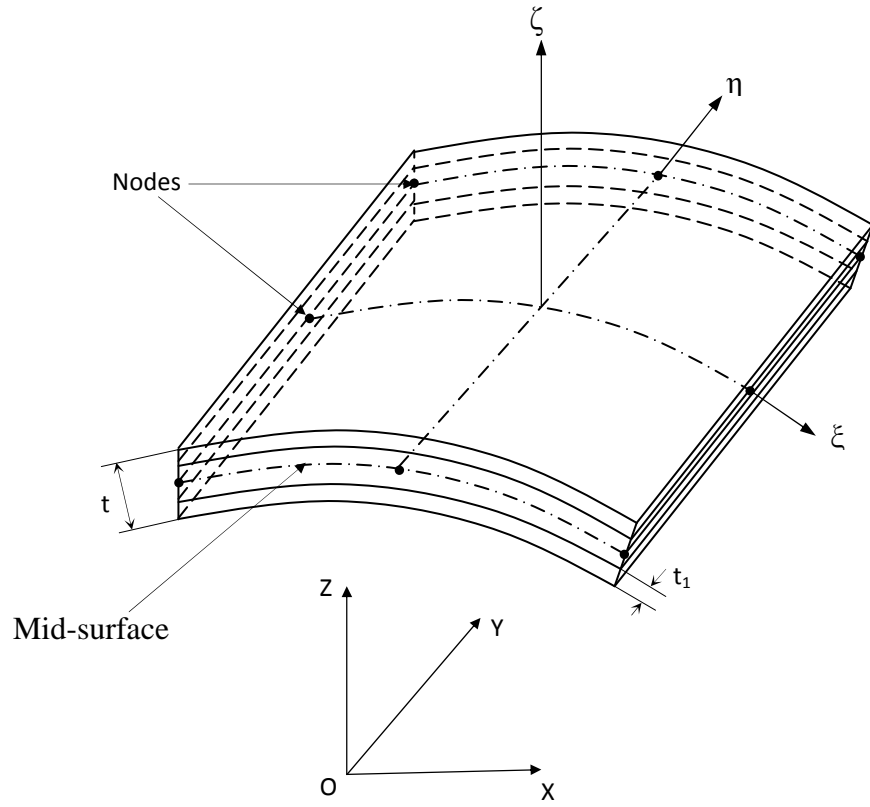


Figure 4. 3: Multi-layer composite shell element

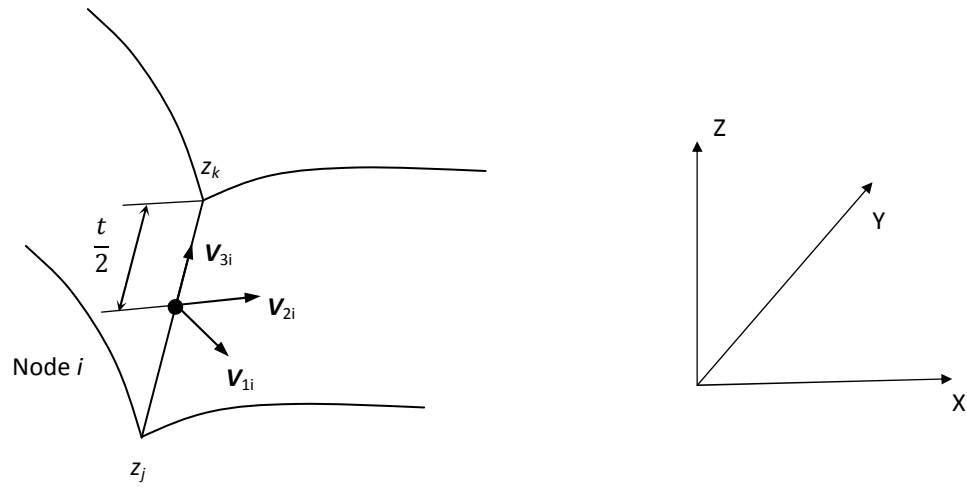


Figure 4. 4: Unit vectors at node i

The global coordinates of any point in the element may be expressed in terms of the position vectors of the nodes and the shape functions as

$$\begin{Bmatrix} x \\ y \\ z \end{Bmatrix} = \sum_{i=1}^8 N_i(\xi, \eta) \begin{Bmatrix} x_i \\ y_i \\ z_i \end{Bmatrix} + \sum_{i=1}^8 N_i(\xi, \eta) \zeta \frac{t}{2} \mathbf{V}_{3i} \quad (4.45)$$

where x_i, y_i, z_i and \mathbf{V}_{3i} are respectively the mid-surface coordinates and the unit vector in the thickness direction defined by

$$x_i = \frac{x_j + x_k}{2}, \quad y_i = \frac{y_j + y_k}{2}, \quad z_i = \frac{z_j + z_k}{2} \quad (4.46)$$

and

$$\mathbf{V}_{3i} = \begin{Bmatrix} l_{3i} \\ m_{3i} \\ n_{3i} \end{Bmatrix}, \quad \text{with } l_{3i} = \frac{(x_j - x_k)}{\|x_j - x_k\|}, \quad m_{3i} = \frac{(y_j - y_k)}{\|y_j - y_k\|}, \quad n_{3i} = \frac{(z_j - z_k)}{\|z_j - z_k\|} \quad (4.47)$$

The unit vector \mathbf{V}_{2i} is chosen along the longitudinal axis of the cylindrical shell, and the unit vector \mathbf{V}_{1i} is obtained from the cross product of \mathbf{V}_{2i} and \mathbf{V}_{3i} .

The N_i are the same shape functions as defined by Eq. (4.2) with the same numbering pattern (Figure 4.2).

4.2.2 Displacement Field

The first order displacement field of Eq. (2.17) will be used to derive the element formulation. The nodal and element degrees of freedom are given by Eq. (4.1). The element displacements consist of the mid-surface node displacements, namely u_i, v_i, w_i and two small rotations θ_{xi} and θ_{yi} about \mathbf{V}_{1i} and \mathbf{V}_{2i} , respectively, as shown in Figure 4.5. Note that, $\mathbf{V}_{1i}, \mathbf{V}_{2i}$ and \mathbf{V}_{3i} are mutually perpendicular, and that \mathbf{V}_{1i} and \mathbf{V}_{2i} are tangent to the element mid-surface at node i . Notes θ_{xi} and θ_{yi} may differ from node to node in a single element.

The displacement components u , v , w , of an arbitrary point in the element in global Cartesian coordinates can be expressed in terms of nodal displacements as follows

$$\begin{Bmatrix} u \\ v \\ w \end{Bmatrix} = \sum_{i=1}^8 N_i(\xi, \eta) \begin{Bmatrix} u_i \\ v_i \\ w_i \end{Bmatrix} + \sum_{i=1}^8 N_i(\xi, \eta) \zeta \frac{t}{2} [d_i] \begin{Bmatrix} \theta_{xi} \\ \theta_{yi} \end{Bmatrix} \quad (4.48)$$

where u_i , v_i , and w_i are the nodal displacements. Since the isoparametric formulation is used, the N_i are the same shape functions as those used in the geometric definition (Eq. (4.2)). Further, $[d_i]$ is a matrix of direction cosines of the unit vectors \mathbf{V}_{1i} and \mathbf{V}_{2i} at the i -th nodal point (see Figure 4.5)

$$[d_i] = \begin{bmatrix} -l_{2i} & l_{1i} \\ -m_{2i} & m_{1i} \\ -n_{2i} & n_{1i} \end{bmatrix} \quad (4.49)$$

The nodal and element displacement may be expressed, respectively, by the vectors

$$\begin{aligned} \{q_i\} &= \{u_i, v_i, w_i, \theta_{xi}, \theta_{yi}\}^T \\ \{q\} &= \{q_1, q_2, \dots, q_8\}^T \end{aligned} \quad (4.50)$$

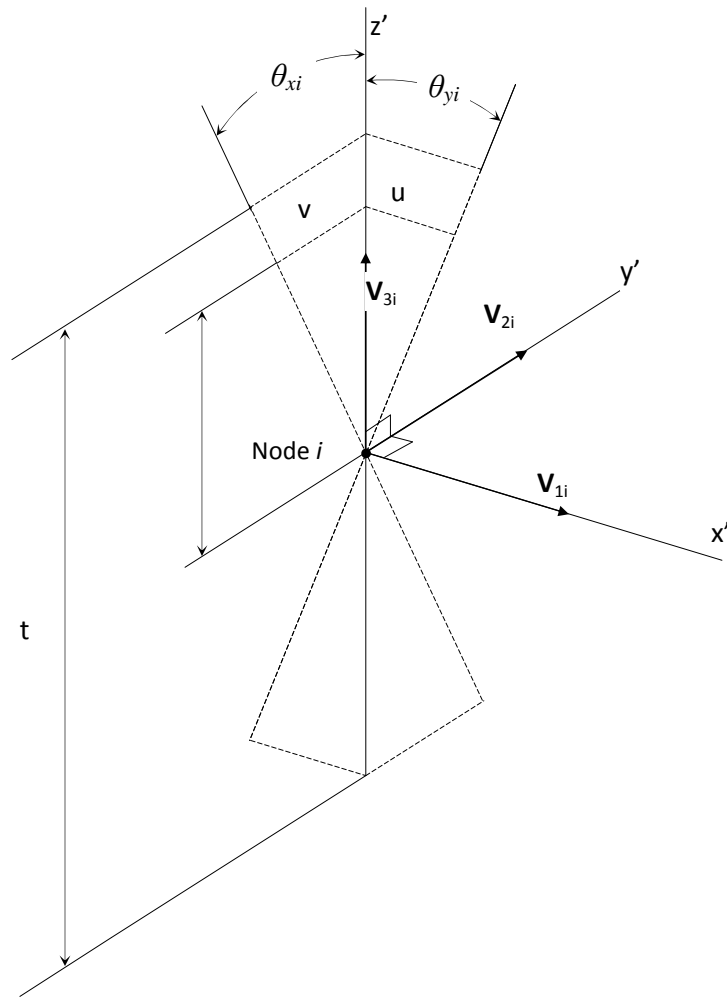


Figure 4. 5: Nodal displacements

4.2.3 Kinematics

The relationship between strain and displacement is obtained following the same procedure as for the plate element. Some steps will be skipped in order to avoid redundancy.

The kinematic relations in a matrix form are given by

$$\begin{Bmatrix} \epsilon_x \\ \epsilon_y \\ \epsilon_z \\ \epsilon_{xy} \\ \epsilon_{yz} \\ \epsilon_{xz} \end{Bmatrix} = \begin{bmatrix} 1 & 0 & 0 & 0 & 0 & 0 & 0 & 0 & 0 \\ 0 & 0 & 0 & 0 & 1 & 0 & 0 & 0 & 0 \\ 0 & 0 & 0 & 0 & 0 & 0 & 0 & 0 & 1 \\ 0 & 1 & 0 & 1 & 0 & 0 & 0 & 0 & 0 \\ 0 & 0 & 0 & 0 & 0 & 1 & 0 & 1 & 0 \\ 0 & 0 & 1 & 0 & 0 & 0 & 1 & 0 & 0 \end{bmatrix} \begin{Bmatrix} u_x \\ u_y \\ u_z \\ v_x \\ v_y \\ v_z \\ w_x \\ w_y \\ w_z \end{Bmatrix} \quad (4.51)$$

The derivative with respect to the global coordinates is obtained through the Jacobian matrix. The 3x3 Jacobian matrix required for this element is

$$[J] = \begin{bmatrix} x_{,\xi} & y_{,\xi} & z_{,\xi} \\ x_{,\eta} & y_{,\eta} & z_{,\eta} \\ x_{,\zeta} & y_{,\zeta} & z_{,\zeta} \end{bmatrix} \quad (4.52)$$

with determinant of $[J] = |J|$

The components of the Jacobian matrix are derived from Eq. (4.45) as follows:

$$\begin{aligned} x_{,\xi} &= \sum_{i=1}^8 N_{i,\xi} x_i + \sum_{i=1}^8 N_{i,\xi} \zeta \frac{t}{2} l_{3i} \\ x_{,\eta} &= \sum_{i=1}^8 N_{i,\eta} x_i + \sum_{i=1}^8 N_{i,\eta} \zeta \frac{t}{2} l_{3i} \\ x_{,\zeta} &= \sum_{i=1}^8 N_i \frac{t}{2} l_{3i} \\ y_{,\xi} &= \sum_{i=1}^8 N_{i,\xi} y_i + \sum_{i=1}^8 N_{i,\xi} \zeta \frac{t}{2} m_{3i} \\ y_{,\eta} &= \sum_{i=1}^8 N_{i,\eta} y_i + \sum_{i=1}^8 N_{i,\eta} \zeta \frac{t}{2} m_{3i} \\ y_{,\zeta} &= \sum_{i=1}^8 N_i \frac{t}{2} m_{3i} \end{aligned} \quad (4.53)$$

$$\begin{Bmatrix} u,x \\ u,y \\ u,z \\ v,x \\ v,y \\ v,z \\ w,x \\ w,y \\ w,z \end{Bmatrix} = \sum_{i=1}^8 \begin{bmatrix} a_i & -d_i l_{2i} & d_i l_{1i} \\ b_i & -e_i l_{2i} & e_i l_{1i} \\ c_i & -f_i l_{2i} & f_i l_{1i} \\ a_i & -d_i m_{2i} & d_i m_{1i} \\ b_i & -e_i m_{2i} & e_i m_{1i} \\ c_i & -f_i m_{2i} & f_i m_{1i} \\ a_i & -d_i n_{2i} & d_i n_{1i} \\ b_i & -e_i n_{2i} & e_i n_{1i} \\ c_i & -f_i n_{2i} & f_i n_{1i} \end{bmatrix} \begin{Bmatrix} u_i \\ v_i \\ w_i \\ \theta_{xi} \\ \theta_{yi} \end{Bmatrix} \quad (4.57)$$

where

$$\begin{aligned} a_i &= InJ_{11}N_{i,\xi} + InJ_{12}N_{i,\eta} \\ b_i &= InJ_{21}N_{i,\xi} + InJ_{22}N_{i,\eta} \\ c_i &= InJ_{31}N_{i,\xi} + InJ_{32}N_{i,\eta} \\ d_i &= \frac{t}{2}(a_i\zeta + InJ_{13}N_i) \\ e_i &= \frac{t}{2}(b_i\zeta + InJ_{23}N_i) \\ f_i &= \frac{t}{2}(c_i\zeta + InJ_{33}N_i) \end{aligned} \quad (4.58)$$

The strain-displacement relationship is derived from Eq. (4.57) and the strain displacement relation, Eq. (4.6), as

$$\begin{aligned} \{\varepsilon\} &= \sum_{i=1}^8 [B_i] \{q_i\} \\ \{\varepsilon\} &= [B] \{q\} \end{aligned} \quad (4.59)$$

where

$$[B_i] = \begin{bmatrix} a_i & & -d_i l_{2i} & & d_i l_{1i} \\ & b_i & & -e_i m_{2i} & e_i m_{1i} \\ & & c_i & -f_i n_{2i} & f_i n_{1i} \\ b_i & a_i & & -e_i l_{2i} - d_i m_{2i} & e_i l_{1i} + d_i m_{1i} \\ & c_i & b_i & -f_i m_{2i} - e_i n_{2i} & f_i m_{1i} + e_i n_{1i} \\ c_i & & a_i & -d_i n_{2i} - f_i l_{2i} & d_i n_{1i} + f_i l_{1i} \end{bmatrix} \quad (4.60)$$

The $[B]$ matrix here is made up of eight (6x5) blocks of $[B_i]$.

The components of the strain based modified complementary energy principle are given in the element coordinates system. Therefore, they have to be transformed into local coordinates. The element stiffness matrix obtained in local coordinates will then be transformed into global coordinates for coherence in the assembly.

4.2.4 Strain Transformation

The strain components at any point in the local coordinates system are given by

$$\{\varepsilon\} = \begin{Bmatrix} \varepsilon_{x'} \\ \varepsilon_{y'} \\ \varepsilon_{z'} \\ \gamma_{x'y'} \\ \gamma_{y'z'} \\ \gamma_{x'z'} \end{Bmatrix} \quad (4.61)$$

The global and local strains vectors are related through a strain transformation matrix as follows

$$\{\varepsilon\} = [T_e]\{\varepsilon\} \quad (4.62)$$

in which $[T_e]$ is given by equation (2.16b).

The direction of the local axes is shown in Figure 4.5. For the case of the cylindrical shell defined by the scalar field

$$g(x, y, z) = x^2 + y^2 \quad (4.63)$$

the unit vector \mathbf{V}_3 normal to the surface (x', y') is defined by

$$V_3 = \frac{\text{grad } g}{|\text{grad } g|} \quad (4.64)$$

The transformation of global displacements (u, v, w) to the local orthogonal displacements (u', v', w') is given by

$$\begin{Bmatrix} u \\ v \\ w \end{Bmatrix} = [L] \begin{Bmatrix} u' \\ v' \\ w' \end{Bmatrix} \quad (4.65)$$

where $[L]$ is the matrix of the three perpendicular unit vectors V_1, V_2, V_3 in the x', y', z' directions and constructed as follows:

$$[L] = [V_1, V_2, V_3] \quad (4.66)$$

The transformation of global derivative of the displacements u, v and w to the local derivatives of the local orthogonal displacements is given by a standard operation,

$$\begin{bmatrix} u',_{x'} & v',_{x'} & w',_{x'} \\ u',_{y'} & v',_{y'} & w',_{y'} \\ u',_{z'} & v',_{z'} & w',_{z'} \end{bmatrix} = [L]^T \begin{bmatrix} u,_{x} & v,_{x} & w,_{x} \\ u,_{y} & v,_{y} & w,_{y} \\ u,_{z} & v,_{z} & w,_{z} \end{bmatrix} [L] \quad (4.67)$$

Substituting Eq. (4.59) into Eq. (4.62), the strain components in local coordinates become

$$\{\varepsilon'\} = [T_e]^{-1} [B] \{q\} \quad (4.68)$$

The nodal and element displacements in local coordinates are expressed, respectively, as

$$\begin{aligned} \{q'_i\} &= \{u'_i, v'_i, w'_i, \theta_{xi}, \theta_{yi}\}^T \\ \{q'\} &= \{q'_1, q'_2, \dots, q'_8\}^T \end{aligned} \quad (4.69)$$

The element displacements in global and local coordinates are related by

$$\{q\} = [DT] \{q'\} \quad (4.70)$$

Here, the transformation matrix $[DT]$ is defined by

$$\{\sigma'\} = [T_c]\{\sigma\} \quad (4.76)$$

in which

$$[T_c] = [T_e]^{-T} \quad (4.77)$$

Upon substituting Eqs. (4.62) and (4.76) into Eq. (4.75), the constitutive relations in global coordinates are expressed as

$$\{\sigma\}^m = [CG]^m \{\varepsilon\}^m \quad (4.78)$$

where

$$[CG] = [T_c]^T [C] [T_c] \quad (4.79)$$

The in-plane strain-function method is used to find the stresses in local coordinates which are given by:

$$\begin{Bmatrix} \sigma'_x \\ \sigma'_y \\ \sigma'_{xy} \end{Bmatrix} = \begin{bmatrix} c_{11} & c_{12} & c_{14} \\ c_{12} & c_{22} & c_{24} \\ c_{14} & c_{24} & c_{44} \end{bmatrix} \begin{Bmatrix} \varepsilon'_x \\ \varepsilon'_y \\ \varepsilon'_{xy} \end{Bmatrix} \quad (4.80)$$

4.2.6 Stress Interpolation

The stresses are obtained through the strain functions defined in the previous chapter. Here, element FELM36 will be used to demonstrate the detailed procedure of obtaining the element stiffness matrix. The expressions of the in-plane strain functions for FELM36 are given by

$$\begin{aligned} \varepsilon'_x &= \beta_1 + \beta_4 x' + \beta_7 y' + \beta_{10} x' y' + \beta_{13} x'^2 + \beta_{16} y'^2 + z' (\beta_{19} + \beta_{22} x' \\ &\quad + \beta_{25} y' + \beta_{28} x' y' + \beta_{31} x'^2 + \beta_{34} y'^2) \\ \varepsilon'_y &= \beta_2 + \beta_5 x' + \beta_8 y' + \beta_{11} x' y' + \beta_{14} x'^2 + \beta_{17} y'^2 + z' (\beta_{20} + \beta_{23} x' \\ &\quad + \beta_{26} y' + \beta_{29} x' y' + \beta_{32} x'^2 + \beta_{35} y'^2) \end{aligned} \quad (4.81)$$

$$\begin{aligned}\epsilon'_{xy} = & \beta_3 + \beta_6x' + \beta_9y' + \beta_{12}x'y' + \beta_{15}x'^2 + \beta_{18}y'^2 + z'(\beta_{21} + \beta_{24}x' \\ & + \beta_{27}y' + \beta_{30}x'y' + \beta_{33}x^2 + \beta_{36}y^2)\end{aligned}$$

From the constitutive equations, one obtains

$$\begin{aligned}\sigma'_x{}^m &= c_{11}^m\epsilon'_x + c_{12}^m\epsilon'_y + c_{14}^m\epsilon'_{xy} \\ \sigma'_y{}^m &= c_{12}^m\epsilon'_x + c_{22}^m\epsilon'_y + c_{24}^m\epsilon'_{xy} \\ \sigma'_{xy}{}^m &= c_{14}^m\epsilon'_x + c_{24}^m\epsilon'_y + c_{44}^m\epsilon'_{xy}\end{aligned}\tag{4.82}$$

Note that the coefficients of the stiffness matrix are not transformed, because they are already transformed into element coordinates.

Substituting the strain expressions, Eq. (4.81) into Eq. (4.82) one has

$$\begin{aligned}\sigma'_x{}^m = & c_{11}^m[\beta_1 + \beta_4x' + \beta_7y' + \beta_{10}x'y' + \beta_{13}x'^2 + \beta_{16}y'^2 + z'(\beta_{19} \\ & + \beta_{22}x' + \beta_{25}y' + \beta_{28}x'y' + \beta_{31}x'^2 + \beta_{34}y'^2)] \\ & + c_{12}^m[\beta_2 + \beta_5x' + \beta_8y' + \beta_{11}x'y' + \beta_{14}x'^2 + \beta_{17}y'^2 + z'(\beta_{20} \\ & + \beta_{23}x' + \beta_{26}y' + \beta_{29}x'y' + \beta_{32}x'^2 + \beta_{35}y'^2)] \\ & + c_{14}^m[\beta_3 + \beta_6x' + \beta_9y' + \beta_{12}x'y' + \beta_{15}x'^2 + \beta_{18}y'^2 + z'(\beta_{21} \\ & + \beta_{24}x' + \beta_{27}y' + \beta_{30}x'y' + \beta_{33}x^2 + \beta_{36}y^2)]\end{aligned}\tag{4.83}$$

$$\begin{aligned}\sigma'_y{}^m = & c_{12}^m[\beta_1 + \beta_4x' + \beta_7y' + \beta_{10}x'y' + \beta_{13}x'^2 + \beta_{16}y'^2 + z'[\beta_{19} \\ & + \beta_{22}x' + \beta_{25}y' + \beta_{28}x'y' + \beta_{31}x'^2 + \beta_{34}y'^2]] \\ & + c_{22}^m[\beta_2 + \beta_5x' + \beta_8y' + \beta_{11}x'y' + \beta_{14}x'^2 + \beta_{17}y'^2 + z'[\beta_{20} \\ & + \beta_{23}x' + \beta_{26}y' + \beta_{29}x'y' + \beta_{32}x'^2 + \beta_{35}y'^2]] \\ & + c_{24}^m[\beta_3 + \beta_6x' + \beta_9y' + \beta_{12}x'y' + \beta_{15}x'^2 + \beta_{18}y'^2 + z'[\beta_{21} \\ & + \beta_{24}x' + \beta_{27}y' + \beta_{30}x'y' + \beta_{33}x^2 + \beta_{36}y^2]]\end{aligned}\tag{4.84}$$

$$\begin{aligned}
\sigma'_{xy} = & c_{14}^m [\beta_1 + \beta_4 x' + \beta_7 y' + \beta_{10} x' y' + \beta_{13} x'^2 + \beta_{16} y'^2 + z' [\beta_{19} \\
& + \beta_{22} x' + \beta_{25} y' + \beta_{28} x' y' + \beta_{31} x'^2 + \beta_{34} y'^2] \\
& + c_{24}^m [\beta_2 + \beta_5 x' + \beta_8 y' + \beta_{11} x' y' + \beta_{14} x'^2 + \beta_{17} y'^2 + z' [\beta_{20} \\
& + \beta_{23} x' + \beta_{26} y' + \beta_{29} x' y' + \beta_{32} x'^2 + \beta_{35} y'^2] \\
& + c_{44}^m [\beta_3 + \beta_6 x' + \beta_9 y' + \beta_{12} x' y' + \beta_{15} x'^2 + \beta_{18} y'^2 + z' [\beta_{21} \\
& + \beta_{24} x' + \beta_{27} y' + \beta_{30} x' y' + \beta_{33} x'^2 + \beta_{36} y'^2]
\end{aligned} \tag{4.85}$$

Using the equilibrium equations in local coordinates as follows:

$$\sigma'_{x,x} + \sigma'_{xy,y} + \sigma'_{xz,z} = 0 \tag{4.86}$$

$$\sigma'_{xy,x} + \sigma'_{y,y} + \sigma'_{yz,z} = 0 \tag{4.87}$$

$$\sigma'_{xz,x} + \sigma'_{yz,y} + \sigma'_{z,z} = 0 \tag{4.88}$$

the transverse stresses can be deduced. Following the same procedure as in the previous section, all the six stresses are found as

$$\begin{aligned}
\sigma'_x = & c_{11}^m [\beta_1 + \beta_4 x' + \beta_7 y' + \beta_{10} x' y' + \beta_{13} x'^2 + \beta_{16} y'^2 + z' (\beta_{19} \\
& + \beta_{22} x' + \beta_{25} y' + \beta_{28} x' y' + \beta_{31} x'^2 + \beta_{34} y'^2)] \\
& + c_{12}^m [\beta_2 + \beta_5 x' + \beta_8 y' + \beta_{11} x' y' + \beta_{14} x'^2 + \beta_{17} y'^2 + z' (\beta_{20} \\
& + \beta_{23} x' + \beta_{26} y' + \beta_{29} x' y' + \beta_{32} x'^2 + \beta_{35} y'^2)] \\
& + c_{14}^m [\beta_3 + \beta_6 x' + \beta_9 y' + \beta_{12} x' y' + \beta_{15} x'^2 + \beta_{18} y'^2 + z' (\beta_{21} \\
& + \beta_{24} x' + \beta_{27} y' + \beta_{30} x' y' + \beta_{33} x'^2 + \beta_{36} y'^2)]
\end{aligned} \tag{4.89}$$

$$\begin{aligned}
\sigma_y^m &= c_{12}^m [\beta_1 + \beta_4 x' + \beta_7 y' + \beta_{10} x' y' + \beta_{13} x'^2 + \beta_{16} y'^2 + z' [\beta_{19} \\
&\quad + \beta_{22} x' + \beta_{25} y' + \beta_{28} x' y' + \beta_{31} x'^2 + \beta_{34} y'^2] \\
&+ c_{22}^m [\beta_2 + \beta_5 x' + \beta_8 y' + \beta_{11} x' y' + \beta_{14} x'^2 + \beta_{17} y'^2 + z' [\beta_{20} \\
&\quad + \beta_{23} x' + \beta_{26} y' + \beta_{29} x' y' + \beta_{32} x'^2 + \beta_{35} y'^2] \\
&+ c_{24}^m [\beta_3 + \beta_6 x' + \beta_9 y' + \beta_{12} x' y' + \beta_{15} x'^2 + \beta_{18} y'^2 + z' [\beta_{21} \\
&\quad + \beta_{24} x' + \beta_{27} y' + \beta_{30} x' y' + \beta_{33} x'^2 + \beta_{36} y'^2]
\end{aligned} \tag{4.90}$$

$$\begin{aligned}
\sigma_{xy}^m &= c_{14}^m [\beta_1 + \beta_4 x' + \beta_7 y' + \beta_{10} x' y' + \beta_{13} x'^2 + \beta_{16} y'^2 + z' [\beta_{19} \\
&\quad + \beta_{22} x' + \beta_{25} y' + \beta_{28} x' y' + \beta_{31} x'^2 + \beta_{34} y'^2] \\
&+ c_{24}^m [\beta_2 + \beta_5 x' + \beta_8 y' + \beta_{11} x' y' + \beta_{14} x'^2 + \beta_{17} y'^2 + z' [\beta_{20} \\
&\quad + \beta_{23} x' + \beta_{26} y' + \beta_{29} x' y' + \beta_{32} x'^2 + \beta_{35} y'^2] \\
&+ c_{44}^m [\beta_3 + \beta_6 x' + \beta_9 y' + \beta_{12} x' y' + \beta_{15} x'^2 + \beta_{18} y'^2 + z' [\beta_{21} \\
&\quad + \beta_{24} x' + \beta_{27} y' + \beta_{30} x' y' + \beta_{33} x'^2 + \beta_{36} y'^2]
\end{aligned} \tag{4.91}$$

$$\begin{aligned}
\sigma'_z{}^m = & -2z' \left[\left(A_{14}^m + \left(\frac{1}{2}z' + z'^2 \right) C_{14}^m + SA_{14}^m + 2D_{14}^m \right) \beta_{10} \right. \\
& + \left(A_{24}^m + \left(\frac{1}{2}z' + z'^2 \right) C_{24}^m + SA_{24}^m + 2D_{24}^m \right) \beta_{11} \\
& + \left(A_{44}^m + \left(\frac{1}{2}z' + z'^2 \right) C_{44}^m + SA_{44}^m + 2D_{44}^m \right) \beta_{12} \\
& + \left(A_{11}^m + \left(\frac{1}{2}z' + z'^2 \right) C_{11}^m + SA_{11}^m + 2D_{11}^m \right) \beta_{13} \\
& + \left(A_{12}^m + \left(\frac{1}{2}z' + z'^2 \right) C_{12}^m + SA_{12}^m + 2D_{12}^m \right) \beta_{14} \\
& + \left(A_{14}^m + \left(\frac{1}{2}z' + z'^2 \right) C_{14}^m + SA_{14}^m + 2D_{14}^m \right) \beta_{15} \\
& + \left(A_{12}^m + \left(\frac{1}{2}z' + z'^2 \right) C_{12}^m + SA_{12}^m + 2D_{12}^m \right) \beta_{16} \\
& + \left(A_{22}^m + \left(\frac{1}{2}z' + z'^2 \right) C_{22}^m + SA_{22}^m + 2D_{22}^m \right) \beta_{17} \\
& + \left(A_{24}^m + \left(\frac{1}{2}z' + z'^2 \right) C_{24}^m + SA_{24}^m + 2D_{24}^m \right) \beta_{18} \\
& + \left(D_{14}^m + \frac{2}{3}z'^2 C_{14}^m + SD_{14}^m + F_{14}^m \right) \beta_{28} \\
& + \left(D_{24}^m + \frac{2}{3}z'^2 C_{24}^m + SD_{24}^m + F_{24}^m \right) \beta_{29} \\
& + \left(D_{44}^m + \frac{2}{3}z'^2 C_{44}^m + SD_{44}^m + F_{44}^m \right) \beta_{30} \\
& + \left(D_{11}^m + \frac{2}{3}z'^2 C_{11}^m + SD_{11}^m + F_{11}^m \right) \beta_{31} \\
& + \left(D_{12}^m + \frac{2}{3}z'^2 C_{12}^m + SD_{12}^m + F_{12}^m \right) \beta_{32} \\
& + \left(D_{14}^m + \frac{2}{3}z'^2 C_{14}^m + SD_{14}^m + F_{14}^m \right) \beta_{33} \\
& + \left(D_{12}^m + \frac{2}{3}z'^2 C_{12}^m + SD_{12}^m + F_{12}^m \right) \beta_{34} \\
& + \left(D_{22}^m + \frac{2}{3}z'^2 C_{22}^m + SD_{22}^m + F_{22}^m \right) \beta_{35} \\
& \left. + \left(D_{24}^m + \frac{2}{3}z'^2 C_{24}^m + SD_{24}^m + F_{24}^m \right) \beta_{36} \right]
\end{aligned} \tag{4.92}$$

$$\begin{aligned}
\sigma'_{xz}{}^m &= A_{11}^m \beta_4 + A_{12}^m \beta_5 + A_{14}^m \beta_6 + A_{14}^m \beta_7 + A_{24}^m \beta_8 + A_{44}^m \beta_9 \\
&\quad + (A_{14}^m x' + A_{11}^m y') \beta_{10} + (A_{14}^m x' + A_{11}^m y') \beta_{11} \\
&\quad + (A_{44}^m x' + A_{14}^m y') \beta_{12} + 2A_{11}^m x' \beta_{13} + 2A_{12}^m x' \beta_{15} \\
&\quad + 2A_{14}^m y' \beta_{16} + 2A_{24}^m y' \beta_{17} + 2A_{44}^m y' \beta_{18} + D_{11}^m y' \beta_{22} \\
&\quad + D_{12}^m \beta_{23} + D_{14}^m \beta_{24} + D_{14}^m \beta_{25} + D_{24}^m \beta_{26} + D_{44}^m \beta_{27} \\
&\quad + (D_{14}^m x' + D_{11}^m y') \beta_{28} + (D_{24}^m x' + D_{12}^m y') \beta_{29} \\
&\quad + (D_{44}^m x' + D_{14}^m y') \beta_{30} + 2D_{11}^m x' \beta_{31} + 2D_{12}^m x' \beta_{32} \\
&\quad + 2D_{14}^m x' \beta_{33} + 2D_{14}^m y' \beta_{34} + 2D_{24}^m y' \beta_{35} + 2D_{44}^m y' \beta_{36}
\end{aligned} \tag{4.93}$$

$$\begin{aligned}
\sigma'_{yz}{}^m &= A_{14}^m \beta_4 + A_{24}^m \beta_5 + A_{44}^m \beta_6 + A_{12}^m \beta_7 + A_{22}^m \beta_8 + A_{24}^m \beta_9 \\
&\quad + (A_{14}^m y' + A_{11}^m x') \beta_{10} + (A_{22}^m x' + A_{24}^m y') \beta_{11} \\
&\quad + (A_{24}^m x' + A_{44}^m y') \beta_{12} + 2A_{14}^m x' \beta_{13} + 2A_{24}^m x' \beta_{15} \\
&\quad + 2A_{12}^m y' \beta_{16} + 2A_{22}^m y' \beta_{17} + 2A_{24}^m y' \beta_{18} + D_{14}^m y' \beta_{22} \\
&\quad + D_{24}^m \beta_{23} + D_{44}^m \beta_{24} + D_{12}^m \beta_{25} + D_{22}^m \beta_{26} + D_{24}^m \beta_{27} \\
&\quad + (D_{12}^m x' + D_{14}^m y') \beta_{28} + (D_{22}^m x' + D_{24}^m y') \beta_{29} + (D_{24}^m x' \\
&\quad + D_{44}^m y') \beta_{30} + 2D_{14}^m x' \beta_{31} + 2D_{24}^m x' \beta_{32} + 2D_{44}^m x' \beta_{33} \\
&\quad + 2D_{12}^m y' \beta_{34} + 2D_{22}^m y' \beta_{35} + 2D_{24}^m y' \beta_{36}
\end{aligned} \tag{4.94}$$

with

$$A_{kl}^m = \sum_{i=2}^m h_i (C_{kl}^i - C_{kl}^{i-1}) - z' C_{kl}^m + C_{kl}^1 h_1 \tag{4.95}$$

$$D_{kl}^m = \frac{1}{2} \left[\sum_{i=2}^m h_i^2 (C_{kl}^i - C_{kl}^{i-1}) - z'^2 C_{kl}^m + C_{kl}^1 h_1^2 \right] \tag{4.96}$$

$$SA_{kl}^m = 2 \sum_{i=2}^m h_i (A_{kl}^i - A_{kl}^{i-1}) + 2A_{kl}^1 h_1 \quad (4.97)$$

$$SD_{kl}^m = 2 \sum_{i=2}^m h_i (D_{kl}^i - D_{kl}^{i-1}) + 2D_{kl}^1 h_1 \quad (4.98)$$

$$F_{kl}^m = \sum_{i=2}^m \frac{4}{3} h_i^3 (C_{kl}^i - C_{kl}^{i-1}) + \frac{4}{3} C_{kl}^1 h_1^3; \quad (4.99)$$

Defining

$$AD_{kl}^m = -2 * Z' \left(A_{kl}^m + \left(\frac{1}{2} Z' + z'^2 \right) C_{kl}^m + SA_{kl}^m + 2 * D_{kl}^m \right) \quad (4.100)$$

$$DF_{kl}^m = -2 * z' \left(D_{kl}^m + \left(\frac{2}{3} z'^2 \right) C_{kl}^m + SD_{kl}^m + F_{kl}^m \right) \quad (4.101)$$

the stresses can be written in matrix form in terms of $\{\beta\}$ as follows:

$$\{\sigma'\}^m = [P']^m \{\beta\} \quad (4.102)$$

where

$$[P']^m = \text{see next page} \quad (4.103)$$

$$[P']^m = \begin{bmatrix} C_{11} & C_{12} & C_{14} & C_{11}x' & C_{12}x' & C_{14}x' & C_{11}y' & C_{12}y' & C_{14}y' \\ C_{12} & C_{22} & C_{24} & C_{12}x' & C_{22}x' & C_{24}x' & C_{12}y' & C_{22}y' & C_{24}y' \\ 0 & 0 & 0 & 0 & 0 & 0 & 0 & 0 & 0 \\ C_{14} & C_{24} & C_{44} & C_{14}x' & C_{24}x' & C_{44}x' & C_{14}y' & C_{24}y' & C_{44}y' \\ 0 & 0 & 0 & A_{11} & A_{12} & A_{14} & A_{14} & A_{24} & A_{44} \\ 0 & 0 & 0 & A_{14} & A_{24} & A_{44} & A_{12} & A_{22} & A_{24} \end{bmatrix}$$

$$\begin{bmatrix} C_{11}x'y' & C_{12}x'y' & C_{14}x'y' & C_{11}x'^2 & C_{12}x'^2 & C_{14}x'^2 & C_{11}y'^2 & C_{12}y'^2 & C_{14}y'^2 \\ C_{12}x'y' & C_{22}x'y' & C_{24}x'y' & C_{12}x'^2 & C_{22}x'^2 & C_{24}x'^2 & C_{12}y'^2 & C_{22}y'^2 & C_{24}y'^2 \\ AD_{14} & AD_{24} & AD_{44} & AD_{11} & AD_{12} & AD_{14} & AD_{12} & AD_{22} & AD_{24} \\ C_{14}x'y' & C_{24}x'y' & C_{44}x'y' & C_{14} & C_{24}x'^2 & C_{44}x'^2 & C_{14}y'^2 & C_{24}y'^2 & C_{44}y'^2 \\ A_{14}x' + A_{11}y' & A_{24}x' + A_{12}y' & A_{44}x' + A_{14}y' & 2A_{11}x' & 2A_{12}x' & 2A_{14}x' & 2A_{14}y' & 2A_{24}y' & 2A_{44}y' \\ A_{12}x' + A_{14}y' & A_{22}x' + A_{24}y' & A_{24}x' + A_{44}y' & 2A_{14}x' & 2A_{24}x' & 2A_{44}x' & 2A_{12}y' & 2A_{22}y' & 2A_{24}y' \end{bmatrix}$$

$$\begin{bmatrix} C_{11}z' & C_{12}z' & C_{14}z' & C_{11}z'x' & C_{12}z'x' & C_{14}z'x' & C_{11}z'y' & C_{12}z'y' & C_{14}z'y' \\ C_{12}z' & C_{22}z' & C_{24}z' & C_{12}z'x' & C_{22}z'x' & C_{24}z'x' & C_{12}z'y' & C_{22}z'y' & C_{24}z'y' \\ 0 & 0 & 0 & 0 & 0 & 0 & 0 & 0 & 0 \\ C_{14}z' & C_{24}z' & C_{44}z' & C_{14}z'x' & C_{24}z'x' & C_{44}z'x' & C_{14}z'y' & C_{24}z'y' & C_{44}z'y' \\ 0 & 0 & 0 & D_{11} & D_{12} & D_{14} & D_{14} & D_{24} & D_{44} \\ 0 & 0 & 0 & D_{14} & D_{24} & D_{44} & D_{12} & D_{22} & D_{24} \end{bmatrix}$$

$$\begin{bmatrix} C_{11}z'x'y' & C_{12}z'x'y' & C_{14}z'x'y' & C_{11}z'x'^2 & C_{12}z'x'^2 & C_{14}z'x'^2 & C_{11}z'y'^2 & C_{12}z'y'^2 & C_{14}z'y'^2 \\ C_{12}z'x'y' & C_{22}z'x'y' & C_{24}z'x'y' & C_{12}z'x'^2 & C_{22}z'x'^2 & C_{24}z'x'^2 & C_{12}z'y'^2 & C_{22}z'y'^2 & C_{24}z'y'^2 \\ DF_{14} & DF_{24} & DF_{44} & DF_{11} & DF_{12} & DF_{14} & DF_{12} & DF_{22} & DF_{24} \\ C_{14}z'x'y' & C_{24}z'x'y' & C_{44}z'x'y' & C_{14}z'x'^2 & C_{24}z'x'^2 & C_{44}z'x'^2 & C_{14}z'y'^2 & C_{24}z'y'^2 & C_{44}z'y'^2 \\ D_{14}x' + D_{11}y' & D_{24}x' + D_{12}y' & D_{44}x' + D_{14}y' & 2D_{11}x' & 2D_{12}x' & 2D_{14}x' & 2D_{14}y' & 2D_{24}y' & 2D_{44}y' \\ D_{12}x' + D_{14}y' & D_{22}x' + D_{24}y' & D_{24}x' + D_{44}y' & 2D_{14}x' & 2D_{24}x' & 2D_{44}x' & 2D_{12}y' & 2D_{22}y' & 2D_{24}y' \end{bmatrix}^m$$

To form the [P'] matrix, the local coordinates x' , y' , and z' need to be expressed in term of global coordinates x , y , and z . For a cylindrical shell in which the origin of the global Cartesian coordinates coincides with the center of the cylinder, the coordinate transformations (while taking in account the translation of the origin) are given by the following expression.

$$\begin{aligned}x' &= \frac{1}{r_i} [z_i(x - x_i) - x_i(z - z_i)] \\y' &= y \\z' &= \frac{1}{r_i} [x_i(x - x_i) + z_i(z - z_i)]\end{aligned}\tag{4.104}$$

where

$$r_i = \sqrt{(x_i^2 + z_i^2)}$$

4.2.7 Development of Stiffness Matrix

After forming the [P'] and [B'] matrices, the following layered matrices based on Eqs (3.16) and (3.17) are found to be:

$$[H'^i] = \int_{V_n} [P']^{iT} [S]^{iT} [P']^i dV,\tag{4.105}$$

$$[G'^i] = \int_{V_n} [P']^{iT} [B'] dV\tag{4.106}$$

Since the matrices $[P]^i$ and $[B]$ are expressed in the normalized coordinates system, the element volume is rewritten using the following standard transformation formula demonstrated by Murnaghan [81]:

$$dV = |J|d\xi d\eta d\zeta\tag{4.107}$$

By substituting Eq. (4.107) into Eq. (4.105) and Eq. (4.106) the $[H^i]$ and $[G^i]$ matrices can be expressed as

$$H^i = \int_{-1}^{+1} \int_{-1}^{+1} \int_{-1}^{+1} [P']^{iT} [S]^{iT} [P']^i |J| d\xi d\eta d\zeta, \quad (4.108)$$

$$G^i = \int_{-1}^{+1} \int_{-1}^{+1} \int_{-1}^{+1} [P']^{iT} [B'] |J| d\xi d\eta d\zeta \quad (4.109)$$

These integrals are carried out numerically using the Gaussian quadrature method.

However, the compliance and stress-parameters matrices change from one layer to another; they are not continuous functions of ζ . Therefore the thickness concept is utilized by splitting the limits of integration through each layer. This is done by modifying the variable ζ to ζ_m in any i -th layer such that ζ_m varies from -1 to +1 in the layer. The change of variable is obtained from

$$\zeta = -1 + 2 \left[\sum_{i=1}^m t_i - t_i(1 - \zeta_m) \right] / t \quad (4.110)$$

and

$$d\zeta = \frac{t_i}{t} d\zeta_m \quad (4.111)$$

Here, t_i is the thickness of layer m and t the element thickness.

Upon substituting of Eq. (4.111) into Eqs (4.108) and (4.109) the $[H]^i$ and $[G]^i$ matrices take the following form:

$$[H']^i = \frac{t_i}{t} \int_{-1}^{+1} \int_{-1}^{+1} \int_{-1}^{+1} [P']^{iT} [S]^{iT} [P']^i |J| d\xi d\eta d\zeta_m, \quad (4.112)$$

$$[G']^i = \frac{t_i}{t} \int_{-1}^{+1} \int_{-1}^{+1} \int_{-1}^{+1} [P']^{iT} [B'] |J| d\xi d\eta d\zeta_m \quad (4.113)$$

Applying the Gauss quadrature formula, one obtains

$$[H']^i = \sum_1^{NX} \sum_1^{NY} \sum_1^{NZ} P'^{iT} S^{iT} P'^i |J| W_x W_y W_z, \quad (4.114)$$

$$[G']^i = \sum_1^{NX} \sum_1^{NY} \sum_1^{NZ} [P']^{iT} [B'] |J| W_x W_y W_z, \quad (4.115)$$

Here, W_x , W_y , and W_z are the convergence parameters associated with the number of Gauss points, NX , NY , and NZ respectively. The element matrices $[H']$ and $[G']$ can then be obtained by summing the contribution of all layers

$$[H'] = \sum_{i=1}^{NL} [H']^i \quad (4.116)$$

$$[G'] = \sum_{i=1}^{NL} [G']^i \quad (4.117)$$

where NL is the total number of layers. After computing the inverse of the $[H']$ matrix, the stiffness matrix for that element is formed by using Eq. (3.22)

$$[K'] = [G']^T [H']^{-1} [G'] \quad (4.118)$$

To assemble the final stiffness matrix, the element stiffness matrix has to be transformed from local to global coordinates. The finite element system of equations is given in the local coordinate system as

$$[K']\{q'\} = \{Q'\} \quad (4.119)$$

where $\{q'\}$ is the vector of generalized displacements (Eq. (2.69)) and $\{Q'\}$ the element load vector. Using the transformation matrix $[DT]$ defined in Eq. (4.71), these can be expressed in global coordinates system as

$$\{q'\} = [DT]\{q\} \quad (4.120)$$

and

$$\{q'\} = [DT]\{Q\} \quad (4.121)$$

Upon substituting Eqs. (4.120) and (4.121) into (4.119) one obtains

$$[K'] [DT]\{q\} = [DT]\{Q\} \quad (4.122)$$

Modifying this equation by pre-multiplying both side by one gets

$$[DT]^{-1} [K'] [DT]\{q\} = \{Q\} \quad (4.123)$$

Therefore, the element stiffness matrix in global coordinates system $[Ke]$ is derived as

$$[Ke] = [DT]^{-1} [K'] [DT] \quad (4.124)$$

Finally, the global stiffness matrix is obtained through algebraic addition of all element stiffness matrices.

The external force vectors are derived from the modified complementary energy formulation and expressed as (Eq. (3.17))

$$\{Q\}^T = \int_{S_n} \{\bar{T}\}^T dS \quad (4.125)$$

The prescribed boundary tractions are approximated for each element using the same isoparametric eight-node shape functions, N_i , as defined by Ep. (4.2). Therefore the element force vector is said to be a “kinematically consistent nodal load vector” [148], and is computed as

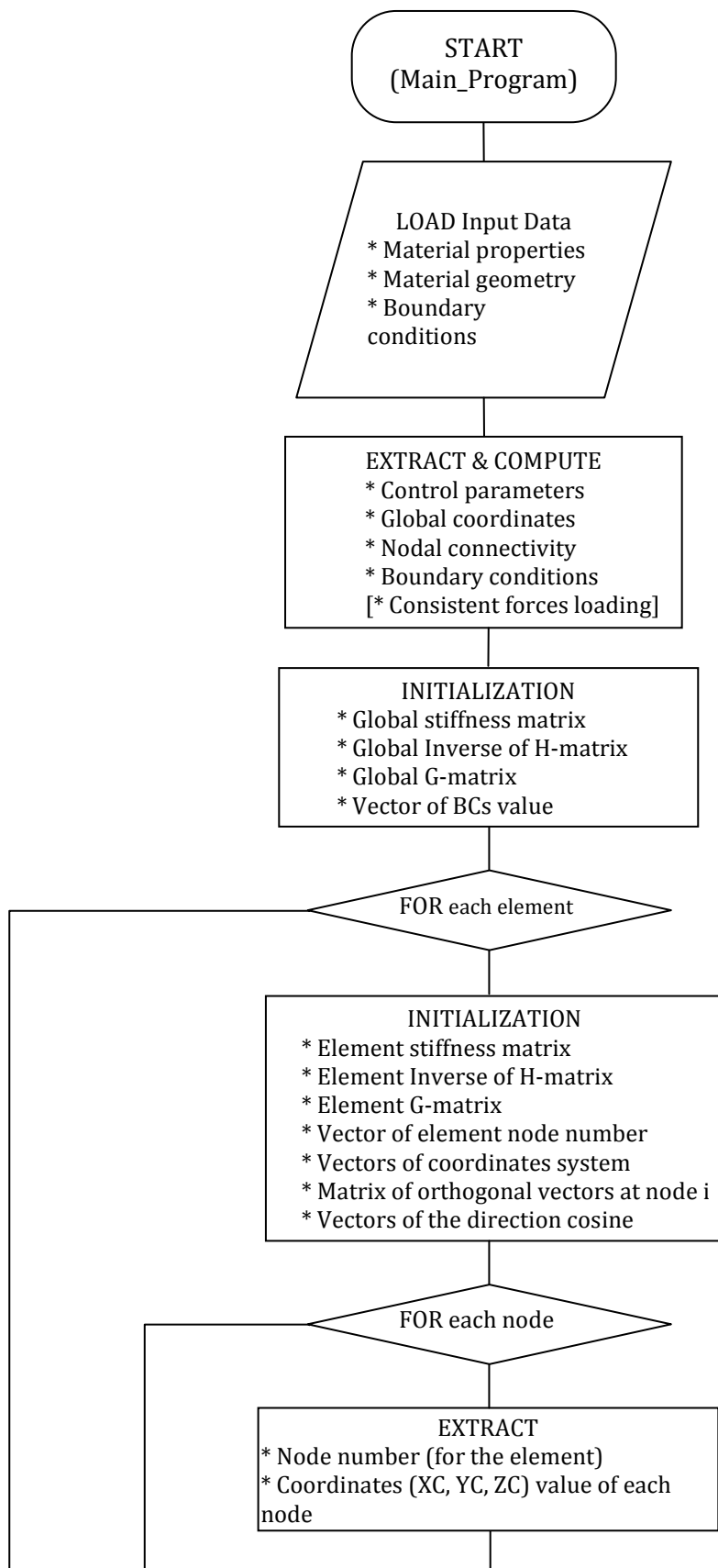
$$\{Q_i\} = \int_{S_n} [N]^T \{\bar{T}\} dS \quad (4.126)$$

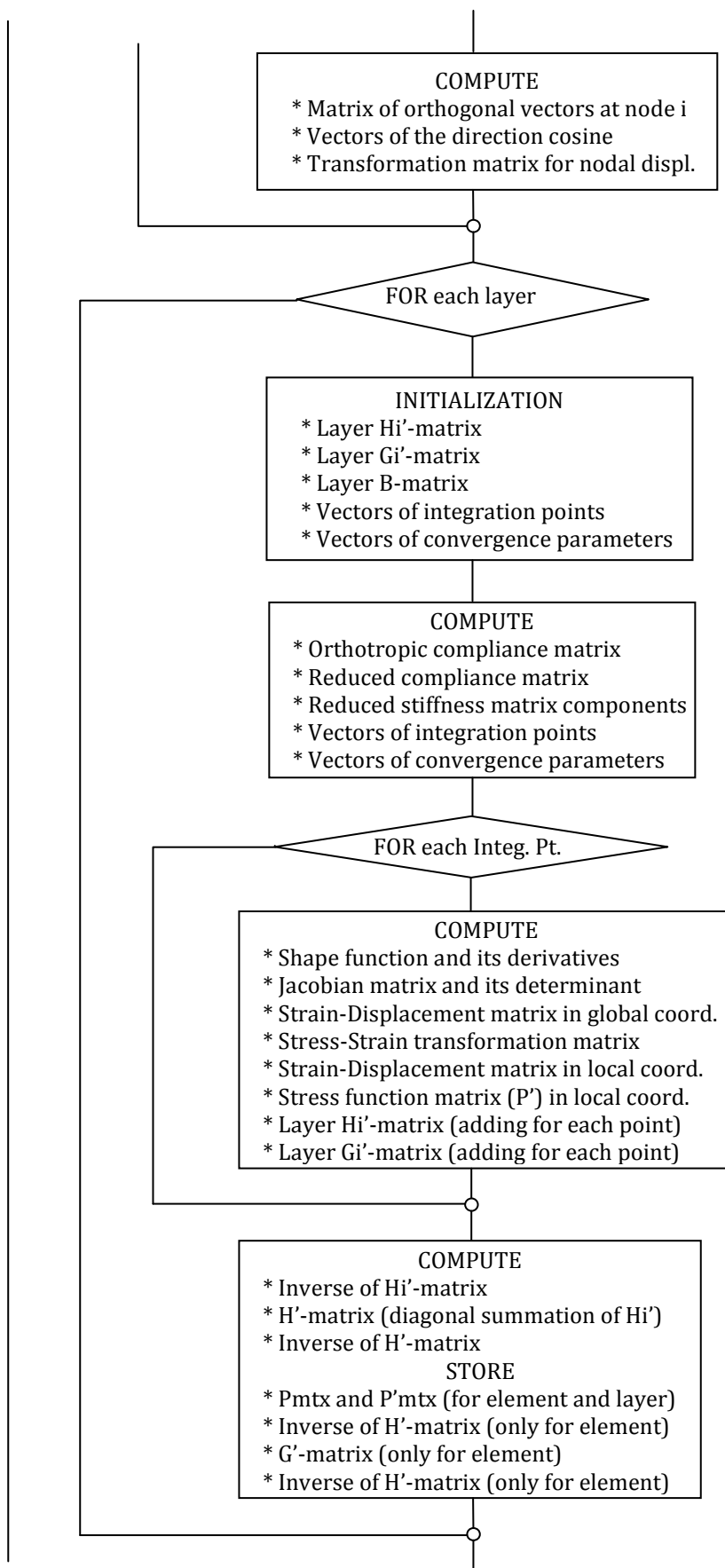
The global force matrix is also obtained by assembling all the element matrices through algebraic summation. After calculating the nodal displacements, $\{q\}$, the strain parameters and the stresses are obtained using Eqs (4.42) and (4.43), respectively.

4.3 Numerical Implementation (Development of FE code)

4.3.1 Flowchart

The finite element programs for either plates or shells analysis are developed using MATLAB language [160]. Both codes follow closely the formulation procedure of the previous sections and they can perform the static analysis of composite laminated plates and shells under various loading conditions such as concentrated load, simple or double sinusoidal load, distributed load, self weight or internal pressure. A detailed flowchart of the shell element implementation is given in Figure 4.7.





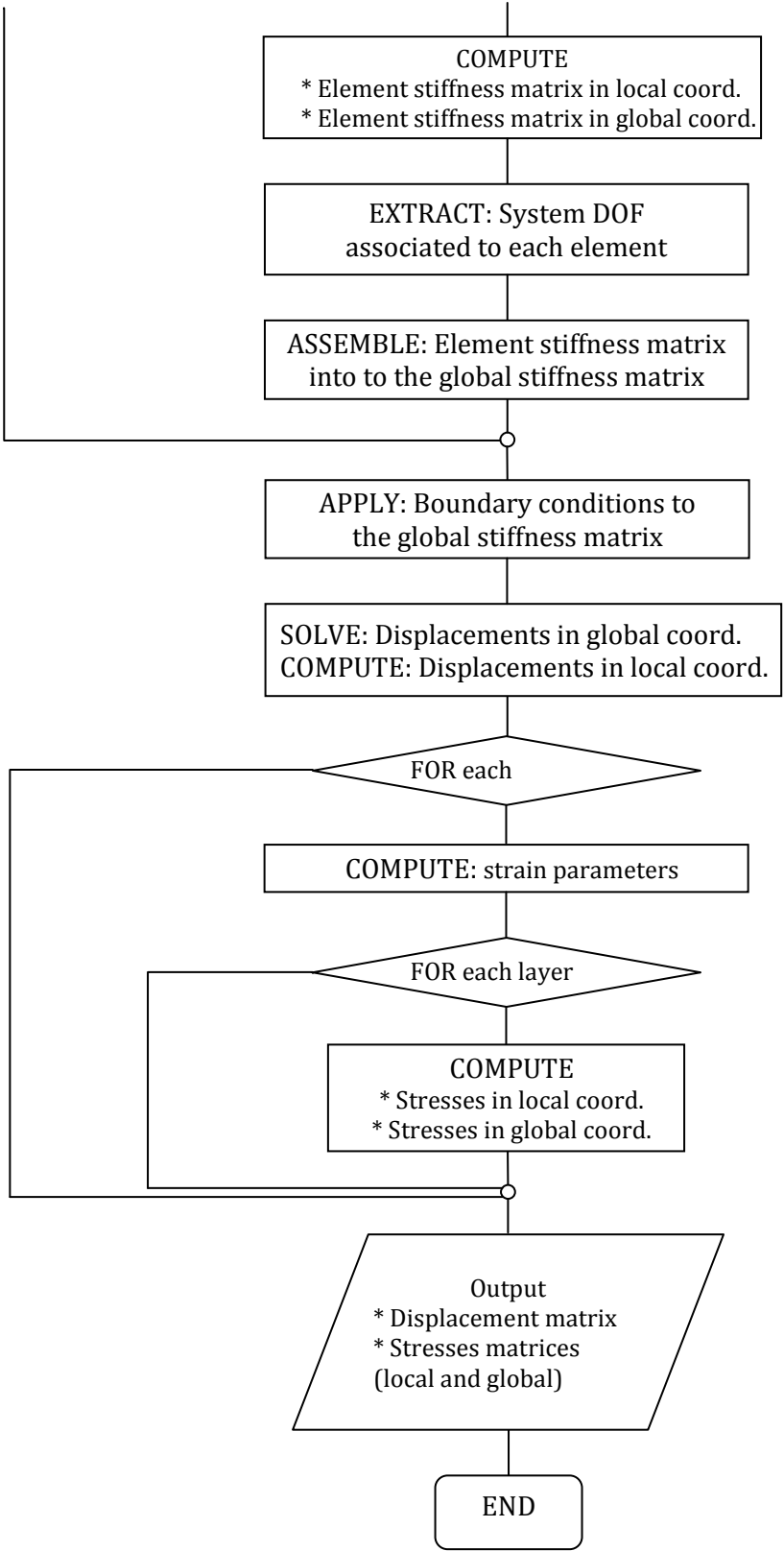


Figure 4.7: Flow chart of the MCPSOLIDSHELL program

4.3.2 Matlab Code Input

All inputs are specified in one input data file and read by the main program. The data file contains, the material properties with the elastic coefficients given in the principal material directions, the basic element description (total number of layers, nodes, DOF per node), the nodal coordinates and their connectivity to each element, and the loading and boundary conditions. The code for plate analysis can be found in Appendix B.

The finite element system of equations is solved easily in MATLAB using the anti-slash (\) notation. The zero energy mode is analyzed automatically and a feedback message is generated when the solution is close to being singular. All the proposed elements were successfully tested.

CHAPTER 5

SAMPLE ANALYSES AND VERIFICATION

To assess the accuracy of the present strain-based elements formulated via the use of a modified complementary principle, the static bending analysis of several example problems for various geometry and material properties is analyzed. Displacements and stresses are investigated and the results are compared with the results from other models in the literature (or those presented in Chapter 2) as well as three-dimensional elasticity solutions. A criterion of 5% percent difference with the referenced solution is considered as acceptable in this study. The rate of convergence and the shear locking phenomenon are addressed by examining elements with lower order formulation (FELM36 and FELM48) because these are the ones likely to exhibit shear locking problems.

To simplify the presentation in this Chapter, the higher order elements which are the main focus of this investigation are classified within two main categories, Type I elements and Type II elements. Each category is separated into two subgroups, “Serendipity” associated elements and “Lagrange” associated elements. Thus, there are four subgroups described as follows:

- i) The Type I elements have independent higher order rotational strain basis functions – elements identified with ‘I’ at the end of the nomenclature (such as TELM36I). For the first subgroup of Type I elements, the in-plane basis polynomials strain function are the same as the “serendipity” basis polynomials ($\{1, x, y, xy, x^2, y^2, x^2y, xy^2\}$). The second subgroup is composed of elements whose basis strain functions are complete third order basis polynomials

$(\{1, x, y, xy, x^2, y^2, x^2y, xy^2, x^3, y^3\})$. They will be referred to as the “Lagrange” type elements.

- ii) The type II elements have a non-linear variation of the rotational strain functions. Its first subgroup is made of elements having the same basis in-plane polynomials function as the “Serendipity” one, and the other subgroup as “Lagrange” complete basis polynomials, as previously defined.

Table 5.1 shows the elements used to analyze the different example problems classified in sub-groups. Although all the twenty-one elements were scrutinized in this investigation, the discussions are limited to elements which exhibit meaningful results.

Table 5.1: Third order elements used to analyze different case problems

Elements classification	Type I Elements with independent higher order strain functions	Type II Elements with non-linear variation of the rotational basis strain functions
Elements consistent with the “Serendipity” element	TELM45I, TELM51I, TELM54I, TELM60I, TELM72I, (Type I-S)	TELM36, TELM422, TELM482, (Type II-S)
Elements with the complete “Lagrange” element	TELM542I, TELM57I, TELM602I, TELM66I, TELM78I, TELM84I, TELM90I, (Type I-L)	TELM42, TELM54, TELM54, TELM60. (Type II-L)

The use of a convergence parameter will be discussed in relation with the type of structure analyzed. The convergence parameter is a direct proportional coefficient to the z terms. The convergence parameters are generally smaller than one, thus their inverse may provide an easier number for graphical presentation. To highlight the importance of the convergence parameter, two figures are given for each characteristic – boundary

conditions or thicknesses. In the first (Figure a)), the evaluation of the error (compared to the exact elasticity solution or the percentage difference if compared to an analytical solution) starts with the convergence parameter equal to one, meaning a strain function without weighing factor. The second (Figure b)) shows the change in error when the range of convergence parameters which gives an excessive error is removed. The elements associated with a non-linear variation of the rotational basis strain functions are presented right after the analysis of elements associated with independent strain functions.

5.1 Displacement Examples

Although most of the discussion and attentions is focused on improving the transverse stresses, it is still important that the new elements also perform well for the displacements. For the bending of plates, the transverse displacement, w , is the most important of these. Thus, it will receive the most attention when comparison results are available without however neglecting the in-plane displacements. In the present analyses, all layers constituting a plate or a shell are assumed to be of constant thickness. The dimensions of the plate along the x-axis will be labeled a , and b along the y-axis, as shown in Figure 5.1. The letter 'S' is used as the ratio of thickness to span ($S=h/a$). The generalized displacements are u_0 , v_0 , w_0 , θ_x , and θ_y .

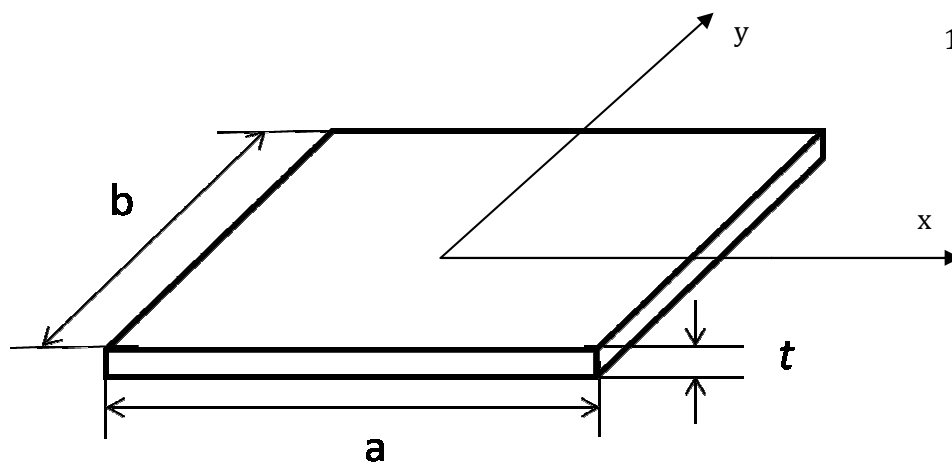


Figure 5. 1: Geometry and axes orientation for a plate

5.1.1 Deflection of an Isotropic Square Plate

An isotropic square plate with sides of length a , various thicknesses t , and under both a concentrated and a uniformly distributed load P is analyzed. Also, two different boundary conditions (simply supported and clamped edges) are selected for the analysis. In order to check the convergence rate of the results, the number of elements is varied from one to sixteen. Because of symmetry, only one quadrant of the plate is analyzed. Four meshing sizes are used, with the number of elements per side varying from one to four.

The material properties are given as

$$E = 26.0E06 \text{ psi}$$

$$\nu = 0.3$$

a) Boundary Conditions 1: Simply Supported Edges

The top surface of the plate is subjected to a uniformly distributed load of 1 psi.

The boundary conditions are

$$\text{at } x = 0, \quad y = 0; \quad w = 0;$$

$$\text{at } x = 5 \text{ in.}, \quad u_0 = \theta_y = 0;$$

$$\text{at } y = 0, \quad w = \theta_y = 0;$$

$$\text{at } y = 5 \text{ in.}, \quad v_0 = \theta_x = 0$$

The exact solutions using classical plate theory (Section 2.2.1) of both a simply supported and clamped square plate are presented by Timoshenko and Young [107].

The displacement solution for the simply supported square plate problem is given in a series form as follows:

$$w_0(x, y) = \frac{16Q_0}{\pi^6 D} \sum_{k=1}^{\infty} \sum_{l=1}^{\infty} \frac{\sin\left(\frac{k\pi x}{a}\right) \sin\left(\frac{l\pi y}{a}\right)}{kl \left[\left(\frac{k}{a}\right)^2 + \left(\frac{l}{a}\right)^2 \right]^2} \quad (5.1)$$

where D is the flexural rigidity of the plate defined in Eq. (2.30). The expression of the maximum deflection given is by

$$w_{max} = 0.0046 \frac{Q_0 a^4}{D} \quad (5.2)$$

The transverse displacement is normalized for comparison purpose through the following equation

$$w_N = w_0 \frac{D}{Q_0 a^4} * 100 \quad (5.3)$$

The finite element results for a thin ($S = 0.01$) and a very thin ($S = 0.005$) plate are presented in Table 2. The convergence analysis of the center deflection in terms of the ratio of the finite element results to the analytical result is illustrated in Figures 5.2 and 5.3. The analysis is done using elements FELM36 and FELM48 for both plates. One notes that no shear locking is observed. Also noticeable is the rapid convergence of both types of elements. They give excellent accuracy with a mesh of only four elements. Thus, they can be used for plate analysis. Note that element FELM48 has a slower convergenve

rate. One reason is that its in-plane strain function has more higher order terms than FELM36.

Table 5.2: Normalized center deflection of an isotropic simply supported square plate

S= h/a =0.01			
N*	Analytical solution	FELM36	FELM48
1	0.4062	0.3335	0.3025
2	0.4062	0.3985	0.3982
3	0.4062	0.4035	0.4034
4	0.4062	0.4049	0.4049
S= h/a =0.005			
N	Analytical solution	FELM36	FELM48
1	0.4062	0.3329	0.3012
2	0.4062	0.3981	0.3979
3	0.4062	0.4032	0.4031
4	0.4062	0.4046	0.4046

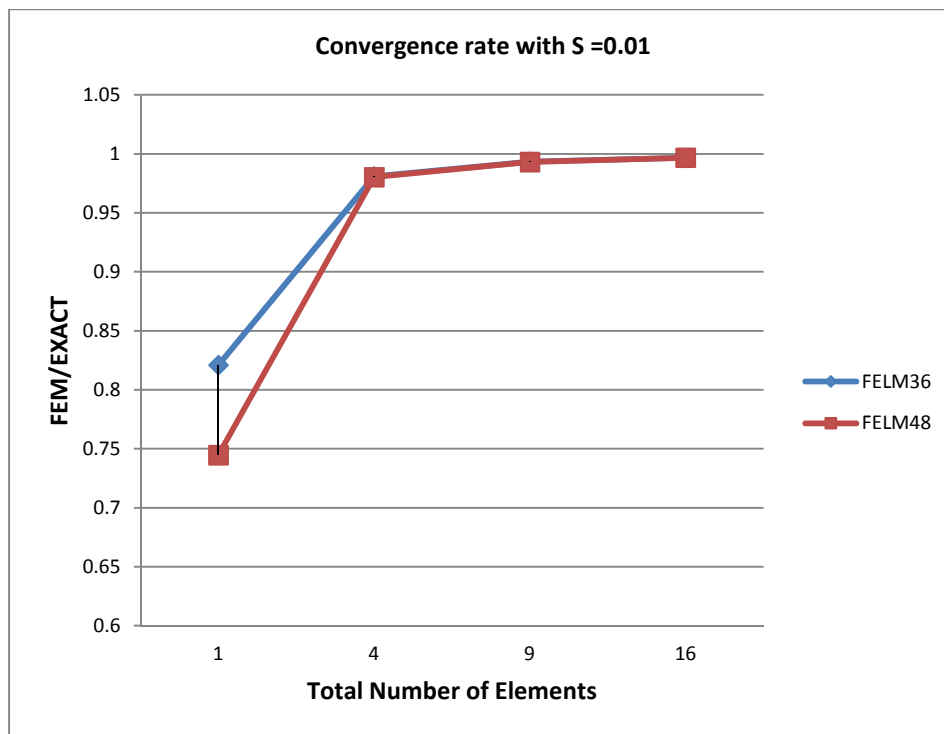


Figure 5.2: Convergence rate of the center deflection for a thin isotropic simply supported plate ($S=0.01$).

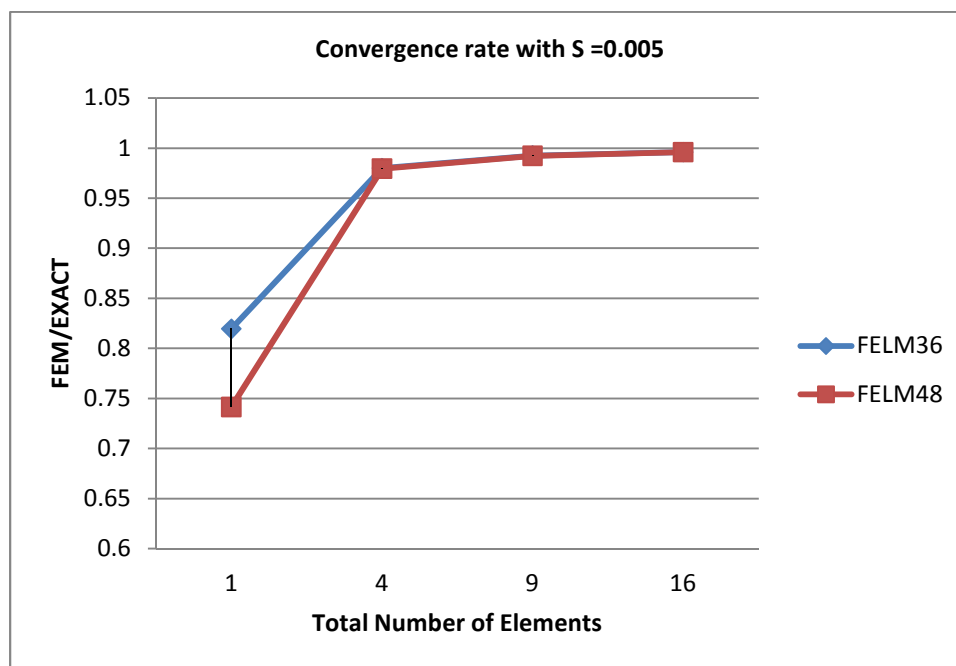


Figure 5.3: Convergence rate for a moderately thin isotropic simply supported plate ($S=0.005$).

b) Boundary Conditions 2: Clamped Edges

In this case, the same material properties and geometry as in *a)* is used. However, the load condition becomes a transverse concentrated load of 100 lbs. at the center of the top surface of the plate. The boundary conditions for clamped edges are given as

$$\text{at } x = 0, \quad u_0 = v_0 = w = \theta_x = \theta_y = 0;$$

$$\text{at } x = 5 \text{ in,} \quad u_0 = \theta_y = 0;$$

$$\text{at } y = 0, \quad u_0 = v_0 = w = \theta_x = \theta_y = 0;$$

$$\text{at } y = 5 \text{ in,} \quad v_0 = \theta_x = 0.$$

The expression of the maximum deflection is given by [107]

$$w_{max} = 0.0056 \frac{Q_0 a^4}{D} \quad (5.4)$$

The transverse displacement at the center of the plate (maximum deflection) is normalized by the following equation

$$w_N = w_{max} \frac{D}{Q_0 a^4} * 100 \quad (5.5)$$

Table 5.3 shows the results for the thin and very thin clamped square plate. The number of elements starts with four because one element is not enough to represent the proper behavior of a clamped edge plate. It can be observed from Figure 5.5 that there is a slower rate of convergence in comparison with the simply supported case. The displacements are better predicted for the thin plate. As before, FELM48 has a slower rate of convergence.

Table 5. 3: Normalized center deflection of an isotropic clamped square plate

S= h/a =0.01			
N	Analytical solution	FELM36	FELM48
1	---	---	---
2	0.5600	0.3924	0.3716
3	0.5600	0.5070	0.4923
4	0.5600	0.5288	0.5281
S= h/a =0.005			
N	Analytical solution	FELM36	FELM48
1	---	---	---
2	0.5600	0.3846	0.3664
3	0.5600	0.5017	0.4865
4	0.5600	0.5232	0.5178

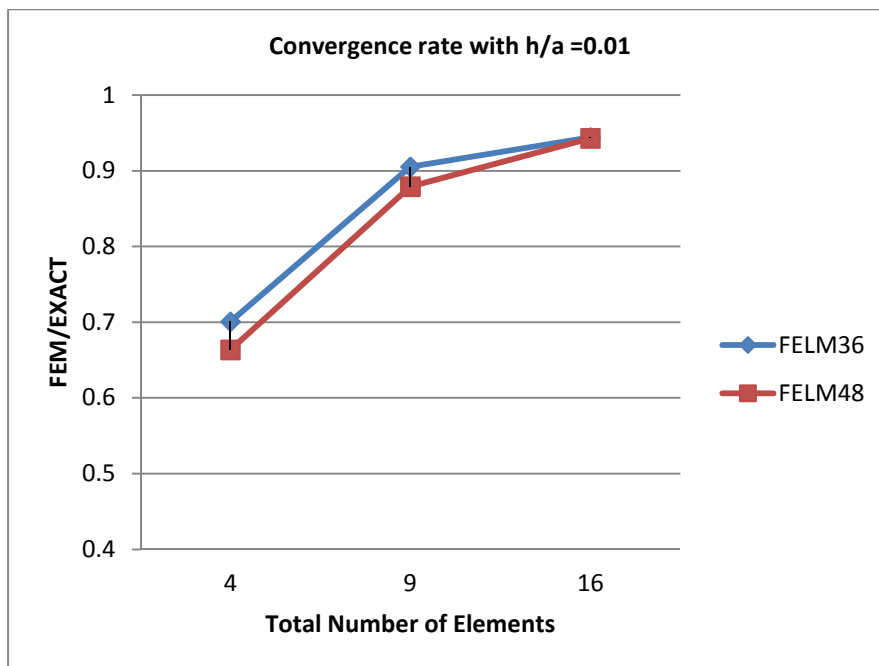


Figure 5. 4: Normalized center deflection of an isotropic clamped square plate ($S=0.01$).

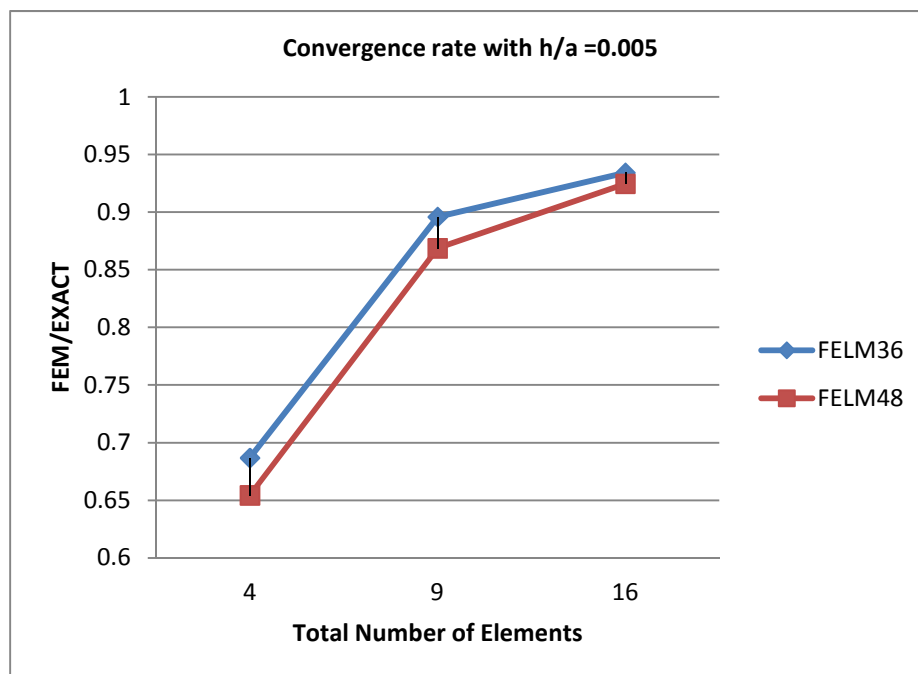


Figure 5. 5: Normalized center deflection of an isotropic clamped square plate ($S=0.005$).

5.1.2 Displacements of Two-Layered Angle-Ply Composite Square Plate

In this section, a composite laminated square plate with two angle-ply ($\pm\theta$) lamina is analyzed (Figure 5.6). The side lengths are equal to a , with a total thickness of t . The two layers have equal thickness and are made of the same material. The top surface of the plate is subjected to a uniformly distributed pressure loading of magnitude Q_0 .

The mechanical properties of each layer are as follows:

$$E_{11} = 40.0E06 \text{ psi} \quad E_{22} = 1.0E06 \text{ psi}$$

$$G_{12} = G_{23} = 0.5E06 \text{ psi}$$

$$\nu_{12} = \nu_{23} = 0.25$$

Dimensions: $a = 10 \text{ in}$ $t = 0.2 \text{ in}$

Boundary Conditions: The plate is simply supported on all four edges as shown in Figure 5.6. Since the laminate structure is not symmetric and the boundary conditions are set up as follows:

$$\text{at } x = 0 \text{ and } 10, \quad w = u_0 = \theta_x = 0;$$

$$\text{at } x = 0 \text{ and } 10, \quad w = v_0 = \theta_y = 0.$$

Whitney [156] provides an analytical solution by using a Fourier series approach. Spilker [76] noticed an error in Whitney's calculation. He also formulated a solution using a hybrid displacement formulation for thick plates. Spilker's elements were formulated such that generalized displacements were completely independent for each layer, thus, using more computer time to solve the problem. Also, he used ten elements along each side of the plate. This case study uses only four elements per side, for a total number of sixteen elements (compared to one hundred elements used by Spilker). Afshari

[150] also uses sixteen first order theory elements to analyze this problem. All of their results are used for comparison purpose. The displacement results are presented in Tables 5.4 and 5.5. The number in the bracket is the percentile displacement error computed using the following equation:

$$Error = \left(1 - \frac{U_{EXACT}}{U_{FEM}}\right) * 100 \quad (5.6)$$

One can notice that the results for the transverse displacements, for both FELM36 and FELM48, are in excellent agreement with the exact analytical solution for both fiber orientations. Although, the in-plane displacements results are very good (less than 3.65 %), they give poorer results compared to the other solutions. One reason is that FELM36 in-plane basis strain functions are two terms short of the “serendipity” basis polynomials (missing the terms xy^2 , and x^2y), while those of FELM48 are augmented by two terms (x^3 , and y^3).

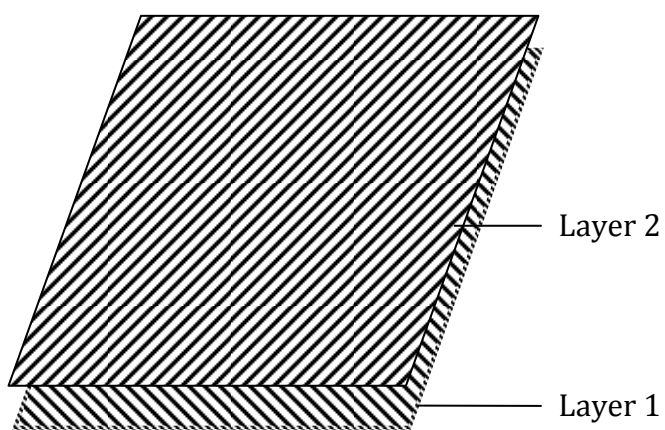
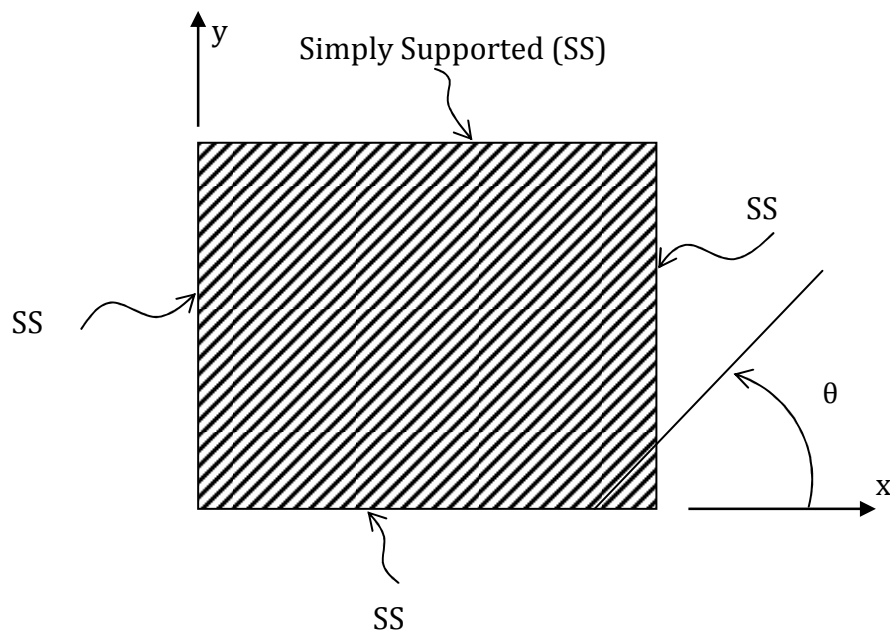


Figure 5. 6: Boundary conditions, fiber orientation and stacking lay up of angle-ply square plate.

Table 5. 4: Displacement of a simply supported two layer anti-symmetric square composite plate with fiber orientation $\theta=\pm 35^\circ$

	Approach	Uo	Vo	W
$\theta = \pm 35^\circ$	Exact [156]	0.01465	0.01610	0.9451
	Spilker [76]	0.01460 (-0.34)	0.01600 (-0.62)	0.9600 (1.55)
	Afshari [150]	0.01463 (-0.14)	0.01619 (0.56)	0.9570 (1.24)
	FELM36	0.01498 (2.20)	0.01671 (3.65)	0.9481 (0.32)
	FELM48	0.01492 (1.81)	0.01661 (3.07)	0.9487 (0.38)

Table 5. 5: Displacement of a simply supported two layer anti-symmetric square composite plate with fiber orientation $\theta=\pm 45^\circ$

	Approach	Uo	Vo	W
$\theta = \pm 45^\circ$	Exact [156]	0.01481	0.01481	0.9152
	Spilker [76]	0.01480 (-0.07)	0.01480 (-0.07)	0.9300 (1.59)
	Afshari [150]	0.01485 (0.27)	0.01485 (0.27)	0.9273 (1.30)
	FELM36	0.01529 (3.14)	0.01529 (3.14)	0.9187 (0.38)
	FELM48	0.0152 (2.57)	0.01520 (2.57)	0.9193 (0.45)

5.1.3 Deflection of a Three-Layered Semi-Infinite Strip

The case analyzed in this section is a three-layer cross-ply (0,90,0) long strip of width, l , in the x -direction and an infinite length in the y -direction. The total thickness varies from thin to thick plate limits. All layers have equal thickness ($h/3$). The other problem information is given as:

Mechanical properties of each layer:

$$E_{11} = 25.0E06 \text{ psi} \quad E_{22} = 1.0E06 \text{ psi}$$

$$G_{12} = 0.5E06 \text{ psi} \quad G_{23} = 0.2E06 \text{ psi}$$

$$\nu_{12} = \nu_{12} = 0.25$$

Sinusoidal loading: $q(x,y) = Q_0 \sin(\pi x/l)$

$l = 10$ in width of the plate

$b = 1$ in width of the strip in the infinite direction

$S = h/l$ thickness to width ratio

Boundary Conditions: symmetric

$$\text{at } x = 0, \quad w = 0;$$

$$\text{at } x = 5, \quad u_0 = \theta_y = 0;$$

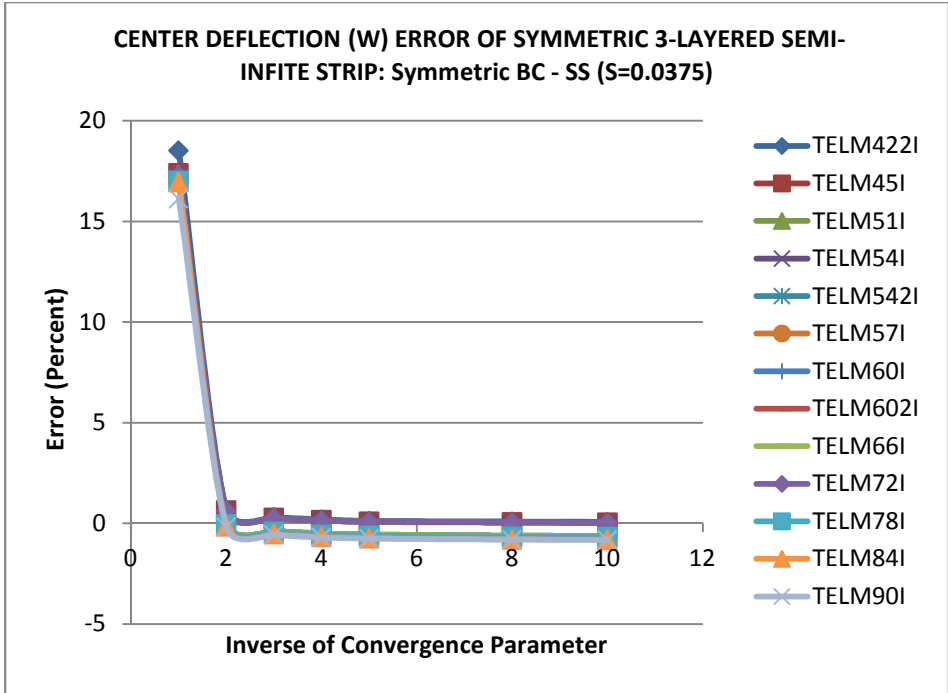
$$\text{at } y = \pm 5, \quad v_0 = \theta_x = 0;$$

Meshing: one half of the strip is modeled with 5 elements (1 x 5)

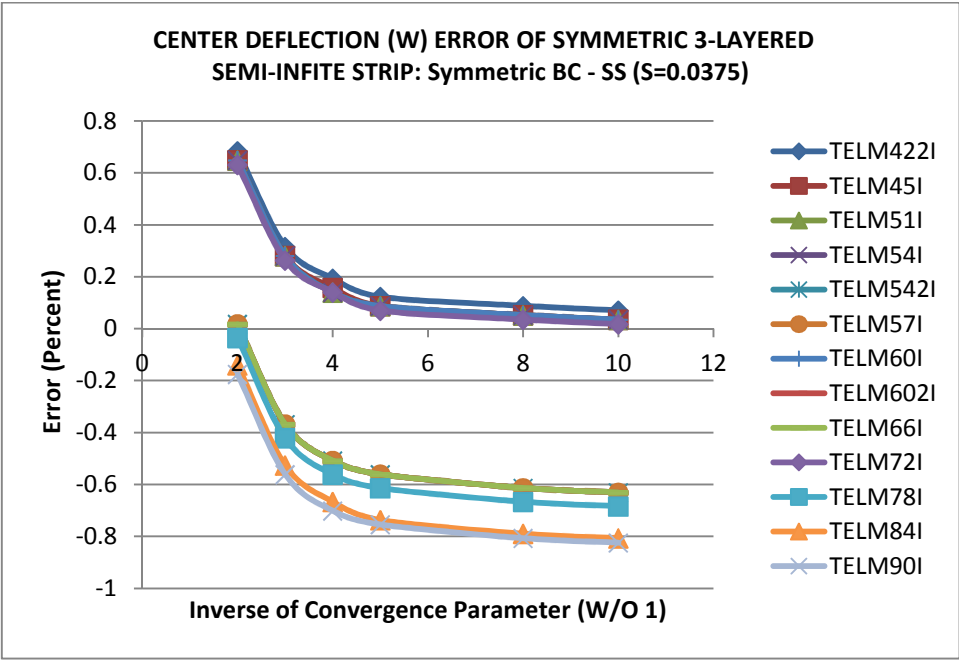
Pagano [4] developed an exact elasticity solution for of problem. Spilker [58] also obtained a solution using a hybrid stress formulation. Spilker's formulation satisfies the top traction free boundary. Both results are used for comparison. In this particular case, all the elements are used to carry out the analysis. The results are presented two fold. The Type I elements are presented first, followed by Type II elements. The evolution of the

percentile error as a function of the inverse of the convergence parameter is presented in Figures 5.7 through 5.10 for the Type I elements, and in Figures 5.11 through 5.15 for Type II. The convergence parameter are generally smaller than one, thus its inverse provides an easier number for graphical presentation.

It can be seen on Figure 5.7a that without the convergence parameter in the formulation of the element strain function ($\alpha = 1$), the error is more than 15%, while a convergence parameter just smaller than one half (Figure 5.7b) reduced the error to less than 1%. This observation is also true for moderately thin plates ($S = 0.05$, see Figure 5.8), moderately thick plates ($S = 0.1$, see Figure 5.9) and very thick plates ($S = 0.25$, see Figure 5.10). One can also notice that the thicker the plate becomes, the higher the error in the absence of convergence parameter. Also, the behavior of the elements follows strictly their classification into subgroups, especially for very thick plates (Figure 5.10). Five Lagrange Type I elements (TELM78I, TELM542I, TELM602I, TELM66I), give less 0.5 % error when the convergence parameter is smaller than 1/3. The other elements have less than 4% error, which is excellent.

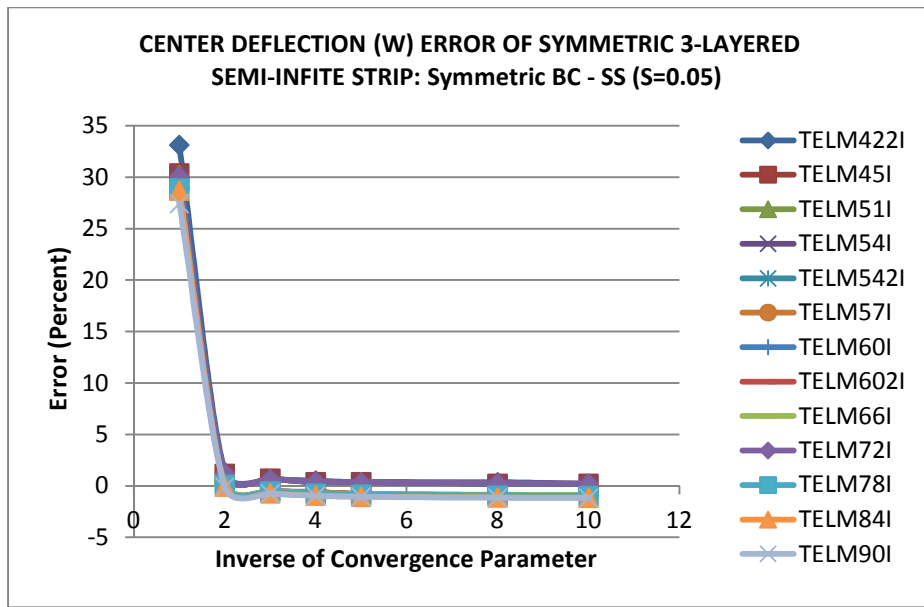


a)

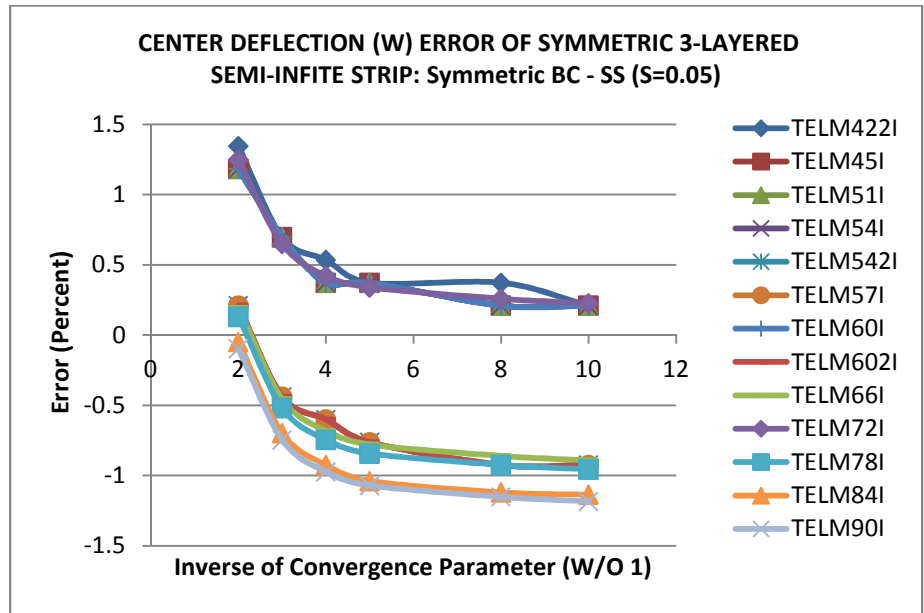


b)

Figure 5. 7: Center deflection error of a thin ($S=0.0375$) symmetric 3-layered semi-infinite strip using Type I elements.

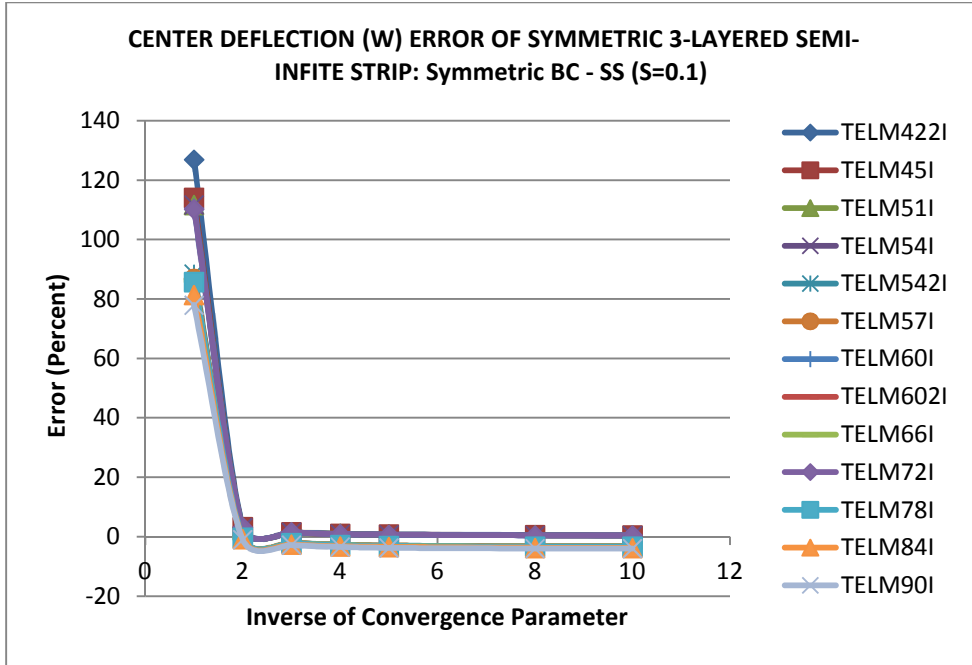


a)

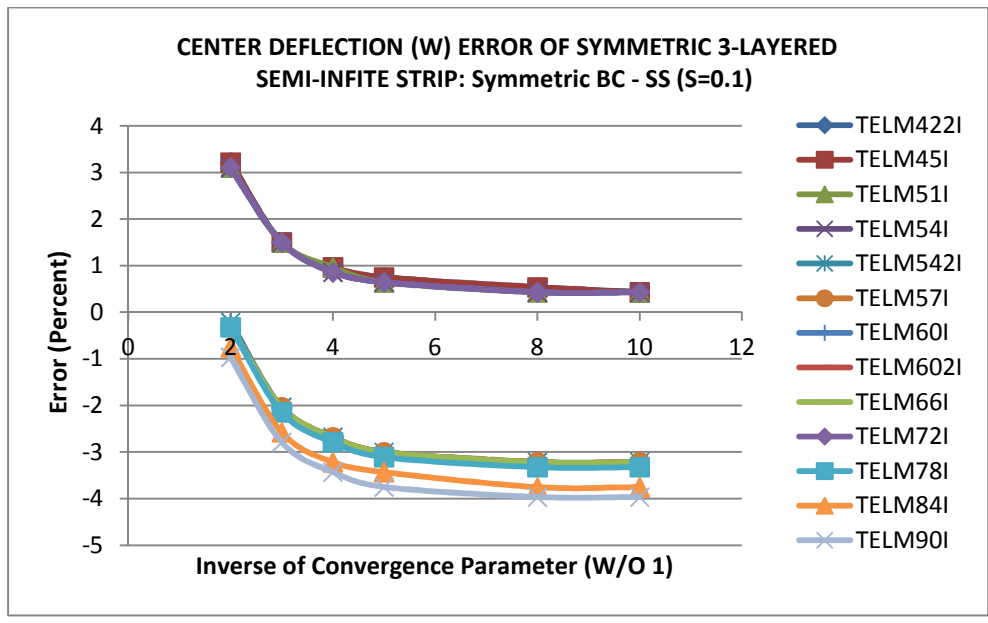


b)

Figure 5. 8: Center deflection error of a moderately thin (S=0.05) symmetric 3-layered semi-infinite strip using Type I elements.

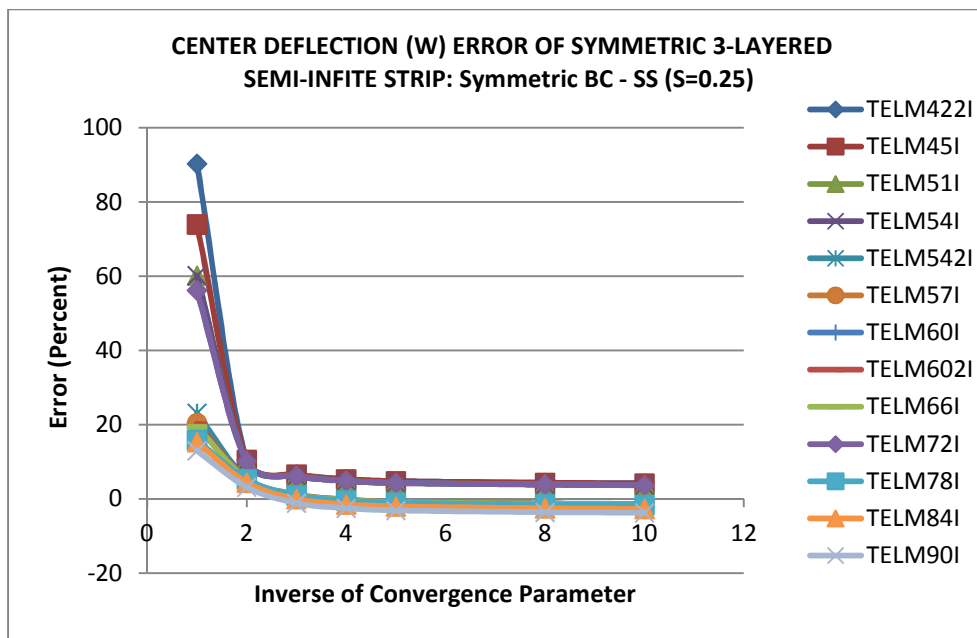


a)

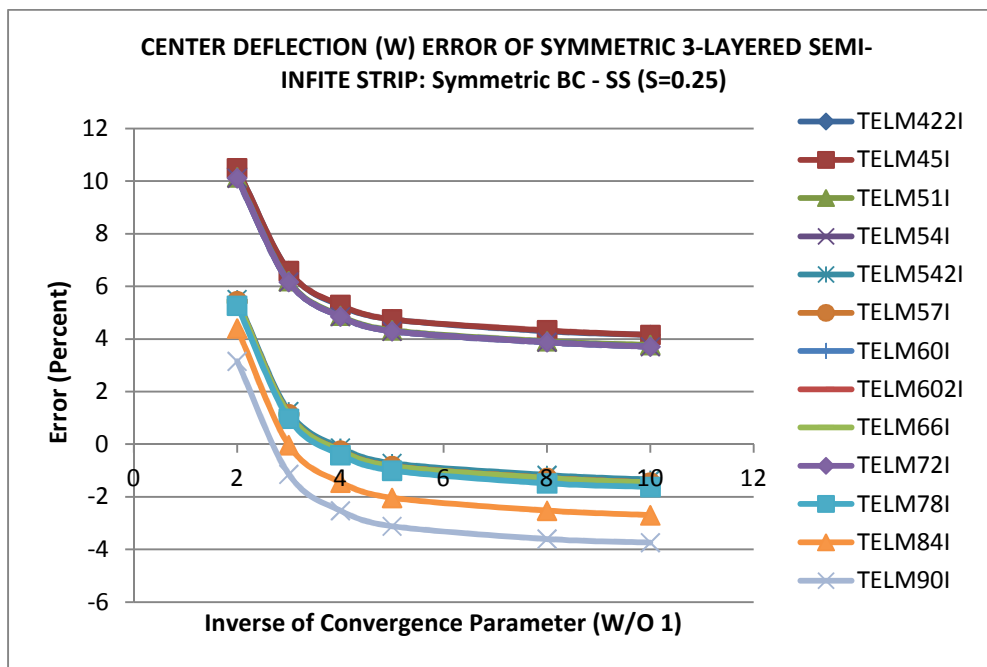


b)

Figure 5. 9: Center deflection error of a moderately thick (S=0.1) symmetric 3-layered semi-infinite strip using Type I elements.



a)



b)

Figure 5. 10: Center deflection error of a very thick (S=0.25) symmetric 3-layered semi-infinite strip using Type I elements.

One can observe from Figure 5.11 that all Type II elements yield excellent performance for thin plates, and none of them has a shear locking problem. Surprisingly, even without a convergence parameter, the results are less than 2% free of error. Also, it can be seen from Figures 5.11b through 5.15b that there are also two groups of elements which correspond exactly to the subgroup of Type II, namely, the “Lagrange” compatible type and the “serendipity” one. One can notice the particular behavior of element TELM60. For very thick plates, it is the only element which converges to the exact elasticity solution when the convergence parameter becomes smaller.

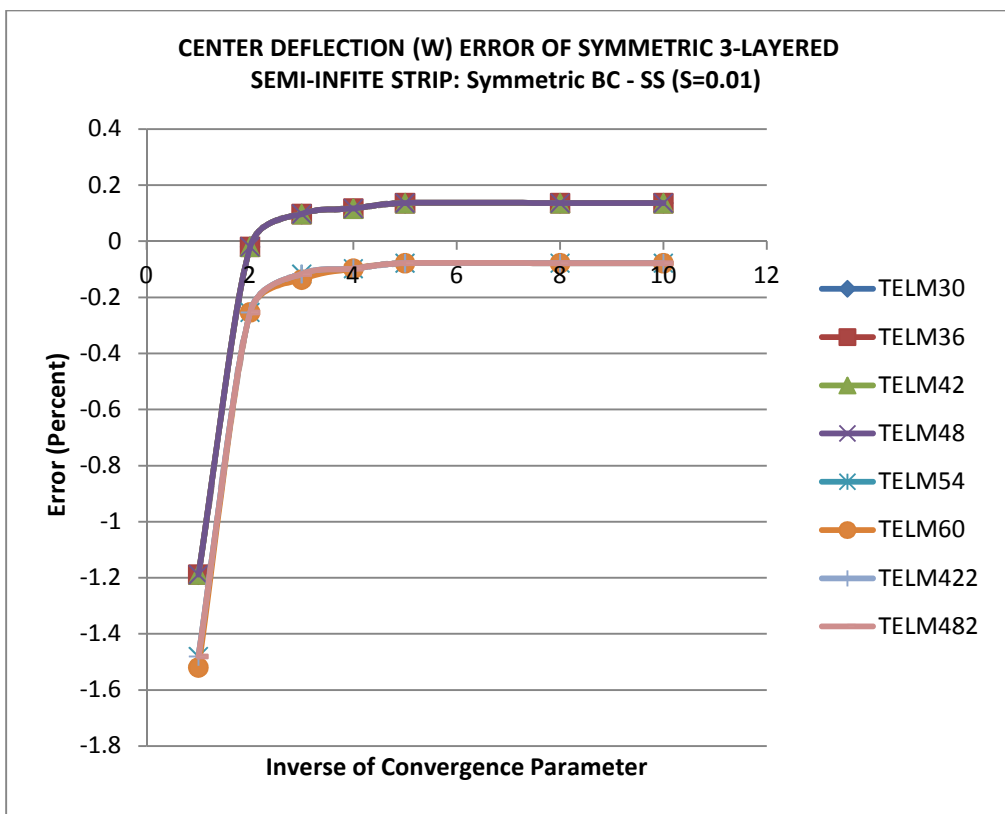
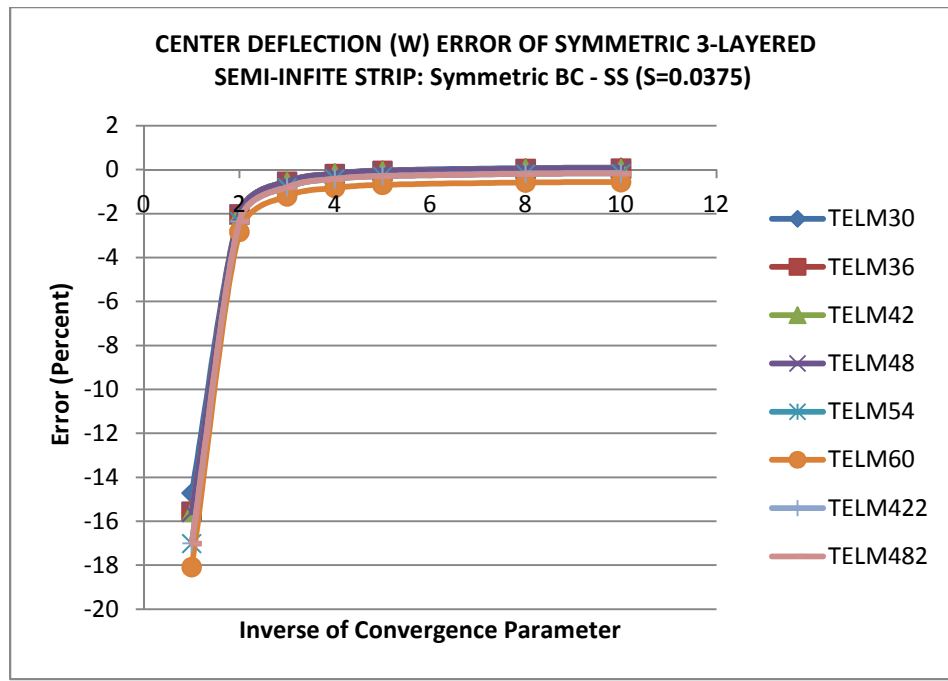
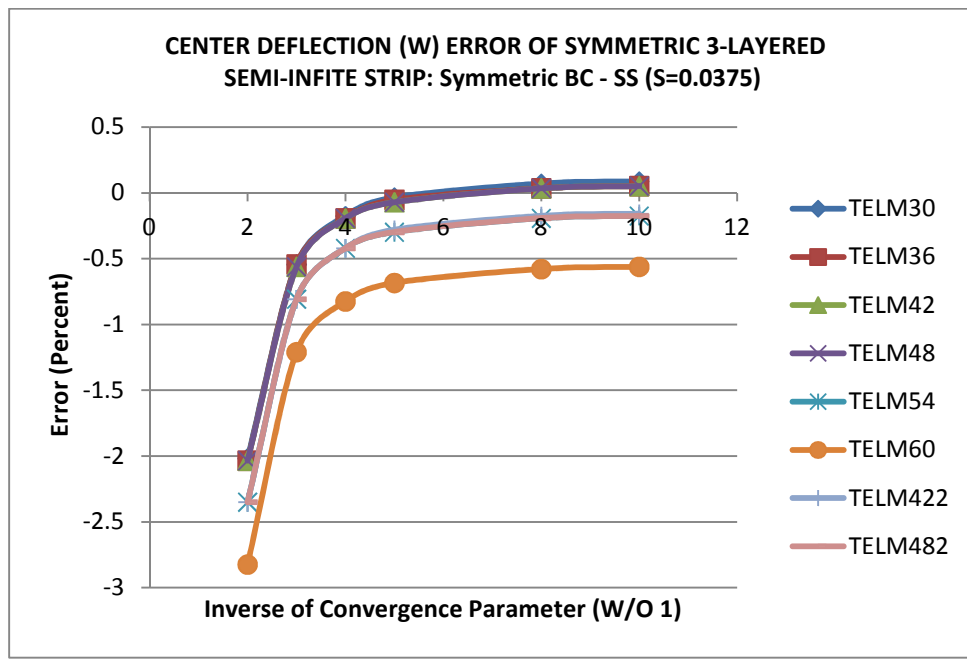


Figure 5. 11: Center deflection error of a very thin (S=0.01) symmetric 3-layered semi-infinite strip using Type II elements.

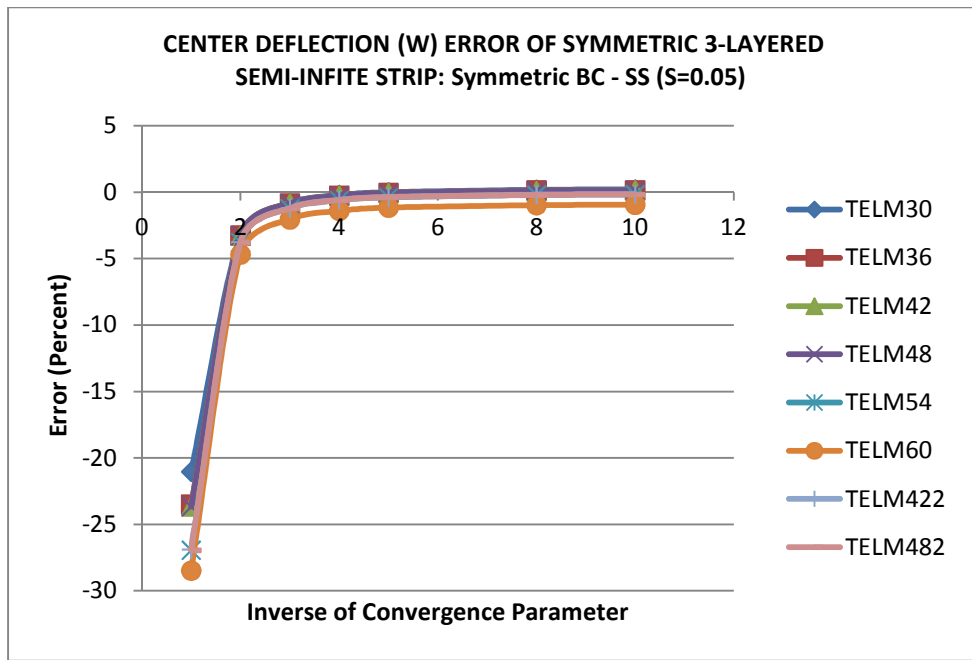


a)

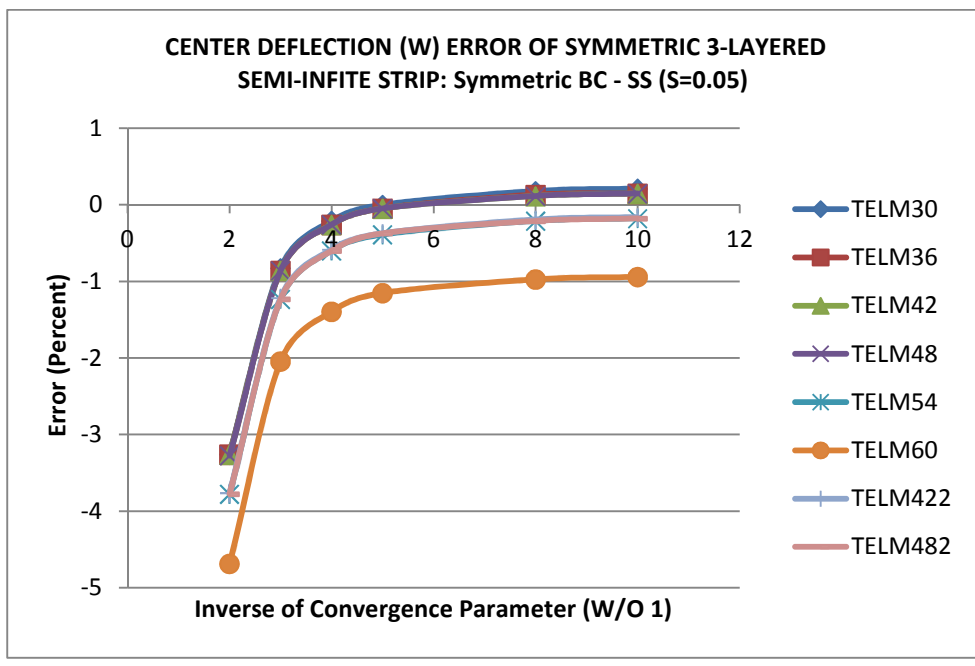


b)

Figure 5. 12: Center deflection error of a thin (S=0.0375) symmetric 3-layered semi-infinite strip using Type II elements.

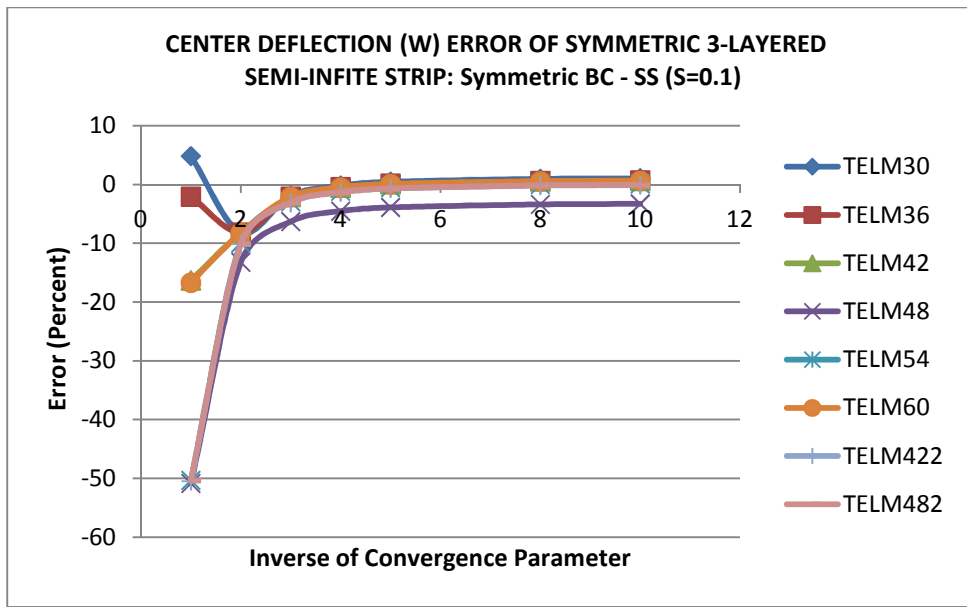


a)

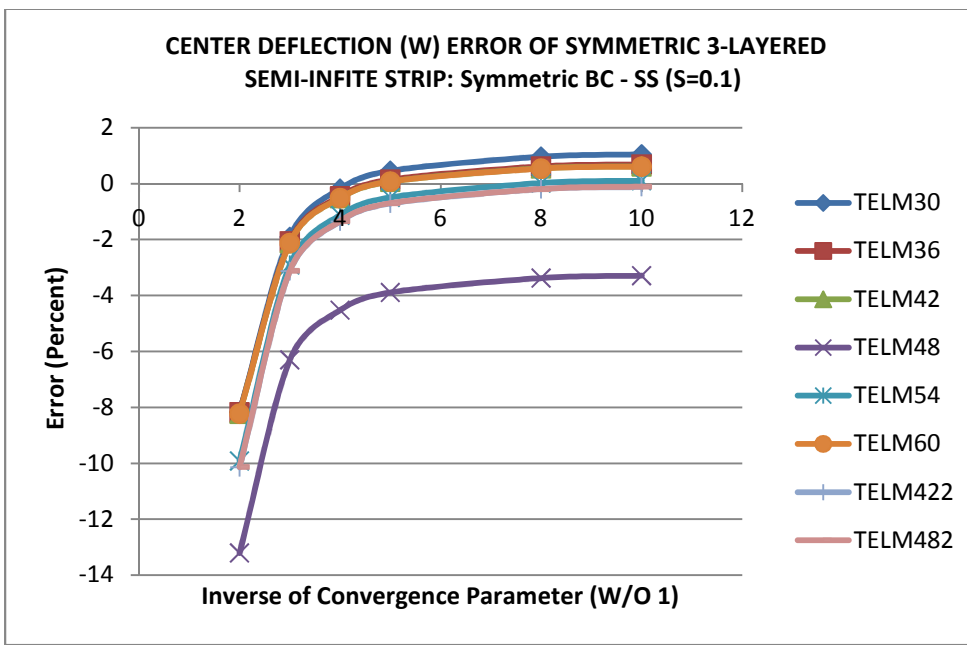


b)

Figure 5. 13: Center deflection error of a moderately thin (S=0.05) symmetric 3-layered semi-infinite strip using Type II elements.

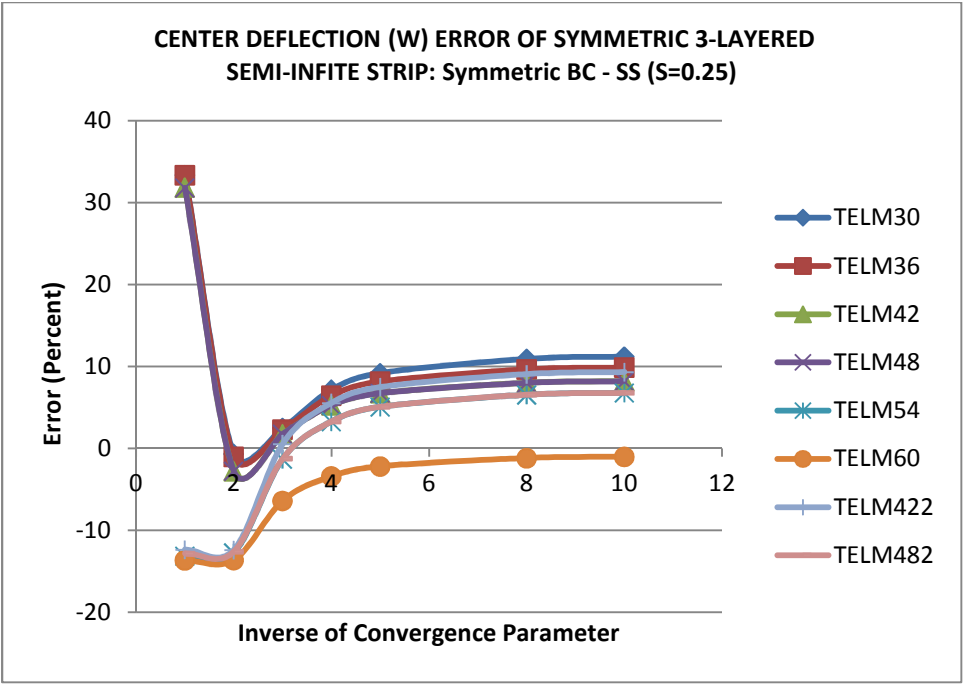


a)

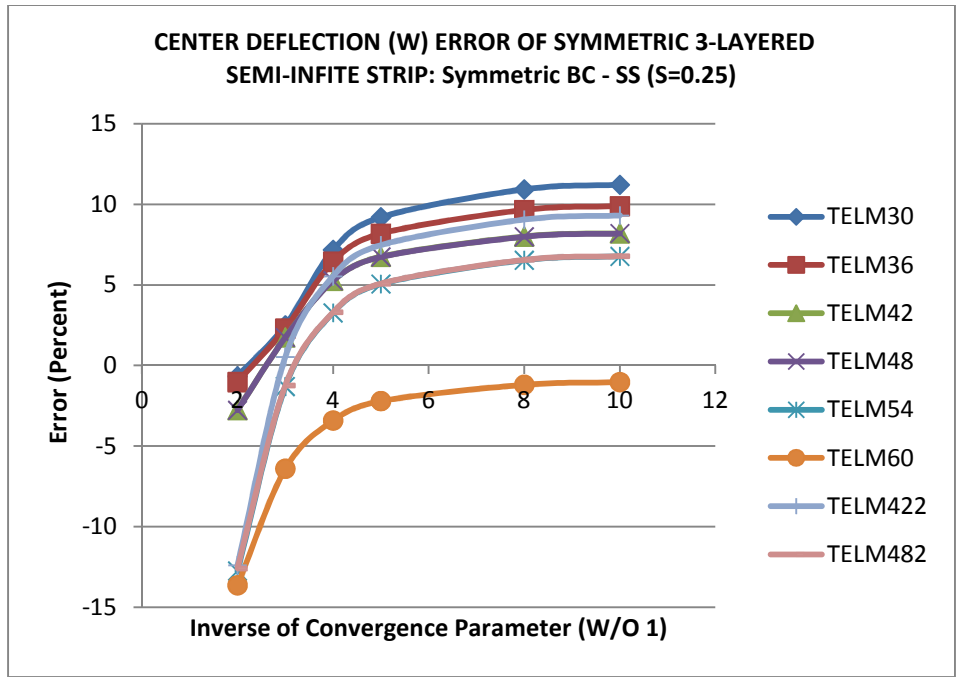


b)

Figure 5. 14: Center deflection error of a moderately thick (S=0.1) symmetric 3-layered semi-infinite strip using Type II elements.



a)



b)

Figure 5. 15: Center deflection error of a very thick (S=0.25) symmetric 3-layered semi-infinite strip using Type II elements.

It can be seen from Figure 5.15 (or Table 5.6) that for very thick plates the range of convergence parameters which give less than 5% error is between 1/3.3 and 1/2.7.

Table 5.6 presents the center deflection error for a very thick plate as a function of the convergence parameter.

Table 5. 6: Center deflection error of a very thick ($S=0.25$) symmetric 3-layered semi-infinite strip using Type II elements.

Elements	Inverse of convergence parameters						
	1.00	2.00	3.00	4.00	5.00	8.00	10.00
TELM30	33.38	-0.67	2.50	7.17	9.20	10.93	11.21
TELM36	33.36	-1.03	2.29	6.44	8.18	9.65	9.89
TELM42	31.86	-2.77	1.75	5.26	6.75	8.00	8.21
TELM48	31.80	-2.78	1.74	5.26	6.74	7.99	8.20
TELM54	-13.15	-12.75	-1.31	3.27	5.06	6.53	6.77
TELM60	-13.65	-13.64	-6.40	-3.41	-2.21	-1.20	-1.03
TELM422	-12.37	-12.40	0.53	5.54	7.46	9.05	9.30
TELM482	-12.82	-12.59	-1.25	3.30	5.08	6.56	6.79

The particular behavior of element TEM60 is due to the fact it is a complete “Lagrangian” type for both the in-plane strain and the rotational strain functions. It has the highest number of strain parameters. It is also noticed that there is less of a distinction between serendipity and Lagrange Type II elements.

In summary, all elements perform very well from very thin to moderately thick plates. It has been confirmed that there is no shear locking effect for very thin plates for all the proposed elements. Also, there is no need for a convergence parameter when analyzing the displacements of very thin to moderately thick of plates. Any value greater than 1/4 gives less than 1% error for thin to moderately thick plates. However, more attention needs to be paid to the element type when analyzing thick plates. Spilker's [58] solution has 5.16% error in comparison to the exact elasticity solution.

5.1.4 Deflection of an Anti-Symmetric Cross-Ply Square Plate with Various Edge Boundary Conditions.

The previous square plate is also analyzed here using different boundary conditions and a different loading. Khdeir and Reddy [62] worked out a Levy-type solution using both the first and third order theories of Sections 2.2 and 2.3. The following material properties are used for each layer

$$\begin{aligned} E_{11} &= 25.0E06 \text{ psi} & E_{22} &= 1.0E06 \text{ psi} \\ G_{12} &= 0.5E06 \text{ psi} & G_{23} &= 0.2E06 \text{ psi} \\ \nu_{12} &= \nu_{12} = 0.25 \end{aligned}$$

The loading is assumed to be sinusoidal: $q(x,y) = Q_0 \cos(\pi x/a) \sin(\pi y/b)$

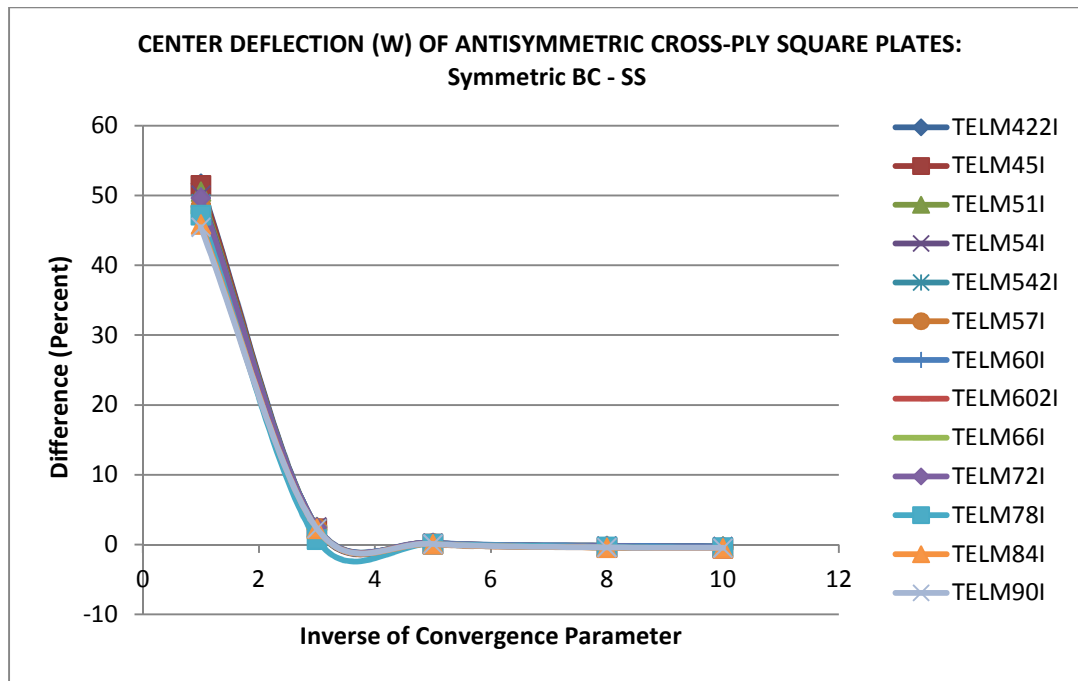
$$\begin{aligned} a &= 10 \text{ in} && \text{length of the plate} \\ b &= 10 \text{ in} && \text{width of the plate} \\ S &= 0.1 && \text{moderately thick} \end{aligned}$$

Six different boundary conditions, combinations of simply supported and clamped edges, are used as presented in Table 5.

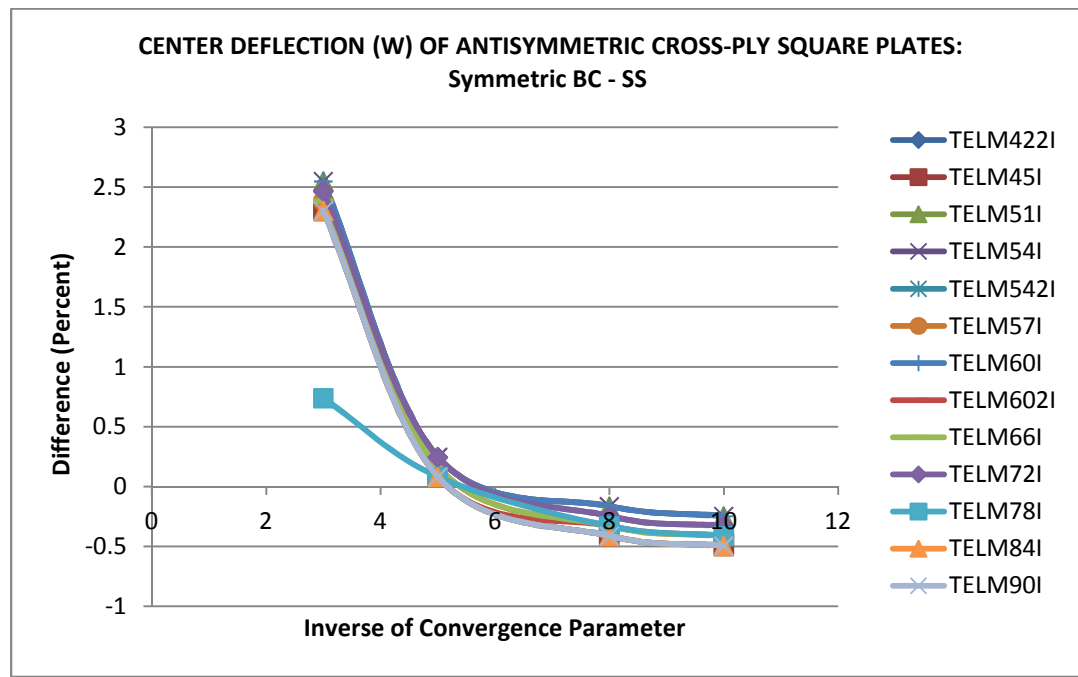
Table 5. 7: Nomenclature for the boundary condition

Symmetric analysis:	Non-symmetric analysis:
SS: simply supported on both ends	SC: simply supported and clamped
CC: clamped on both ends	FC: free and clamped edge
FF: free BC on both ends	FS: free BC and simply supported

The results for Type I elements are shown in Figures 5.16 through 5.21. One can observe that the convergence parameter is necessary for all type of boundary conditions for an accurate analysis. Also, all the element solutions converge towards the exact analytical solution when the weighting becomes smaller. For Type I elements, there is no distinction between its subgroups. The Serendipity and the Lagrange categories behave equally well. All give more than 98% accuracy when the convergence parameter is smaller than $1/3$.

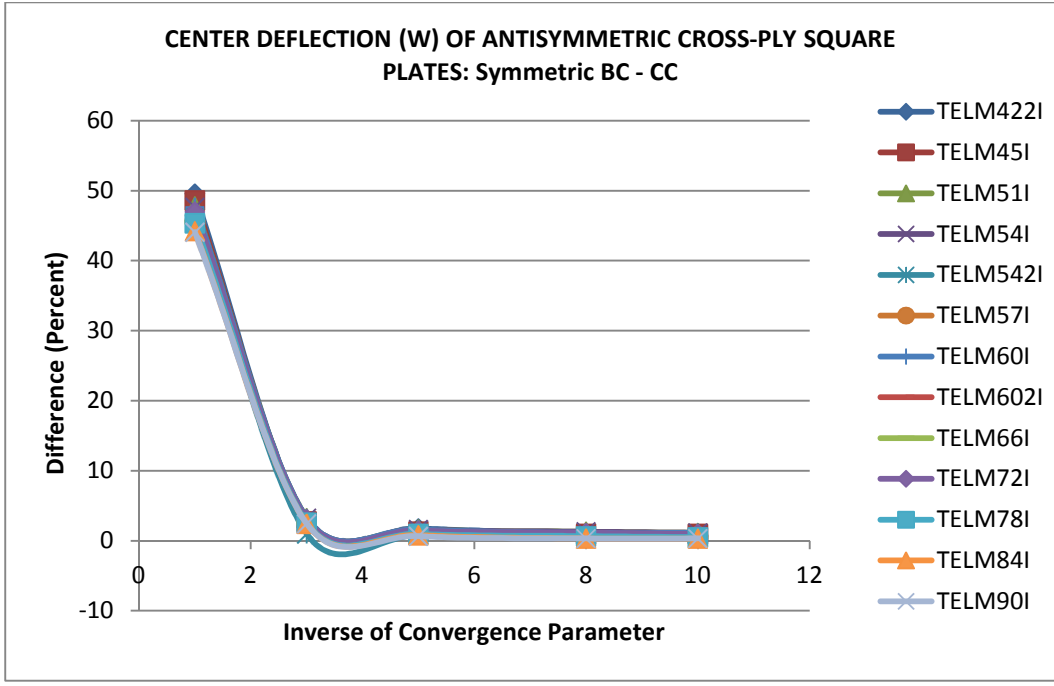


a)

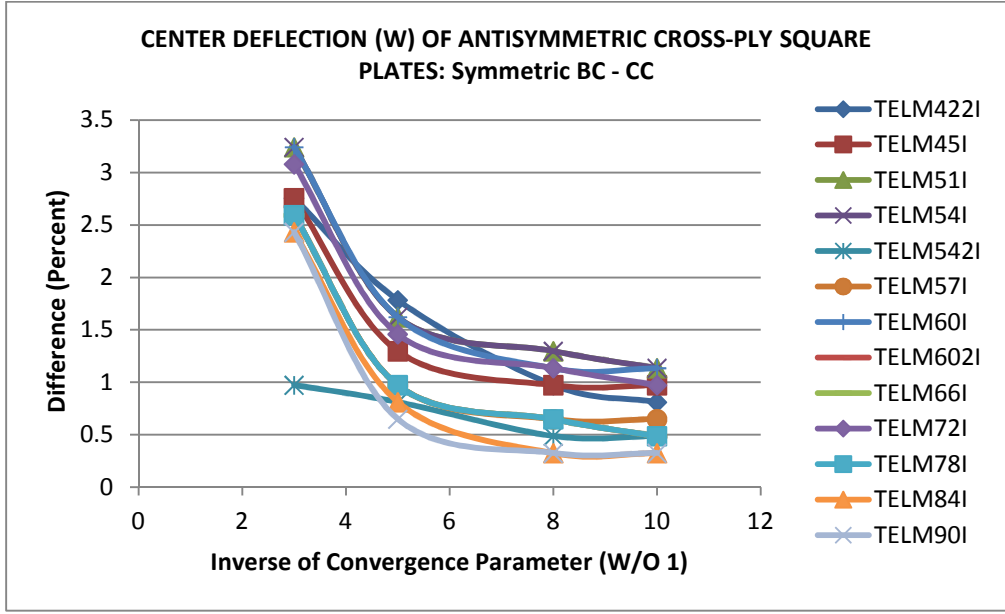


b)

Figure 5. 16: Center deflection of antisymmetric cross-ply square plates (SS BCs) using Type I elements.

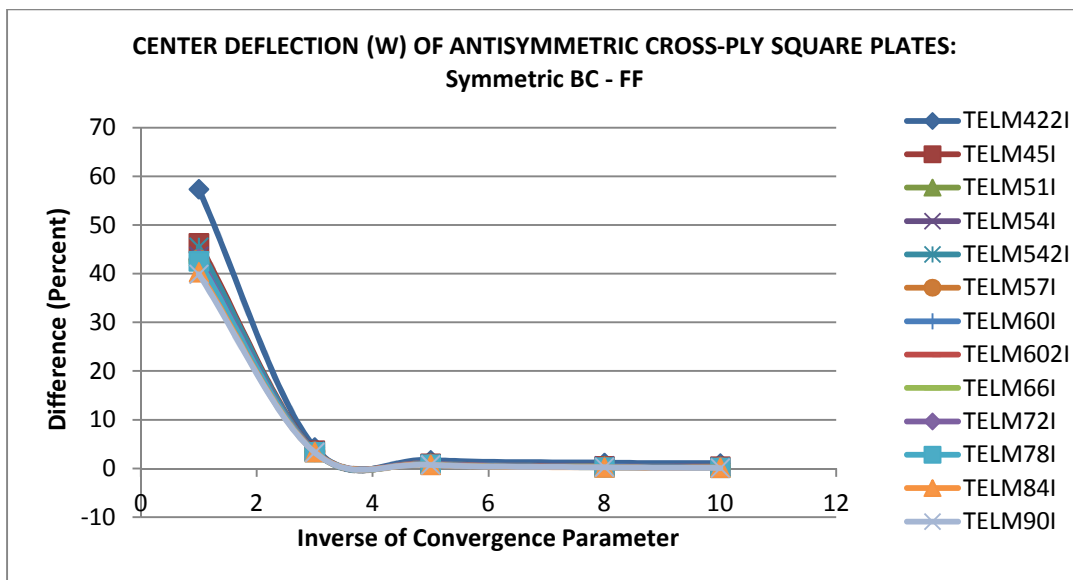


b)

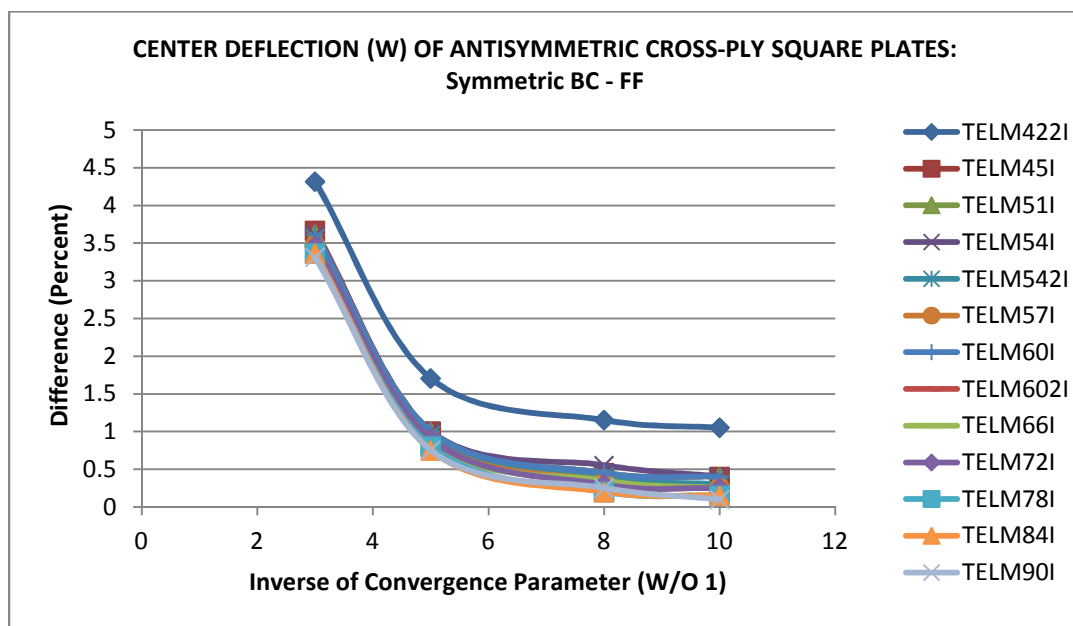


b)

Figure 5. 17: Center deflection of antisymmetric cross-ply square plates (CC BCs) using Type I elements.

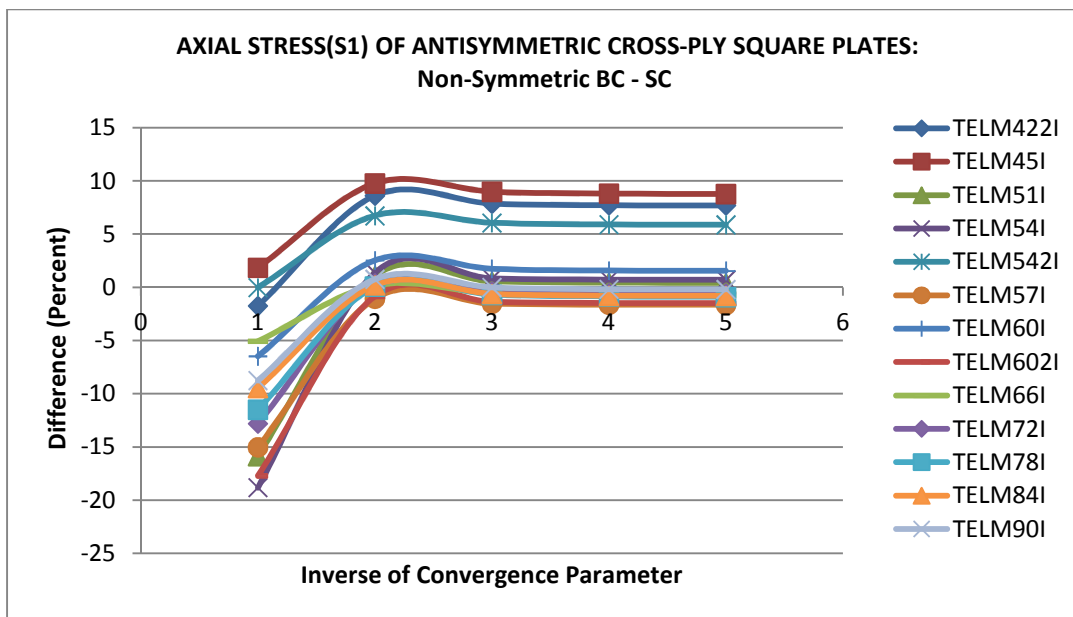


a)

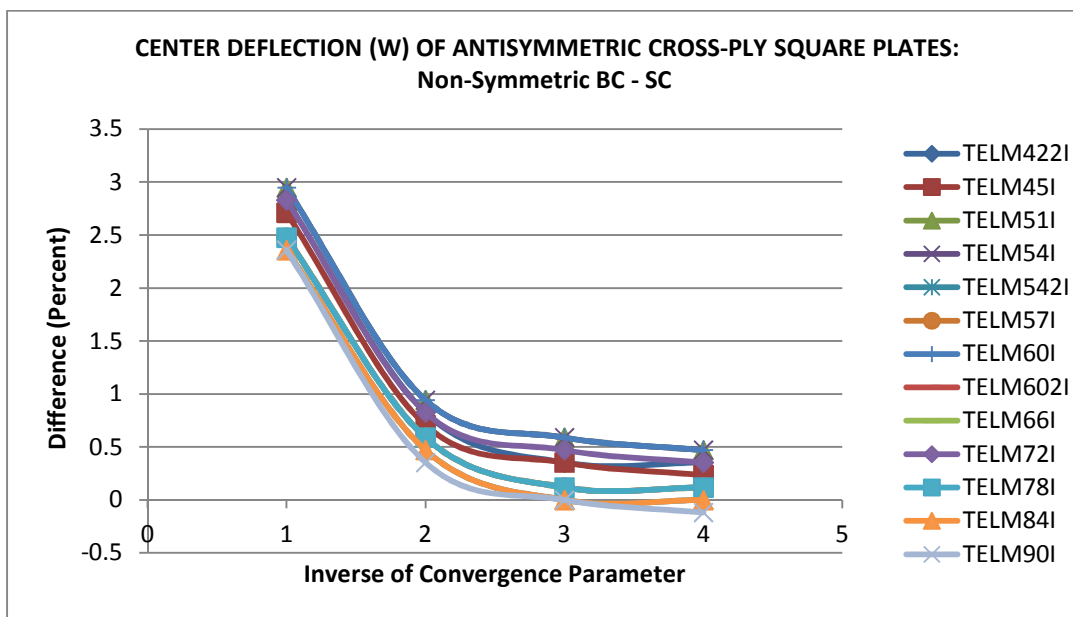


b)

Figure 5. 18: Center deflection of antisymmetric cross-ply square plates (FF BCs) using Type I elements.

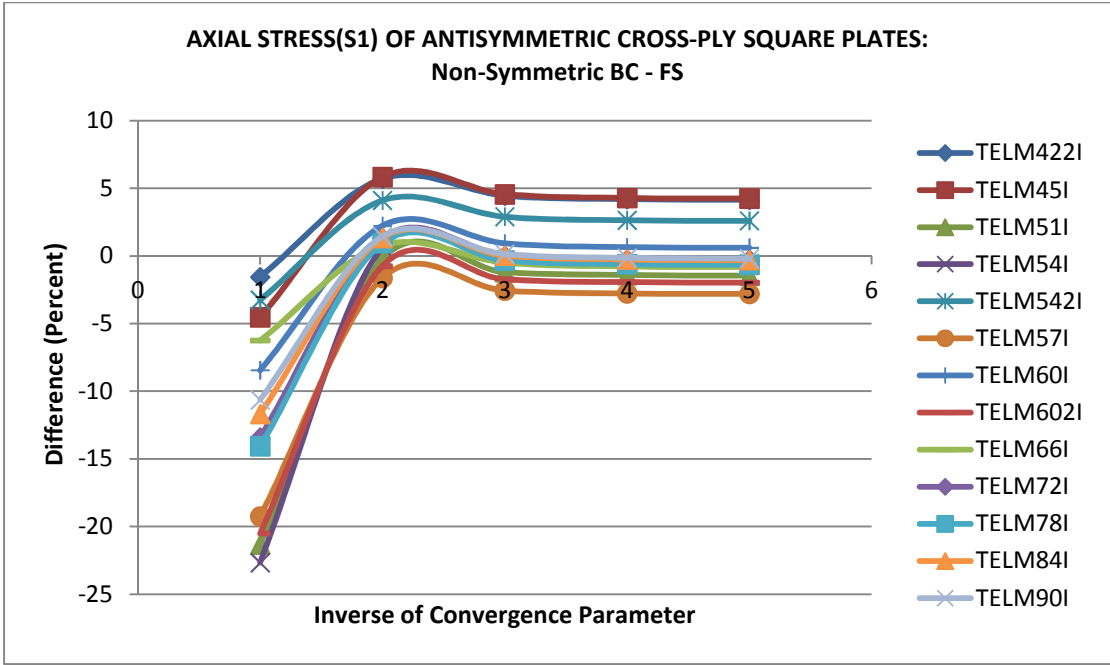


a)

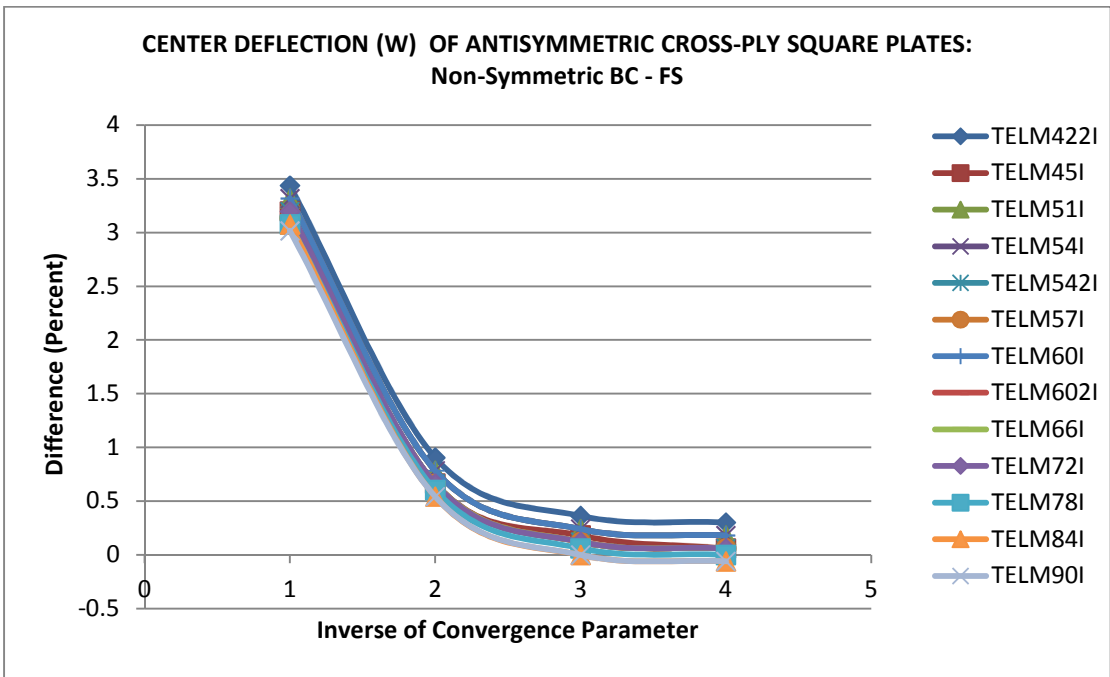


b)

Figure 5. 19: Center deflection of antisymmetric cross-ply square plates (SC BCs) using Type I elements.

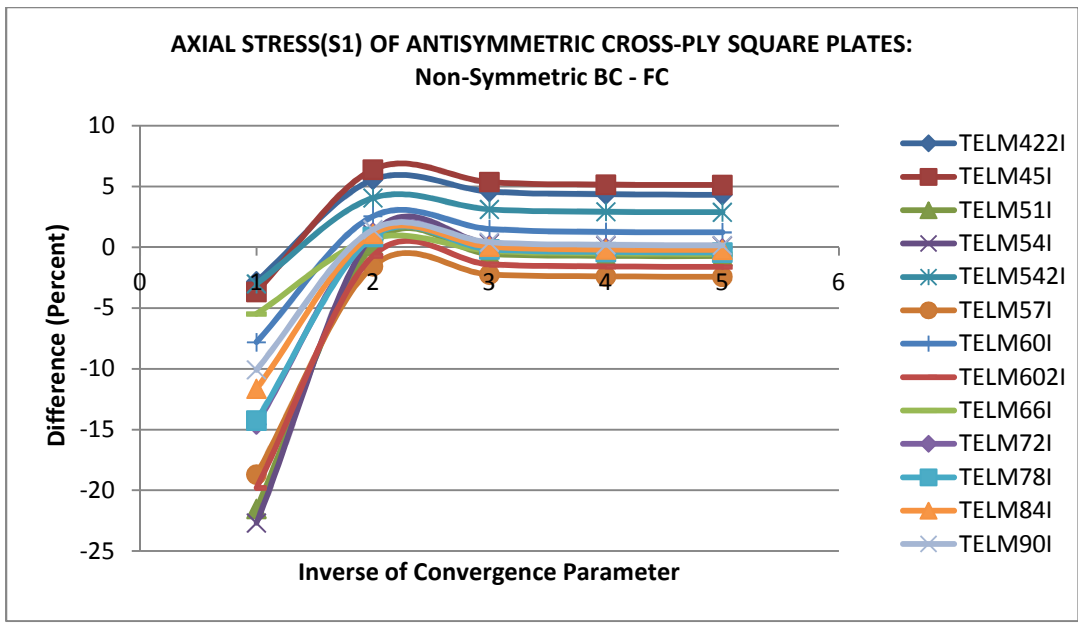


a)

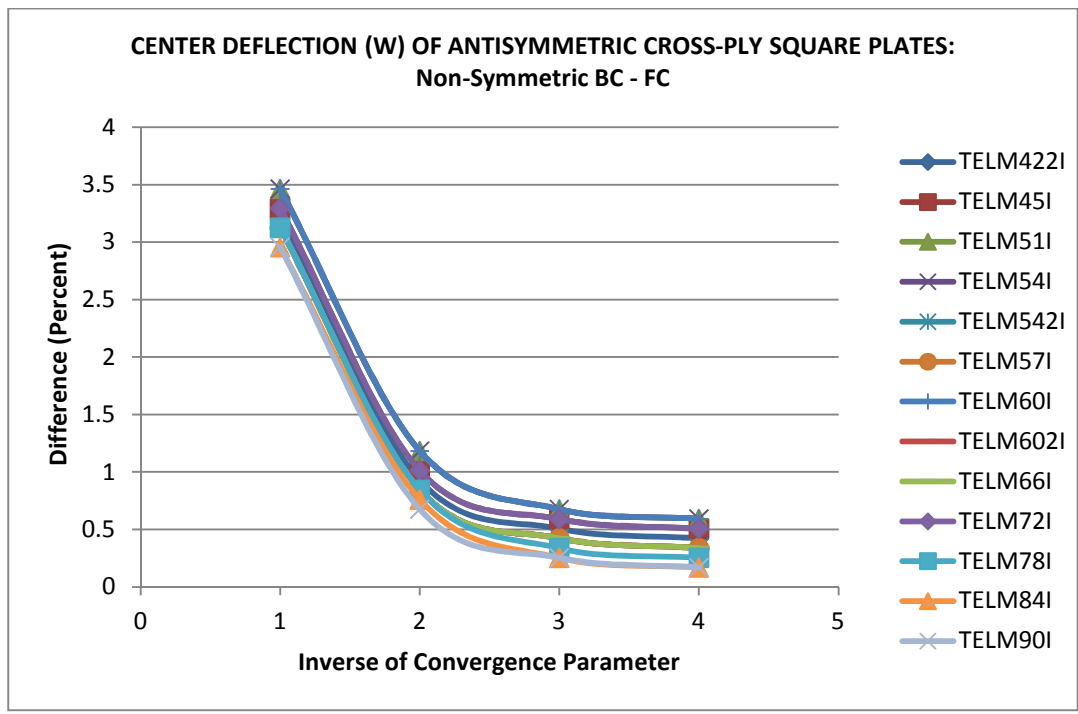


b)

Figure 5. 20: Center deflection of antisymmetric cross-ply square plates (SS BCs) using Type I elements.



a)



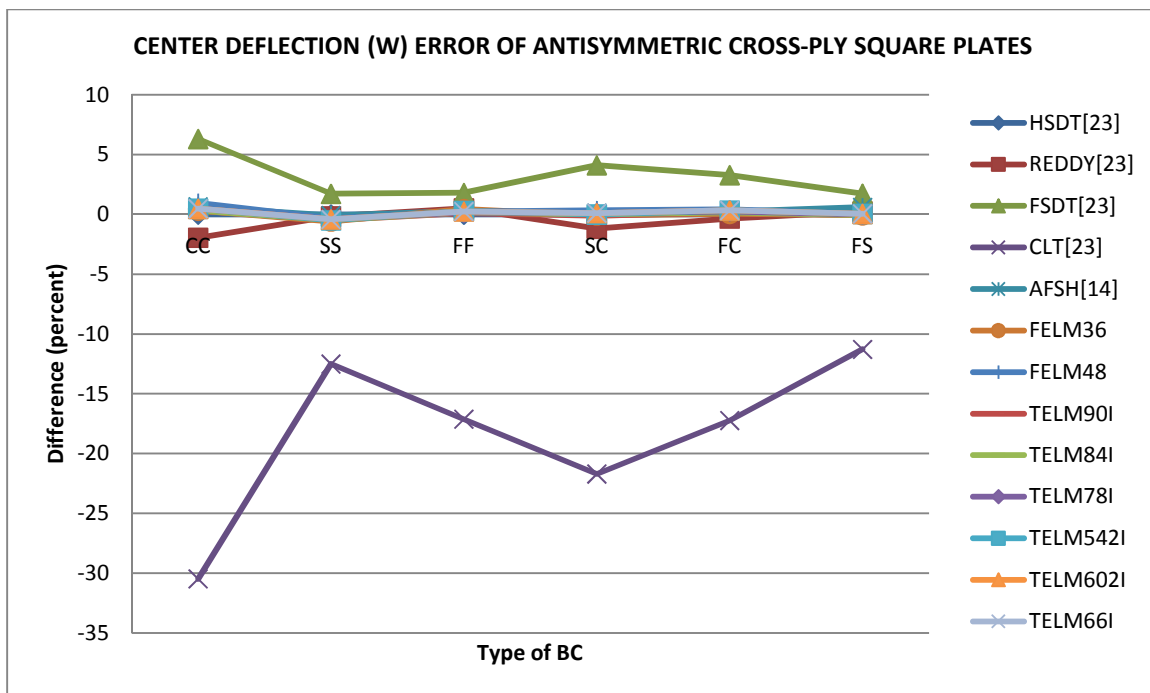
b)

Figure 5. 21: Center deflection of antisymmetric cross-ply square plates (FC BCs) using Type I elements.

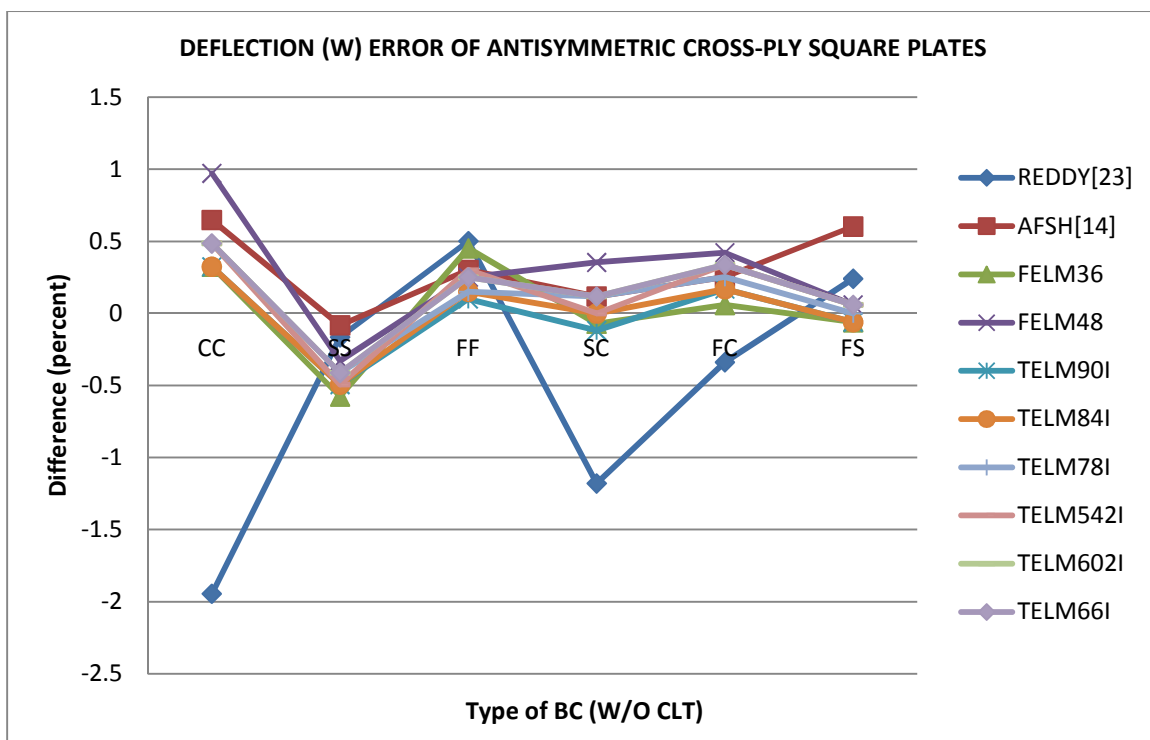
Six elements (TELM84I, TELM90I, TELM78I, TELM542I, TELM602I) give less than 0.5% difference when the weighing factor is 1/10. The results are compared to Reddy's analytical and finite element solutions. Afshari's solution is also integrated in the comparison table shown in Table 5.8. Figure 5.22 gives a graphical comparison for the five best elements mentioned above.

Table 5. 8: Nondimensional center deflection of antisymmetric cross-ply square plates with Various Edge BCs – Comparison with other results.

Elements	Symmetric boundary conditions			Non-Symmetric boundary conditions		
	SS	CC	FF	SC	FS	FC
TSDT[23]	1.216	0.617	1.992	0.848	1.658	1.184
REDDY[23]	1.214	0.605	2.002	0.838	1.662	1.180
FSDT[23]	1.237	0.656	2.028	0.883	1.687	1.223
CLT[23]	1.064	0.429	1.651	0.664	1.471	0.980
AFSH[14]	1.215	0.621	1.998	0.849	1.668	1.187
FELM36	1.209	0.619	2.001	0.8474	1.657	1.185
FELM48	1.212	0.623	1.997	0.851	1.659	1.189
TELM422I	1.212	0.622	2.013	0.851	1.663	1.189
TELM45I	1.210	0.623	2.000	0.850	1.659	1.190
TELM51I	1.213	0.624	2.000	0.852	1.661	1.191
TELM54I	1.213	0.624	2.000	0.852	1.661	1.191
TELM542I	1.210	0.620	1.998	0.848	1.659	1.188
TELM57I	1.211	0.621	1.997	0.849	1.659	1.188
TELM60I	1.213	0.624	2.000	0.852	1.661	1.191
TELM602I	1.211	0.620	1.997	0.849	1.659	1.188
TELM66I	1.211	0.620	1.997	0.849	1.659	1.188
TELM72I	1.212	0.623	1.997	0.851	1.659	1.190
TELM78I	1.211	0.620	1.995	0.849	1.658	1.187
TELM84I	1.210	0.619	1.995	0.848	1.657	1.186
TELM90I	1.210	0.619	1.994	0.847	1.657	1.186



a)

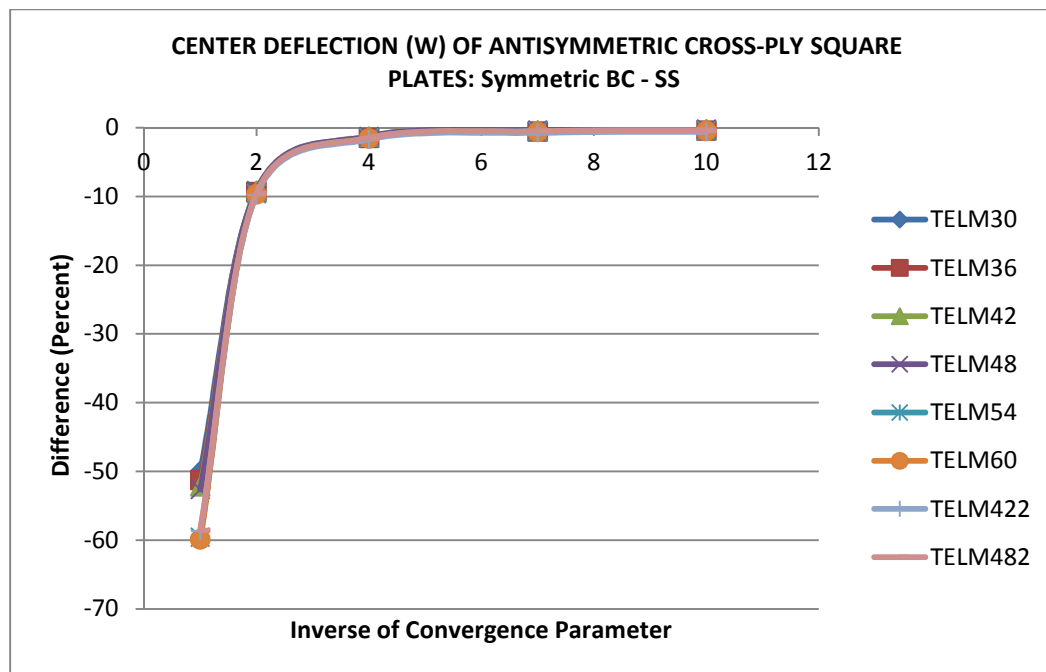


b)

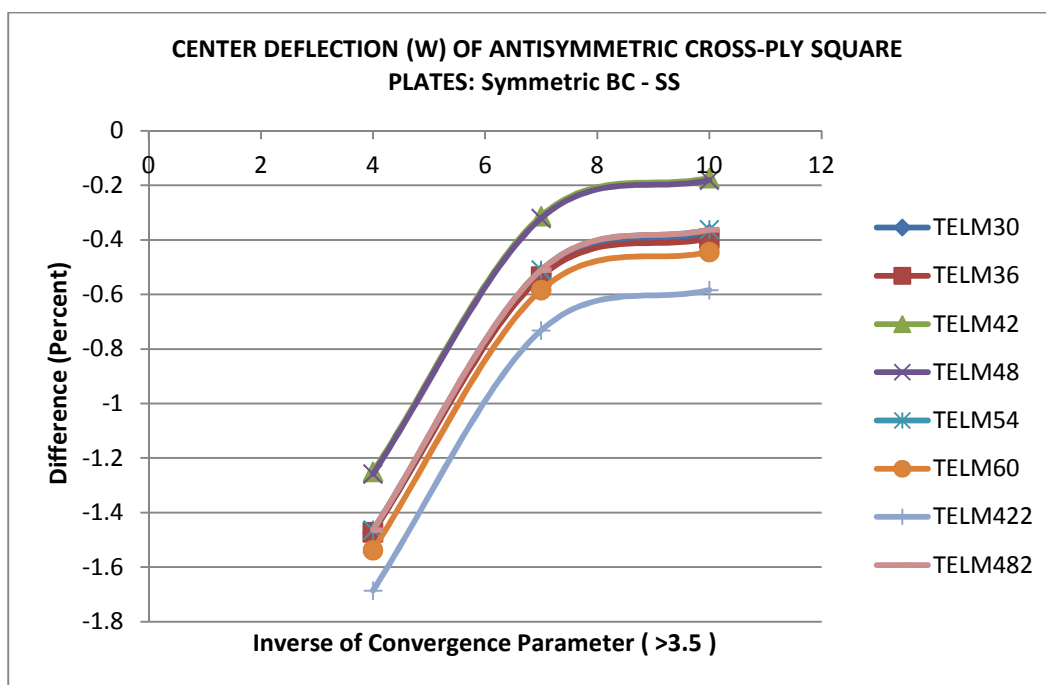
Figure 5. 22: Center deflection comparison of antisymmetric cross-ply square plates with various edge BCs

Figure 5.22a shows that the Classical Lamination Theory (CLT) gives between a 12 and 30% difference with the analytical solution. Removing it from the comparison, one gets Figure 5.22b. It can be noticed that all elements behave well. However, Reddy's third order element is less accurate than the proposed Type I elements of the present study. All the first order elements agree with analytical solution because the structure analyzed is within the limits of plate analysis ($S = 0.1$).

Figures 5.23 through 5.28 show the transverse displacement analysis of the same composite square plate using Type II elements. It can be noticed that without a convergence parameter the difference is more than 60%, while the use of a convergence parameter smaller than $1/5$ give less than 1% difference between the present elements solutions and the analytical one. A closer look at Figure 5.24b reveals a difference between the Serendipity subgroup and the Lagrange one. The latter one performs better, although the difference is not significant. Also, element TELM60 is the most consistent in converging to the analytical solutions for all boundary conditions except for the SS BC (Figure 5.23b).

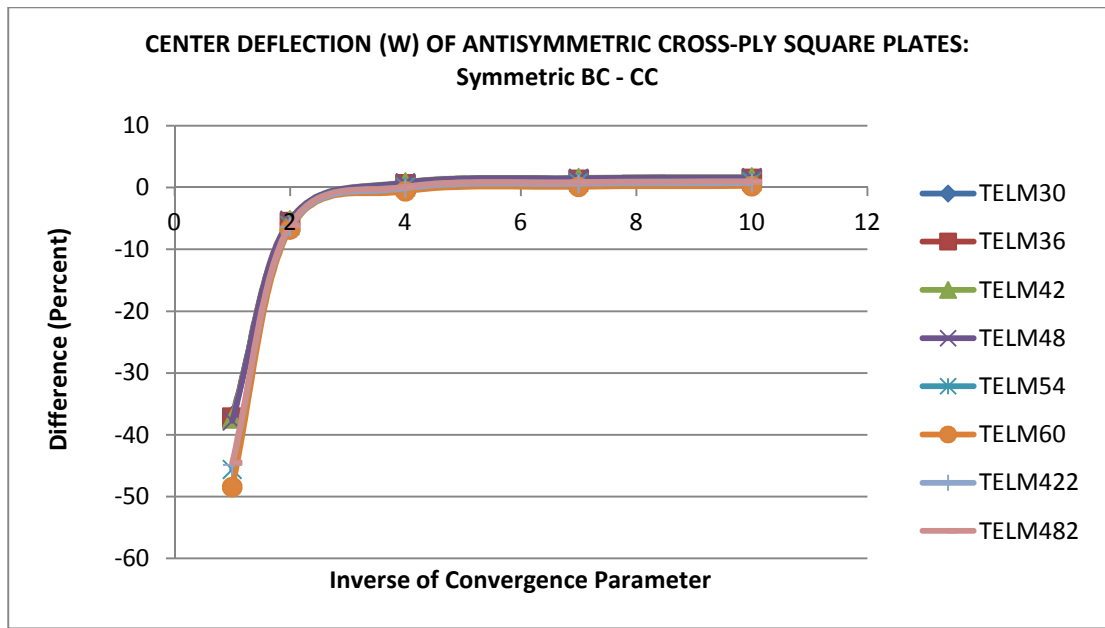


a)

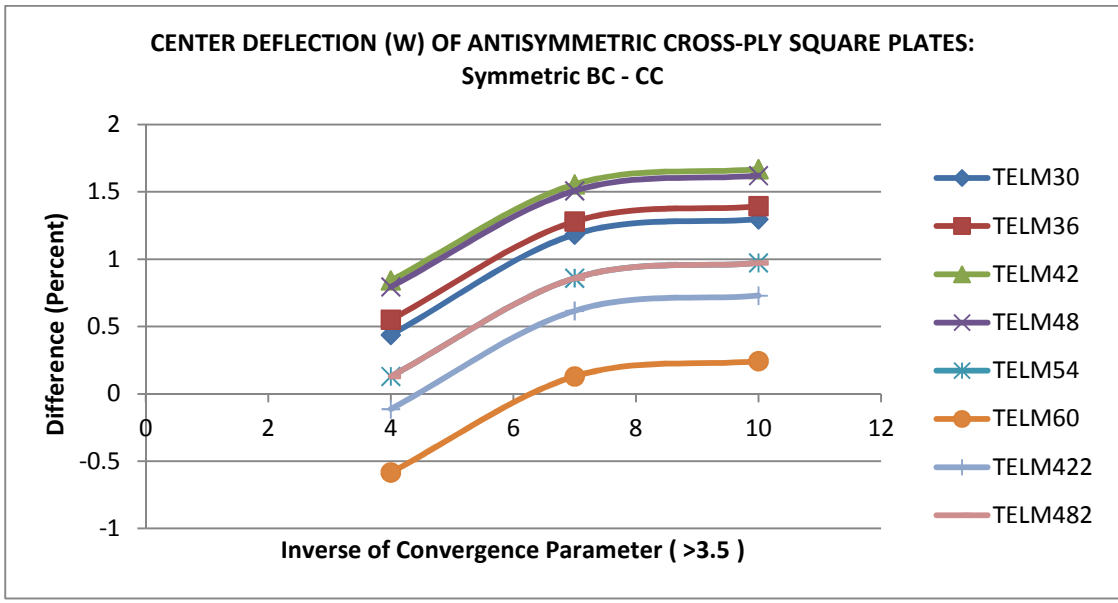


b)

Figure 5. 23: Center deflection of antisymmetric cross-ply square plates (SS BCs) using Type II elements.

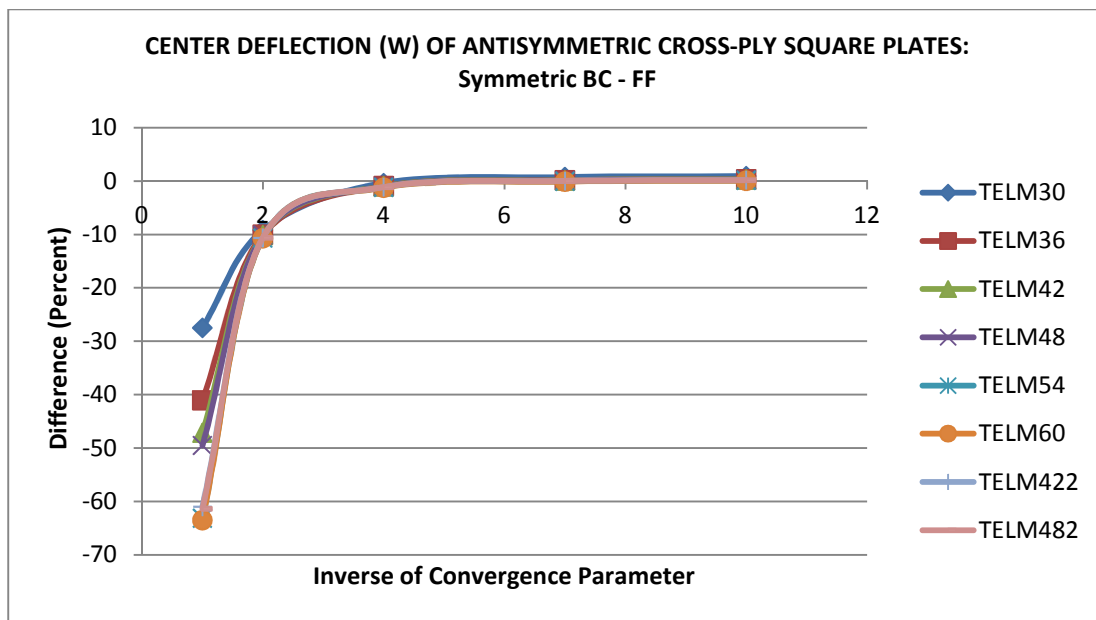


a)

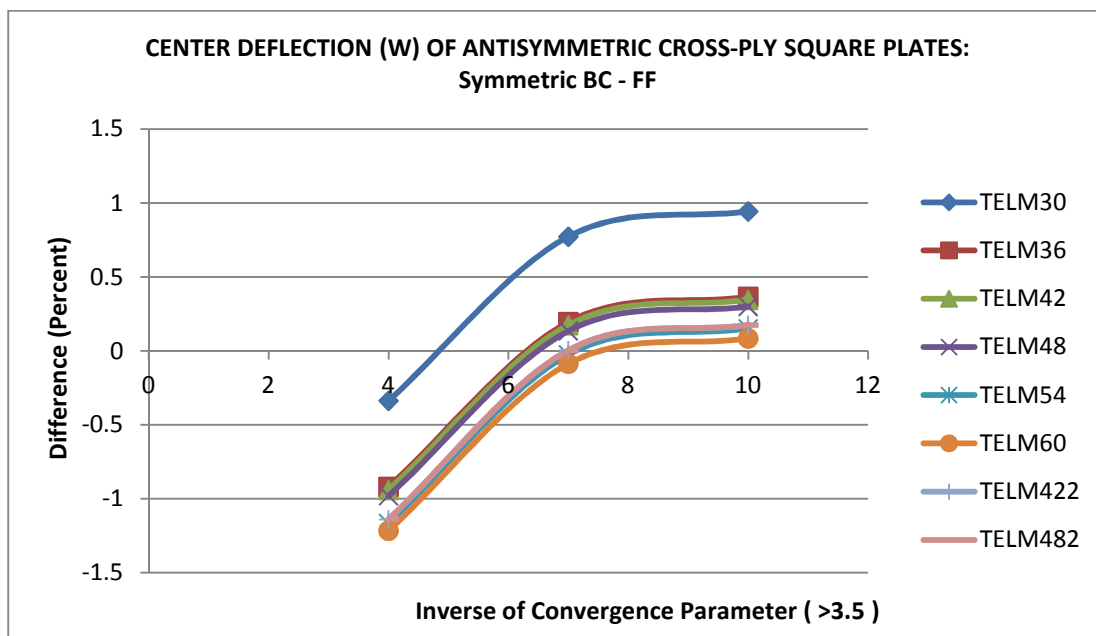


b)

Figure 5. 24: Center deflection of antisymmetric cross-ply square plates (CC BCs) using Type II elements.

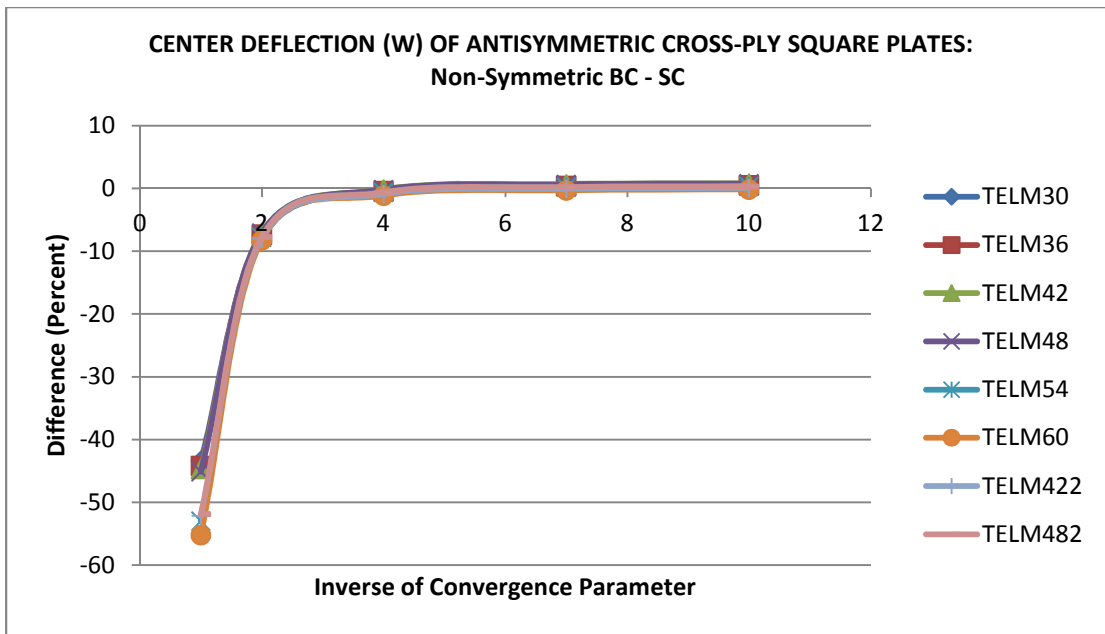


a)

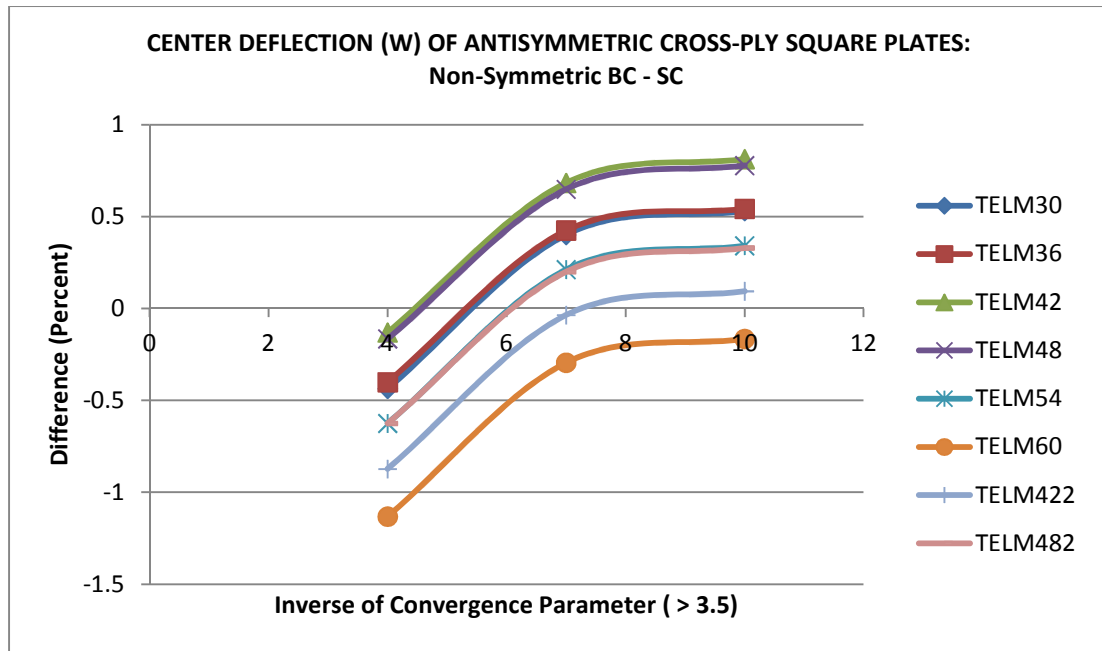


b)

Figure 5. 25 : Center deflection of antisymmetric cross-ply square plates (FF BCs) using Type II elements.

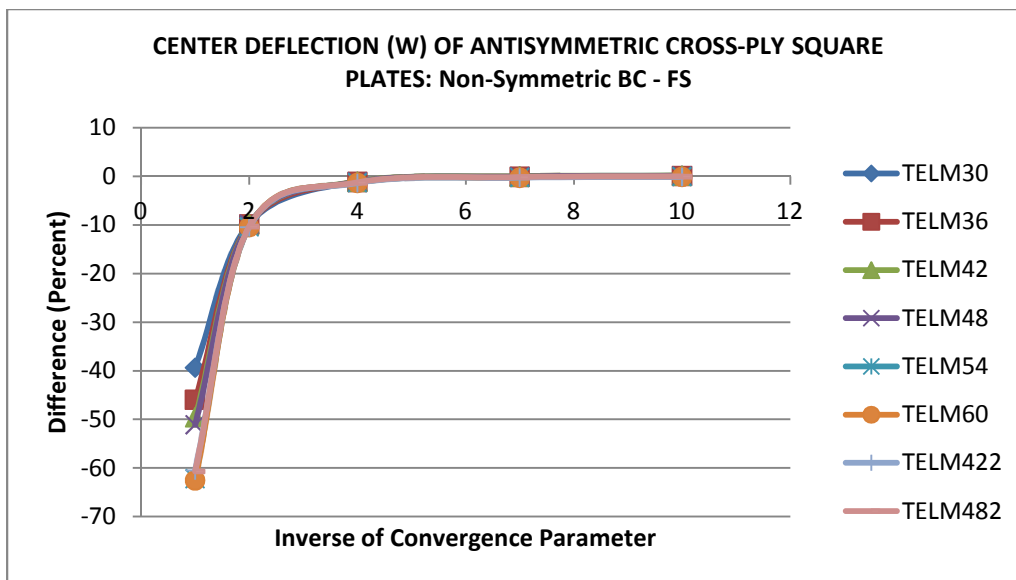


a)

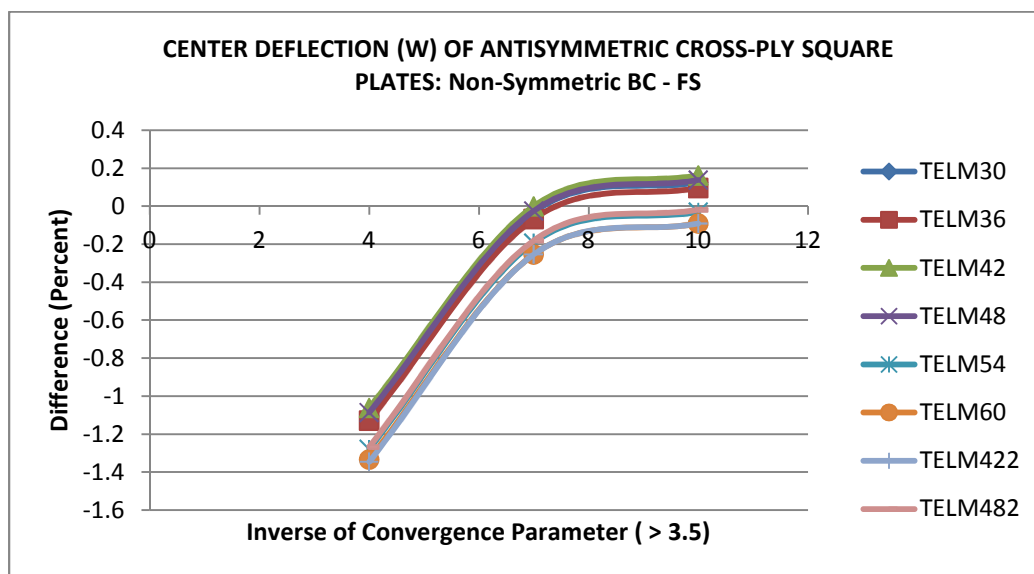


b)

Figure 5. 26: Center deflection of antisymmetric cross-ply square plates (SC BCs) using Type II elements.

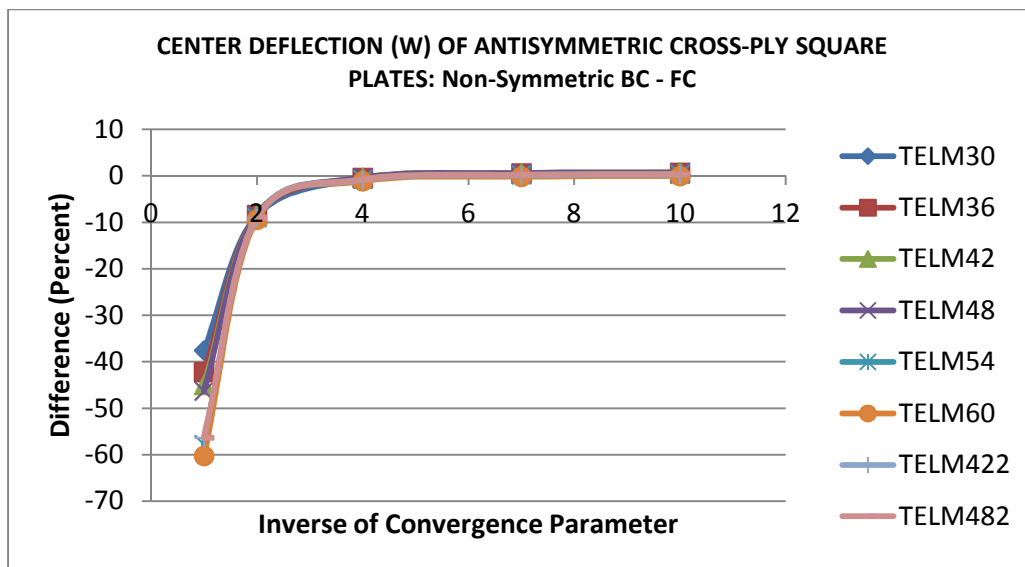


a)

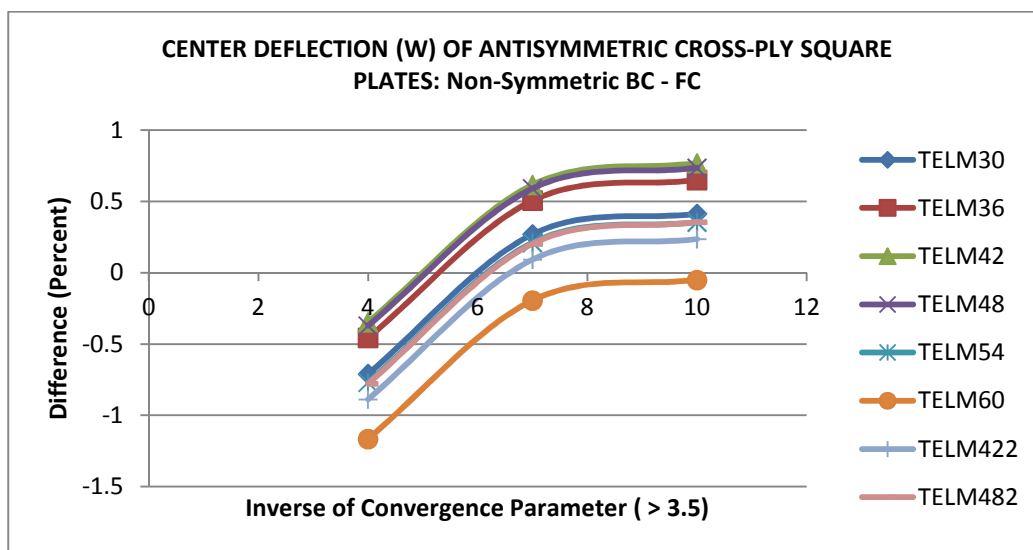


b)

Figure 5. 27: Center deflection of antisymmetric cross-ply square plates (FS BCs) using Type II elements.



a)



b)

Figure 5. 28: Center deflection of antisymmetric cross-ply square plates (FC BCs) using Type II elements.

Overall, displacement results for moderately thick antisymmetric square plates under sinusoidal loading have demonstrated the excellent performance of both Type I and Type II elements for various boundary conditions. A convergence parameter smaller than $1/3$ works well for all the elements.

All the elements have been used to analyze various laminated composites plates. For very thin to moderately thick plates, all the elements predict excellent results when compared to the exact elasticity solutions if the convergence parameter is smaller than $1/10$. However, for very thick plates, one should choose carefully the elements and the convergence parameter. Also noticeable, is that a convergence parameter smaller than $1/6$ gives less than 1% error for all Type II. Further, the best elements of the Type I category are the Lagrange subgroup, with the higher number of strain parameters. Therefore, the use of Lagrange Type II is cost effective for this case.

In the next Section, isotropic and laminated composite shell problems are analyzed using the proposed elements.

5.1.5 Barrel Vault Under Gravity Load

This case is a well-known benchmark problem (called Scordelis-Lo roof). The geometry of the problem is given in Figure 5.29. The roof is subjected to a distributed gravity load and is supported at each end by rigid diaphragm. The analytical solution for the maximum transverse deflection (point B in Figure 5.29) is reported by Kwon and Bang [157]. Other properties of the problem are given as:

Material properties: Isotropic

$$E = 3.0E06 \text{ psi}$$

$$\nu = 0.0$$

Dimensions: $a = 600 \text{ in.}$

$$R = 300 \text{ in.}$$

$$t = 3 \text{ in.}$$

$$\theta = 40^\circ$$

Loading: own weight of 90 lb/ft^2

Boundary Conditions: rigid support at both curved edges and free for the other two.

Meshing: using symmetry, only one fourth of the roof is discretized. 16 elements are used for this analysis as shown in Figure 5.29.

The results are given in Table 5 along with those obtained by Simo et al. [158], Reddy [24] and Kwon and Bang. Only the first order elements are used, since the material is isotropic. The two elements give very good results considering that they use only 65 nodes. Reddy's solution in comparison used more than three times the same number of nodes. It should be noted that early in this investigations, flat shell elements

were used to implement the higher order strain-based formulation proposed here. They performed poorly for this problem. The solid-shell formulation adopted here is more cumbersome to implement, but gives very good results for isotropic shells.

Table 5.9: Center deflection of the free edge of a Barrel Vault and comparison with other results.

Simo et al. [158]	Reddy [24] (289 nodes)	Ref. [157]	FELM36 (65 nodes)	FELM48 (65 nodes)
3.6288	3.6170	3.5088	3.5781	3.3727

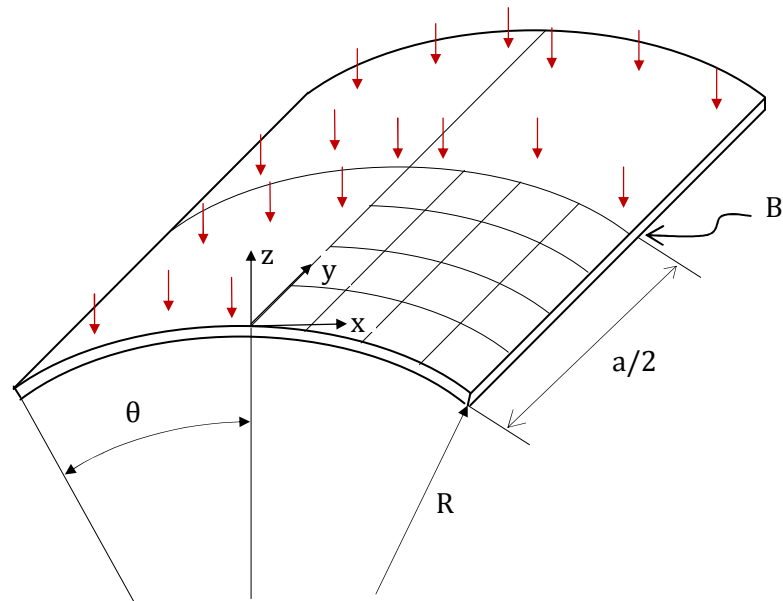


Figure 5. 29: Barrel Vault geometry and meshing (Scordelis-Lo Roof problem).

5.1.6 Pinched Cylinder Analysis

The pinched cylinder problem is, like the previous case, a benchmark problem for testing shell elements. It is considered by Belyschko et al. [159] as an “obstacle course” that any new shell element must pass. It tests an element’s ability to characterize both the state of constant transverse strain and the complexity of the state of membrane strain of shells in bending. Figure 5.30 shows the geometry of the cylinder. The cylinder is subjected to two diametrically opposite point loads of magnitude 1.0. Both ends of the cylinder are rigidly restrained by diaphragms. The analytical solution can be found in Ref. [157]. Other data of the problem are given as follows:

Material properties : Isotropic

$$E= 10.5E07 \text{ psi}$$

$$\nu = 0.315$$

Dimensions: $a = 10.35 \text{ in.},$

$$R=5 \text{ in.},$$

$$t=0.094 \text{ in.},$$

Loading: point load of 100 lb at the center (Figure 5.30).

Boundary conditions: rigid end diaphragms.

Meshing : in using symmetry, only one eighth of the roof is analyzed. 25 elements are used for this analysis as shown in Figure 5.30.

The two first order elements, FELM36 and FELM48, are used for the analysis as was the case for the other isotropic structures.

The numerical results are given in Table 5.10 along with the results from other researchers.

Table 5.10: Center deflection of a pinched cylinder and comparison with other results.

Analytical solution [157]	Kwon & Bang	FELM36	FELM48
0.1139	0.1087	0.24165	0.1186

FELM48 performs very well while FELM36 does not. One possible reason is that FELM36 does not have enough terms in its in-plane basis strain function to account for the complexity of membrane strain in this problem. It has six terms, two terms shy of the “serendipity” elements and four missing terms compared to the complete “Lagrange” type elements.

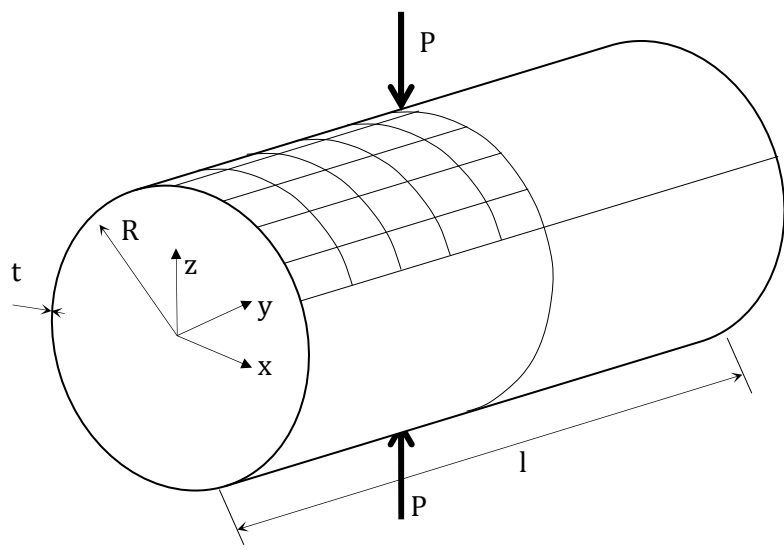


Figure 5. 30: Pinched cylinder geometry and meshing.

5.1.7 Maximum Transverse Deflections of a Two-Layered Cross-Ply Laminated Cylindrical Shell Roof of Various Thickness

The problem considered is similar to the Barrel Vault problem of Section 5.1.5 as the geometry and loading conditions are the same. However, the roof is a laminated composite. Reddy [24] used a displacement finite element model to analyze this problem. His results appear to be the only ones available for comparison. The material properties are

$$E_{11} = 25.0 \text{ E06 psi}, \quad E_{22} = 1.0 \text{ E06 psi}$$

$$G_{12} = 0.5 \text{ E06 psi}, \quad G_{23} = 0.2 \text{ E06 psi},$$

$$\nu_{12} = \nu_{21} = 0.25$$

Boundary condition:

$$\text{at } y = 0 \text{ and } 10, \quad u_0 = w_0 = \theta_y = 0;$$

The absence of constraints on the displacement along the x-axis suggests that one must add another constraint in order to avoid rigid body motion. The center of the shell is therefore constrained in the x-direction (at $x = 0$ and $y = 1/2$, $v_0 = 0$).

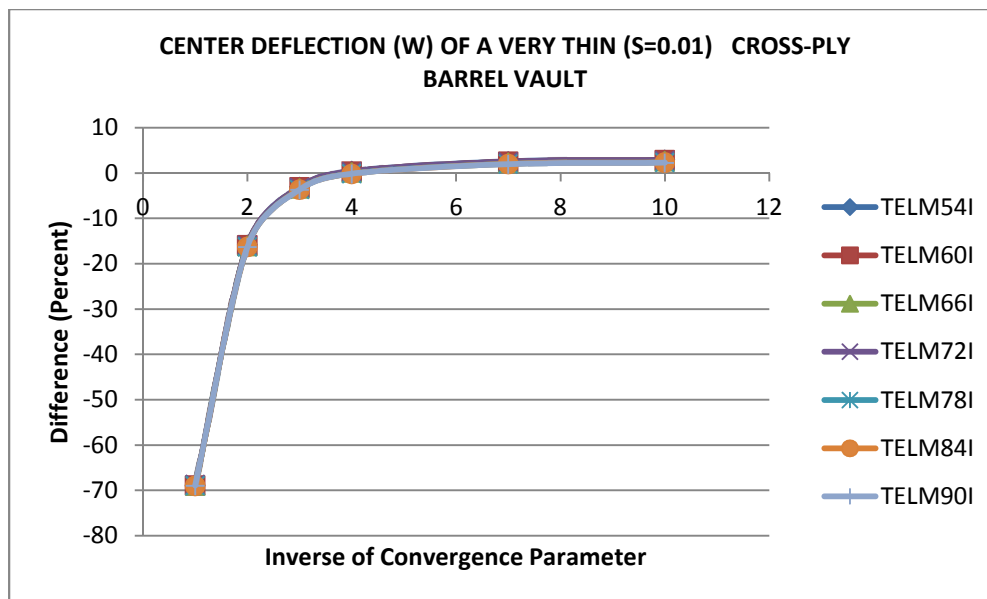
Meshing: the full shell roof is modeled with 16 elements (4 x 4).

The nondimensionalized transverse displacement (w_N), evaluated at the center of the roof, is computed as follows:

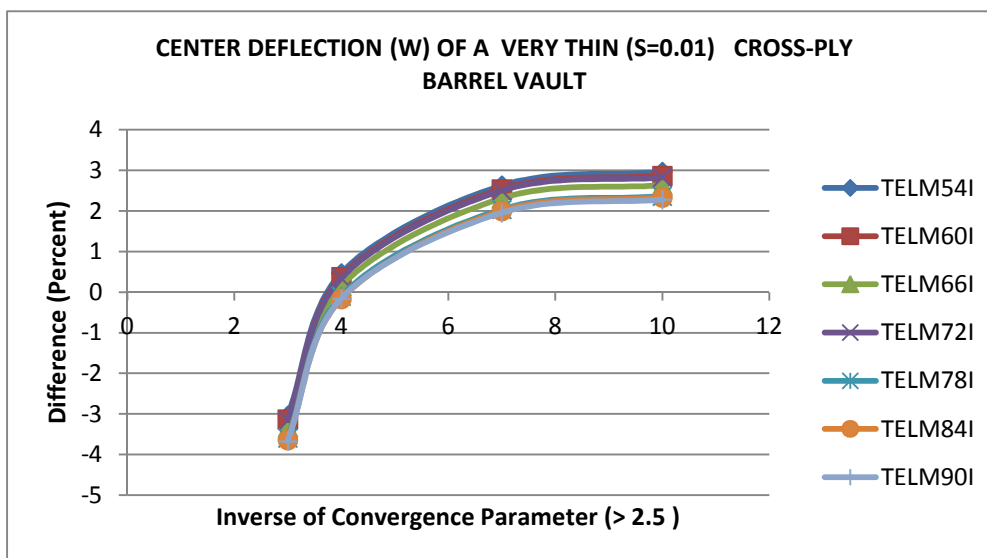
$$w_N = w_{FEM} \frac{10E_1 t^3}{qR^4} \quad (5.7)$$

Very thin to moderately thick shell roofs are analyzed. Eight Type I elements are used for the analysis. Those with the higher number of strain parameters and associated with the Lagrange type element (like FEM48) are selected. However, two “serendipity” types are also analyzed for comparison purpose.

It can be seen from Figures 5.31 through 5.33 that the results are in excellent agreement with the reference solutions. As was the case for the plate analyses, an absence of the convergence parameter yields results that have an over 70 % percent difference. Also, none of the elements converges identically to the analytical solution. However, for the thin to moderately thin composite barrel vaults analyzed all the elements converge towards the reference solution for smaller convergence parameters.

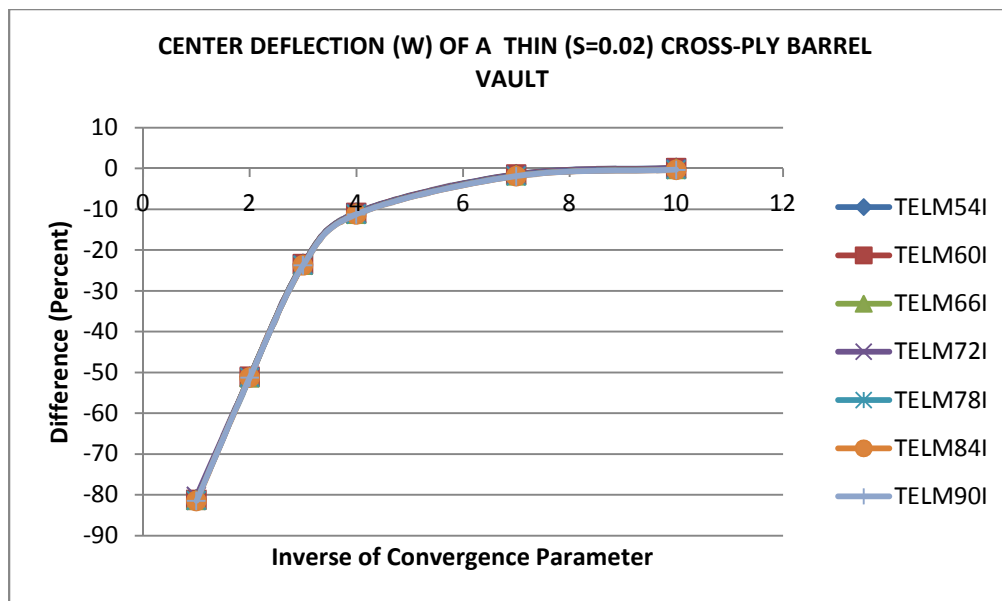


a)

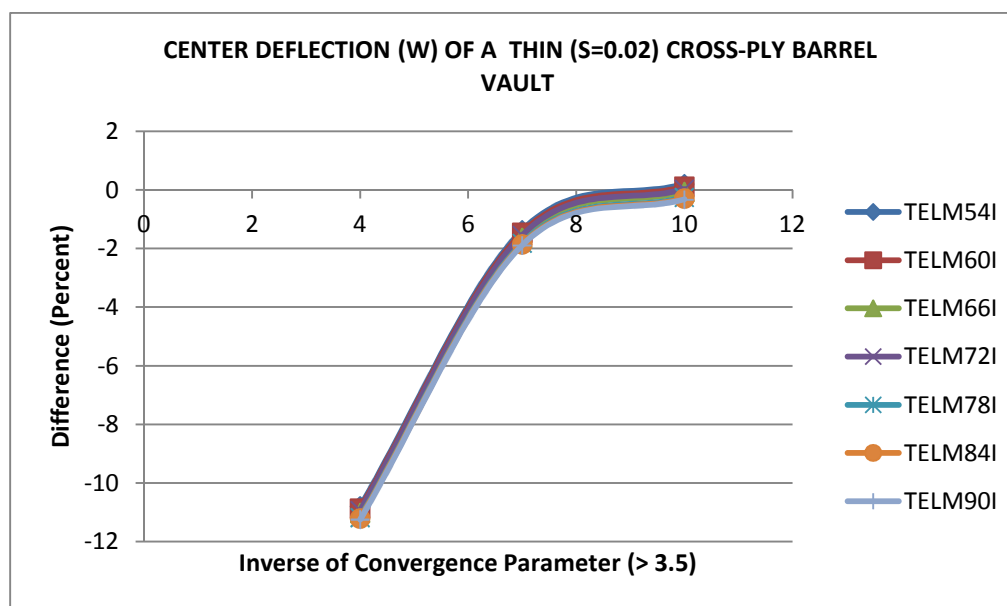


b)

Figure 5. 31: Center deflection of a very thin ($S = 0.01$) cross-ply Barrel Vault using Type I element

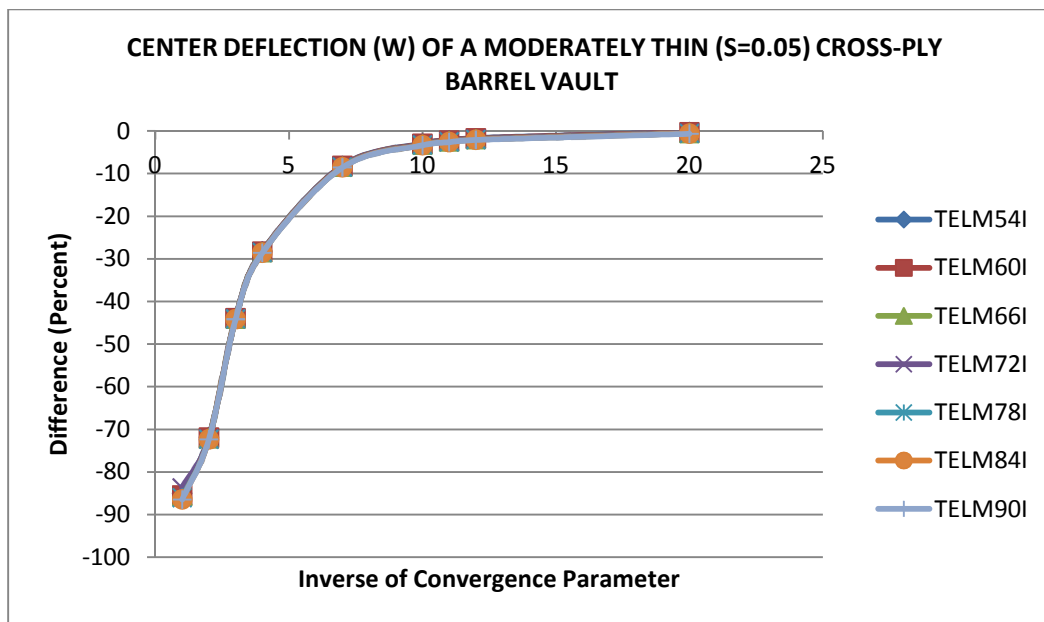


a)

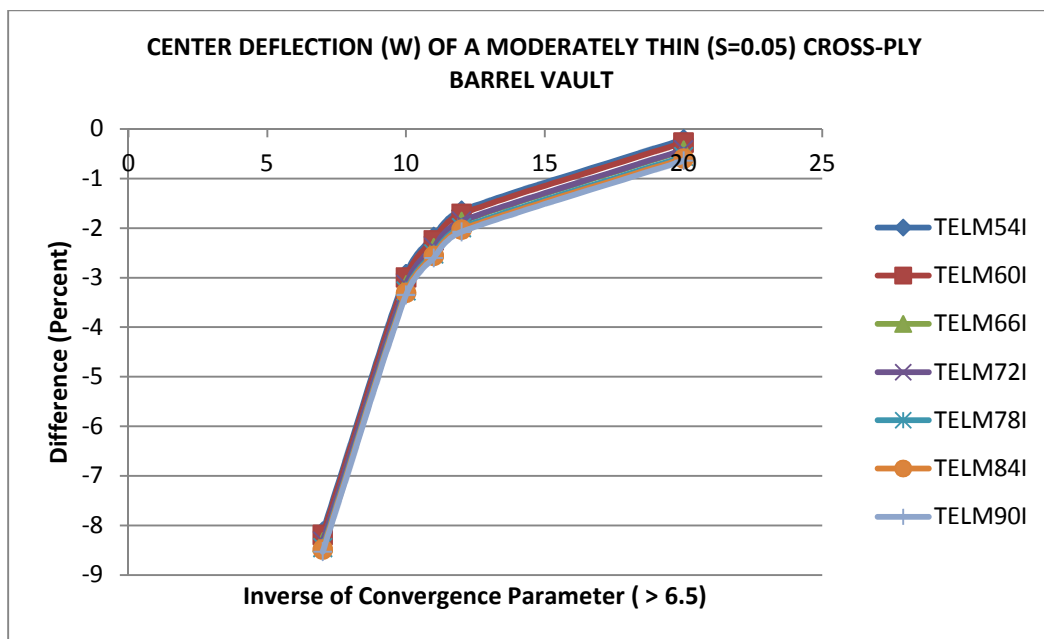


b)

Figure 5. 32: Center deflection of a thin (S=0.02) cross-ply Barrel Vault using Type I element.



b)



b)

Figure 5. 33: Center deflection of a moderately thin (S=0.05) cross-ply Barrel Vault using Type I element.

In the above sections, the displacement of various plates and shells structures subjected to different type of loadings and boundary has been analyzed with the proposed Type I and Type II elements. Very good to excellent results are obtained with these elements, especially for very thin to moderately thick plate and shell structures. The Type I and Type II Lagrange elements perform better for thick plates. Also, the “Pinched Cylinder” test was passed by the first order Lagrangian types.

In the next Section, the same range of convergence parameters will be used for the stress analysis composite laminated plates and shells. The same problems as in Section 5.1 will again be analyzed with Type I and Type II elements.

5.2 Stress Examples

Composite laminated structures fail mostly due to delamination. Thus, an accurate stress analysis of composite plates and shells is very important. Many authors emphasize the importance of the transverse stresses [14, 33, 40, 54]. However, because of the coupling effect in composite laminated structures, it is equally important to have the in-plane stress determined accurately for an effective failure analysis. In this Section, the in-plane and transverse stress results are compared to the exact elasticity or exact analytical solutions when possible. Also, the same categories of elements as in displacement analyses are going to be used. For each case, a summary of the problem data is given.

5.2.1 Bending Stresses of a Simply Supported Isotropic Square Plate

This is the same case as in Section 5.1.1. The problem data are as follows:

Material properties : Isotropic

$$E = 26.0 \text{ E}07 \text{ psi}$$

$$\nu = 0.3$$

Dimensions: $a = 10 \text{ in.}$,

$t=0.2 \text{ in.}$,

Loading: Transversely distributed load of 100 psi on the top surface of the plate.

Meshing : sixteen elements (4 x 4).

Figure 5.33 shows the stress distribution through the thickness of the plate. The element FELM36 result is in excellent agreement with that of classical plate theory.

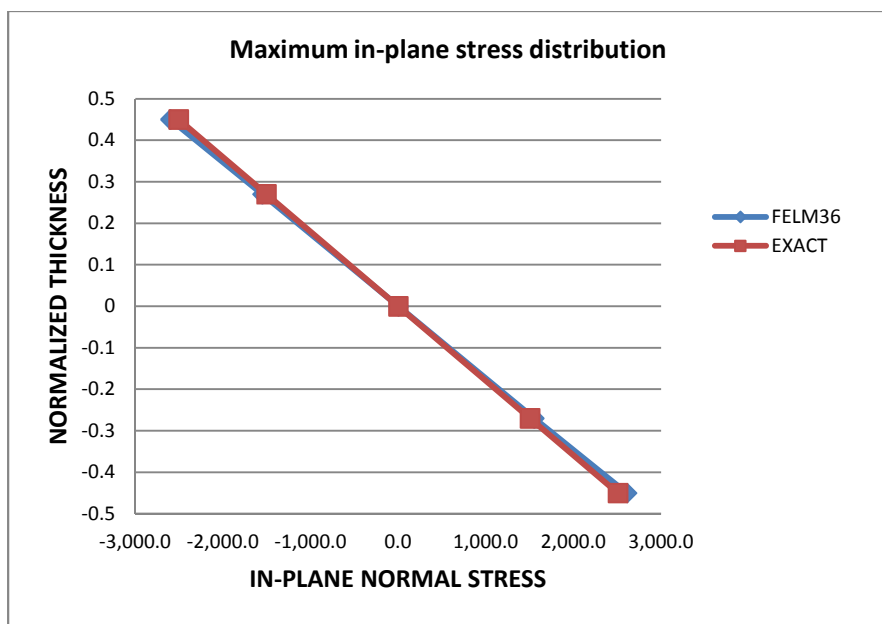


Figure 5.34: Maximum In-plane distribution of an isotropic square plate

5.2.2 Stress Analysis of a Three-Layered Semi-Infinite Strip

The case analyzed is the same as in Section 5.13. It is a three-layer cross-ply (0,90,0) long strip. The material properties of each layer are:

$$E_{11} = 25.0E06 \text{ psi} \quad E_{22} = 1.0E06 \text{ psi}$$

$$G_{12} = 0.5E06 \text{ psi} \quad G_{23} = 0.2E06 \text{ psi}$$

$$\nu_{12} = \nu_{12} = 0.25$$

$$\text{Sinusoidal loading: } q(x,y) = Q_0 \sin(\pi x/l)$$

$$l = 10 \text{ in} \quad \text{width of the plate}$$

$$b = 1 \text{ in} \quad \text{width of the strip in the infinite direction}$$

$$S = h/l \text{ various thickness to width ratio}$$

Boundary Conditions: symmetric case.

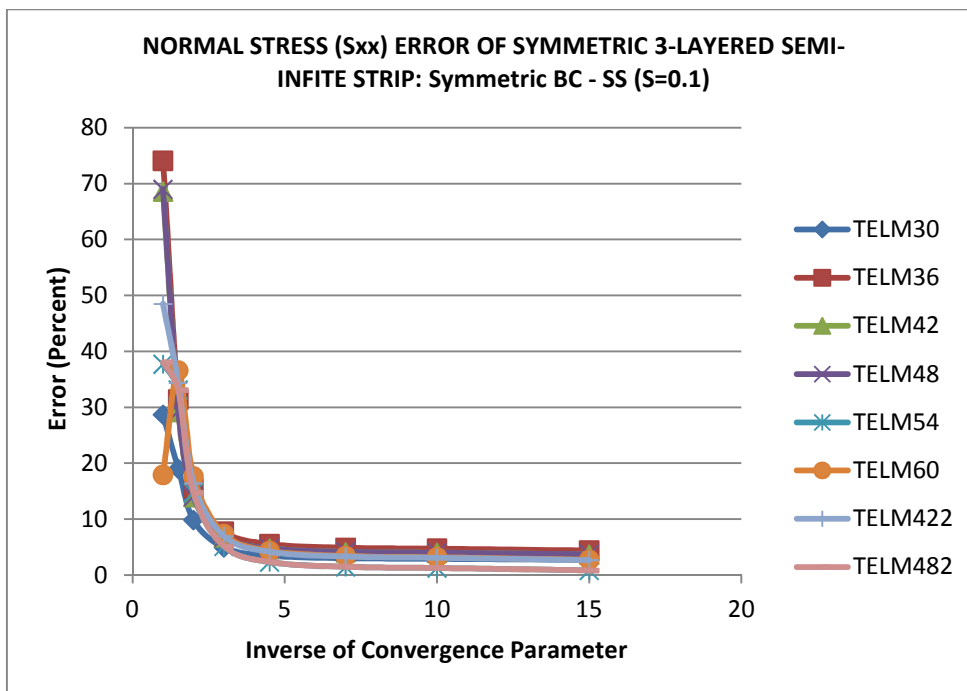
Meshing: one half of the strip is modeled with 5 elements (1 x 5)

The exact elasticity solution of Pagano [4] is used for comparison. The elements associated with independent higher order rotational strain basis functions - element with 'I' at the end of the nomenclature such as (TELM36I) are presented first. For each of the boundary conditions, the difference in percentage between the finite element result and the exact elasticity solution is presented as a function of the convergence parameter. The latter is in fact a convergence factor, since it characterizes how well and fast the element solution converges towards a certain value, not necessarily towards the first order theory solution. It is observed that, in general, the finite element solutions tend to the exact or the analytical value. The convergence parameter is a direct proportional coefficient of the z terms. As the convergence parameters are again generally smaller than one, the inverse may provide a better number for graphical presentation. To highlight the importance of

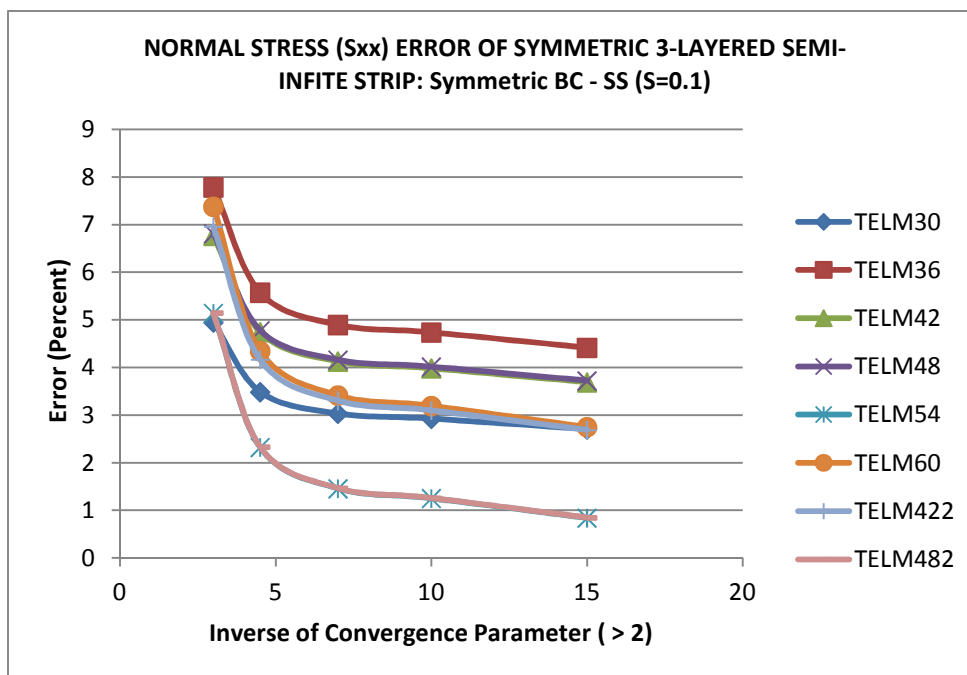
the convergence parameter, two figures are again given for each boundary case. In the first (Figure a)), the evaluation of the error (compare to the exact elasticity solution or the percentage difference if compared to the analytical solution) starts with the convergence parameter equal to one, meaning a strain function without convergence parameter. The second (Figure b)) shows the change in error when the range of weighing factors which gives an excessive error is removed. After the independent functions are analyzed, then the elements associated with a non-linear variation of the rotational basis strain functions are presented.

The following figures illustrate the error evolution of both normal in-plane and transverse shear stresses.

It can be seen in Figures 5.35 and 5.36 that there is very good agreement between the finite element solution and the exact elasticity solution when the convergence parameter is smaller than $1/6$, except for element TELM60 which is the only one giving a poor result for a large range of convergence parameters. This is due to the x^3 and y^3 terms in the transverse strain function. The result is excellent for 3 elements (TELM30, TELM422, TELM482).

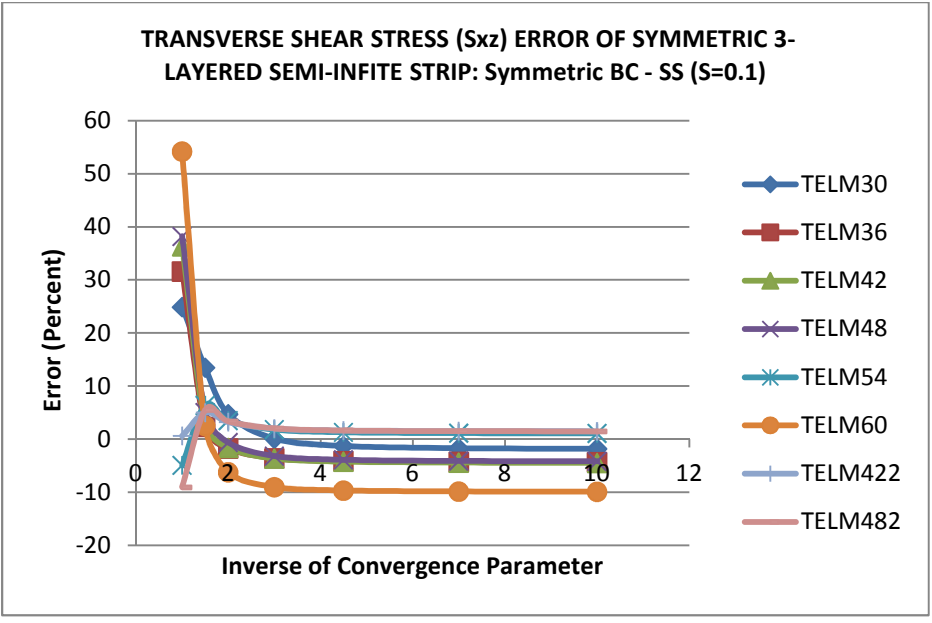


a)

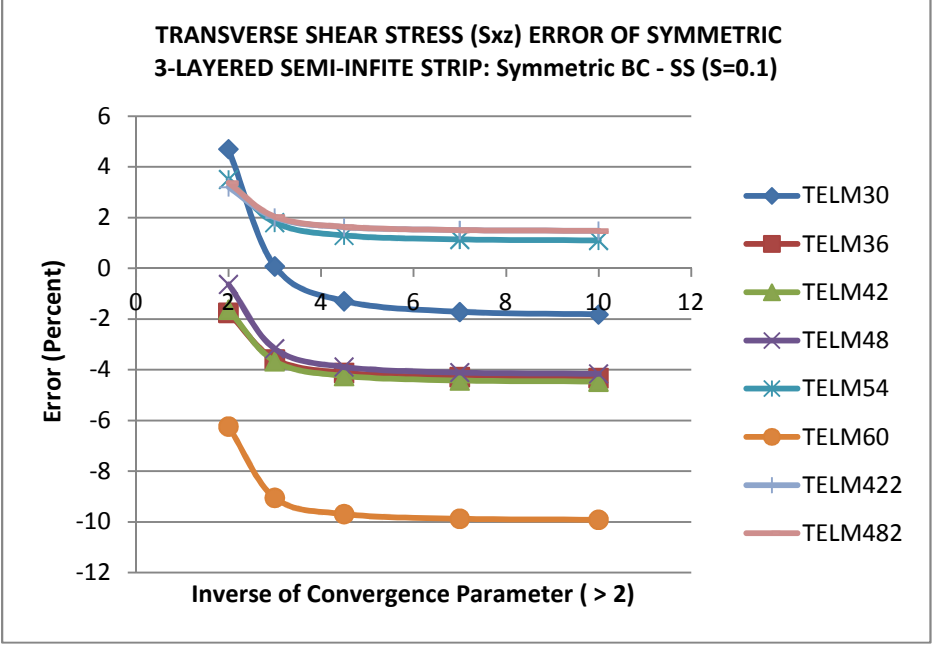


b)

Figure 5. 35: Normal stress evaluation of a symmetric 3-layered semi-infinite strip



a)



b)

Figure 5. 36: Transverse shear stress evaluation of a symmetric 3-layered semi-infinite strip.

5.2.3 Stress Analysis of an Anti-Symmetric Cross-Ply Square Plate with Various Edge Boundaries Conditions.

The square plate of Section 5.1.4 is also analyzed for stresses. As with the displacement case, Khdeir and Reddy [62] solutions are used for comparison. The following material properties are used for each layer:

$$E_{11} = 25.0E06 \text{ psi} \quad E_{22} = 1.0E06 \text{ psi}$$

$$G_{12} = 0.5E06 \text{ psi} \quad G_{23} = 0.2E06 \text{ psi}$$

$$\nu_{12} = \nu_{12} = 0.25$$

The loading is assumed to be Sinusoidal: $q(x,y) = Q_0 \cos(\pi x/a) \sin(\pi y/b)$

$$a = 10 \text{ in} \quad \text{length of the plate}$$

$$b = 10 \text{ in} \quad \text{width of the plate}$$

$$S = 0.1 \quad \text{moderately thick}$$

Six different boundary conditions, as a combination of simply supported and clamped edges, are used as presented in Table 5. 7 of Section 5.1.4.

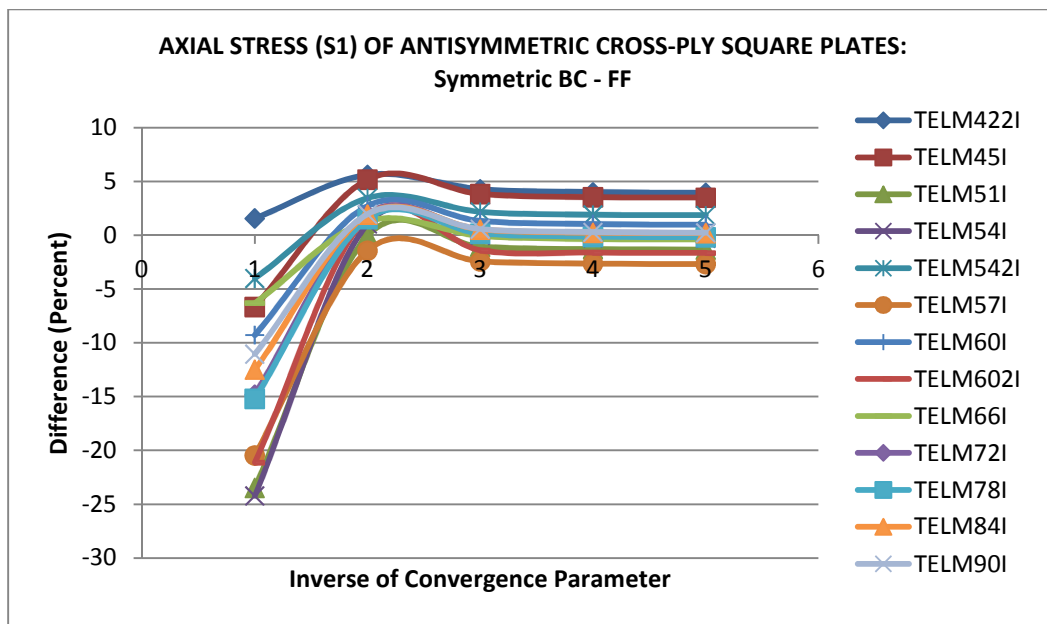
Nomenclature for the boundary condition:

Symmetric analysis:	Non-symmetric analysis:
SS: simply supported on both ends	SC: simply supported and clamped
CC: clamped on both ends	FC: free and clamped edge
FF: free BC on both ends	FS: free BC and simply supported

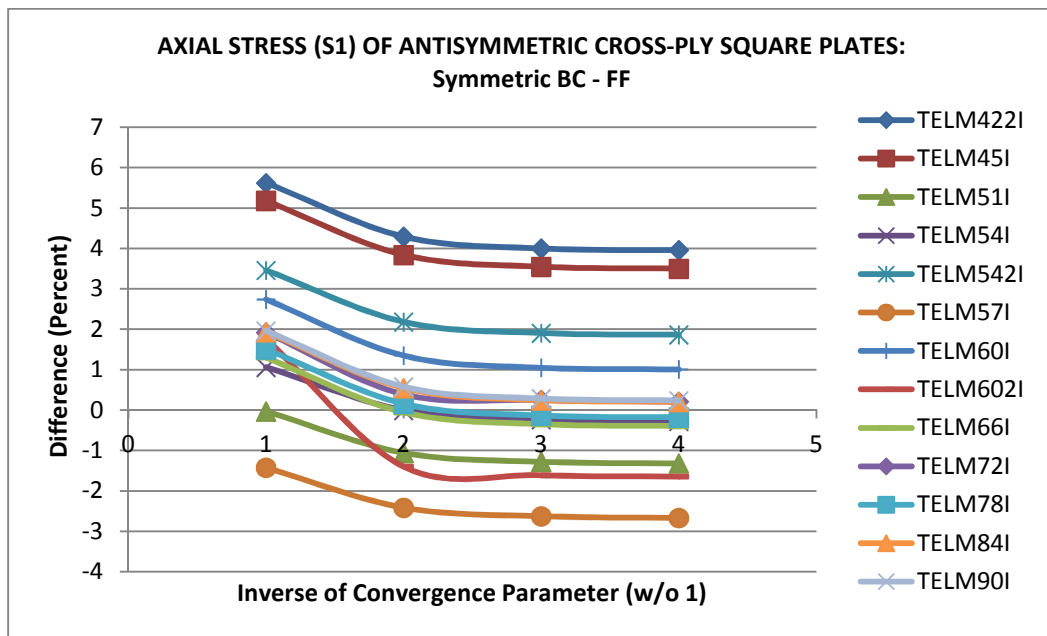
Note that the convergence parameters range used for displacements is also used here, so that the same convergence parameter is applied for both the displacements and

the stresses. Therefore, here the convergence parameters are not correction coefficients applied to a particular component of the analysis; rather, they are applied to the overall behavior of the structure. They thus adjust the coefficients of the strain functions to the complexity of the loading, boundary conditions and geometry. It is a variant of the strain field as defined in Eq. (3.28). The presentation is divided between a comparison of Type I elements and then a combination of the best type I and all the elements of Type II. Also, two figures types illustrate the evolution of the difference between analytical solution and the finite element solution. Figures 5. 37 through 5.45 show the evolution of in-plane normal stresses and the transverse shear stress for Type I elements.

On can notice the good agreement between the finite element solutions and the exact analytical solutions for most elements when the convergence parameter is smaller than $1/8$. However, it can be observed from Figures 5.37b, 5.38b, 5.39b, 5.40b, and 5.41b that the Type I Serendipity elements have poor agreement for the in-plane normal stresses associated with boundary conditions SS and CC (Figure 5.38b and 5.39b). Although some of the results for elements, TELM422I, TELM45I and TELM54I, are within an acceptable agreement in terms of transverse stress analysis, these elements should not be used because of their overall poor performance.

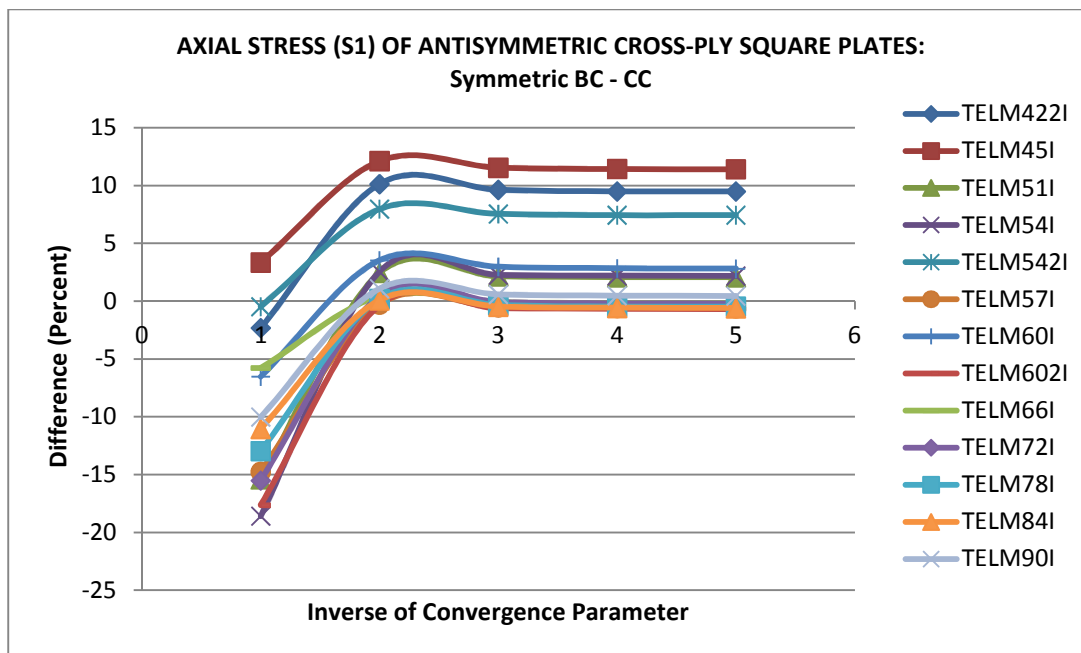


a)

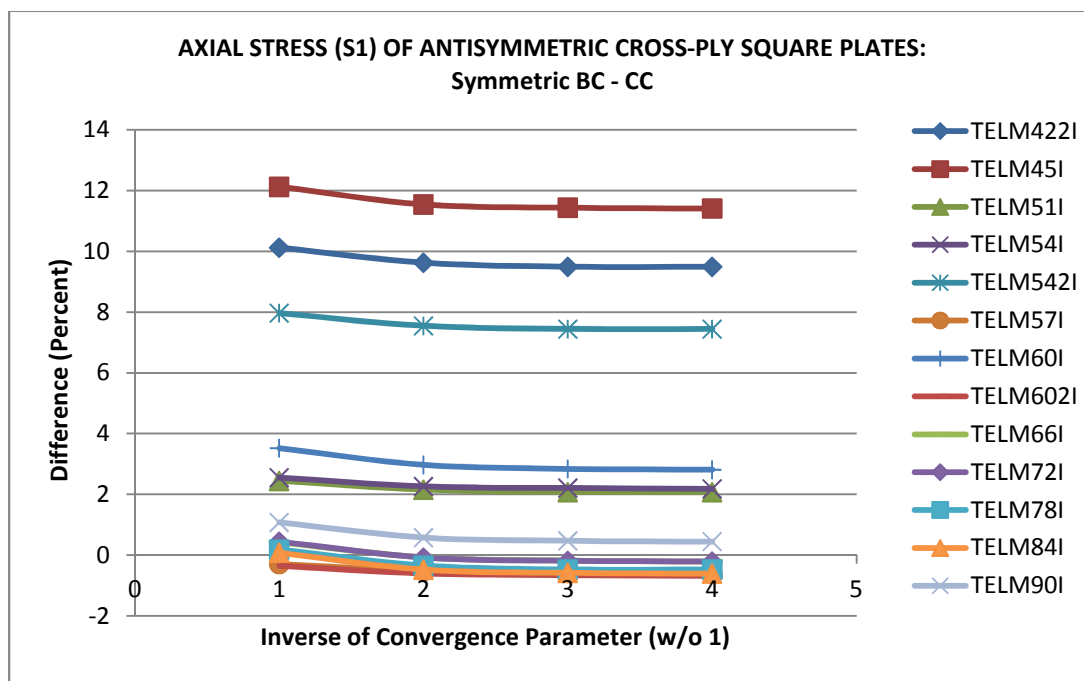


b)

Figure 5. 37: Axial stress (S1) of antisymmetric cross-ply square plates (FF BCs) using Type I elements.

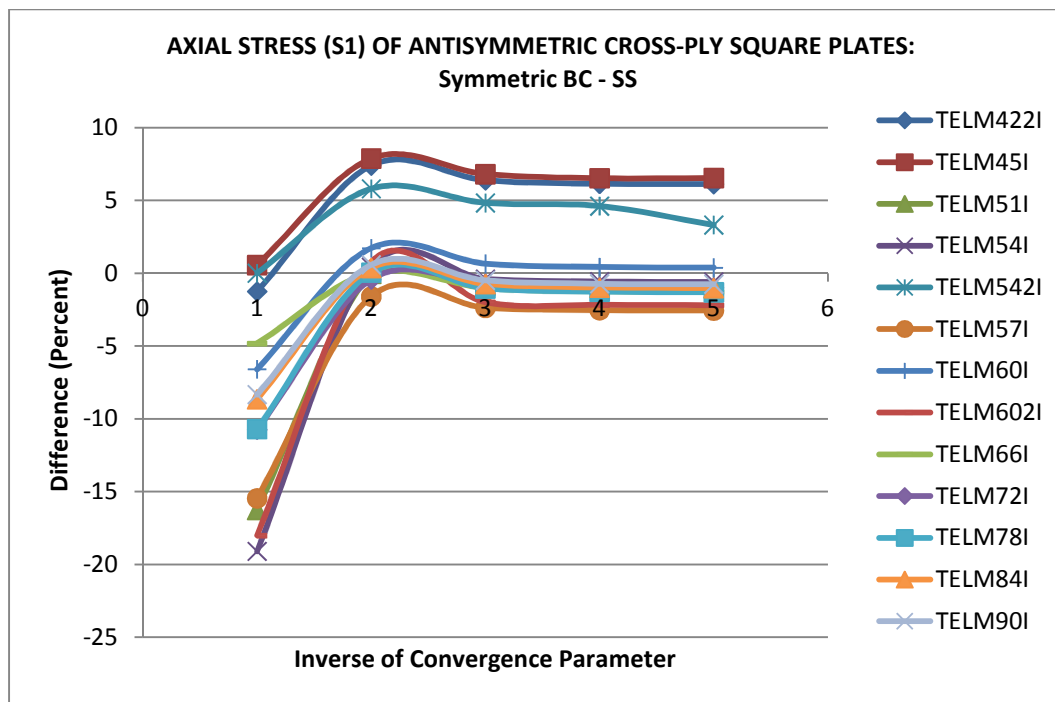


a)

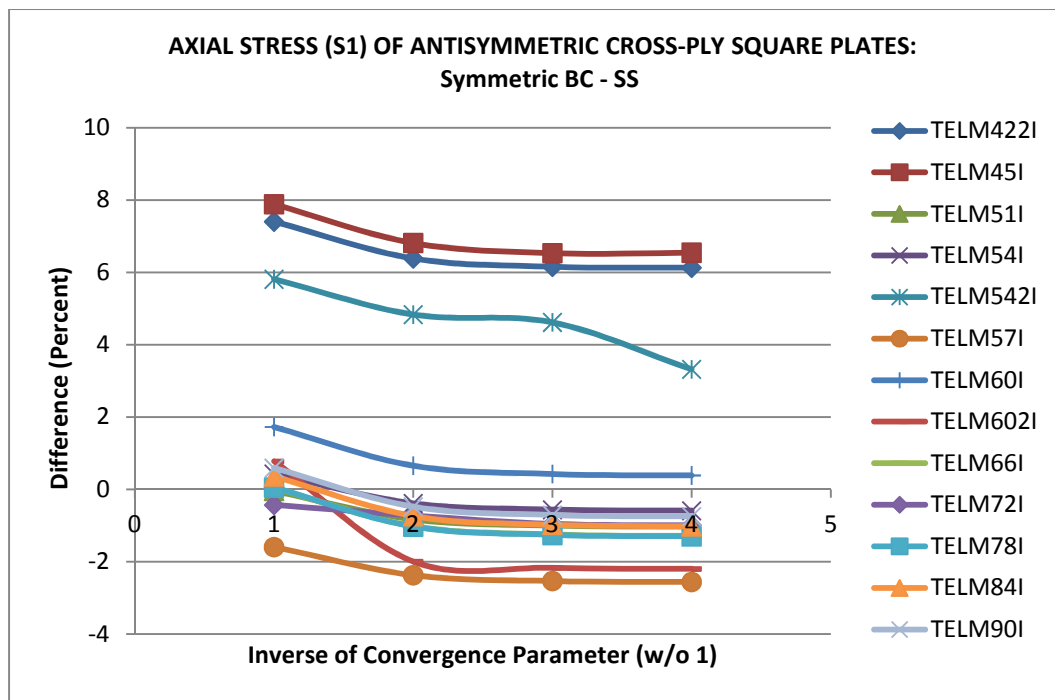


b)

Figure 5. 38: Axial stress (S1) of antisymmetric cross-ply square plates (CC BCs) using Type I elements.

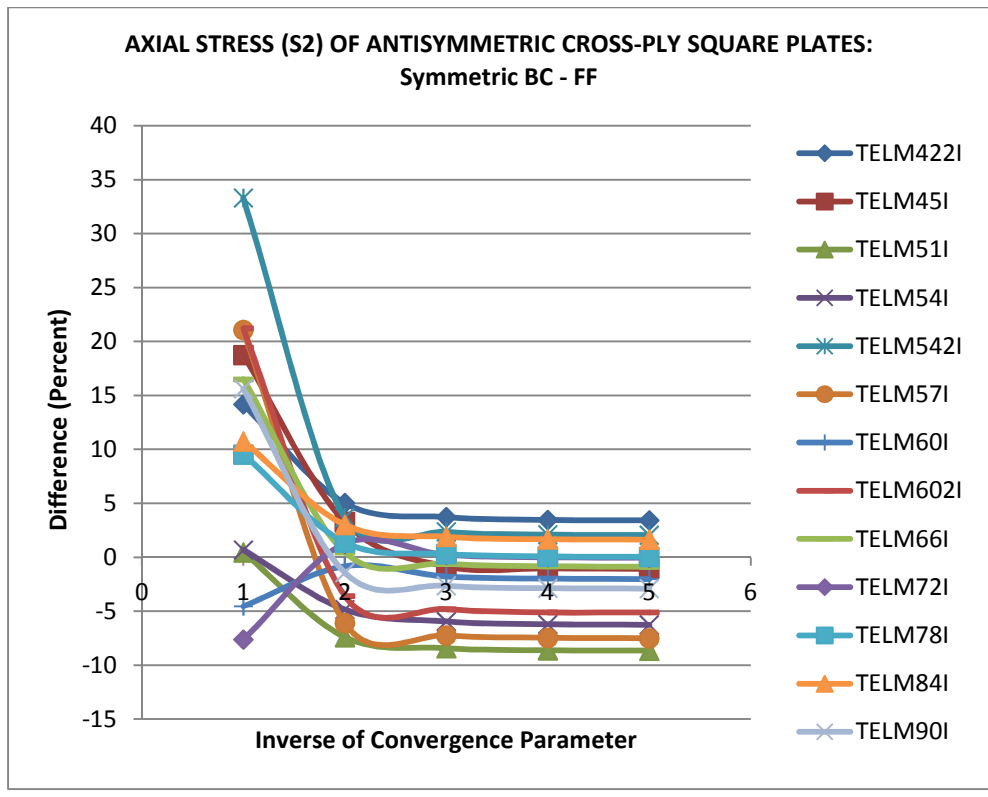


a)

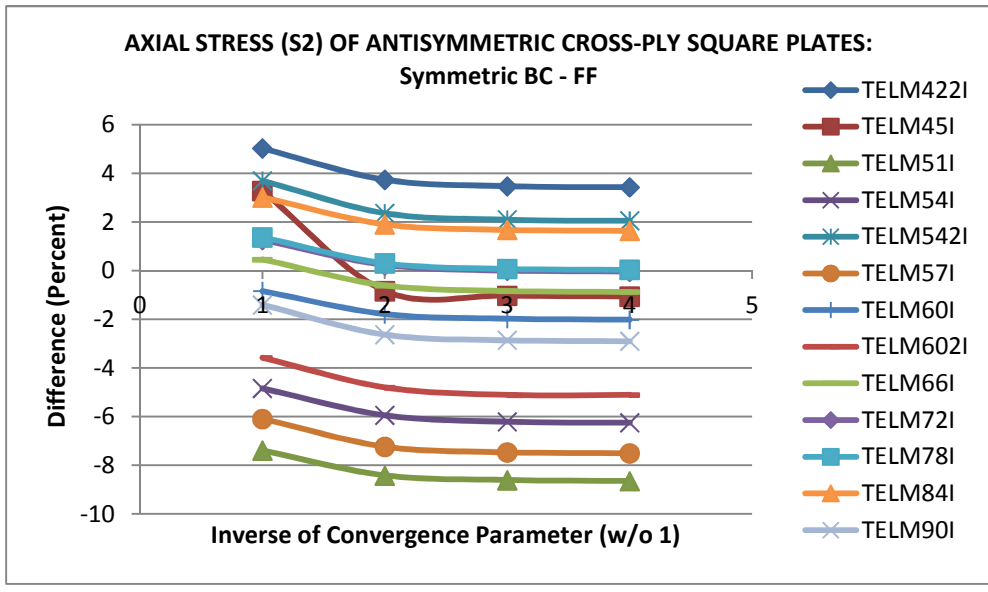


b)

Figure 5. 39: Axial stress (S1) of antisymmetric cross-ply square plates (SS BCs) using Type I elements.

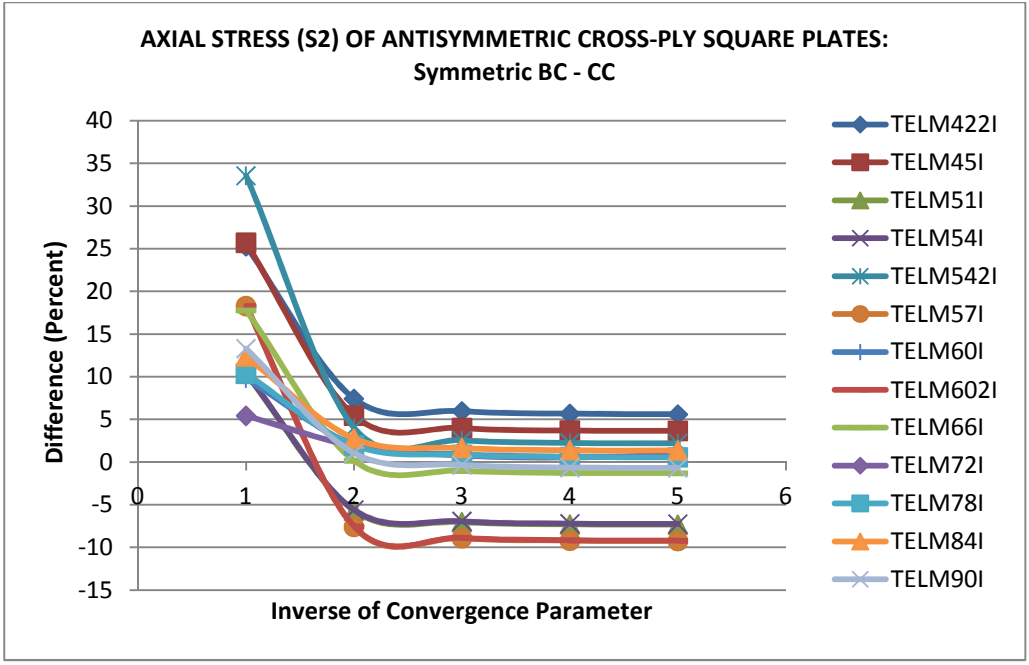


a)

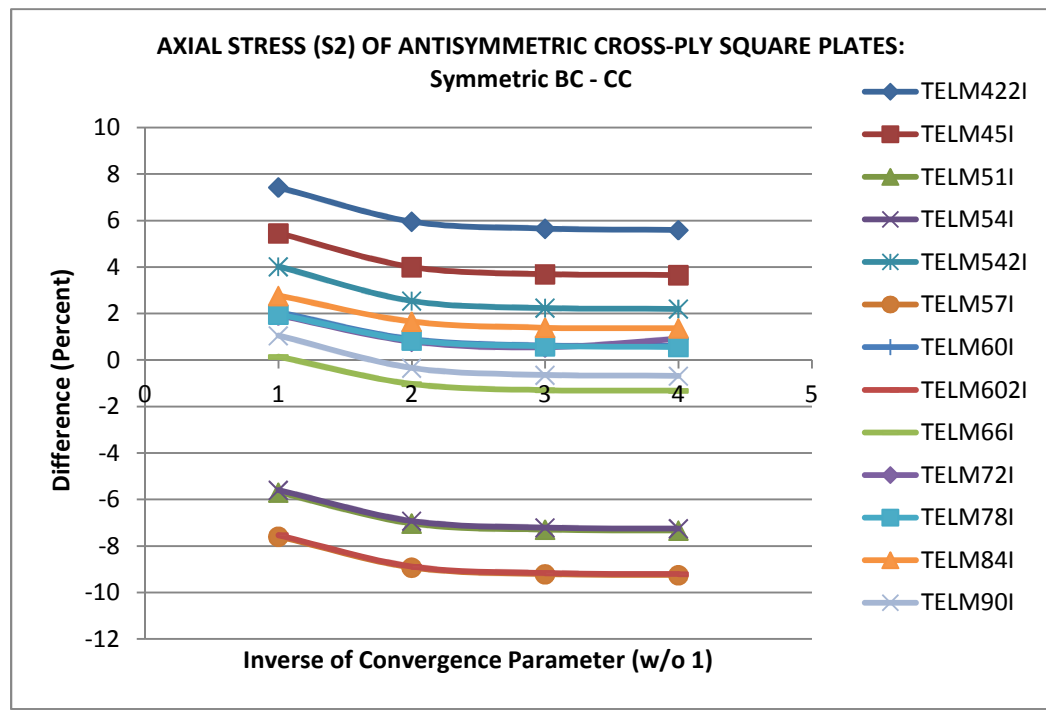


b)

Figure 5. 40: Axial stress (S2) of antisymmetric cross-ply square plates (FF BCs) using Type I elements.

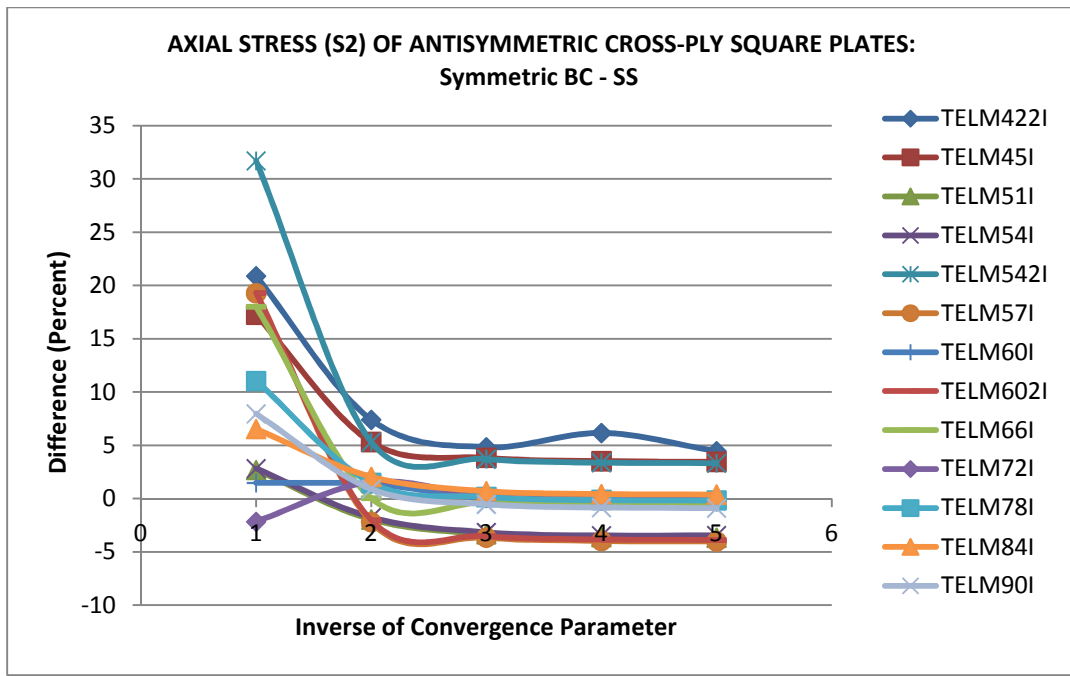


a)

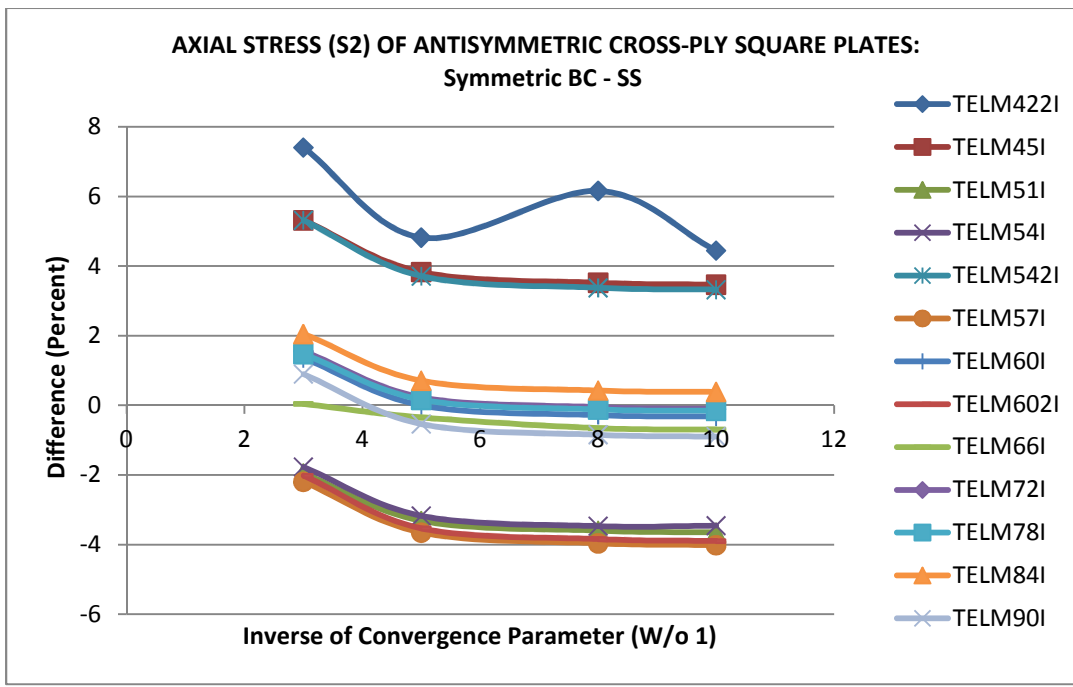


b)

Figure 5. 41: Axial stress (S2) of antisymmetric cross-ply square plates (CC BCs) using Type I elements.

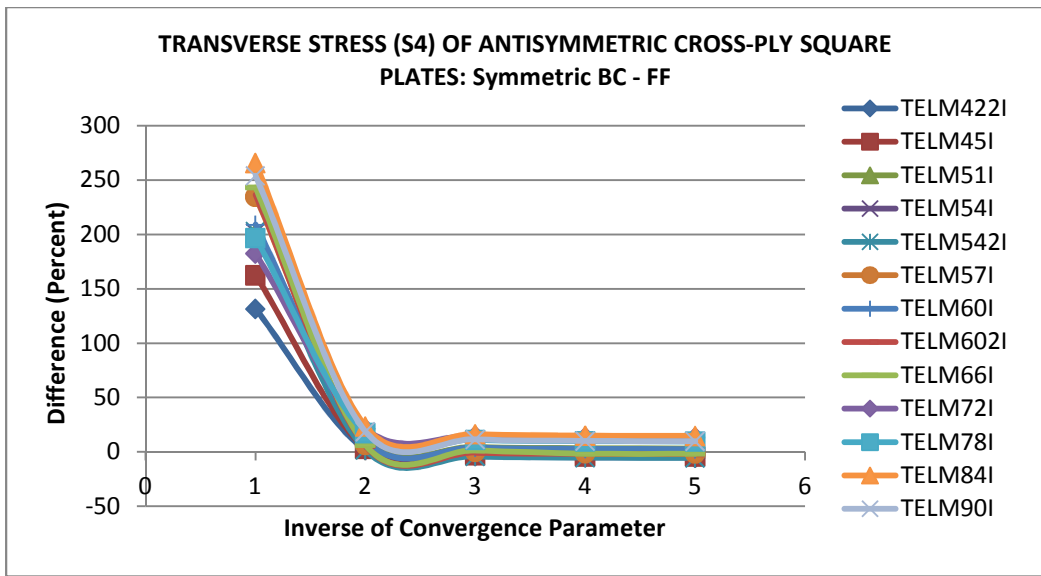


a)

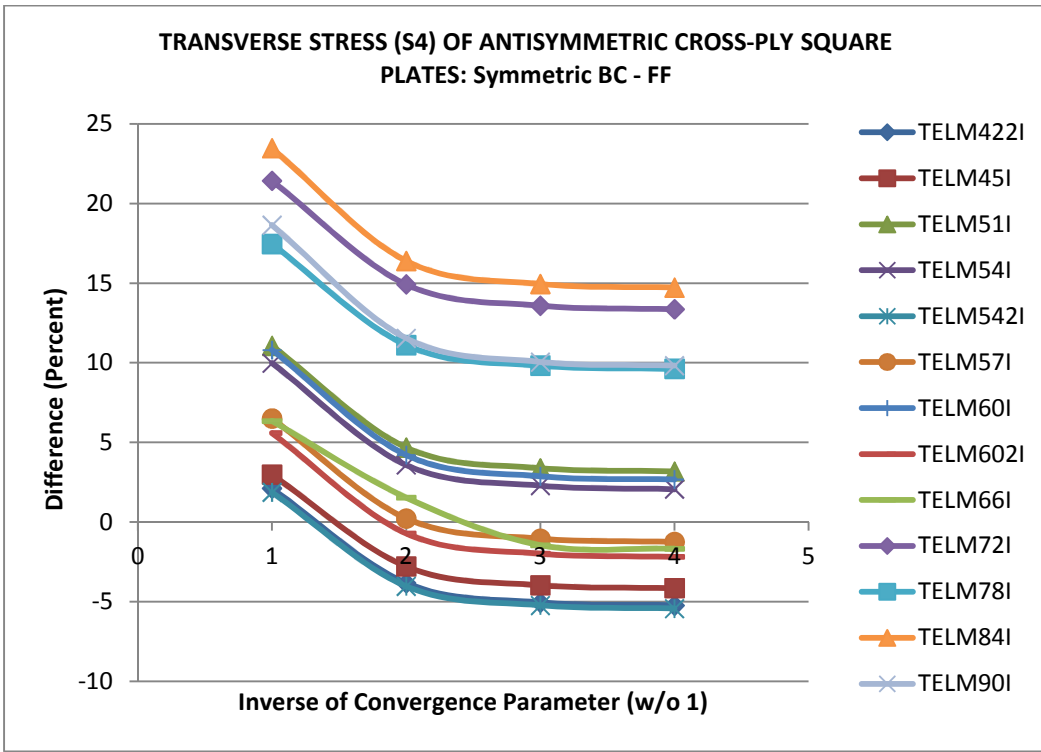


b)

Figure 5. 42: Axial stress (S2) of antisymmetric cross-ply square plates (SS BCs) using Type I elements.

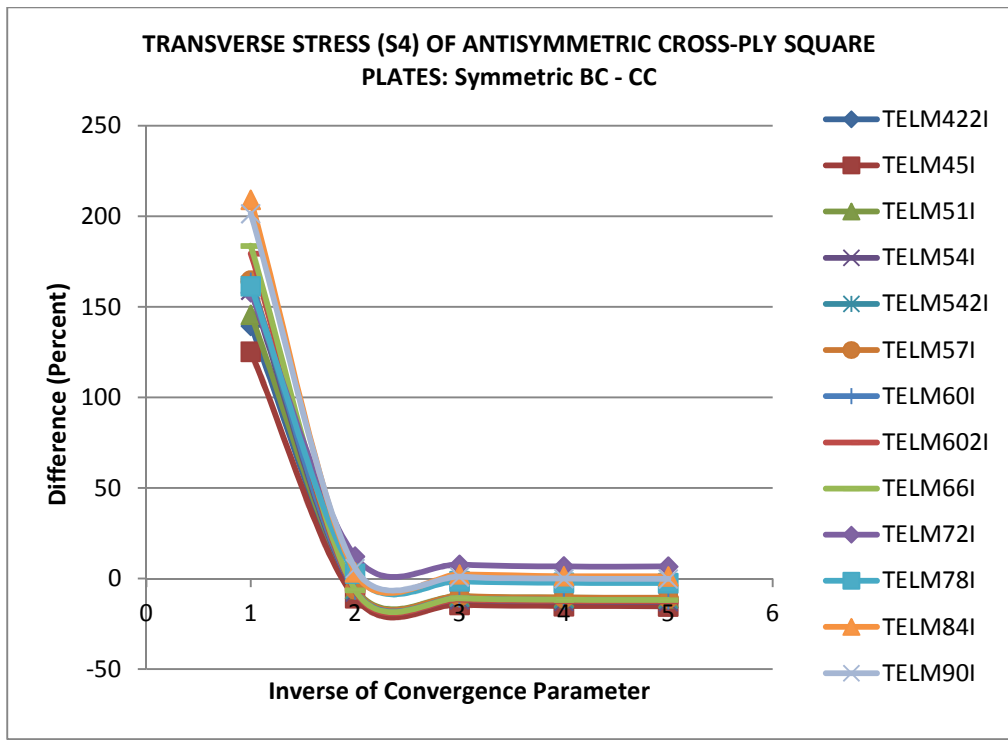


a)

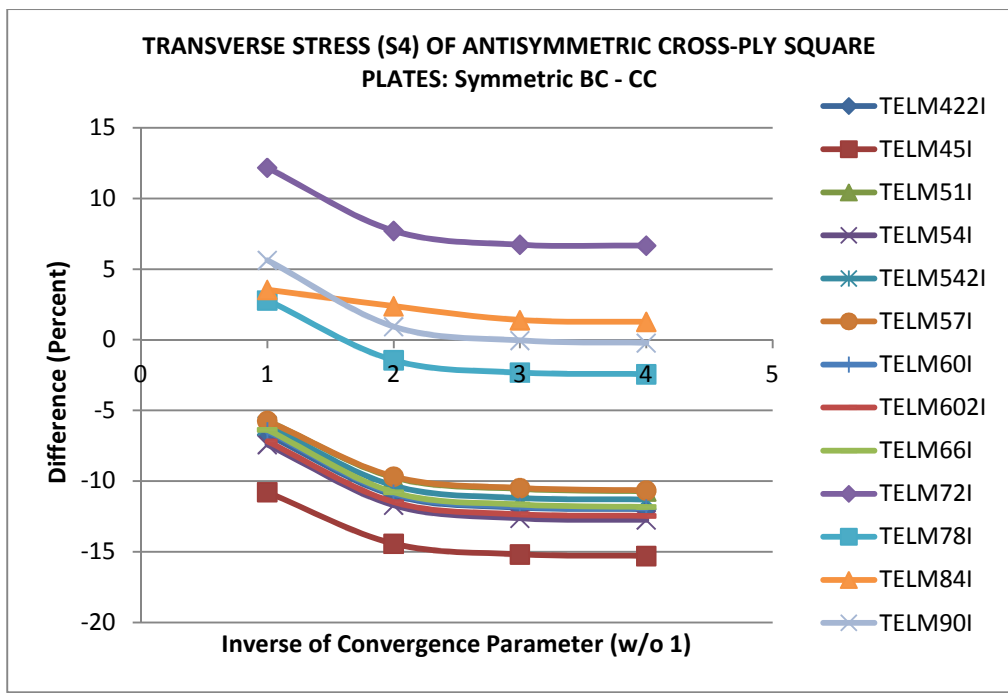


b)

Figure 5. 43: Transverse shear stress (S4) of antisymmetric cross-ply square plates (FF BCs) using Type I elements.

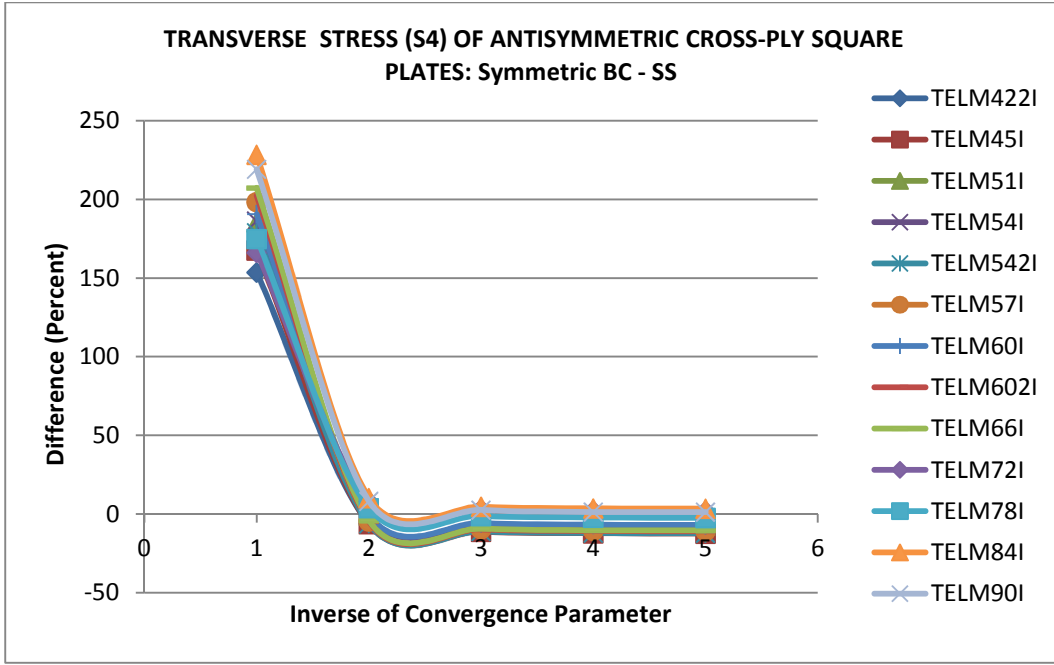


a)

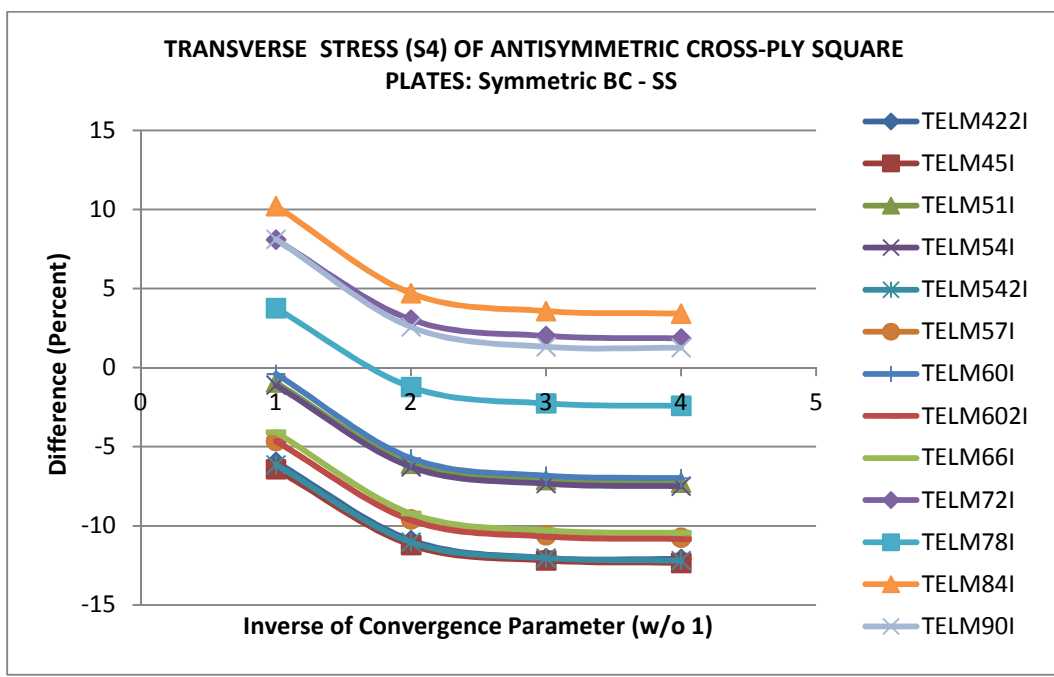


b)

Figure 5. 44: Transverse shear stress (S4) of antisymmetric cross-ply square plates (CC BCs) using Type I elements.



a)



b)

Figure 5. 45: Transverse shear stress (S4) of antisymmetric cross-ply square plates (SS BCs) using Type I elements.

Base on the previous analysis, only five Type I elements are being kept for comparison purposes with Type II elements. They are the most consistent for all the displacement and stress analysis carried out so. Also, the critical boundary conditions that were used to eliminate some elements are chosen for comparison purposes. They are the symmetric boundary conditions. The following Figures, from 5.46 to 5.51, illustrate the behavior of the Type II elements

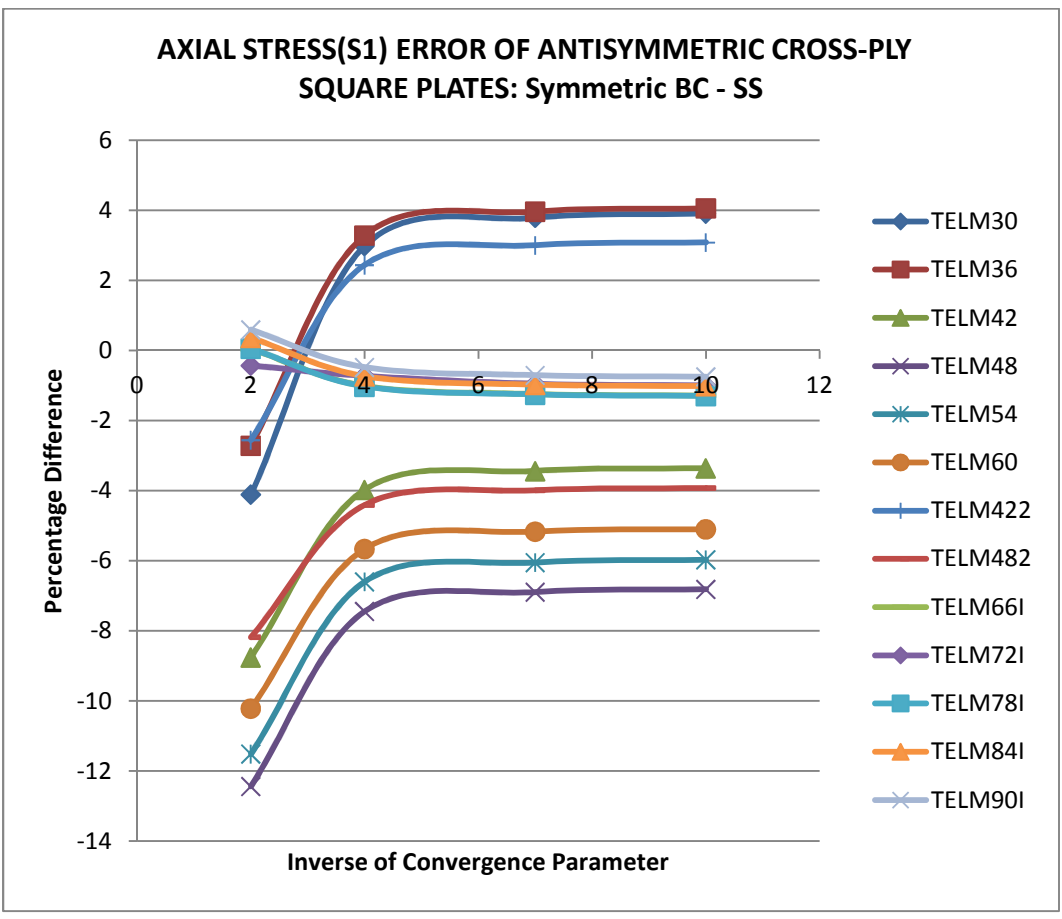


Figure 5. 46: Axial stress (S1) of antisymmetric cross-ply square plates (SS BCs) using Type II and bests of Type I elements.

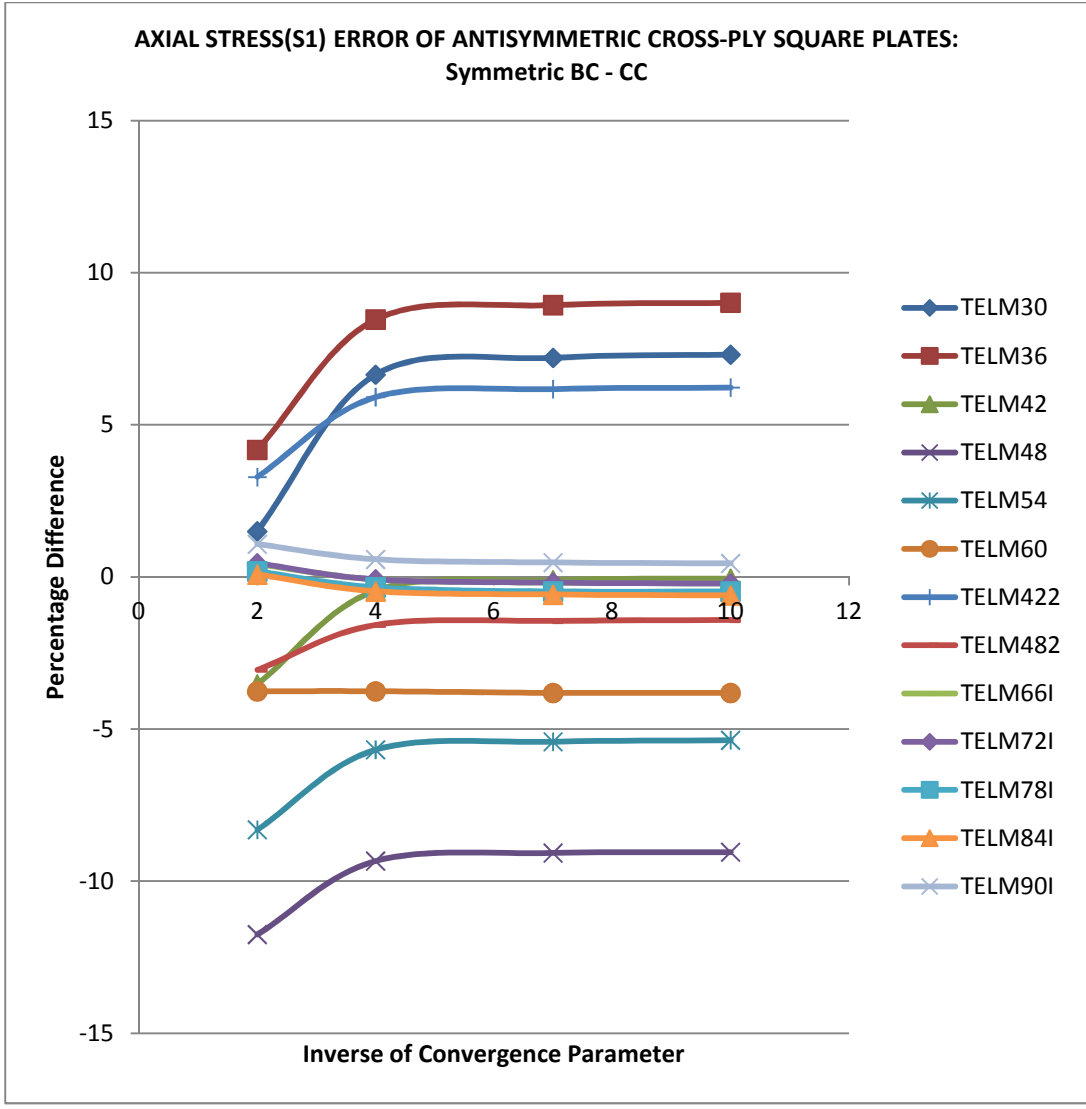


Figure 5. 47: Axial stress (S1) of antisymmetric cross-ply square plates (CC BCs) using Type II and bests of Type I elements.

It can be observed that elements TELM48 and TELM54 are neither convergent to an acceptable agreement, nor possess a convergence parameter range. Thus, they should not be considered recommendable.

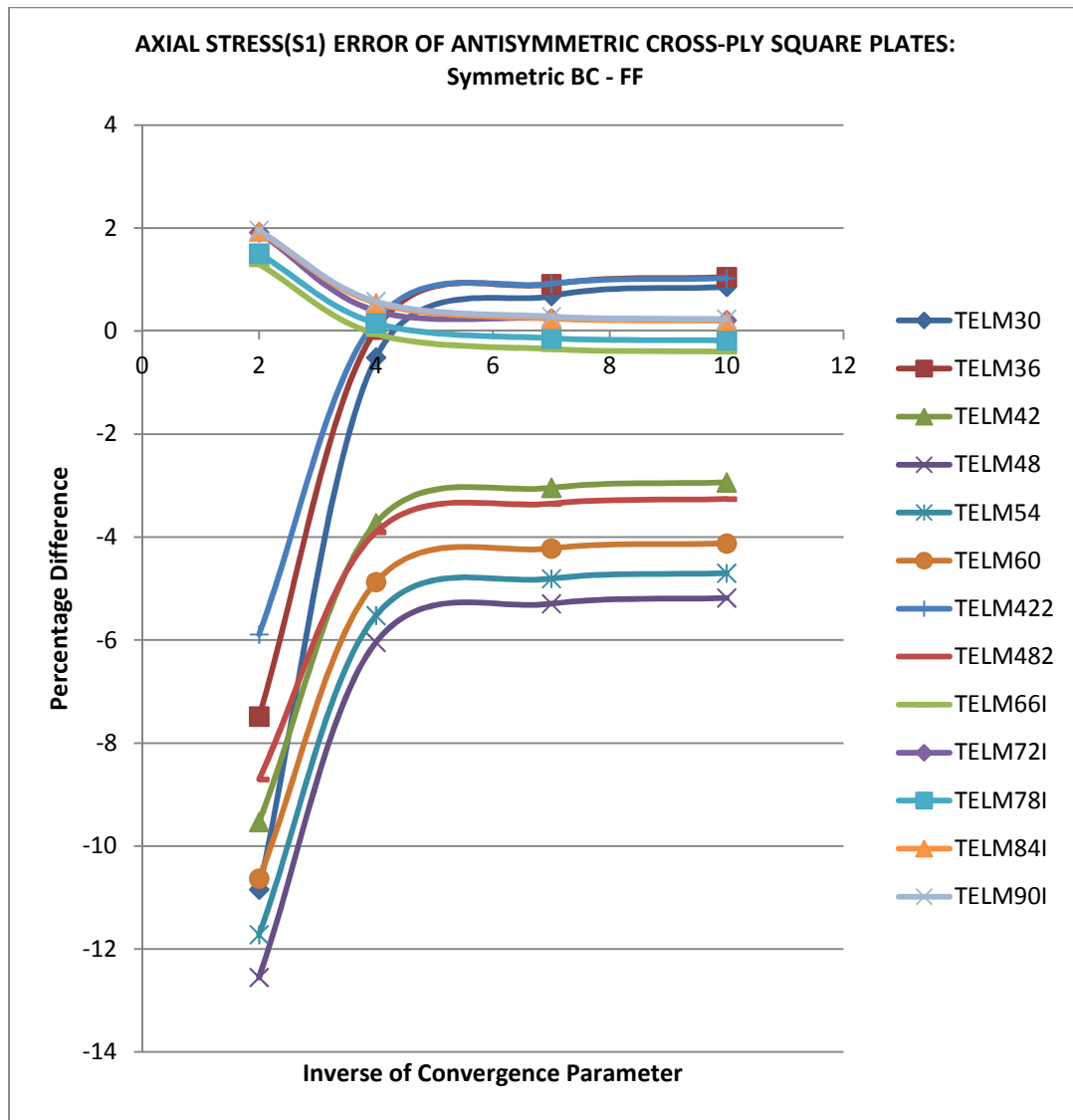


Figure 5. 48: Axial stress (S1) of antisymmetric cross-ply square plates (FF BCs) using Type II and bests of Type I elements.

It is seem that all elements give good results.

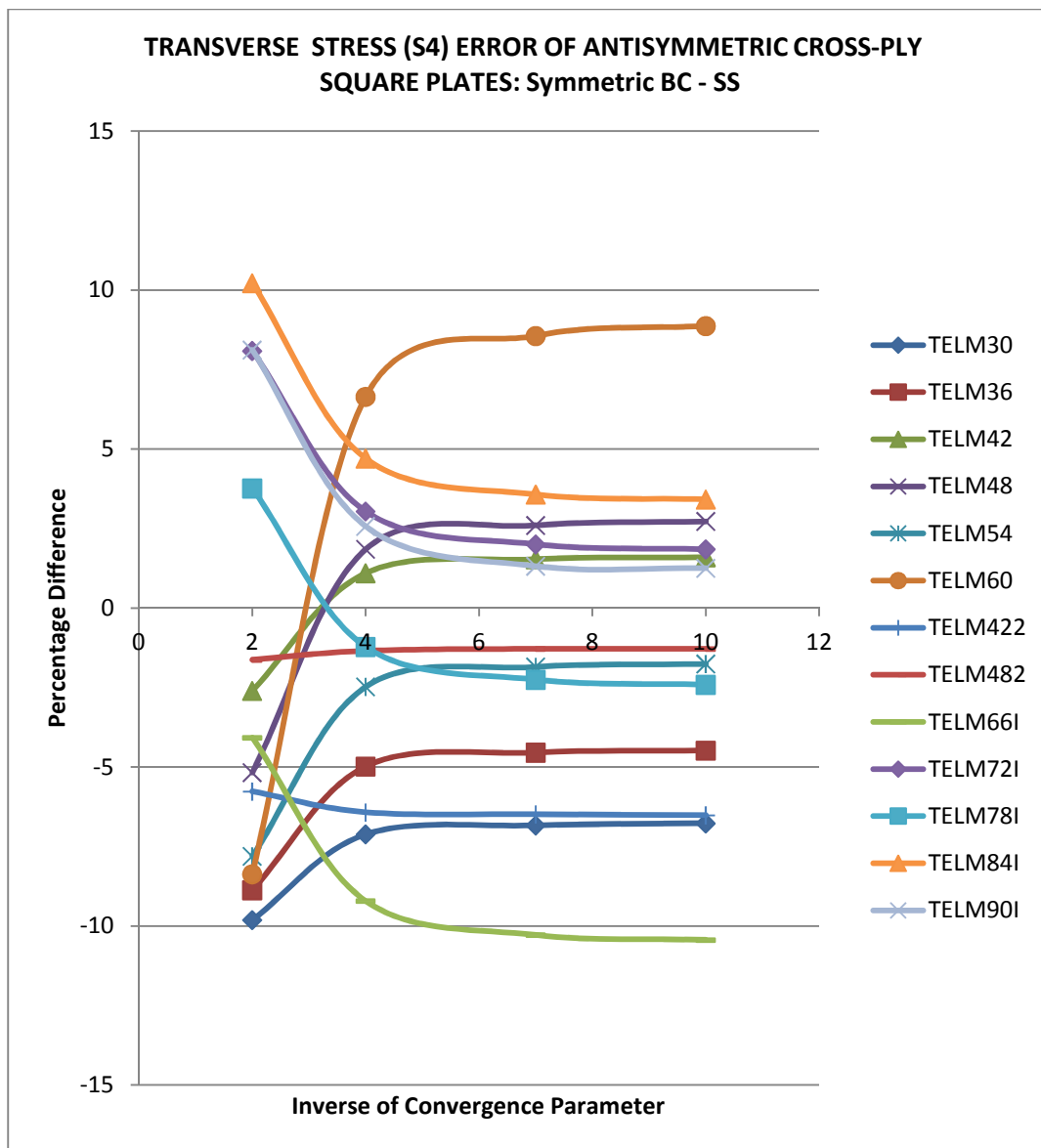


Figure 5. 49: Transverse shear stress (S4) of antisymmetric cross-ply square plates (SS BCs) using Type II and bests of Type I elements.

The figure shows that TELLM30 does not give acceptable results.

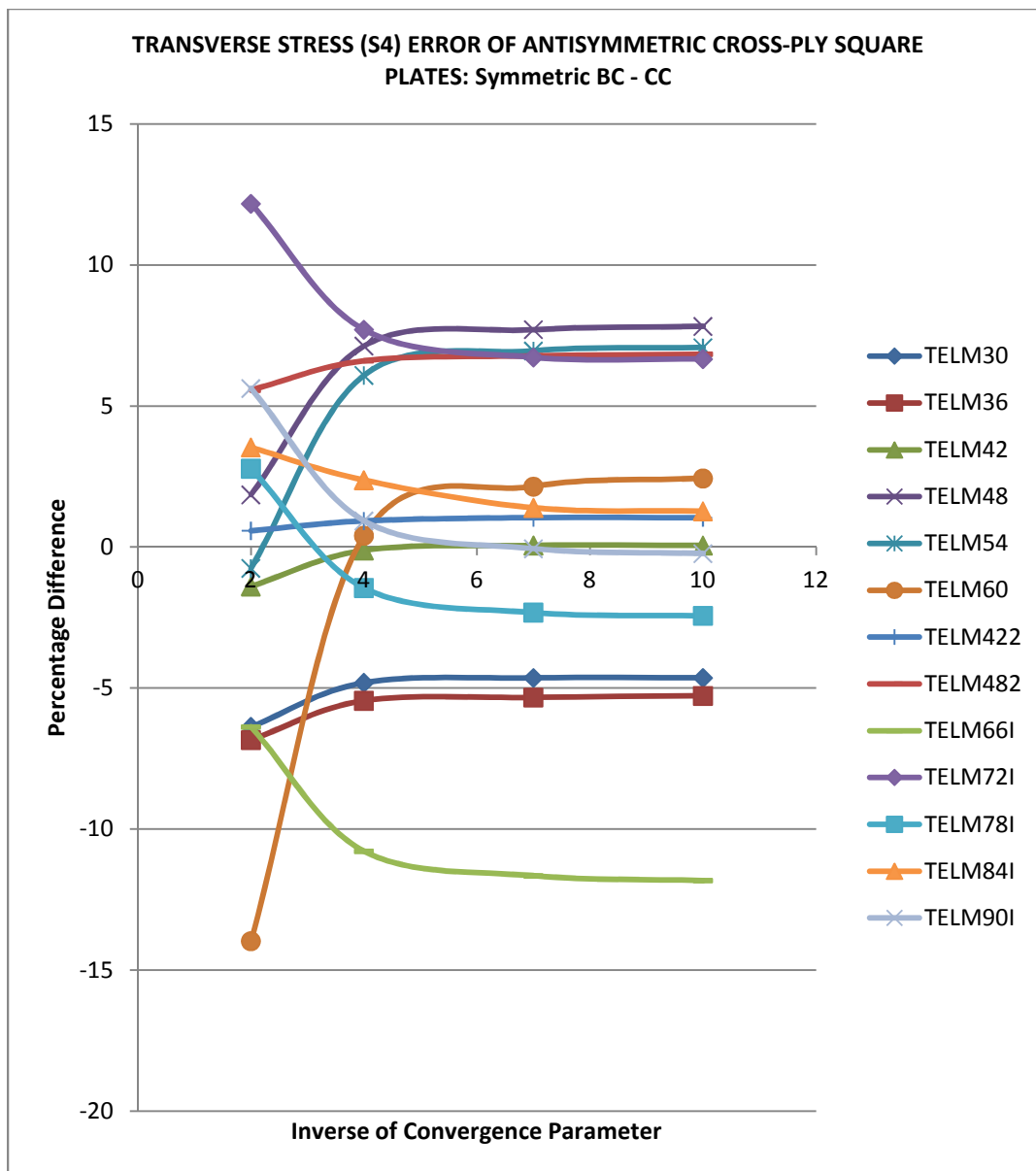


Figure 5. 50: Transverse shear stress (S4) of antisymmetric cross-ply square plates (CC BCs) using Type II and bests of Type I elements.

Here, it seems that TELM36, TELM30, TELM72 do not yield good results.

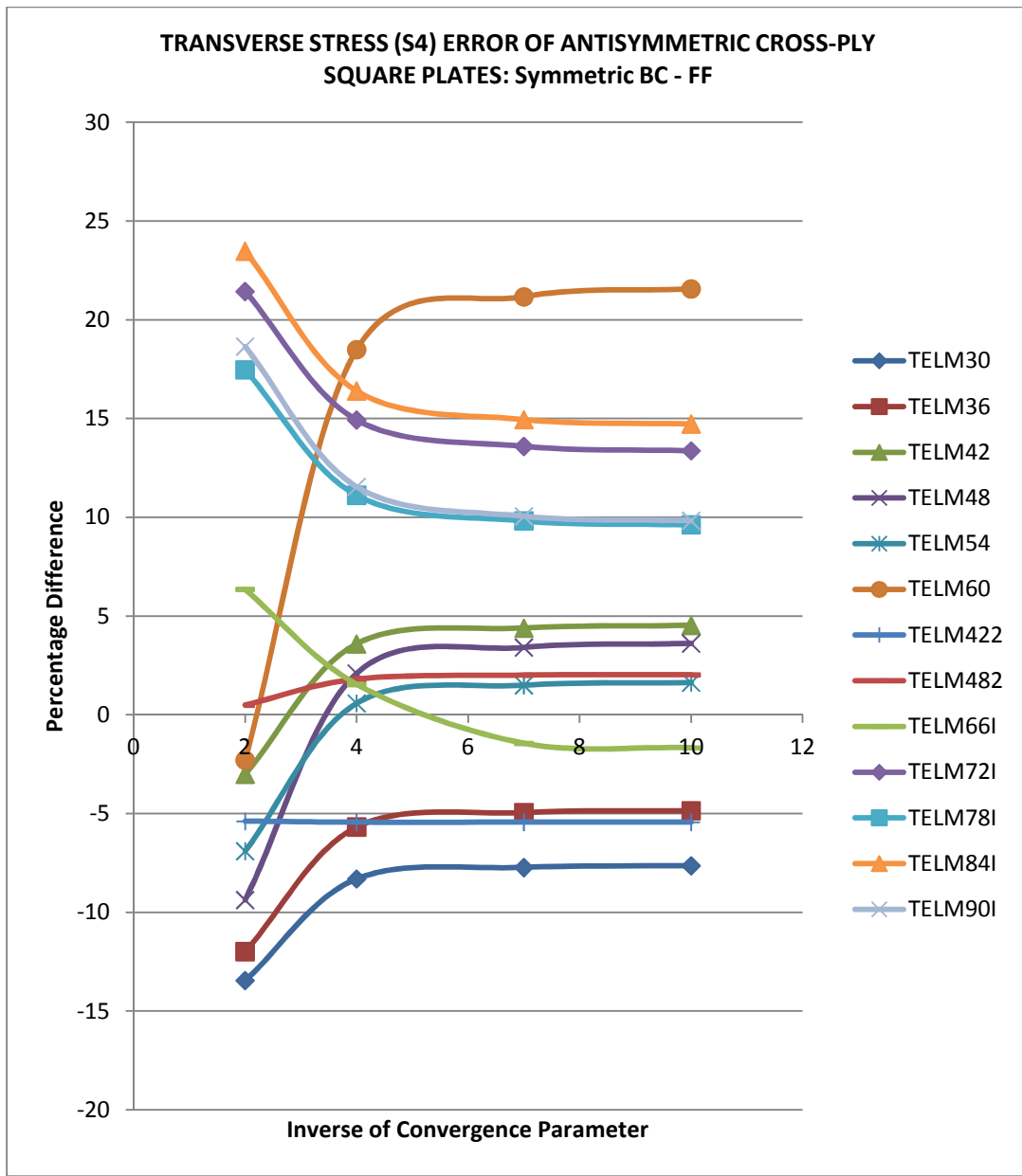


Figure 5. 51: Transverse shear stress (S4) of ant symmetric cross-ply square plates (FF) (BCs) using Type II and bests of Type I elements.

This is the most significant boundary condition combination for laminated composite analysis, the free boundaries. A few elements satisfy the criterion of excellence (5%). These elements are: TELM54, TELM66I TELM482 TELM48 and TELM42.

5.2.4 Stress Analysis of a Two-Layered Cross-Ply Laminated Cylindrical Shell Roof of Various Thicknesses

This case is the same as the one of Section 5.1.7. Reddy [24] used a displacement finite element model to analyze this problem. His results appear to be the only ones available for comparison. The material properties are

$$E_{11} = 25.0 \text{ E06 psi}, \quad E_{22} = 1.0 \text{ E06 psi}$$

$$G_{12} = 0.5 \text{ E06 psi}, \quad G_{23} = 0.2 \text{ E06 psi},$$

$$\nu_{12} = \nu_{21} = 0.25$$

Boundary condition:

$$\text{at } y = 0 \text{ and } 10, \quad u_0 = w_0 = \theta_y = 0;$$

The absence of constraints on the displacement along the x-axis suggests that one must add another constraint in order to avoid rigid body motion. The center of the shell is therefore constrained in the x-direction (at $x = 0$ and $y = 1/2$, $v_0 = 0$).

Meshing: the full shell roof is modeled with 16 elements (4 x 4).

The nondimensionalized normal stresses ($\sigma_x \sigma_y$), evaluated at the bottom and the top of the center of the roof, respectively, are computed as follows:

$$\sigma_{xN} = \sigma_{XFEM} \frac{10t^2}{qR^2}, \quad \sigma_{yN} = \sigma_{yFEM} \frac{10t^2}{qR^2} \quad (5.8)$$

Very thin to moderately thick shell roofs are analyzed. Eight Type I elements are used for the analysis because of the flexibility of their independent strain functions. Those with the higher number of strain parameters and associated with the Lagrange type element are selected. Three “serendipity” type elements are also analyzed for comparison purposes.

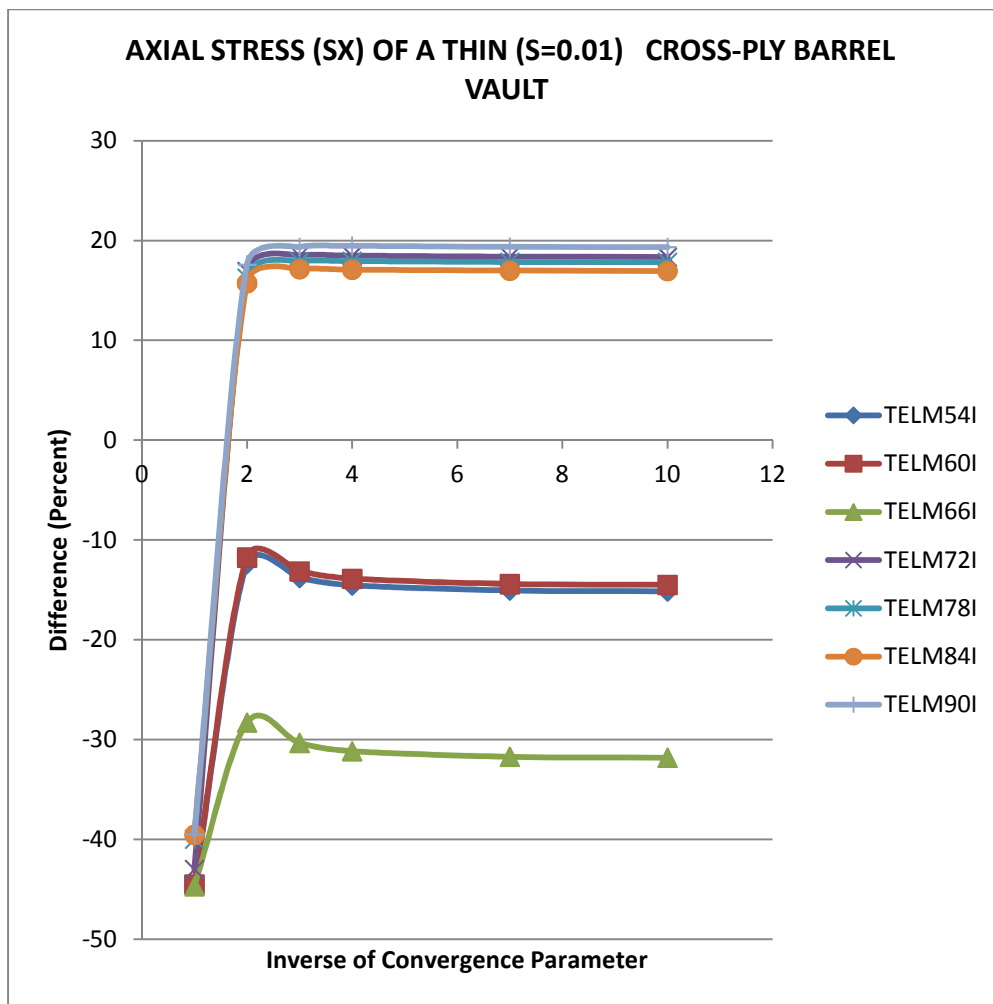


Figure 5. 52: Axial stress (S_x) of thin cross-ply Barrel Vault

It can be noticed that the range of appropriate convergence parameter is reduced considerably, and only three elements can produce a very good result. The rapid variation is due to the curvature of the shell.

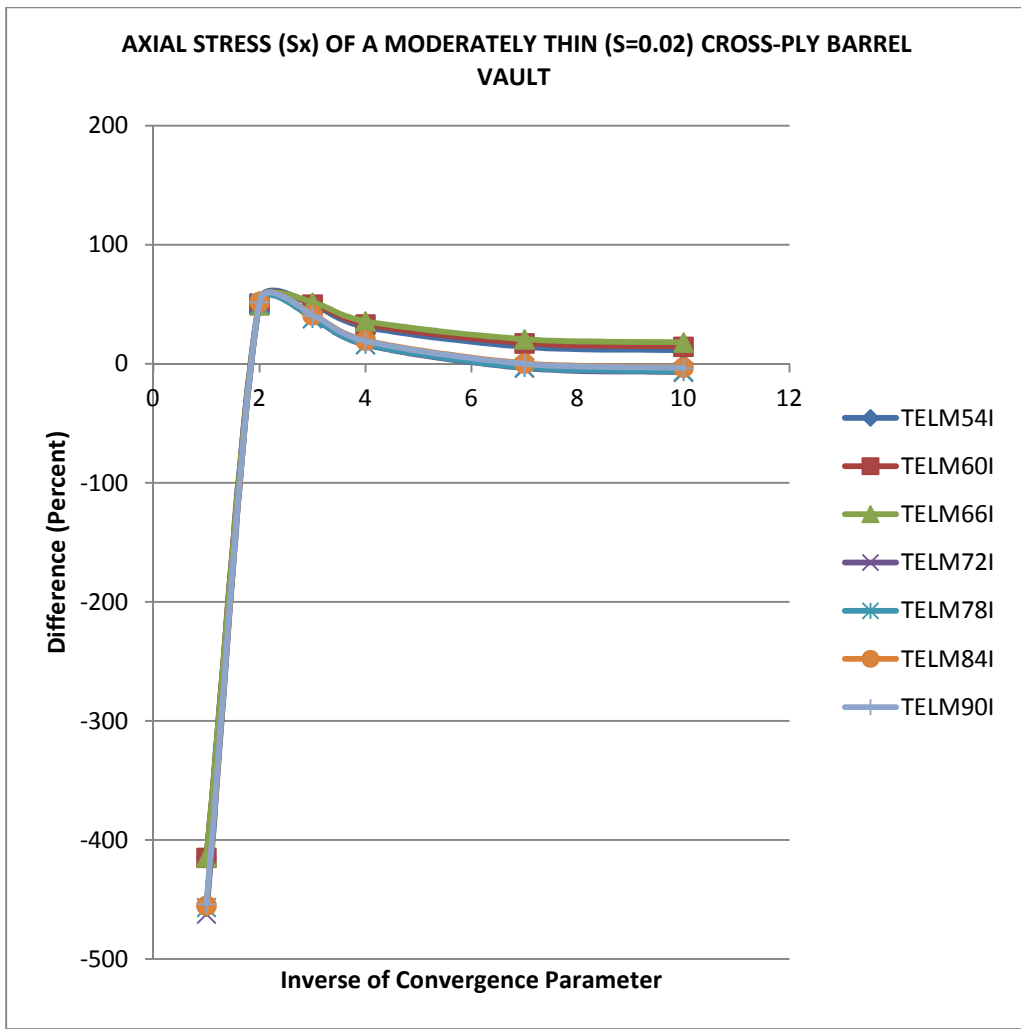


Figure 5. 53: Axial stress (S_x) of a moderately thin cross-ply Barrel Vault.

One can observe that some of the elements have double range of good performance. The percentage difference in between Reddy's solutions and the present is considerable when no convergence parameter is applied. For a larger thickness, the difference is reduced significantly.

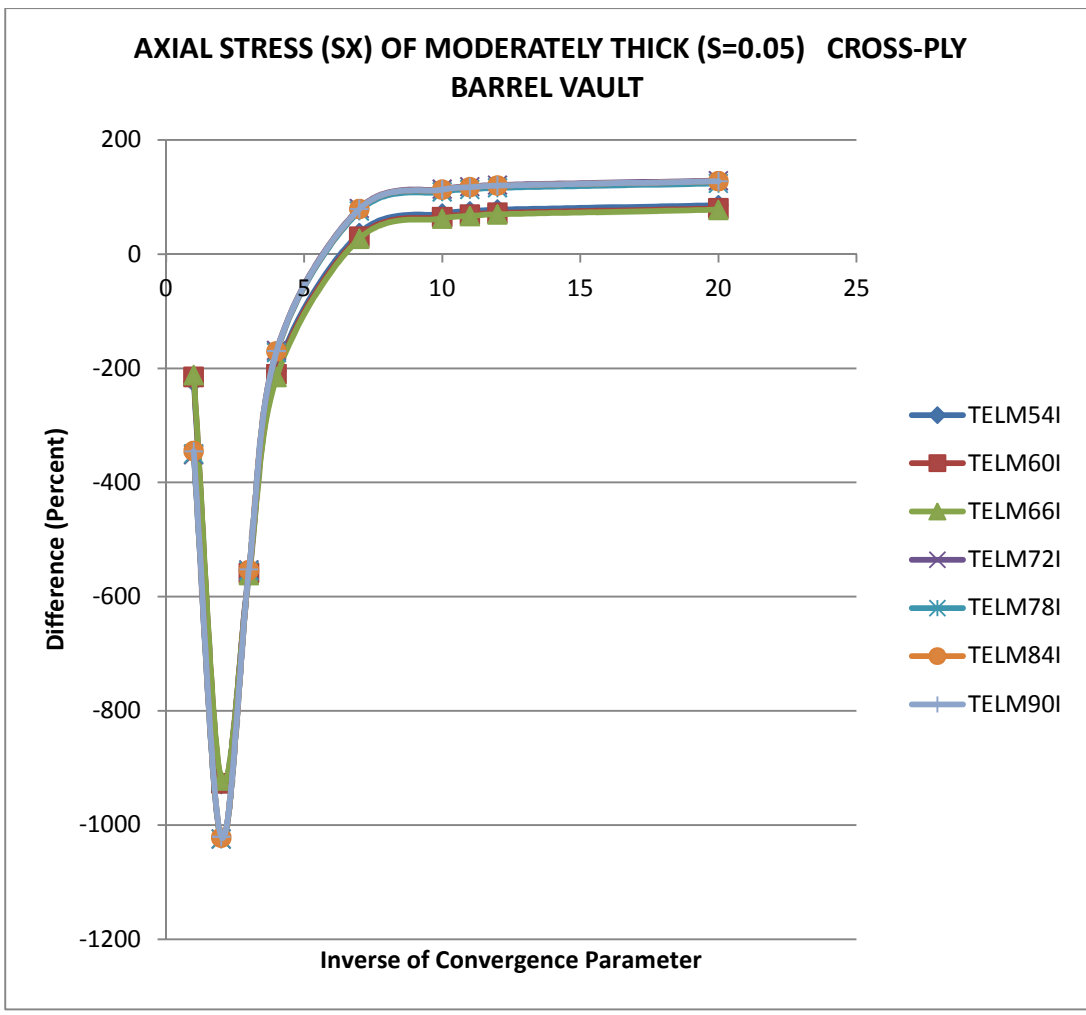


Figure 5. 54: Axial stress (Sx) of a moderately thick cross-ply Barrel Vault

It can be observed from the figure above that all elements have the same type of variation, which is characterized by a considerable increase in the value of the “error” before they start to converge.

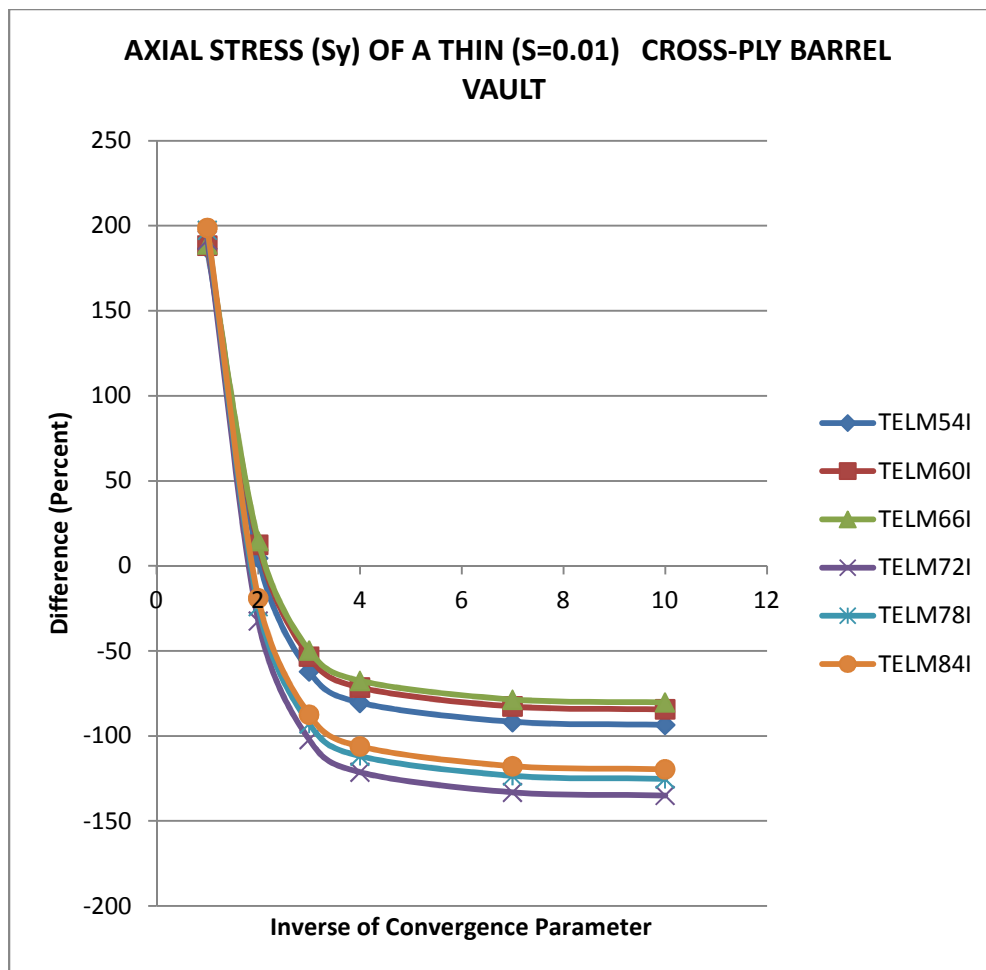


Figure 5. 55: Axial stress (S_y) of a thin cross-ply Barrel Vault

One can observe that all the elements have a good range for the choice of the convergence parameter.

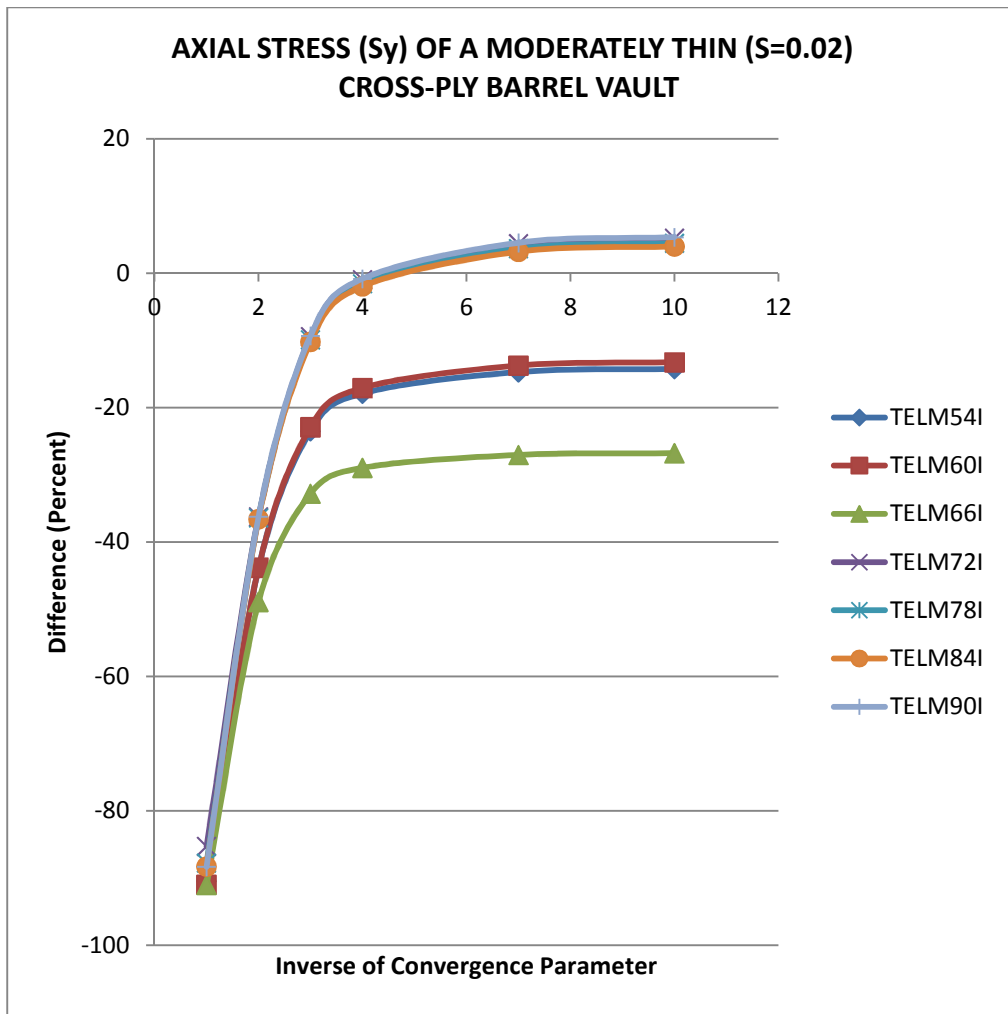


Figure 5. 56: Axial stress (Sy) of a moderately thin cross-ply Barrel Vault

It can be observed that only few elements (TELM90I TELM84I TELM78I) have the possibility of good performance.

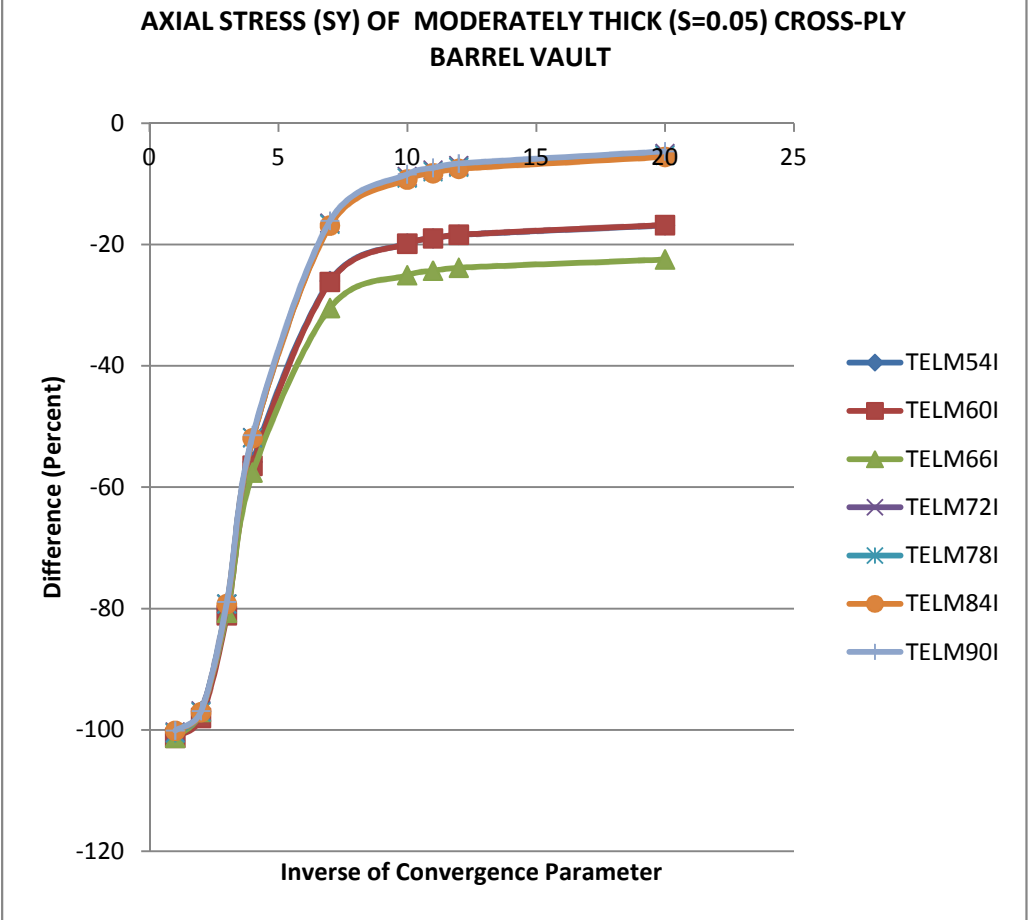


Figure 5. 57: Axial stress (Sy) of a moderately thick cross-ply Barrel Vault

It is seen from the Figure above, that the previous elements (all complete “Lagrangian” type) show an acceptable convergence towards the analytical solution for a moderately thick plate.

The in-plane stress analysis of the Barrel Vault shows that for thin shell structures, the range of good convergence parameters is reduced considerably. For thick shells, one observed a consistent convergence towards the solution. Three Lagrange

elements: TELM90I, TELM84I and TELM78I, give very good results. All the serendipity type elements selected for this analysis performed poorly.

As expected, the range of a choice for the convergence parameter is reduced because of the curvature of the shell. A shell structure loaded so as to cause bending creates additional membrane stresses in comparison with a plate structure. The complexity of the nodal rotation (drilling rotation) in shell structures usually produces instability in the solution. This is probably what is shown in Figure 5.54. All the elements have a large gradient around the convergence parameter of $1/5$.

In summary, the proposed elements work very well for laminated composites plate and shell structures. The Lagrange subgroup elements are excellent for a displacement study, as well as for in and out of plane stress analysis. The independent type I basis strain functions performance depends on the kind of problem analyzed, while the non-linearly dependent elements (type II) are more consistent in converging towards the reference solution. Although shell structures were analyzed with relatively small number of elements (sixteen for the Barrel Vault), the results were good. The number of proposed elements for this investigation seems high but as stated before, none exhibited the type of results or inconsistency which should have eliminated them earlier. This is due to the fact that the basis strain functions added in the variational principle are fully consistent with the displacement field. To make the choice of element easier for analysts of structural composite plate and shell structure, some elements are recommended in the Conclusion for general or selective applications.

CHAPTER 6 SUMMARY – CONCLUSION AND FUTURE WORK

6.1 Summary and Conclusion

New elements were proposed for the displacement and stress analysis of laminated composite plates and shells. The elements are characterized by higher order strain functions which allow for a non-linear variation of the transverse strains. This in turn allows for a more effective representation of the complex nature of composite laminates which are non-homogeneous and anisotropic. A strain-based modified complementary energy principle is used to implement the finite element formulation. This formulation has the advantage of satisfying a priori the inter-element compatibility conditions, the equilibrium within an element and displacement continuity on the boundary. An isoparametric eight node “serendipity” shape function with five degrees of freedom per node is used to approximate both the shape and the displacement functions. The proposed higher-order (in z^3 -terms) strain functions were chosen to be consistent with the displacements assumptions, thus allowing for a non-linear transverse displacement. Full integration schemes (3x3 and 4x4) were used for the Gauss quadrature numerical integration. As part of the formulation, two types of higher order strain functions, characterized by their in-plane basis functions, are proposed (using Pascal’s triangle): (1) those with the same in-plane strain basis functions as the “Serendipity” elements (truncated series of bi-cubic basis functions for which the in-plane strain functions have eight basis components with x^3 and y^3 terms missing), and (2) those which are consistent with the “Lagrange” elements (full series of bi-cubic basis functions with ten basis components). Note that, the “Lagrange” type elements are better suited for the

full integration scheme than the serendipity types. Also, two sub-groups of elements based on the transverse rotations were developed: those with independent higher order transverse rotations, (thus having more strain parameters), and those for which the higher order strain function is associated with the out-of-plane rotation.

A total of twenty-three new elements were investigated (two elements are based on first order strain functions and twenty-one also incorporating third order ones). During the process of this investigation, some elements were eliminated on the basis of poor performance and viability. The usage of the developed elements was demonstrated by the analysis of a range of plate and shell problems. The problems studied had different types of loading (point, distributed, self weight, sinusoidal), various boundary conditions (simply supported, clamped, free, combinations of these types), various geometry and thickness dimensions (very thin, thin, moderately thin, moderately thick and thick plates or shells) and material properties (isotropic or laminated composite). It was demonstrated that the proposed elements are effective and accurate. The use of a convergence parameter allows for more accurate convergence of the solution. The numerical implementation of the formulations was accomplished through the use of two computer codes written in MATLAB. All the displacement and stress analyses of the samples problem were carried out using these programs.

Conclusions drawn from the present study in the use of the proposed elements are as follows:

1. All elements did not show a shear locking effect during the analysis of both plate and shell problems.

2. The convergence parameter allows for the convergence of element strain functions. It is truly different from a correction factor as it does not correct any simplification made in a formulation. As was seen, its absence can result in an up to 50% error or difference with the reference solution. It was also noticed that the thicker the plate becomes, the larger the error when the convergence parameter is absent.
3. All the proposed elements performed well within performance criteria. Good performance was considered to be within 5% error and excellent within 2%. The viability criterion in this case is simply based on the number of strain parameters. This of course is linked to the computational time for obtaining a solution. For instance, although element TELM66 performed well, it was not consider viable element when compared to the recommend elements (see below) since it has more strain parameters than the others.
4. For very thin to moderately thick laminated composite plate problems, any of the proposed elements can be used with a convergence parameter of $1/3$. Excellent results were obtained using only a maximum of sixteen elements for a plate and twenty-five for shell analysis, respectively. For very thick plates, only the recommended strain functions elements should be used.
5. For shell problems, the two proposed first order element performed very well for the Barrel Vault test problem; however only FELM48 passed the pinched cylinder test. Therefore, FELM48 is recommend for isotropic and thin composites plate and shell structures.

6. The elements recommended for any problem are TELM60 (2-2.2), TELM482 (>2), TELM48 (3-4) and TELM42 (2-3.5). The quantity in brackets is the inverse of convergence parameter range.

The results obtained for cylindrical shell type problems while being very good for the displacements, could be improved further if a cylindrical coordinate system is employed in the formulation. While it would simplify the problem of cylindrical shell analysis, it would not allow for an extension of the current investigation to study composite shell intersections. These would be better handled using Cartesian coordinates.

The Lagrange multiplier introduced in the complementary energy principle statement represent an additional displacement field. The latter contributed greatly to the accuracy and robustness of the proposed formulation. It also provided additional equilibrium constraints needed to achieve the desired level of accuracy for both the displacements and stresses. Further, it eliminated the shear locking effect observed in a displacement formulation. How is the strain field of the strain-based MCEP related to the displacement field used as the Lagrange multiplier? How does one chose a basis function such that the element remains robust, stable and do not violate the stability requirements? Those are questions that were answered during the development of the proposed formulation.

For the nineteen failure theories evaluated by the WWFE (during a period of twelve years), none of them, according to the conclusive documents of the exercise could, predict failure stresses within 10% of the measured strengths in more than 40% of the test cases. One reason for this discrepancy is the lack of accurate determination of the state of stress within composites. The present work makes a contribution in that direction. An

accurate state of stress (and displacement) is necessary to obtain accurate results from the use of a failure theory.

6.2 Suggestion for Future Work

The following are recommendation for extensions of the present work:

- a. Extend the analysis to cylindrical shells under internal pressure, by exploring new ways of integrating the surface (boundary) pressure instead of nodal integration.
- b. Investigate the effectiveness of the present elements for laminated composites with a large number of layers.
- c. Integrate the proposed element formulations with an existing failure criterion or with a new criterion which is compatible with the new elements, if necessary.
- d. Investigate composite shell intersection problems using the present elements.

REFERENCES

- [1] Vinson, J. R. and Sierakowski, R. L., 1986, *The Behavior of Structures Composed of Composite Materials*, Martinus Nijhoff, Dordrecht.
- [2] Kaczkowski, Z., 1960, "The Influence of Shear and Rotary Inertia on the Frequencies of an Anisotropic Vibrating Plate," *Bull. Acad. Polonaise Sci.*, Vol. 8, pp. 343-50.
- [3] Ambartsumyan, S. A., 1969, *Theory of Anisotropic Plates*, translated from Russian by T. Cheron, Technomic, Stamford, CT.
- [4] Pagano, N. J., 1969, "Exact solutions for composite laminates in cylindrical bending," *Journal of Composite Materials*, Vol. 3, pp. 398-411.
- [5] Pagano, N. J., 1970, "Exact Solutions for Rectangular Bidirectional Composites and Sandwich Plates," *Journal of Composite Materials*, Vol. 4, pp. 20-34.
- [6] Pagano, N.J., 1970, "Influence of Shear Coupling in Cylindrical Bending of Anisotropic Laminates," *Journal of Composite Materials*, Vol.4, pp. 330-34.
- [7] Srinivas, S. and Rao A. K., 1970, "Bending Vibration and Buckling of Simply Supported Thick Orthotropic Rectangular Plates and Laminates," *Int. J. Solids Struct.*, Vol. 6, pp. 1464-81.
- [8] Srinivas, S., Rao A. K., and Joga Rao C. V., 1969, "Flexure of Simply Supported Thick Homogeneous and Laminated Rectangular Plates," *Zeitschrift fur Angewandte Mathematik und Mechanik*, Vol.49, pp. 449-58.
- [9] Srinivas, S., 1973, "A Refined Analysis of Composite Laminates," *Journal of Sound and Vibration*, Vol.30, pp. 495-507.
- [10] Srinivas, S., Joga Rao, C. V. and Rao R. K., 1970, "An Exact Analysis of the Vibration Analysis of Simply-Supported Homogeneous and Laminated Thick Rectangular Plates," *Journal of Sound and Vibration*, Vol. 12, pp.187-99.
- [11] Jones, A. T., 1970, "Exact Natural Frequencies for Cross-Ply Laminates," *Journal of Composite Materials*, Vol. 4, pp. 476-91.
- [12] Lee, Y. C., Reismann, H., 1969, "Dynamics of Rectangular Plates," *International Journal of Engineering Science*, Vol. 7, pp. 93-113.
- [13] Lee, C. W., 1967, "Three-Dimensional Solution for Simply Supported Thick Rectangular Plates," *Nuclear Engineering and Design*, Vol. 6, pp. 151-62.
- [14] Whitney, J. M., 1969, "The Effect of Transverse Shear Deformation on Bending of Laminated Plates," *Journal of Composite Materials*, Vol. 3, pp. 534-47.

- [15] Pagano, N. J., Hatfield, S. J., 1972, "Elastic Behavior of Multilayered Bidirectional Composites," *AIAA J*, Vol. 10, pp. 20-34.
- [16] Noor, A. K., 1973, "Free Vibration of Multilayered Composite Plates," *AIAA J*, Vol. 11, pp. 1038-39.
- [17] Fan, J. R. and Ye, J. Q., 1990, "A Series Solution of the Exact Equation for Thick Orthotropic Plates," *International Journal of Solids and Structures*, Vol. 26, pp.773-8.
- [18] Kant, T., Gupta, A. B., Pendhari, S. and Desai, Y. M., 2008, "Elasticity Solution for Cross-ply Composite and Sandwich Laminates," *Composite Structures*, Vol. 83, pp. 13-24.
- [19] Kant, T. and Swaminathan, K., 2002, "Analytical Solutions for the Static Analysis of Laminated Composite and Sandwich Plates Based on a Higher Order Refined Theory," *Composite Structures*, Vol. 56, pp. 329-44.
- [20] Teo, T. M. and Liew, K. M., 1999, "Three-Dimensional Elasticity Solutions to Some Orthotropic Plate Problems," *International Journal of Solids and Structures*, Vol. 36, pp. 5301-26.
- [21] Civalek and Baltacioglu, 2010, "Three-Dimensional Elasticity Analysis of Rectangular Composite Plates," *Journal of Composites Materials*, Vol. 44, pp. 17.
- [22] Liew, K. M., Zhang, J. Z., Ng, T. Y. and Meguid, S. A., 2003, "Three-Dimensional Modeling of Elastic Bonding in Composite Laminates using Layerwise Differential Quadrature," *International Journal of Solids and Structures*, Vol. 40, pp.1745-64.
- [23] Zhang, J. Z., Ng, T. Y. and Liew, K. M., 2003, "Three-Dimensional Theory of Elasticity for Free Vibration Analysis of Composite Laminates via Layerwise Differential Quadrature Modeling," *International Journal for Numerical Methods in Engineering*, Vol. 57 pp. 1819-44.
- [24] Reddy, J. N., 2004, *Mechanics of Laminated Plates and Shells: Theory and Analysis*, 2nd Ed. CRC Press, New York.
- [25] Widera, G. E. O., and Fan, H., 1991, "Refined Engineering Beam Theory Base on the Asymptotic Expansion Approach," *AIAA Journal*, Vol. 29, pp. 444-9.
- [26] Wang, Y. Y., Lam, K. Y. and Liu, G. R., 2000, "Bending Analysis of Classical Symmetric Laminated Plates By The Strip Element Method," *Mechanics of Composite Materials and Structures*, Vol. 7, pp. 225-47.
- [27] Reissner, E. and Stavsky Y., 1961, "Bending and Stretching of Certain Types of Aeolotropic Elastic Plates," *Journal of Applied Mechanics*, Vol. 8, pp. 402-8.
- [28] Stavsky, Y., 1961, "Bending and Stretching of Laminated Aeolotropic Plates,"

Journal of Engineering Mechanics, ASCE, 87 (EM6), pp. 31-56.

- [29] Dong, S. B., Pister, K. S., and Taylor, R. L., 1962, "On the Theory of Laminated Anisotropic Shells and Plates," *Journal of Aeronautical Science*, Vol. 29, pp. 969-75.
- [30] Whitney, J. M. and Leissa, A. W., 1969, "Analysis of Heterogeneous Anisotropic Plates," *Journal of Applied Mechanics*, Vol. 36, pp. 261-6.
- [31] Whitney, J. M. and Pagano, N. J., 1970, "Shear Deformation in Heterogeneous Anisotropic Plates," *Journal of Applied Mechanics*, Vol. 37, pp. 1031-6.
- [32] Reissner, E., 1972, "A Consistent Treatment of Transverse Shear Deformations in Anisotropic Plates," *AIAA Journal*, Vol. 10, pp.716-8.
- [33] Reissner, E., 1979, "Note on the Effect of Transverse Shear Deformation in Laminated Anisotropic Plates," *Computer Methods in Applied Mechanics and Engineering*, Vol. 20, pp. 203-9.
- [34] Reddy, J. N., 2002, *Energy Principles and Variational Methods in Applied Mechanics*, Second Edition, John Wiley, New York.
- [35] Whitney, J. M., 1973, "Shear Correction Factors for Orthotropic Laminates under Static Load," *Journal of Applied Mechanics*, Vol. 40, pp. 302-4.
- [36] Bert, C. W., 1973, "Simplified Analysis of Static Shear Correction Factors for Beams of Homogeneous Cross Section," *Journal of Composite Materials*, Vol. 7, pp. 525-9.
- [37] Wittrick, W. H., 1987, "Analytical Three-Dimensional Elasticity Solutions to Some Plate Problems and Some Observations on Mindlin's Plate Theory," *International Journal of Solids Structures*, Vol. 23, pp. 441-464.
- [38] Lo, K. H., Christensen, R. M., and Wu, E. M., 1977, "A Higher Order Theory of Plate Deformation Part 2; Laminated Plates," *Journal of Applied Mechanics*, Vol. 44, pp. 669-76.
- [39] Krishna Murty, A. V., 1977, "Higher Order Theory for Vibration of Thick Plates," *AIAA Journal*, Vol. 15, pp. 1823-4.
- [40] Murthy, M. V. V., 1981, "An Improved Transverse Shear Deformation Theory for Laminate Anisotropic Plates," NASA Technical Paper 1903, pp. 1-37.
- [41] Reddy, J. N., 1984, "A Simple Higher-Order Theory for Laminated Composite Plates," *Journal of Applied Mechanics*, Vol. 51, pp. 745-52.
- [42] Pryor C.W., and Barker, R. M., 1971, "A Finite-Element Analysis Including Transverse Shear Effects for Applications to Laminated Plates," *AIAA Journal*, Vol.

9, pp. 912-7.

- [43] Noor, A.K. and Mathers, M.D., 1977, "Finite Element Analysis of Anisotropic Plates," *International Journal for Numerical Methods in Engineering*, Vol. 11, pp. 289-307.
- [44] Panda, S.C. and Natarajan, R., 1979, "Finite Element Analysis of Laminated Composite Plates," *International Journal for Numerical Methods in Engineering*, Vol. 14, pp. 69-79.
- [45] Reddy, J.N., 1980, "A Penalty Plate-Bending Element for the Analysis of Laminated Anisotropic Composite Plates," *International Journal for Numerical Methods for Engineering*, Vol. 15, pp. 1187-1206.
- [46] Lakshminarayana, H. V. and Murthy S., 1984, "Shear-Flexible Triangular Finite Element Model for Laminated Composite Plates," *International Journal for Numerical Methods for Engineering*, Vol. 20, pp. 591-623.
- [47] Engblom, J. J. and Ochoa, O. O., 1985, "Through-the-Thickness Stress Predictions for Laminated Plates of Advanced Composite Materials," *International Journal for Numerical Methods in Engineering*, Vol. 21, pp. 1759-76.
- [48] Engblom, J. J. and Ochoa, O. O., 1986, "Finite Element Formulation Including Interlaminar Stress Calculations," *Comput. and Struct.*, Vol. 23, pp. 241-9.
- [49] Pandya, B. N. and Kant, T., 1988, "Flexural Analysis of Laminated Composites Using Refined Higher-Order CO Plate Bending Elements," *International Journal for Numerical Methods in Engineering*, Vol. 66, pp. 173-98.
- [50] Kwon, Y. K. and Akin, J. E., 1987, "Analysis of Layered Composite Plates Using a High-Order Deformation Theory," *Comput. and Struct.*, Vol. 27, pp. 619-23.
- [51] Spilker, R. L. and Jakobs, M., 1986, "Hybrid Stress Reduced-Mindlin Elements for Thin Multilayer Plates," *International Journal for Numerical Methods in Engineering*, Vol. 23, pp. 555-78.
- [52] Haas, D. J. and Lee, S. W., 1987, "A Nine-Node Assumed-Strain Finite Element for Composite Plates and Shells," *Comput. and Struct.*, Vol. 26, pp. 445-452, 1987.
- [53] Mawenya, A. S. and Davies, J. D., 1974, "Finite Element Bending Analysis of Multilayer Plates," *International Journal for Numerical Methods in Engineering*, Vol. 8, pp. 215-25.
- [54] Chaudhuri, R.A., 1986, "An Equilibrium Method for Prediction of Transverse Shear Stresses in a Thick Laminated Plate," *Comput. and Struct.*, Vol. 23, pp. 139-46.
- [55] Chaudhuri, R. A. and Seide, P., 1987, "An Approximate Semi-Analytical Method for Prediction of Interlaminar Shear Stresses in an Arbitrarily Laminated Thick

- Plate,” *Comput. and Struct.*, Vol. 25, pp. 627-36.
- [56] Owen, D. R. J. and Li, Z. H., 1987, “A Refined Analysis of Laminated Plates by Finite Element Displacement Methods-I. Fundamentals and Static Analysis,” *Comput. and Struct.*, Vol. 26, pp. 907-14.
- [57] Owen, D. R. J. and Li, Z.H., 1987, “A Refined Analysis of Laminated Plates by Finite Element Displacement Methods--II. Vibration and Stability,” *Comput. and Struct.*, Vol. 26, pp. 915-23.
- [58] Spilker, R. L., 1980, “A Hybrid-Stress Finite-Element Formulation for Thick Multilayer Laminates,” *Comput. and Struct.*, Vol. 11, pp. 507-14.
- [59] Liou, W. J. and Sun, C. T., 1987, “A Three-Dimensional Hybrid Stress Isoparametric Element for the Analysis of Laminated Composite Plates,” *Comput. and Struct.*, Vol. 25, pp. 241-49.
- [60] Carrera, E., 2000, “An Assessment of Mixed and Classical Theories on Global and Local Response of Multilayered Orthotropic Plates,” *Composite Structures*, Vol. 20, pp. 183-98.
- [61] Zhang, Y. X. and Yang, C. H., 2009, “Recent Developments in Finite Element Analysis for Laminated Composite Plates,” *Composite Structures*, Vol. 88, pp. 147-57.
- [62] Khdeir, A. A., and Reddy J. N., 1991, “Analytical Solutions of Refined Plate Theories of Cross-Ply Composite Laminates,” *Journal of Pressure Vessel Technology*, Vol. 113, pp. 570-78.
- [63] Zienkiewicz, O. C., 1977, *The Finite Element Method*, McGraw Hill, Berkshire.
- [64] Zienkiewicz, O. C., Taylor, R. L., Too, J. M., 1971, “Reduced Integration Techniques in General Analysis of Plates and Shells,” *International Journal for Numerical Methods for Engineering*, Vol. 3, pp. 275-90.
- [65] Harbok, M. M., Hrudey, T. M., 1984, “A Review and Catalogue of Plate Bending Finite Elements,” *Computers and Structures*, Vol. 19, pp. 479-95.
- [66] Pian, T. H. H., 1964, “Derivation of Element Stiffness Matrices by Assumed Stress Distribution,” *AIAA Journal*, Vol. 2, pp. 1333-6.
- [67] Pian, T. H. H., Chen D. P., Kang, D., 1983, “A New Formulation of Hybrid/Mixed Finite Element,” *Computers and Structures*, Vol. 16, pp. 81-7.
- [68] Pian, T. H. H., 1966, “Element Stiffness Matrices for Boundary Compatibility and for Prescribed Boundary Stresses Proc. Conf. on Matrix Methods in Structural Mechanics,” pp. 457-77, Wright Patterson Air Force Base, Dayton, Ohio.

- [69] Pian, T. H. H., and Tong, P., 1969, "Rationalization in Deriving Element Stiffness Matrix Assumed-Stress Approach. PMC. Second Conf, on Matrix Meth," in *Structural Mech.*, pp 457-77, AFFDL-TR-66-80, Wright-Paterson Air Force Base, Dayton, Ohio.
- [70] Pian, T. H. H., 1973, "Hybrid Elements, in Numerical and Computer Methods in Structural Mechanics," *S. J. Fen Eds*, pp. 59-78. New York, Academic Press.
- [71] Pian, T. H. H., 1995, "State-of-the-art Development of Hybrid/Mixed Finite Element Method," *Finite Elements in Analysis and Design*, Vol. 21, pp. 5-20.
- [72] Mau, S. T., Tong, P. and Pian, T. H. H., 1972, "Finite element Solutions for Laminated Thick Plates," *J. Composite Materials*, Vol. 6, pp. 304-11.
- [73] Spilker, R. L., 1979, "On the Formulation of Thick Laminated Plates," *Computers and Structures*, Vol. 2, pp.507-14.
- [74] Spilker, R. L., 1984, "Short Communications, An Invariant Eight-Node Hybrid-Stress Element for Thin and Thick Multilayered Laminated Plates," *Int. J. for Num. Meth. Eng*, Vol. 20, pp. 573-87.
- [75] Spilker, R. L., 1982, "Hybrid-Stress Eight-Node Elements for Thin and Thick Multilayer Laminated Plates," *International Journal for Numerical Methods for Engineering*, Vol. 18, pp. 801-82.
- [76] Spilker, R. L., Chou, S. C., and Orringer O., 1977, "Alternate Hybrid-Stress Elements for Analysis of multilayered Composite Plates," *J. Composite Mat.*, Vol. 11, pp. 51-70.
- [77] Spilker, R.L., Munir, N. I., 1980, "A Hybrid-Stress Quadratic Serendipity Element Mindlin Plate Bending Element," *Compo. Struc.*, Vol. 12, pp. 11-21.
- [78] Shtayerman, I. Ya., 1924, "Theory of Symmetrical Deformation of Anisotropic Elastic Shells," *Izvestia Kievsk. Politekh. I Sel.-Khoz. Inst.*, Vol. 1 (in Russian).
- [79] Ambartsumian, S. A., 1966, "Some Current Aspects of the Theory of Anisotropic Layered Shells," *Applied Mechanics Surveys*.
- [80] Bert, C. W., 1975, "Analysis of Shells," *Structural Design and Analysis*, Vol. 7, PP. 240-2.
- [81] Lekhnitskii, S. G., 1941, "Bending of inhomogeneous anisotropic thin plates of a symmetric layup," *Applied Mathematics and Mechanics*, Vol. 5, (in Russian).
- [82] Lekhnitskii, S. G., 1963, *Theory of Elasticity of an Anisotropic Body*, Gostekhisdat, Moscow. 1950. First ed., English translation by Holden-day.

- [83] Lekhnitskii, S. G., 1968, *Anisotropic Plates*, Gostekhisdat, Moscow. 1957. Second ed., English translation by S. W. Tsai and T. Cheron, Gordon and Breach Science Publishers, New York.
- [84] Budynas, R. and Nisbett, J., 2007, *Shigley's Mechanical Engineering Design*, 8th ed., New York, McGraw-Hill.
- [85] Barbero, E. J., 2011, *Introduction to Composites Materials Design*, CRC Press, New York.
- [86] Tsai, S. W., 1988, *Composites Design*, Think Composites, Dayton.
- [87] Voyiadis, G. Z. and Katta, P. I., 2005, *Mechanics of Composite Materials with Matlab*, Springer, Berlin.
- [88] Reddy, J. N. and Miravete, A., 1995, *Practical Analysis of Composite Laminates*, CRC Press, New York.
- [89] Hwang, T. K., Hong, C. S. and Kim, C. G., 2003, "Size Effect on the Fiber Strength of Composite Pressure Vessels," *Compos. Struct.*, Vol. 59, pp. 489-98.
- [90] Kam, T. Y., Liu, Y. W. and Lee, F. T., 1997, "First-Ply Failure Strength of Laminated Composite Pressure Vessels," *Compos. Struct.*, Vol. 38, pp. 65-70.
- [91] Lekhnitskii, S. G., 1981, *Theory of Elasticity of an Anisotropic Body*, Nauka, Moscow. 1977. Second Ed., English Translation by Mir Publishers, Moscow.
- [92] Roy, A. K. and Tsai SW., 1988, "Design of Thick Composite Cylinders," *J. Press. Vessel Tech.*, Vol. 110, pp.255-62.
- [93] Bogdanovich, A. E., 1993, "Three-Dimensional Analysis of Anisotropic Spatially Reinforced Structures," *Composites Manufacturing*, Vol. 4, pp. 173-86.
- [94] Bogdanovich, A. E. and C. M. Pastore, 1996, *Mechanics of Textile and Laminated Composites with Application to Structural Analysis*, Chapman & Hall (London and New York).
- [95] Parnas, L. and Katirci, N., 2002, "Design of Fiber-Reinforced Composite Pressure Vessels under Various Loading Conditions," *Compos. Struct.*, Vol. 58, pp.83-95.
- [96] Johnson, M. W. and Reissner, E., 1959, "On the Foundations of the Theory of Thin Elasticity Shells," *Journal of Mathematical Physics*, Vol. 37, pp. 371-92.
- [97] Reissner, E., 1964, "On Asymptotic Expansions for Circular Cylindrical Shells," *Journal of Applied Mechanics*, Vol. 31, pp. 245-52.
- [98] Johnson, M. W. and Widera, G. E. O., 1969, "An Asymptotic Dynamic Theory for Cylindrical Shells," *Studies in Appl. Math.*, Vol. 48, pp. 205-26.

- [99] Chung, S.W. and Widera, G. E. O., 1972, "A Theory for Nonhomogeneous Anisotropic Cylindrical Shells," *J. Composite Materials*, Vol. 6, p. 14.
- [100] Logan, D. and Widera, G. E. O., 1980, "Refined Theories for Nonhomogeneous Anisotropic Cylindrical Shells: Part I-Derivation," *Journal of the Engng. Mechanics Div., Proc. of ASCE*, Vol. 106, pp. 1053-74.
- [101] Logan, D. and Widera, G. E. O., 1980, "Refined Theories for Nonhomogeneous Anisotropic Cylindrical Shells: Part II-Application," *Journal of Engng. Mechanics Div., Proc. of ASCE*, Vol. 106, p. 1075.
- [102] Widera, G. E. O., Johnson, M. W. and Logan, D., 1980, "An Asymptotic Analysis of Layered Tube," *Mechanics Today – Eric Reissner Symposium*, Vol. 5, pp. 543-60.
- [103] Yang H. T. Y., Saigal S., Masud A. and Kapania, R. K., 2000, "A Survey of Recent Shell Finite Elements," *International Journal for Numerical Methods in Engineering*, Vol. 47, pp. 101-27.
- [104] Ahmad S., Irons B. M. and Zienkiewicz O. C., 1990, "Analysis of Thick and Shell Structures by Curved Granite Element," *International Journal for Numerical Methods in Engineering*, Vol. 2, pp. 419-59.
- [105] Ramm E., 1977, "A Plate/Shell Element for Large Deflection and Rotations," *Formulations and Computational Algorithms in Finite Element Analysis*, Bathe, KJ., Oden, JT., Wunderlich, W (Eds). MIT Press: Cambridge, MA.
- [106] Dvorkin E. N. and Bathe K. J., 1984, "A Continuum Mechanics Based Four-node Shell Element for General Non-linear Analysis," *Engineering Computations*, Vol. 1 pp. 77-88.
- [107] Liu W. K., Law E. S., Lam D. and Belytschko T., 1986, "Resultant-stress Degenerated-Shell Element," *Computer Methods in Applied Mechanics and Engineering*, Vol. 55, pp. 259-300.
- [108] Hughes T. J. R., Masud A. and Harari I., 1995, "Numerical Assessment of some Membrane Elements with Drilling Degrees of Freedom," *Computers and Structures*; Vol. 55, pp. 297-314.
- [109] Meek J. L. and Tan H. S., 1986, "A Faceted Shell Element with Loaf Nodes," *International Journal for Numerical Methods in Engineering*, Vol. 23, pp. 49-67.
- [110] Chang, R. R., 2000, "Experimental and Theoretical Analyses of First-Ply Failure of Laminated Composite Pressure Vessels," *Compos. Struct.*, Vol. 49, pp.237-43.
- [111] Mirza S., Bryan A. and Noori M., 2001, "Fiber-Reinforced Composite Cylindrical Vessel with Lugs," *Compos. Struct.*, Vol. 53, pp.143-51.

- [112] Onder, A., Sayman, O., Dogan, T. and Tarakcioglu, N., 2009, "Burst Failure Load of Composite Pressure Vessels," *Composites Structures*, Vol. 89, pp. 159-166.
- [113] Timoshenko, S. and Young, D. H., 1962, *Elements of Strength of Materials*, Van Nostrand, Princeton.
- [114] Tsai, S. W., 1964, "Structural Behavior of Composite Materials," NASA CD-71.
- [115] Tsai, S. W., 1965, "Strength Characteristics of Composite Materials," NASA CD-224.
- [116] Tsai, S. W., 1968, "Strength Theory of Filamentary Structures," in *Fundamental Aspects of Fiber -Reinforced Plastic Composites*, Wiley Interscience, New York.
- [117] Tsai, S. W. and Wu, E. M., 1971, "A General Theory of Strength for Anisotropic Materials," *J. Composite Materials*, Vol. 5, pp. 58-80.
- [118] Tsai S. W., Adams D. F. and Doner D. R., 1966, "Effect of Constituent Materials Properties on the Strength of Fiber-Reinforced Materials," AFML-TR-66-190.
- [119] Tsai, S. W., 1984, "A Survey of Macroscopic Failure Criteria for Composite Materials," *Journal of Reinforced Plastic and Composites*, Vol. 3, pp. 40-62.
- [120] Hashin Z. and Rosen, W., 1964, "The Elastic Moduli of Fiber-Reinforced Materials," *Journal of Applied Mechanics*, Vol. 31, pp. 223-232.
- [121] Hashin, Z., 1965, "On Elastic Behavior of Fiber-Reinforced Materials of Arbitrary Transverse Phase Geometry," *Journal of Mechanism and Physics of Solids*, Vol. 13, pp. 119-134.
- [122] Hashin, Z., 1985, "Analysis of Cracked Laminates: A Variational Approach," *Mechanics of Materials*, Vol. 4, pp. 121-136.
- [123] Puck, A. and Schumann, H., 2002, "Failure Analysis of FRP Laminates by Means of Physically Based Phenomenological Models," *Composites Sciences and Technology*, Vol. 62, pp. 1633-1662.
- [124] Failure of Polymeric Composite Structures: Mechanisms and Criteria for Prediction of Performance. SERC/I.Mech.E Annual Expert Meeting, 23–25 September 1991, Sopwell House, St. Albans, UK [A report compiled by C.E. Neal-Sturgess].
- [125] Hinton M. J. and Soden P. D., 1998, "Failure Criteria for Composite Laminates," *Compos. Sci. Technol.*, Vol. 58, pp.1001–10.
- [126] Soden P. D., Hinton M. J. and Kaddour A. S., 1998, "Comparison of the Predictive Capabilities of Current Failure Theories for Composite Laminates," *Compos. Sci. Technol.*, Vol. 58, pp. 1225–54.

- [127] Hinton M. J., Kaddour A. S. and Soden P. D., 2002, "A Comparison of the Predictive Capabilities of Current Failure Theories for Composite Laminates, Judged Against Experimental Evidence," *Compos. Sci. Technol.*, Vol. 62, pp 1489-1529.
- [128] Soden P. D. Hinton M. J. and Kaddour A. S., 2004, "Recommendations for Designers and Researchers Resulting from the World-Wide Failure Exercise," *Compos. Sci. Technol.*, Vol. 64, pp 589-604.
- [129] Adali S Verijenko V. E., et al., 1995, "Optimization of Multilayered Composite Pressure Vessels using Exact Elasticity Solution," *Compos. Press. Vessels Ind.* Vol. 302, pp. 203-312.
- [130] Sun, X. K., Du, S. Y., Wang, G. D., 1999, "Bursting Problem of Filament -Wound Composite Pressure Vessels," *Int. J. Press. Vessels Piping*, Vol. 76, pp. 55-9.
- [131] Bakaiyan, H. Hosseini, H. Ameri E., 2009, "Analysis of Multi-Layered Filament-Wound Composite Pipes under Combined Internal Pressure and Thermomechanical Loading with Thermal Variations," Vol. 88, pp.532-41.
- [132] Hyer, M. W., 2009, *Stress Analysis of fiber-Reinforced Composite Materials*, Destech, Lancaster.
- [133] Reissner, E., 1945, "The Effect of Transverse Shear Deformation on the Bending of Elastic Plates," *J. Appl. Mech.*, Vol. 12, pp. 69-77.
- [134] Mindlin, R. D., 1951 "Influence of Rotatory Inertia and Shear on Flexural Motions of Isotropic, Elastic Plates," *J. Appl. Mech.*, Vol. 18, pp. 31-8.
- [135] Yang, P. C., Norris C. H. and Stavsky, Y., 1966 "Elastic Wave Propagation in Heterogeneous Plates," *Int. J. Solids Struct.*, Vol. 2, pp. 665-84.
- [136] Essenburg, F., 1975, "On the Significance of the Inclusion of the Effect of Transverse Normal Strain in Problems Involving Beams with Surface Constraints," *J. Appl. Mech.*, Vol. 42, pp. 127-32.
- [137] Whitney J. M. and Sun C. T., 1973, "A Higher order Theory for Extension Motions of Laminated Plates," *J. Sound Vibrat.*, Vol. 30, pp. 85-97.
- [138] Nelson R. B. and Lorch D. R., 1974, "A refined Theory of Laminated Orthotropic Plates," *J. Appl. Mech.*, Vol. 41, pp. 177-83.
- [139] Reissner, E., 1975, "On the Transverse Bending of Plates, Including the Effects of Transverse Shear Deformation," *Int. J. Solids Struct.*, Vol. 11, pp. 569-73.
- [140] Lo K. H., Christensen R. M. and Wu E. M., 1977, "A High-order Theory of plate Deformation, Part I: Homogenous Plates," *J. Appl. Mech.*, Vol.44, pp. 663-8.

- [141] Lo K. H., Christensen R. M. and Wu E. M., 1977, "A Higher-order Theory of Plate Deformation, Part II: Laminated Plates," *J. Appl. Mech.*, Vol. 44, pp. 669-76.
- [142] Levinson, 1980, "An Accurate Simple Theory of the Static and Dynamics of Elastic Plates," *Mech. Res. Communications*, Vol. 7, pp. 343-50.
- [143] Bhimaraddi A. and Stevens L. K., "A Higher Order Theory for Free Vibration of Orthotropic, Homogeneous, and Laminated Rectangular Plates," *J. Appl. Mech.*, Vol. 51, pp. 195-8.
- [144] Krishna Murty A. V. and Vellaichamy S., 1987, "On the Higher Order Shear Deformation Theory of Laminated Composite Panels," *Composite Structure*, Vol. 8, pp. 247-70.
- [145] Panda, S.C. and Natarajan, R., 1979, "Finite Element Analysis of Laminated Composite Plates," *International Journal for Numerical Methods for Engineering*, Vol. 11, pp. 69-79.
- [146] Pandya, B. N. and Kant, T., 1988, "Flexural Analysis of Laminated Composites using Refine Higher Order C^0 Plate Bending Elements," *Comput. Meth. Appl. Mech. Engng.*, Vol. 66, pp. 173-198.
- [147] Wunderlich, W. and Pilkey, W. D., 2002, *Mechanics of Structures: Variational and Computational Methods*, CRC Press, New York.
- [148] Cook, Robert D., 2002, *Concepts and Applications of Finite Element Analysis*, Wiley & Sons, Hoboken, N.J.
- [149] Pian, T. T. H., 1972, "Finite Element Methods in Continuum Mechanics," *Advances in Applied Mechanics*, Edited by C-S Yih, Vol. 12, Academic Press, N.Y.
- [150] Afshari, P., 1992, "Finite Element Analysis of Composite Plates by use of the Modified Complementary Energy Principle," *Ph.D. Thesis*, Mechanical Engineering, University of Illinois at Chicago.
- [151] Washizu, K., 1982, *Variational Methods in Elasticity & Plasticity*, 3rd ed., Pergamon Press, Oxford.
- [152] Felippa, C.A., 1994, "A survey of Parameterized Variational Principles and Applications to Computational Mechanics," *Comput. Methods Appl. Mech. Eng.* 113, pp. 109-139.
- [153] Spilker R. L., Maskeri S. M. and Kania E., 1964, "Plane Isoparametric Hybrid-Stress Elements: Invariance and Optimal Sampling," *Int., Journal for Num., Methods in Eng.*, Vol. 17, 1469-96.
- [154] William K. J., "Finite Element Analysis of Cellular Structure," *Ph. D. Dissertation*, Dept. Civil Eng., Univ. of Cal., Berkeley, Dec. 1969.

- [155] Jones, R. M., 1975, *Mechanics of Composite Materials*, Scripta, District of Columbia.
- [156] Whitney J. M., 1970, "The Effect of Boundary Conditions on the Response of Composites," *J. Comp. Matls.*, Vol. 4, pp. 192-203.
- [157] Kwon, Y. W. and Bang, H., 2000, *The Finite Element Method using MATLAB*, Second Ed., CRC, New York.
- [158] Simo, J. C., Fox, D. D. and Rifai, M. S., 1989, "On a Stress Resultant Geometrically Exact Shell Model. Part II: The Linear Theory," *Computer Methods in Applied Mechanics and Engineering*, Vol. 73, pp. 53-92.
- [159] Belytschko T., Liu WK, Ong, J. and Lam, D, 1985, "Stress Projection for Membrane and Shear Locking in Shell Finite Element," *Computer Methods in Applied Mechanics and Engineering*, Vol.51, pp. 221-258.
- [160] MATLAB MathWorks Inc. 2012.

APPENDIX A

Example Elasticity Solution for a Composite Cylindrical Shell

The anisotropic material structure in a composite material combined with the curvature in the geometry offer substantial mathematical complexity in finding exact three-dimensional elasticity solutions for laminated cylinders. However, the load condition of a uniformly distributed pressure on the inner surface of the cylinder considerably simplifies the analysis. The present investigation will provide an exact analytical solution for anisotropic thick laminated composite cylinders subjected to internal pressure loading. The material properties and geometries are taken from the work of Onder et al. [112]. The closed-form solution will be written in Matlab code.

1 Material and mechanical properties

The material is E-glass/Epoxy with the fiber and resin properties given in Table A1.

Table A1 Fiber and resin properties

	E (GPa)	σ_{TS} (MPa)	P (g/cm ³)	ϵ_t (%)
E-Glass	73.0	2400	2.6	4
Epoxy resin	3.4	50	1.2	6

The mechanical properties of the composite are given in Table A2.

Table A2 Mechanical properties of the composite

E_1 (GPa)	E_2 (GPa)	G_{12} (GPa)	G_{23} (GPa)	$\nu_{12} = \nu_{13}$	ν_{23}	X_t (MPa)	$Y_t = Z_t$ (MPa)	X_c (MPa)	$Y_c = Z_c$ (MPa)	S (MPa)
36.5	15.0	6.4	1.6	0.24	0.22	1050	43	938	106	88

2 Geometry

A filament wound composite pressure vessel as shown in Figure A1 is considered.

Here, r , θ , and z are the radial, tangential and axial coordinate axes, respectively.

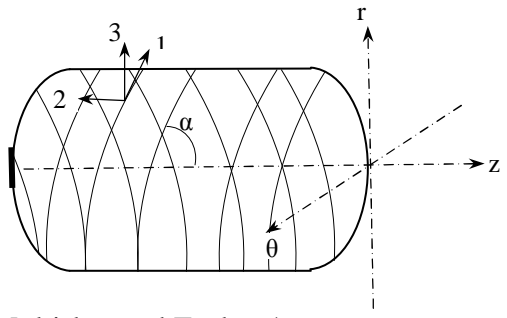


Figure A1 Multi-layered E-glass/epoxy pressure vessel

Geometry of the sample is shown in Figure A2 (Onder et al. [112]).

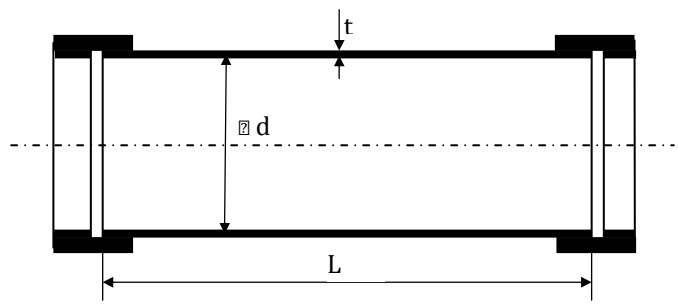


Figure A2 Geometry of the specimen.

Dimensions:

$$L = 400 \text{ mm} \qquad t = 2.5 \text{ mm}$$

$$d = 100 \text{ mm}$$

3 Analytical solution

Consider a three dimensional model stressed as shown in Figure A3.

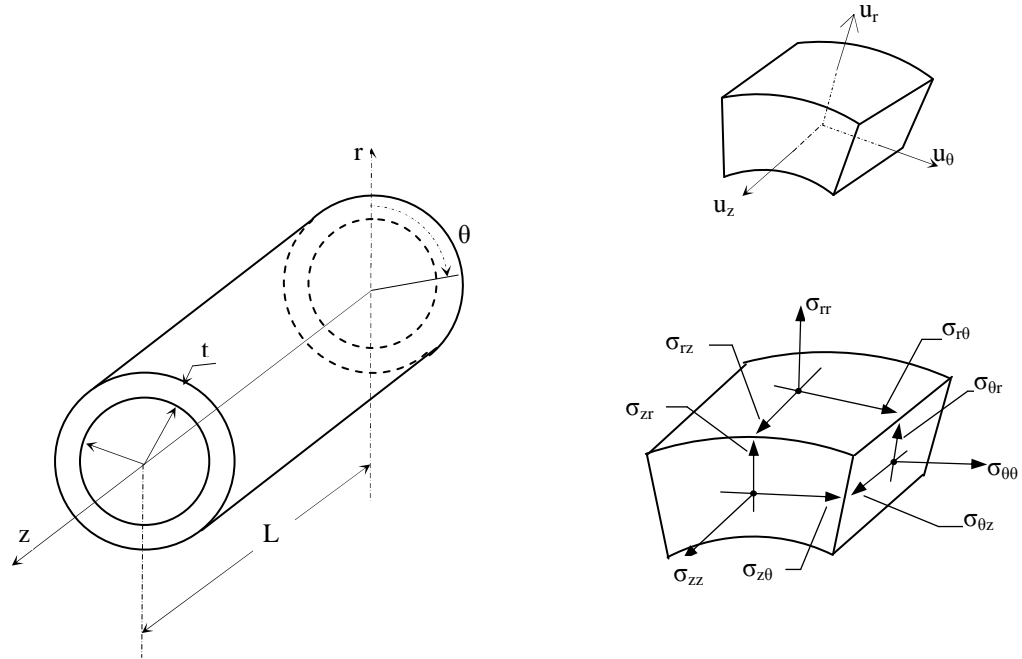


Figure A3 Three-dimensional elasticity model.

Problems of linear elasticity theory are governed by three sets of equations which can be expressed in terms of cylindrical coordinates (r, θ, z) as follows:

Stress equilibrium equations:

$$\begin{aligned} \frac{\partial \sigma_{rr}}{\partial r} + \frac{1}{r} \frac{\partial \sigma_{r\theta}}{\partial \theta} + \frac{\partial \sigma_{rz}}{\partial z} + \frac{1}{r} (\sigma_{rr} - \sigma_{\theta\theta}) + F_r &= 0 \\ \frac{\partial \sigma_{r\theta}}{\partial r} + \frac{1}{r} \frac{\partial \sigma_{\theta\theta}}{\partial \theta} + \frac{\partial \sigma_{\theta z}}{\partial z} + \frac{2}{r} \sigma_{r\theta} + F_\theta &= 0 \\ \frac{\partial \sigma_{rz}}{\partial r} + \frac{1}{r} \frac{\partial \sigma_{\theta z}}{\partial \theta} + \frac{\partial \sigma_{zz}}{\partial z} + \frac{1}{r} \sigma_{rz} + F_z &= 0 \end{aligned} \quad (\text{A.1})$$

Stress-strain relations (constitutive equation)

$$\sigma_{ij} = C_{ijkl} \varepsilon_{kl} \quad (\text{A.2})$$

or

$$\varepsilon_{ij} = S_{ijkl} \sigma_{kl} \quad (\text{A.3})$$

Strain-displacement relations (kinematics)

$$\begin{aligned}
 \varepsilon_{rr} &= \frac{\partial u_r}{\partial r} ; \quad \varepsilon_{\theta\theta} = \frac{1}{r} \left(\frac{\partial u_\theta}{\partial \theta} + u_r \right) ; \quad \varepsilon_{zz} = \frac{\partial u_z}{\partial z} \\
 \varepsilon_{r\theta} &= \frac{1}{2} \left(\frac{1}{r} \frac{\partial u_r}{\partial \theta} + \frac{\partial u_\theta}{\partial r} - \frac{u_r}{r} \right) ; \\
 \varepsilon_{\theta z} &= \frac{1}{2} \left(\frac{\partial u_\theta}{\partial z} + \frac{1}{r} \frac{\partial u_z}{\partial \theta} \right) ; \quad \varepsilon_{rz} = \frac{1}{2} \left(\frac{\partial u_r}{\partial z} + \frac{\partial u_z}{\partial r} \right)
 \end{aligned} \tag{A.4}$$

where

σ_{ij} = stress tensor component

u_{ij} = displacement tensor component

ε_{ij} = strain tensor component

F_i = prescribed body force component

C_{ijkl} = elastic stiffness coefficient

S_{ijkl} = elastic compliance coefficient

Here, $i, j = r, \theta, z$ and repeated indices imply the use of the summation convention.

An elasticity problem consists of solving the above equations for the domain V . Along the boundary S_n , the surface tractions T_i are prescribed, and along the remaining boundary S_u the displacements u_i are specified. The surface tractions T_i are related to the stresses by

$$\sigma_{ij} n_j = T_i \tag{A.5}$$

where n_j are the direction cosines of the surface normal.

To match a benchmark example, a filament wound pressure vessels made of $(\pm\alpha)$ angle-ply lay ups is studied. Figure 4 shows a magnified view of two adjacent layers.

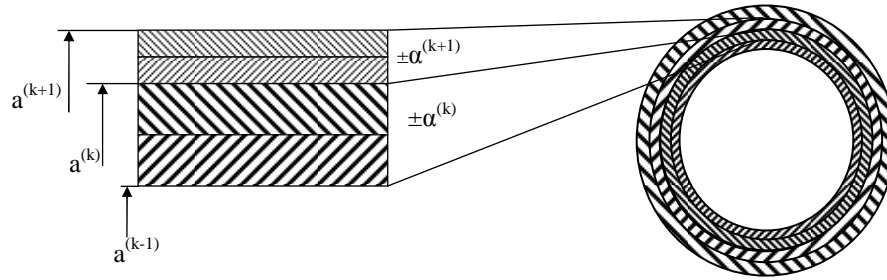


Figure A4 Enlarged view of the cross section

For a closed-end cylinder, the strain in the z-direction is assumed to be constant, i.e., $\varepsilon_z^{(k)} = \varepsilon_z^o$.

Due to cylindrical orthotropy, axisymmetric loading, and ignoring the longitudinal bending deformation due to end closures, the current case is reduced to that of a generalized plain strain problem. Define new material constants such as

$$R_{ij}^{(k)} = S_{ij}^{(k)} - \frac{S_{iz}^{(k)} S_{jz}^{(k)}}{S_{zz}^{(k)}} \quad (i,j=r, \theta) \quad (\text{A.6})$$

$$\nu_{iz}^{(k)} = \frac{S_{iz}^{(k)}}{S_{zz}^{(k)}} \quad (i,j=r, \theta) \quad (\text{A.7})$$

Let $T^{(k)}$ be the normal traction acting on the interface between k^{th} and $(k+1)^{\text{th}}$ layers.

Then, the radial, hoop, and longitudinal stresses are, respectively :

$$\sigma_{rr}^{(k)} = A^{(k)} \left[\left(\frac{r}{a^{(k)}} \right)^{g^{(k)}-1} - \left(\frac{a^{(k)}}{r} \right)^{g^{(k)}+1} \right] + B^{(k)} \left[- \left(\frac{r}{a^{(k)}} \right)^{g^{(k)}-1} + (c^{(k)})^{2g^{(k)}} \left(\frac{r}{a^{(k)}} \right)^{g^{(k)}+1} \right] \quad (\text{A.8})$$

$$\sigma_{\theta\theta}^{(k)} = A^{(k)} g^{(k)} \left[\left(\frac{r}{a^{(k)}} \right)^{g^{(k)}-1} + \left(\frac{a^{(k)}}{r} \right)^{g^{(k)}+1} \right] - B^{(k)} g^{(k)} \left[\left(\frac{r}{a^{(k)}} \right)^{g^{(k)}-1} + (c^{(k)})^{2g^{(k)}} \left(\frac{a^{(k)}}{r} \right)^{g^{(k)}+1} \right] \quad (\text{A.9})$$

$$\sigma_{zz}^{(k)} = (\varepsilon_{zz}^0 - S_{rz}^{(k)} \sigma_{rr}^{(k)} - \sigma_{\theta\theta}^{(k)} \frac{S_{\theta z}^{(k)}}{S_{zz}^{(k)}}) \quad (\text{A.10})$$

where

$$A^{(k)} = \frac{T^{(k-1)} (c^{(k)})^{g^{(k)}+1}}{1 - (c^{(k)})^{2g^{(k)}}}$$

$$B^{(k)} = \frac{T^{(k)}}{1 - (c^{(k)})^{2g^{(k)}}}$$

$$c^{(k)} = \frac{a^{(k-1)}}{a^{(k)}}$$

$$g^{(k)} = \left[\frac{R_{rr}^{(k)}}{R_{\theta\theta}^{(k)}} \right]^{0.5}$$

The displacement components are:

$$u^{(k)}(r) = r[R_{\theta r}^{(k)} \sigma_{rr}^{(k)} + R_{\theta\theta}^{(k)} \sigma_{\theta\theta}^{(k)} + \nu_{\theta z}^{(k)} \varepsilon_z^0]; \quad v^{(k)} = 0; \quad w^{(k)} = L\varepsilon_z^0 \quad (\text{A.11})$$

To find the axial strain ε_z^o , the axial stress $\sigma_{zz}^{(k)}$, is assumed that the axial traction can be satisfied on the average, i.e.

$$\sum_{k=1}^m 2\pi \int_{a^{k-1}}^{a^k} \sigma_{zz}^{(k)} r dr = \pi(T^{in})a^2 \quad (\text{A.12})$$

where T^{in} is the internal pressure.

The interface normal tractions, $T^{(k)}$'s, are determined by satisfying the contact condition of the interfaces

$$u^{(k)} = u^{(k+1)} \quad \text{at } r = a^{(k)} \quad (\text{A.13})$$

A MATLAB code was written to implement this elasticity solution.

APPENDIX B

```

%-----
%           THIS IS A FINITE ELEMENT           %
%           PROGRAM THAT USES A MODIFIED       %
%           COMPLEMENTARY ENERGY PRINCIPLE TO %
%           ANALYZE LAMINATED COMPOSITE PLATES %
%           WRITTEN BY MARTIN-CLAUDE DOMFANG S.J. %
%-----

clc; clear;
%
%-----
% LOAD IN INPUT DATA FILE (from working directory)
%-----
load INPUT1.DAT -ASCII

%-----
% CREATE OUTPUT DATA FILE (Text file in working directory)
%-----
fid = fopen('OUTPUT1.txt', 'a');

% READ IN AND WRITE OUT THE TYPE OF THE METHOD
IMETH=INPUT1(1,1);

V1=now;           % CURRENT DATE
str1=char(datestr(V1)); % TRANSFORM TO STRING

if IMETH==0
    fprintf(fid, '%\n', ...
        'THIS IS THE DISPLACEMENT METHOD OBTAINED ON : ');
    fprintf(fid, '%s%\n', str1);
elseif IMETH==1
    fprintf(fid, '\n');
    fprintf(fid, '%s%\n', 'THIS IS A TSDT HYBRID METHOD OBTAINED ON : ');
    fprintf(fid, '%s%\n', str1);
else
    fprintf(fid, '%s%\n', 'ERROR IN TYPING THE METHOD');
end
fprintf(fid, '\n\n');

% READ IN AND WRITE OUT THE TYPE OF THE ANALYSIS TO BE DONE
ANTYPE=INPUT1(2,1);

if ANTYPE==0
    fprintf(fid, '%s%\n', 'THIS IS A MODAL AND STATIC ANALYSIS');
elseif ANTYPE==1
%     fprintf(fid, '%s%\n', 'THIS IS A STATIC ANALYSIS ');

```

```

else
    fprintf(fid, '%s%\n', 'ERROR IN TYPING THE ANALYSIS TYPE');
end
%    fprintf(fid, '\n\n');%

% READ IN AND WRITE OUT THE TYPE OF STRESS CALCULATION
ISTRES=INPUT1(4,1);

if ISTRES==0
    fprintf(fid, '%s', 'STRESSES CALCULATED USING DISPLACEMENT METHOD');
elseif ISTRES==1
%    fprintf(fid, 'STRESSES CALCULATED USING USING HYBRID WITH SZZ = 0.0');
elseif ISTRES==2
    fprintf(fid, '%s%\n', 'SIX STRESS COMPONENTS CALCULATED USING HYBRID');
else
    fprintf(fid, '%s%\n', 'ERROR IN TYPING THE STRESSES ANALYSIS TYPE')
end

% READ IN AND WRITE OUT THE NUMBER OF STRESS FUNCTIONS
NBETA=INPUT1(5,1);
%    fprintf(fid, ...
%    '%g IS THE NUMBER OF STRESS FUNCTIONS 3rd HSDT\n', NBETA)

% READ IN AND WRITE OUT THE INTEGRATION SCHEME (Using GAUS Function)
[NGPX,NGPY,NGPZ,GAUSS,WEIGHT] = GAUSS;
%    fprintf(fid, '\n');%

% READ IN AND WRITE OUT SOME CONSTANTS
NUMLAYER=INPUT1(6,1);
NUMNODE =INPUT1(6,2);
NUMELE =INPUT1(6,3);
NUMDOFPN =INPUT1(6,4);
NUMNODEPE =INPUT1(6,5);
NUMDOFPE =INPUT1(6,6);
NUMDOFSTRUCT=NUMDOFPN*NUMNODE;
%    fprintf(fid, 'NUMBER OF LAYERS ARE : %g \n\n', NUMLAYER);
%    fprintf(fid, 'NUMBER OF D.O.F FOR THE STRUCTURE IS: %g
\n\n', NUMDOFSTRUCT);

% READ IN AND WRITE OUT THE MATERIAL PROPERTIES
% AND DIRECTION OF EACH LAYER

%INITIALIZATION
PHI =zeros(1,NUMLAYER);
TH =zeros(1,NUMLAYER);
E11 =zeros(1,NUMLAYER);
E22 =zeros(1,NUMLAYER);
NU12 =zeros(1,NUMLAYER);
NU23 =zeros(1,NUMLAYER);
G12 =zeros(1,NUMLAYER);
G23 =zeros(1,NUMLAYER);

```

```

DENS =zeros(1,NUMLAYER);
MATPROP=zeros(NUMLAYER,9);

% fprintf(fid,'%s%\n', 'MATERIAL PROPERTIES:')
% fprintf(fid,'\n');%
% fprintf(fid,'%s%\n', ...
% 'LAYER PHI TH E11 E22 NU12 NU23 G12 G23 DENS')
% fprintf(fid,'\n');%
for I = 1:NUMLAYER
% fprintf(fid,'\n');%
PHI(I) =INPUT1(6+I,1);
TH(I) =INPUT1(6+I,2);
E11(I) =INPUT1(6+I,3);
E22(I) =INPUT1(6+I,4);
NU12(I) =INPUT1(6+I,5);
NU23(I) =INPUT1(6+I,6);
G12(I) =INPUT1(6+I,7);
G23(I) =INPUT1(6+I,8);
DENS(I) =INPUT1(6+I,9);
MATPROP(I,:)=[PHI(I) TH(I) E11(I) E22(I) NU12(I) NU23(I) ...
G12(I) G23(I) DENS(I)];
% fprintf(fid, ...
% '%2.0f %8.0f %5.2f %9.1E %9.1E %5.2f %5.2f %9.1E %7.E %6.3f\n', ...
% I,MATPROP(I,:));%
end
% fprintf(fid,'\n');%
% fprintf(fid,'ALPAH IN DEGREE : %g \n', PHI(1));

% CALCULATING THE LOCATION OF THE REFERENCE PLANE AND
% THE DISTANCE OF EACH LAYER H(LN) TO THE REF. PLANE.

%INITIALIZATION
HT =0;
HREF =0;
H =zeros(1,NUMLAYER+1);

for I = 1:NUMLAYER
HT=HT+TH(1,I);
H(1,1)=0.5*HT;
end
for I = 1:NUMLAYER
HREF=HREF+TH(1,I);
H(I+1)=0.5*HT-HREF;
end

% READ SOME INPUT DATA

% READ(15,*) A,B,Q0
LDR=7+NUMLAYER; % ROW, LOADINGS
A=INPUT1(LDR,1); % LENGTH OF THE PLATE

```

```

B=INPUT1(LDR,2);      % WIDTH OF THE PLATE
Q0=INPUT1(LDR,3);    % INTENSITY OF THE DISTRIBUTED LOAD
Po=INPUT1(LDR,4);    % INTENSITY OF THE CONCENTRATED LOAD
LPo=INPUT1(LDR,5);   % LOCALIZATION OF THE CONCENTRATED LOAD
NN=zeros(1,NUMNODE);
CORD=zeros(3,NUMNODE);
ICON=zeros(8,NUMELE);
ELR=LDR+NUMNODE+1;   % ROW, ELEMENT
NWCLR = ELR+NUMELE;  % ROW, NUMB OF NODES WITH CONC LOADS
NNWCL = INPUT1(NWCLR,1); %NUMB OF NODES WITH CONC. LOADS

% fprintf(fid,'%s%\n\n','NODE NUMBER  X-CORD   Y-CORD   Z-CORD')
% fprintf(fid,'\n');%

% READ IN THE COORDINATES AND CONNECTIVITY OF NODES AND ELEMENETS
for I = 1:NUMNODE
    NN(I)= INPUT1(LDR+I,1);
    CORD(1,I)=INPUT1(LDR+I,2);
    CORD(2,I)=INPUT1(LDR+I,3);
    CORD(3,I)=INPUT1(LDR+I,4);
%     fprintf(fid,'%6.0f %12.3f %11.3f %12.3f\n',NN(I),CORD(:,I));%
end
%     fprintf(fid,'\n\n');%
%     VERIF1=[NN' CORD']

%     fprintf(fid,'%s%\n', ...
%     'ELEMENT NUMBER N1  N2  N3  N4  N5  N6  N7  N8')
%     fprintf(fid,'\n');%

for I = 1:NUMELE
    ICON(1,I)=INPUT1(ELR+I-1,1);
    ICON(2,I)=INPUT1(ELR+I-1,2);
    ICON(3,I)=INPUT1(ELR+I-1,3);
    ICON(4,I)=INPUT1(ELR+I-1,4);
    ICON(5,I)=INPUT1(ELR+I-1,5);
    ICON(6,I)=INPUT1(ELR+I-1,6);
    ICON(7,I)=INPUT1(ELR+I-1,7);
    ICON(8,I)=INPUT1(ELR+I-1,8);
%     fprintf(fid, ...
%     '%8.0f %9.0f %5.0f %5.0f %5.0f %5.0f %5.0f %5.0f %5.0f \n', ...
%     NN(I),ICON(:,I));%
end

% END OF INPUT DATA
% -----

% PRINT OUT THE ENTERIES FOR THE S AND C MATRIX
%     PRNT_MATMTX(NUMLAYER,E11,E22,NU12,NU23,G12,G23,PHI);
%     fprintf(fid,'\n');%
% PRINT OUT THE NODE COORDINATE FOR EACH ELEMENT
%     PRNT_COORD(NUMELE,ICON,CORD);

```

```

%      fprintf(fid,'\n');%
%-----
% COMPUTE THE CONSISTANT FORCES WITH
% FULL INTEGRATION SCHEME IS PERFORMED
%-----

FORC=zeros(1,NUMDOFSTRUCT);
EFORC_ELT=zeros(NUMDOFPE,NUMELE);
for EN=1:NUMELE
    EFORC=zeros(1,NUMDOFPE);

% CALL GLOBAL COORDINATES
[XC,YC,ZC]=GCOORD(EN,ICON,CORD);

    for NX=1:3
        for NY=1:3

            XSI=GAUSS(NX,3);
            WX=WEIGHT(NX,3);
            ETA=GAUSS(NY,3);
            WY=WEIGHT(NY,3);

% CALL SHAPE FUNCTION
[SF,SFXI,SFET,XIDX,XIDY,ETDX,ETDY,X,Y,JAC]=SHAP(XSI,ETA,XC,YC);

% CALL THE STRETCHING PART OF THE "B" MATRIX
SHMS=BSRMAS(SF);

WC=WX*WY*JAC;

% CALL SINUSOIDAL FORCE
EFORC=SINUF1(NUMDOFPE,SHMS,EFORC,WC,X,A,Q0);
% EFORC=SINUF2(NUMDOFPE,SHMS,EFORC,WC,X,Y,A,B,Q0);
% CALL DISTRIBUTED FORCES
% EFORC=DISTF(NUMDOFPE,SHMS,EFORC,WC,Q0);

    for LN=1:NUMLAYER % BEGIN LOOP FOR NUMBER OF LAYERS
%
        for NZ=1:2
            ZTA=GAUSS(NZ,2);
            WZ=WEIGHT(NZ,2);
            W=WX*WY*WZ*JAC*TH(LN)/2;
            Z=0.5*(H(LN)+H(LN+1)+ZTA*(H(LN+1)-H(LN)));

% CALL THE BENDING PART OF THE "B" MATRIX
SHMS=BBNMAS(SHMS,Z);

        end
    end
end
end

```

```

EFORC_ELT(:,EN)=EFORC(:);

% CALL ASEMBLE FUNCTION
FORC = ASEMBF(EN,NUMNODEPE,NUMDOFPN,EFORC,ICON,FORC);

end

DISTFORC=FORC;
EFORC_ELT;

%-----
% ADDING CONCENTRATED FORCES TO DISTRIBUTED FORCES
CONCFORC=FORC;
CONCFORC(1,LPo)=FORC(1,LPo)+Po;

%-----
% CREATES THE BCs FROM INPUT FILE DIRECTLY
%-----
% NUMBER OF FIXED NODES

FIXNR = NWCLR+NNWCL+1;    % ROW NUMBER OF FIXED NODES
NFIXN = INPUT1(FIXNR,1);  % NUMBER OF FIXED NODES

BCDOF=BOUNDARYDOF(NFIXN);

% BEGIN LOOP FOR STRAIN FUNCTIONS
%-----

%STR_FCT=[42 45 51 54 57 60 66 72 78 84 90];
STR_FCT=60; %[42 48];
% STR_FCT=[30 36 42 48 54 60];

% NUMBER OF TEST FUNCTION NTF
NTF=length(STR_FCT);

fprintf(fid,...
'TELM: -1/az = 1    2    3    4    5    8    10\n');
%,Daz(3),Daz(4),Daz(5),Daz(6),Daz(7),Daz(8)
fprintf(fid,'\n');%

for INB=1:NTF

% NUMBER OF UNKNOW BETAS FOR EACH STRAIN FUNCTION
NBETA=STR_FCT(INB);

```

```

aZ=0;
% Daz=-[1  2  3  4  5  8  10];
% Daz=-20 ;
Daz=[1.0 1.5];% 2.0 3.0 4.5 7.0 10

WS=length(Daz);

Matrix_W=zeros(1,WS);
NORLDSIG1=zeros(1,WS);
NORLDSIG2=zeros(1,WS);
NORLDSIG4=zeros(1,WS);
NORLDSIG11=zeros(WS,9);
NORLDSIG13=zeros(WS,9);
NORSIGM13_1_2=zeros(WS,9);

%-----
% BEGINNING OF HYBRIDS METHODS
% -----
for Iz = 1:WS

HM=zeros(NBETA,NBETA,NUMELE);
InvHM=zeros(NBETA,NBETA,NUMELE);
HM_L_E=zeros(NBETA,NBETA,NUMELE,NUMLAYER);
GM=zeros(NBETA,40,NUMELE);
GM_L_E=zeros(NBETA,40,NUMELE,NUMLAYER);
BIGK =zeros(NUMDOFSTRUCT,NUMDOFSTRUCT);
NB=NBETA;

    aZ=Daz(Iz);

for EN=1:NUMELE    % BEGIN LOOP FOR NUMBER OF ELEMENTS

    % INITIALIZE THE ELEMENT STIFFNESS MATRIX
    BMTX=zeros(6,40);

    % CALL THE COORDINATES OF THE ELEMENT
    [XC,YC,ZC] =GCOORD(EN,ICON,CORD);

    % EXTRACT CONNECTED NODE VECTOR FOR (EN)-TH ELEMENT
    NOD=zeros(1,NUMNODEPE);
    for I=1:NUMNODEPE
        NOD(I)=ICON(I,EN);
    end
    %    B1=0

    % START THE INTEGRATION (XSI AND EAT SUMMATIONS)
    for NX=1:NGPX
    %    NX

        for NY=1:NGPY

```

```

%      NY

XSI=GAUSS(NX,NGPX);
WX=WEIGHT(NX,NGPX);
ETA=GAUSS(NY,NGPY);
WY=WEIGHT(NY,NGPY);

% CALL THE 2-D SHAPE FUNCTION
[SF,SFXI,SFET,XIDX,XIDY,ETDX,ETDY,X,Y,JAC]= SHAP(XSI,ETA,XC,YC);

%
%      VERELXEZ1=[EN XSI ETA ];
%      display(' ');
%      display('ELT  XSI  ETA');
%      display(num2str(VERELXEZ1));

% ADDING THE STRETCHING PART OF THE B MATRIX
[BMTX] = BSRMTX(SF,SFXI,SFET,XIDX,XIDY,ETDX,ETDY,BMTX);
%      BMTX;

% FORM THE 'B', 'H' AND 'G' MATRICES FOR EACH LAYER

for LN=1:NUMLAYER % BEGIN LOOP FOR NUMBER OF LAYERS
%      LN
[S,C] = MATMTX2(NUMLAYER,E11,E22,NU12,NU23,G12,G23,PHI);
[CMOD, SMOD] = MODMAT(NUMLAYER,C,S); % REDUCED THE SIZE OF C & S

for NZ=1:NGPZ
%      NZ
%      B1=B1+1
ZTA=GAUSS(NZ,NGPZ);
WZ=WEIGHT(NZ,NGPZ);
W=WX*WY*WZ*JAC*TH(LN)/2;
%      DISPLAY1=[EN LN JAC W]

Z=0.5*(H(LN)+H(LN+1)+ZTA*(H(LN+1)-H(LN)));

%      WRITE(27,*) 'ELT =',EN,'LAY =',LN,'XSI',XSI,'ETA=',ETA,'ZTA=',ZTA,
%      VERELXEZ=[EN LN XSI ETA ZTA X Y Z];
%      display(' ');
%      display('ELT  LAY  XSI  ETA  ZTA  X  Y  Z');
%      display(num2str(VERELXEZ));

% ADD THE BENDING PART OF THE B MATRIX
BMTX = BBN3MTX1(BMTX,Z,aZ);

if NBETA == 30
P = NP3MTX30422(C,X,Y,Z,aZ,LN,H);
elseif NBETA == 36
P = NP3MTX36SN(C,X,Y,Z,aZ,LN,H);
elseif NBETA == 42

```

```

        P = NP3MTX42LN542(C,X,Y,Z,aZ,LN,H); %2
    % P = NP3MTX42SL60(C,X,Y,Z,aZ,LN,H);
    % P = P3MTX422(C,X,Y,Z,aZ,LN,H);
elseif NBETA == 45
    P = P3MTX45(C,X,Y,Z,aZ,LN,H);
elseif NBETA == 48
%       P = P3MTX48(C,X,Y,Z,aZ,LN,H);
    % P = NP3MTX48LL66(C,X,Y,Z,aZ,LN,H); % 2
    P = NP3MTX48SS72(C,X,Y,Z,aZ,LN,H);
elseif NBETA == 51
    P=P3MTX51(C,X,Y,Z,aZ,LN,H);
elseif NBETA == 54
    % P=P3MTX54(C,X,Y,Z,aZ,LN,H);
    % P=P3MTX542(C,X,Y,Z,aZ,LN,H);
    P=NP3MTX54LN78(C,X,Y,Z,aZ,LN,H);
elseif NBETA == 57
    P=P3MTX57(C,X,Y,Z,aZ,LN,H);
elseif NBETA == 60
%   P=P3MTX602(C,X,Y,Z,aZ,LN,H);
%   P=P3MTX60(C,X,Y,Z,aZ,LN,H);
    P=NP3MTX60LL90(C,X,Y,Z,aZ,LN,H);
elseif NBETA == 66
    P=P3MTX66(C,X,Y,Z,aZ,LN,H);
elseif NBETA == 72
    P=P3MTX72(C,X,Y,Z,aZ,LN,H);
elseif NBETA == 78
    P=P3MTX78(C,X,Y,Z,aZ,LN,H);
elseif NBETA == 84
    P=P3MTX84(C,X,Y,Z,aZ,LN,H);
elseif NBETA == 90
    P=P3MTX90(C,X,Y,Z,aZ,LN,H);
else
    fprintf(fid,...
        '%s%\n','ERROR IN THE NUMBER OF STRESS PARAMENTERS');
end

% REDUCE THE SIZE OF B AND P MATRICES SO THAT THE ZERO ENTERIES
% WON'T MAKE THE MATRICES SINGULAR MPT=TRANPOSE OF MP
[MBMTX,MPT] = MODBMXHYB(BMTX,P);

% CALCULATE THE MODIFIED VERSION OF G MATRIX
GM = MODGMTX(MBMTX,MPT,EN,W,NBETA,GM);%

% CALCULATE ONE ENTRY OF THE 'H' MATRIX FOR 5 STRESSES
HM = HMTX2(EN,LN,SMOD,W,MPT,NBETA,HM);

end % END LOOP ON NZ-INTEGRATION
end % END LOOP ON NUMBER OF LAYER
end % END LOOP ON NY-INTEGRATION

```

```

end      % END LOOP ON NX-INTEGRATION
% PUT HM IN S SQUARE MATRIX FORMFOR THE INVERSE
HHM=zeros(NBETA,NBETA);
for LL=1:NBETA
    for JJ=1:NBETA
        HHM(LL,JJ)=HM(LL,JJ,EN);
    end
end

% COMPUTE THE INVERSE OF HHM = HI
HI=NEWINV(NBETA,HHM);

for LL=1:NBETA
    for JJ=1:NBETA
        HM(LL,JJ,EN)=HI(LL,JJ);
%     InvHM(LL,JJ,EN)=HI(LL,JJ);
    end
end

% COMPUTES THE ELEMENT SFIFFNESS MATRIX FOR HYBRID STRESS
EKM = ELMKMXHYB(HM,GM,NBETA,NUMDOFPE,EN);
%     SIZE_EKM=size(EKM)

% EXTRACT SYSTEM DOFS ASSOCIATED WITH ELEMENT
[EDOFIND]=ELDOFAS(NOD,NUMNODEPE,NUMDOFPN);% [1x40]

% ASSEMBLY OF ELEMENT MATRICES INTO THE SYSTEM MATRIX
[BIGK]=ASMBLBIGK(BIGK,EKM,EDOFIND);%

end      % END LOOP FOR NUMBER OF ELEMENTS

FORCES = DISTFORC; % JUST PUT POINT LOAD=0

% APPLY THE BOUNDARY CONDITIONS
BCVAL =zeros(1,NUMDOFSTRUCT);
[BIGKM,FORCM]=APLYBCS(BIGK,FORCES,BCDOF,BCVAL);

% SOLVE FOR A SET OF LINEAR EQUATIONS WITH PIVOTING AND SCALING
DISP = ELIM(NUMDOFSTRUCT,BIGKM,FORCM,NUMDOFSTRUCT+1);% SAME AS
MATLAB

% PRINT THE FIXED DISPLACEMENTS
%     PRNT_FIXDOF(NUMNODE,NUMDOFPN)

% PRINT THE DISPL. CALL
PRDISP(NUMDOFSTRUCT,NUMNODE,NUMDOFPN,DISP)
%     DISPMTX=PRDISP(NUMNODE,NUMDOFPN,DISP);

```

```

% PRINT THE DISPL AT NODE 33. CALL
PRDISP(NUMDOFSTRUCT,NUMNODE,NUMDOFPN,DISP)
% PRNT_DISP33=PRDISP33(NUMNODE,NUMDOFPN,DISP);
% PRNT_DISP65=PRDISYMP65(NUMNODE,NUMDOFPN,DISP);

% PRNT_DISP_STRIP17=PRDISTRIP117(NUMNODE,NUMDOFPN,DISP);

% PRNT_DISP_STRIP11=PRDISTRIP1B11(NUMNODE,NUMDOFPN,DISP);
% NW=PRDISTRIP1B11_Simple_Mtx(NUMNODE,NUMDOFPN,DISP);

% PRNT_DISP_CP4A21=PRDISTCP4A21(NUMNODE,NUMDOFPN,DISP);
% PRNT_DISP_CP4A21=PRDISTCP4A21_SIMPLE(NUMNODE,NUMDOFPN,DISP);

% PRNT_DISP_CP4B33=PRDISTCP4B33(NUMNODE,NUMDOFPN,DISP);
% PRNT_DISP_CP4B33=PRDISTCP4B33_SIMPLE(NUMNODE,NUMDOFPN,DISP);
% NW=PRDISTCP4B33_SIMPLE_M(NUMNODE,NUMDOFPN,DISP);

DW=100*E22(1)*HT^3/(Q0*A^4);

NW= DW*DISP(83);
Matrix_W(Iz)=NW;

% PRINT THE DISPL AT NODE 33 and its surroundings

% PRNT_DISP33Plus=PRDISP33Plus(NUMNODE,NUMDOFPN,DISP);
% PRNT_DISP33Plus=PRDISP52933(NUMNODE,NUMDOFPN,DISP);
% endif % END FOR DISPLACEMENT METHOD LOOP

% THE BETAS ARE FOUND FOR EACH ELT
BETA =zeros(NBETA,NUMELE);
for EN=1:NUMELE
BETA =
BETAS(NBETA,NUMDOFPE,NUMNODEPE,NUMDOFPN,EN,ICON,HM,GM,BETA,DISP);
end

% PRINT THE LOCATION OF THE POINT WITHIN THE ELEMENT
% fprintf(fid,'\n');%
% fprintf(fid,'%s%\n','% ELEMENT POINT POSITION');
% fprintf(fid,'\n');%
% fprintf(fid,'%6.0f %18.3f \n', ELPT(1),ELPT(3));%
% fprintf(fid,'\n');%
%
% fprintf(fid,'%s%\n', ...
'% X Y Z SXX SYX SZZ SXY SYZ SXZ');
% fprintf(fid,'\n');%

NGPZ=3;
SIGMAMTX=zeros(NGPZ,7,NUMELE,NUMLAYER,NGPX*NGPY);

```

```

for EN=1:NUMELE
%   fprintf(fid,'\n\n');%
%   PRNT_ELEMENT_COORD(EN,ICON,CORD);

    BMTX=zeros(6,40);

% CALL THE COORDINATES OF THE ELEMENT
[XC,YC,ZC]=GCOORD(EN,ICON,CORD);

for LN=1:NUMLAYER

%   fprintf(fid,'\n');%
%   fprintf(fid,'%s%\n','ELEMENT LAYER LAYER POSITION');
%   fprintf(fid,'\n');%
%   fprintf(fid,'%4.0f %9.0f %15.3f \n', EN,LN,H(LN));%
%   fprintf(fid,'\n');%
%
%   fprintf(fid,'%s%\n', ...
% ' X   Y   Z   SXX   SYY   SZZ   SXY   SYZ   SXZ');
%   fprintf(fid,'\n');%

    XYP=0;

    for NX=1:NGPX
    for NY=1:NGPY

        XYP=XYP+1;

        XSI=GAUSS(NX,NGPX);
        ETA=GAUSS(NY,NGPY);

%   CALL THE SHAPE FUNCTION
[SF,SFXI,SFET,XIDX,XIDY,ETDX,ETDY,X,Y,JAC]= SHAP(XSI,ETA,XC,YC);

%   CALL THE STRETCHING PART OF THE "B" MATRIX
[BMTX] = BSRMTX(SF,SFXI,SFET,XIDX,XIDY,ETDX,ETDY,BMTX);

% INITIALIZE THE NUMBER OF Z WITHIN THE TOTAL THICKNESS
NZZ=0;

% INITIALIZE THE STRESSES WITHIN LAYER LN
SIGNZZ=zeros(NGPZ,7);

for NZ=1:NGPZ

% THE NUMBER OF Z WITHIN THE TOTAL THICKNESS
NZZ=NZZ+1;

ZTA=GAUSS(NZ,NGPZ);
Z=0.5*(H(LN)+H(LN+1)+ZTA*(H(LN+1)-H(LN)));

```

```

VCORD=[X Y Z];

%      CALL THE BENDING PART OF THE "B" MATRIX
BMTX = BBN3MTX1(BMTX,Z,aZ);

if NBETA == 30
    P = NP3MTX30422(C,X,Y,Z,aZ,LN,H);
elseif NBETA == 36
    P = NP3MTX36SN(C,X,Y,Z,aZ,LN,H);
elseif NBETA == 42
    P = NP3MTX42LN542(C,X,Y,Z,aZ,LN,H); %2
    % P = NP3MTX42SL60(C,X,Y,Z,aZ,LN,H);
    % P = P3MTX422(C,X,Y,Z,aZ,LN,H);
elseif NBETA == 45
    P = P3MTX45(C,X,Y,Z,aZ,LN,H);
elseif NBETA == 48
%      P = P3MTX48(C,X,Y,Z,aZ,LN,H);
    % P = NP3MTX48LL66(C,X,Y,Z,aZ,LN,H); %2
    P = NP3MTX48SS72(C,X,Y,Z,aZ,LN,H);
elseif NBETA == 51
    P=P3MTX51(C,X,Y,Z,aZ,LN,H);
elseif NBETA == 54
    % P=P3MTX54(C,X,Y,Z,aZ,LN,H);
    % P=P3MTX542(C,X,Y,Z,aZ,LN,H);
    P=NP3MTX54LN78(C,X,Y,Z,aZ,LN,H);
elseif NBETA == 57
    P=P3MTX57(C,X,Y,Z,aZ,LN,H);
elseif NBETA == 60
%      P=P3MTX602(C,X,Y,Z,aZ,LN,H);
%      P=P3MTX60(C,X,Y,Z,aZ,LN,H);
    P=NP3MTX60LL90(C,X,Y,Z,aZ,LN,H);
elseif NBETA == 66
    P=P3MTX66(C,X,Y,Z,aZ,LN,H);
elseif NBETA == 72
    P=P3MTX72(C,X,Y,Z,aZ,LN,H);
elseif NBETA == 78
    P=P3MTX78(C,X,Y,Z,aZ,LN,H);
elseif NBETA == 84
    P=P3MTX84(C,X,Y,Z,aZ,LN,H);
elseif NBETA == 90
    P=P3MTX90(C,X,Y,Z,aZ,LN,H);
else
    fprintf(fid,...
        '%s%\n','ERROR IN THE NUMBER OF STRESS PARAMENTERS');
end

% REDUCE THE SIZE OF B AND P MATRICES SO THAT THE ZERO ENTERIES
% WON'T MAKE THE MATRICES SINGULAR MPT=TRANPOSE OF MP
[MBMTX,MPT] = MODBMXHYB(BMTX,P);

```

```

SXX=0.0;
  SYY=0.0;
  SZZ=0.0;
  SXY=0.0;
  SYZ=0.0;
  SXZ=0.0;
  X1=X;
  Y1=Y;
  Z1=Z;

if ISTRES == 1

  for J=1:NBETA
    SXX=SXX+MPT(J,1)*BETA(J,EN);
    SYY=SYY+MPT(J,2)*BETA(J,EN);
    %   SZZ=SZZ+MPT(J,3)*BETA(J,EN);
    SXY=SXY+MPT(J,3)*BETA(J,EN);
    SYZ=SYZ+MPT(J,4)*BETA(J,EN);
    SXZ=SXZ+MPT(J,5)*BETA(J,EN);
  end

  SHOW=[X1 Y1 Z1 SXX SYY SZZ SXY SYZ SXZ];
  CALSIG=[X1 Y1 Z1 SXX SYY SYZ SXZ];    %SHOW;
  SIGNZP(NZP,:)=CALSIG(1,:);

% FORM THE MATRIX OF ALL STRESSES AND THEIR POSITION
SIGMAMTX(:, :, EN, LN, XYP)=SIGNZP(:, :);

% % LOCATION WHERE TO COMPUTE THE STRESSES
% %   ELPT=[6,1,9];
%   fprintf(fid, ...
%   ' %1.2f %5.2f %6.3f %10.2E %10.2E %2.0f %10.2E %10.2E %10.2E\n',SHOW);%
%   end

elseif ISTRES ==2

  for J=1:NBETA

    SXX=SXX+P(1,J)*BETA(J,EN);
    SYY=SYY+P(2,J)*BETA(J,EN);
    SZZ=SZZ+P(3,J)*BETA(J,EN);
    SXY=SXY+P(4,J)*BETA(J,EN);
    SYZ=SYZ+P(5,J)*BETA(J,EN);
    SXZ=SXZ+P(6,J)*BETA(J,EN);
  end

%   fid = fopen('OUTPUT1.txt','a');

  SHOW=[X1 Y1 Z1 SXX SYY SZZ SXY SYZ SXZ];

%   fprintf(fid, ...

```

```

%   '%1.2f %5.2f %5.2f %10.2E %10.2E %2.0f %10.2E %10.2E %10.2E\n',SHOW);%
%       fclose(fid);%       Close the OUTPUT file

    else
    fprintf(fid,'\n');%
    fprintf(fid,'%s%\n','INCORRECT TYPE OF TYPE OF STRESS');
    fprintf(fid,'\n');%

    end

    end % END LOOP ON NZ-INTEGRATION
end % END LOOP ON NY-INTEGRATION
end % END LOOP ON NX-INTEGRATION
end % END LOOP ON LAYER
end % END LOOP ON ELEMENT

% end % END LOOP FOR HYBRID METHOD

% LOCATION WHERE TO COMPUTE THE STRESSES

% CALSIG=NZP * [X1 Y1 Z1 SXX SYY SXY] ;
% SIGM11_5_14=SIGMAMTX(:,4,5,.,14);
% SIGM11_5_15=SIGMAMTX(:,4,5,.,15);
SIGM13_1_1_1=SIGMAMTX(1,7,1,1,2);
SIGM13_1_1_2=SIGMAMTX(2,7,1,1,2);
SIGM13_1_1_3=SIGMAMTX(3,7,1,1,2);
SIGM13_1_2_1=SIGMAMTX(1,7,1,2,2);
SIGM13_1_2_2=SIGMAMTX(2,7,1,2,2);
SIGM13_1_2_3=SIGMAMTX(3,7,1,2,2);
SIGM13_1_3_1=SIGMAMTX(1,7,1,3,2);
SIGM13_1_3_2=SIGMAMTX(2,7,1,3,2);
SIGM13_1_3_3=SIGMAMTX(3,7,1,3,2);
SIGM13_1_2=[SIGM13_1_1_1 SIGM13_1_1_2 SIGM13_1_1_3 ...
SIGM13_1_2_1 SIGM13_1_2_2 SIGM13_1_2_3 ...
SIGM13_1_3_1 SIGM13_1_3_2 SIGM13_1_3_3];

% COMPUTE THE STRESS SIGMA2

% EXTRAPOLATION SCHEME
%-----

% SIGMA11_LN = SIGMA11_CASE2SS(SIGMAMTX,NGPZ,NGPX,NGPY)
% SIGMA13_LN = SIGMA13_CASE2SS(SIGMAMTX,NGPZ,NGPX,NGPY);
% XSIGMA1_CASE4B = SIGMA1_CASE4B(SIGMAMTX,NGPX,NGPY,2,ZP,YP,XP);
% XSIGMA2_CASE4B = SIGMA2_CASE4B(SIGMAMTX,NGPX,NGPY,1,0.5,YP,XP);
% XSIGMA4_CASE4B = SIGMA4_CASE4B(SIGMAMTX,NGPX,NGPY,LN,0,0,0);
%
% NORLDSIG11(Iz,:)=(1/Q0)*SIGMA11_LN(1,:);
% NORLDSIG13(Iz,:)=(1/Q0)*SIGMA13_LN(1,:);
NORSIGM13_1_2(Iz,:)=(1/Q0)*SIGM13_1_2(1,:);

```

```

% NORLDSIG2(Iz)=0.1*XSIGMA2_CASE4B;
% NORLDSIG4(Iz)=XSIGMA4_CASE4B;

% % CASE 4A SYMMETRIC
% XSIGMA1_CASE4A = SIGMA1_CASE4A(SIGMAMTX,NGPX,NGPY,2,ZP,YP,XP);
% XSIGMA2_CASE4A = SIGMA2_CASE4A(SIGMAMTX,NGPX,NGPY,1,0.5,YP,XP);
% XSIGMA4_CASE4A = SIGMA4_CASE4A(SIGMAMTX,NGPX,NGPY,LN,0,0,0);
%
%     fprintf(fid,'\n');%
%     fprintf(fid, 'NORMALIZED SIGMA1 : %g ', 0.1*XSIGMA1_CASE4A)
%     fprintf(fid,'\n');%
%     fprintf(fid, 'NORMALIZED SIGMA2 : %g ', 0.1*XSIGMA2_CASE4A)
%     fprintf(fid,'\n');%
%     fprintf(fid, 'NORMALIZED SIGMA4 : %g ', XSIGMA4_CASE4A)
%     fprintf(fid,'\n');%
%     fprintf(fid,'%s%\n', ...
%     '----- ');
%     fprintf(fid,'\n');%

end % END OF WEIGHING COEF LOOP

% NORLDSIG11

% fprintf(fid,...
%'CL%g: 1/az = 1   3   4   5   6   8   10  100\n', NBETA);

% PRDISPLACMT_VECTOR(Matrix_W,WS,NBETA);
% PRNTSIGMA11_MTX(NORLDSIG11,WS,NBETA,Daz);
% PRNTSIGMA11_MTX(NORLDSIG13,WS,NBETA,Daz);
% PRNTSIGMA11_MTX(NORSIGM13_1_2,WS,NBETA,Daz);
% PRDISTCP4B33_MATRIX(Matrix_W,WS);
% PRNTSIGMA1_VECTOR(NORLDSIG1,WS);
% PRNTSIGMA2_VECTOR(NORLDSIG2,WS);
% PRNTSIGMA4_VECTOR(NORLDSIG4,WS);
%     fprintf(fid,'\n');%

end % END OF STRAIN FUNCT LOOP

fclose(fid);%     Close the OUTPUT file

```